2007

UNIVERSITY OF CANTERBURY
Te Whare Wānanga o Waitaha
CHRISTCHURCH NEW ZEALAND

Reversible Photoregulation of Binding of the Serine Protease α-Chymotrypsin to a Functional Surface

A thesis submitted in partial fulfilment of the requirements for the Degree of

Doctor of Philosophy in Chemistry

in the University of Canterbury

by

David Pearson

Acknowledgements

Thanks to everyone that has helped out with my PhD:

My supervisors for supervising my work and helping to develop my scientific skills. In particular, Andrew for doing the main supervision, helping to improve my writing, and getting us enough research money to do this project properly, and Alison for her critical reasoning skills and extensive knowledge of cyclic voltammetry.

The Abell and Downard groups, and the rest of the chemistry department, for showing me how to do chemistry and for having good parties, lunches and cakes. Especially Nathan, my other 'supervisor', who also supplied some of the starting materials used in this work.

My family for being encouraging and listening to me talking about chemistry.

My friends, whatever countries they are in at the moment, for helping to distract me from doing too much chemistry.

And my girlfriend Tara, for staying in NZ while I finished my thesis, and for having rich parents who can afford to fly us around in premium economy!

Publications

Work described in this thesis appears in the following publications:

Pearson, D.; Downard, A. J.; Muscroft-Taylor, A.; Abell, A. D., Reversible photoregulation of binding of α-chymotrypsin to a gold surface, *J. Am. Chem. Soc.*, **2007**, 129, 14862-14863**.**

Pearson, D.; Abell, A. D., D-Leu-L-Phe-containing dipeptide inhibitors of chymotrypsin – the role of the N- and C-termini in enzyme affinity, *ARKIVOC*, submitted.

Pearson, D.; Abell, A. D., Photoswitch inhibitors of α-chymotrypsin—increased substitution and peptidic character in peptidomimetic boronate esters, *Org. Biomol. Chem.,* **2006**, 4, 3618.

Abstract

This thesis presents the first example of reversible photoregulation of the binding of a protease, α-chymotrypsin, to a surface. A modular approach is used involving the azobenzene photoswitch group, a surface linker and an enzyme binding group. This approach is designed to be easily extended to the photoregulation of binding of other proteases to surfaces by use of enzyme binding groups selective to these proteases.

Chapter one gives a brief outline of some of the important areas involved in to this work, including molecular switches, proteases and surface modification.

Chapter two describes the synthesis of azobenzene-containing boronate esters designed as photoswitch inhibitors of α-chymotrypsin. Boronate esters were prepared containing the aminophenylboronate group or the peptidomimetic borophenylalanine group for enzyme binding and a range of substituents designed for enzyme affinity and/or surface attachment. Syntheses primarily involved peptide coupling reactions and azobenzene formation by condensation of nitrosobenzenes and anilines. Coupling reactions were successfully carried out using EDCI or isobutyl chlorofomate in several cases where other reagents gave unacceptable decomposition.

Chapter three describes the syntheses and HPLC stability studies of derivatives of a noncovalent α-chymotrypsin inhibitor. Several dipeptide-based compounds containing either an amide group for surface attachment or an azobenzene group for photoswitching were prepared, primarily using peptide coupling reactions. Each compound was incubated with α-chymotrypsin to assess its stability, and all were found by HPLC monitoring to be stable to α-chymotrypsin catalysed hydrolysis.

Chapter four describes syntheses of azobenzene-containing trifluoromethylketones and α-ketoesters designed as photoswitch inhibitors of α-chymotrypsin. Trifluoromethylketones/α-ketoesters containing amine groups for surface attachment were prepared, primarily using peptide coupling reactions, but could not be isolated due to the incompatibility of the electrophilic ketone and primary amine groups. Trifluoromethylketones/α-ketoesters containing terminal alkynes for surface attachment

were prepared either by the attachment of an alkyne substituent group to a symmetrical azobenzene core or by Pd-catalysed reaction of a protected alkyne with an azobenzene having a halide substitutent.

Chapter five describes syntheses of sulfur-containing surface linkers for use in surface attachment of the photoswitch inhibitors described in chapters 2-4. A range of compounds containing disulfide or protected thiol groups for surface attachment and azide or carboxylic acid groups for inhibitor attachment were prepared. Syntheses primarily involved coupling of functionalised alcohols/amides to carboxylic acid-containing disulfides/thioacetates. Selected linkers were attached to azobenzenes by amide coupling or azide-alkyne cycloaddition for surface attachment, photoswitching and/or enzyme assay. Azide-alkyne cycloaddition yields were initially poor, but were improved by use of stoichiometric amounts of copper catalyst.

Chapter six describes UV/vis photoisomerisation studies and enzyme assays carried out to assess enzyme photoswitching of the compounds described in chapters 2-5. The trifluoromethylketones and α-ketoesters described in chapter 4 gave the best results, with moderate inhibition of α-chymotrypsin (μM affinity constants) and up to 5.3 fold changes in inhibition on UV/vis irradiation. Many of the boronate esters described in chapter 2 were found to inhibit α-chymotrypsin, but were somewhat unstable to irradiation. The dipeptide-based compounds described in chapter 3 were inactive against α-chymotrypsin. Good photoisomerisation was obtained for an azobenzene containing a symmetrical disulfide surface linker and poor photoisomerisation was obtained for an azobenzene containing a lipoic acid surface linker.

Chapter seven describes surface attachment of selected photoswitch inhibitors and studies of photoregulated enzyme binding to the resultant functional surfaces. Self assembled monolayers (SAMs) of disulfides were formed on gold surfaces and characterised by electrochemistry and contact angle measurements. Binding of α-chymotrypsin to SAMs containing a photoswitch inhibitor was detected by quartz crystal microbalance (QCM), but was found to be largely irreversible. An alkyne-containing photoswitch inhibitor was attached to a surface plasmon resonance (SPR) chip in a two step procedure involving generation of an azide modified surface followed by azide-alkyne cycloaddition. Binding

of α-chymotrypsin to the resultant modified surface was detected by SPR and successfully regulated by UV/vis irradiation.

Chapter eight provides conclusions for the work described in this thesis and suggests future directions.

Chapter nine gives experimental details for the work described in this thesis.

Abbreviations

Ala	alanine
Asp	aspartic acid
Boc	*tert*-butoxycarbonyl
BOP	benzotriazol-1-yloxy-tris(dimethylamino)phosphonium hexafluorophosphate
Cbz	carbobenzyloxy
CV	cyclic voltammetry/cyclic voltammogram
d	doublet (NMR)
dd	doublet of doublets (NMR)
de	diastereomeric excess
DCM	dichloromethane
DIBAL	diisobutylaluminium hydride
DIEA	diisopropylamine
DMAP	dimethylaminopyridine
DME	dimethoxyethane
DMF	dimethylformamide
DMSO	dimethylsulfoxide
dq	doublet of quartets (NMR)
dt	doublet of triplets (NMR)
EDCI	*N*-ethyl-*N*'-(3-dimethylaminopropyl)carbodiimide hydrochloride
EDTA	ethylenediamine tetraacetic acid
eq	equivalents
Fmoc	9-fluorenylmethoxycarbonyl
Gly	glycine
HATU	*O*-(7-azabenzotriazol-1-yl)-*N*,*N*,*N*′,*N*′-tetramethyluronium hexafluorophosphate
HEPES	4-(2-hydroxyethyl)-1-piperazineethanesulfonic acid
His	histidine
HMDS	hexamethyldisilazane
HMPA	hexamethylphosphoramide
HOAt	*N*-hydroxy-7-azobenzotriazole

HOBt	*N*-hydroxybenzotriazole
HPLC	high performance liquid chromatography
HRMS	high resolution mass spectrometry
Hyp	hydroxyproline
LDA	lithium diisopropylamide
Leu	leucine
LiHMDS	lithium hexamethyldisilazane
Ms	mesyl (methanesulfonyl)
MS	mass spectrometry
NHS	*N*-hydroxysuccinimide
NMM	*N*-methylmorpholine
NMR	nuclear magnetic resonance
OEG	oligoethylene glycol
pet ether	petroleum ether
Phe	phenylalanine
Pro	proline
PSS	photostationary state
QCM	quartz crystal microbalance
qu	quantitative
r.t.	room temperature
SAM	self-assembled monolayer
sat.	saturated
SCE	saturated calomel electrode
SDS	sodium dodecyl sulfate
Ser	serine
SPR	surface plasmon resonance
Suc	succinyl
t	triplet (NMR)
TBAF	tetrabutylammonium fluoride
TEA	triethylamine
TFA	trifluoroacetic acid
THF	tetrahydrofuran
TLC	thin layer chromatography
Tris	tris-(hydroxymethyl)aminomethane

UV	ultraviolet
Val	valine
vis	visible

Chapter One

Introduction

Introduction

1.1 Overview

The aim of this project was to prepare a series of photoswitch enzyme inhibitors for surface attachment, in order to photoregulate enzyme binding to surfaces. To achieve this goal, existing classes of protease inhibitors containing an azobenzene molecular switch were modified to improve molecular switching and to introduce groups for surface attachment. These photoswitch inhibitors were attached to surfaces and enzyme binding and photoswitching studies were carried out at the modified surfaces.

This work is based on previous study of photoswitch inhibitors of the enzyme α-chymotrypsin. The work of Harvey[1-3] focused on the design of inhibitors containing an azobenzene group linked to a peptidomimetic α-ketoester, based on a known inhibitor.[4] This study covered a range of structures and discovered several effective photoswitch inhibitors, with a 2-3 fold change in enzyme activity observed on photoisomerisation. An example compound is shown in Fig. 1.1 that switches from an inhibition constant, K_i, of 240 nM in the *E* form, **1.1**, to 130 nM in the *Z* form, **1.2**. This represents an increase in activity on *E* to *Z* photoswitching.

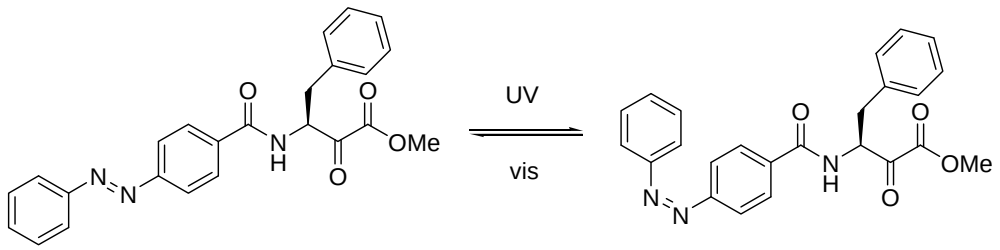

1.1 K_i = 240 nM **1.2** K_i = 130 nM

Fig. 1.1. α-Ketoester photoswitch inhibitor of α-chymotrypsin.[2]

The work of Alexander[5] involved the study of photoswitch enzyme inhibitors containing the trifluoromethylketone enzyme binding group (Fig. 1.2), again based on known inhibitors.[6] This work aimed to increase the potency and/or photoswitching of the compounds by increased derivatisation of the azobenzene group. The inhibitors were less

active than α-ketoesters, but showed better photoswitching of up to 5 fold changes in activity on photoisomerisation.

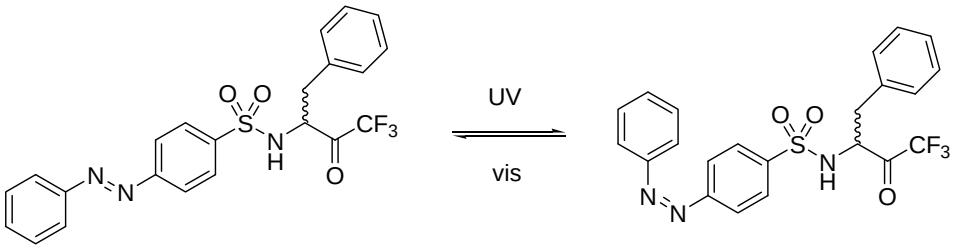

1.3 **1.4**

Fig. 1.2. Trifluoromethylketone photoswitch inhibitor of α-chymotrypsin.[5]

The work described in this thesis involves the study of related inhibitors and those with a third enzyme binding group, the boronate ester, as well as further derivatisation of the azobenzene group and surface attachment of photoswitch inhibitors.

This chapter summarises the major areas involved in this thesis: molecular switching, protease inhibition and surface modification, and gives a brief description of the work presented in this thesis.

1.2 Molecular Switching

A single compound can often exist in different forms such as isomers and excited states that have significantly different molecular shape and function. In certain cases, these different forms can be reversibly interconverted by non-invasive changes in external conditions such as pH, electron transfer, light or heat, and thus can be used as molecular switches. This external control of molecular function is important both in fundamental research of molecular properties and as a first step towards useful molecular devices and technologies. As such, it is currently of interest to develop a variety of molecular switching methods for a range of systems.

Effective, useful molecular switching has various ideal requirements:

1. Efficient and complete switching – a molecular switch should be easily converted completely from one form to another.

2. Significant change in properties on switching – a large difference in properties such as shape or charge should be obtained between the two forms.

3. Reversibility – molecular switching should be completely reversible and stable over a number of switching cycles without side reactions.

4. Ease of synthesis – a molecular switch should be easy to incorporate into a variety of different structures without extensive new synthetic design.

In practice, many molecular switches do not fulfil all of these requirements. However, the most useful switches satisfy most of them. Molecular switches using pH or light control are two of the most important, and will be briefly described below:

1.2.1 pH switching

pH switching has been studied in supramolecular chemistry for the development of nanoscale devices. This form of molecular switching usually requires a change in shape between a protonated and a deprotonated form of a molecule. While protonation/deprotonation clearly has a large impact on the charge of a molecule, shape is not always affected. However, a localised change in charge can significantly alter interactions with neighbouring groups, often leading to a change in shape. This is particularly likely when coordination effects are involved.

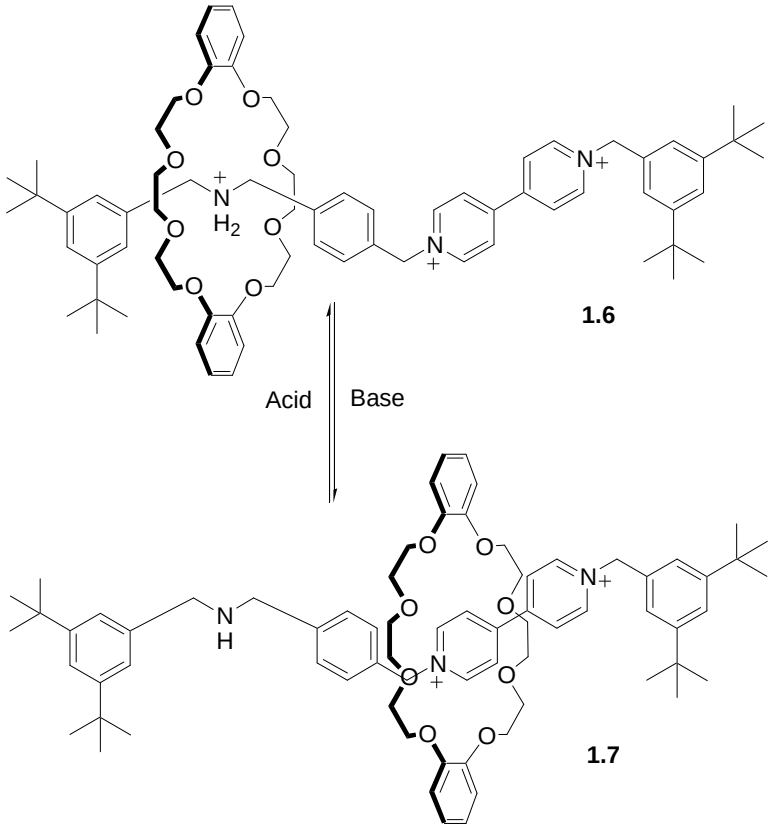

Fig. 1.3. Acid-base molecular switch.[7]

pH switching at a coordination site has been used in the development of 'molecular shuttle' rotaxanes.[7] One such shuttle, shown in Fig. 1.3, consists of a dumbbell shaped unit with two coordination sites, NH_2^+ and bipyridinium^{2+}, and a crown ether ring which surrounds the dumbbell and can coordinate to either site. The ring coordinates to the NH_2^+ site in acidic media (structure **1.6**), and on deprotonation of the group to NH at higher pH the ring moves to the bipyridinium coordination site (structure **1.7**). An extension of this pH switching molecular device is the molecular 'elevator', which consists of three connected molecular shuttles.[8] This large platform structure shifts up and down on pH switching.

1.2.2 Photoswitching

Photoswitching is the isomerisation of a compound resulting from irradiation with light. While many molecules undergo electronic transitions under UV/visible irradiation, only a few reversibly isomerise as a result of a transition.

To fulfil the ideal molecular switching requirements, the photoisomerisation process should have high quantum yield and proceed to completion quickly without side reactions. The isomer formed should be stable to ambient light conditions and to the initial isomerisation wavelength, but be readily isomerised back to the initial state by isomerisation at a different wavelength. Several relatively effective photoswitches that fulfil most of these criteria have been developed and used extensively.

For studies aimed towards information storage, photoswitches are required that are very stable and reversible, and have some easily measurable property change (e.g. colour) rather than a large change in shape on switching. For this purpose, studies have focused on such compounds as diarylethenes and fulgides. Diarylethenes are developed from stilbene **1.8**, which undergoes a photochemical reaction to form dihydrophenanthrene **1.9** (Fig. 1.4).[9] This electrocyclic reaction proceeds under UV irradiation, and the reverse reaction occurs thermally, as shown in Fig. 1.4. Unfortunately, dihydrophenanthrene **1.9** is irreversibly oxidised in the presence of air to phenanthrene **1.10**, which does not undergo photoisomerisation. Stilbene has been systematically improved by the replacement of the phenyl rings by heterocycles, constraining the structure to prevent *E*/*Z* isomerisation about the double bond, and substitution of the *ortho* positions of the aromatic rings to prevent a permanent cyclisation.[10] These modifications have produced stable, thermally irreversible compounds with effective photoswitching from a colourless to a coloured state. For example, compound **1.11** (Fig. 1.4) cyclises on UV irradiation to **1.12**, which is heat stable but reopens to **1.11** on visible irradiation.

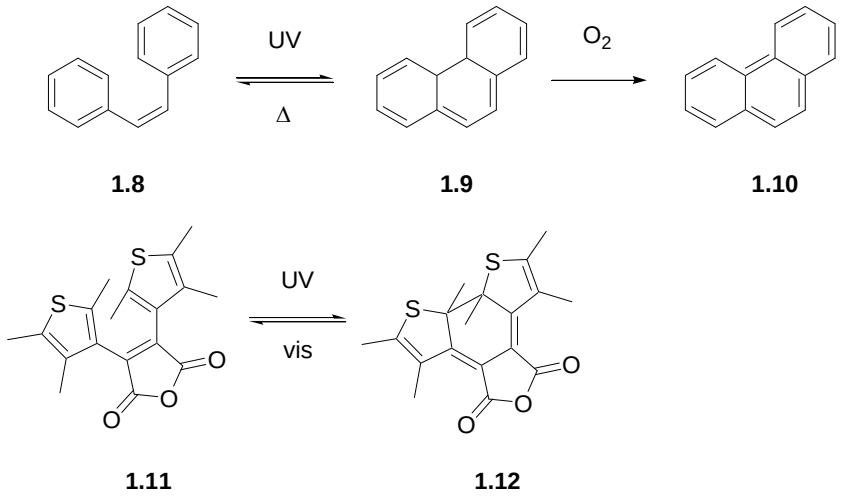

Fig. 1.4. Photoswitching of diarylethenes.

Fulgides are another class of photoisomerisable compounds that undergo a photochemical transition between an 'open' colourless form and a 'closed' coloured form,[11] such as compound **1.13**, which isomerises to **1.14** on UV irradiation (Fig. 1.5). The first fulgides discovered were unstable and thermally reversible due to reactions of the closed form. However, as for diarylethenes, modifications have improved the stability and photoswitching of these compounds.

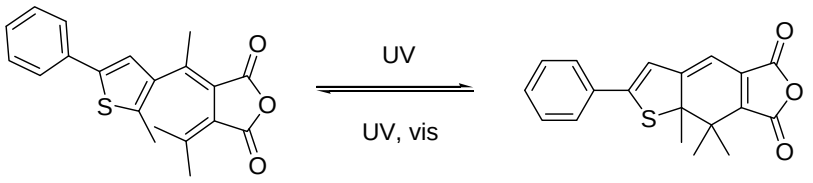

1.13 **1.14**

Fig. 1.5. Photoswitching of fulgides.

The most commonly studied photoswitch is azobenzene. Azobenzenes undergo photoswitching by a simple *E*/*Z* isomerisation, as shown in Fig. 1.6. *E*-Azobenzene **1.15** is the most stable form, but readily undergoes isomerisation to the *Z* isomer **1.16** on UV irradiation. The two isomers have markedly different properties, the major difference being the shape of the isomers. The *E* isomer is a planar molecule with extended π-conjugation through the aromatic structure, whereas the *Z* isomer is a distorted non-planar structure, as steric repulsion between *ortho* hydrogen atoms on the two phenyl rings cause the rings to rotate out of the C-N=N-C plane.[12] Due to these differences in shape, the isomers have different electronic and physical properties. In general the *Z* isomer is more polar than the *E* isomer,[13] which can be observed, for example, by the separation of the isomers on a chromatography column.[14] The measured dipole moments for the isomers are 3.0 D for *Z*-azobenzene and zero for the *E* isomer.[15]

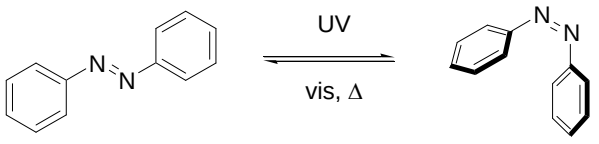

1.15 **1.16**

Fig. 1.6. Photoswitching of azobenzene.

The UV/vis spectra the isomers of azobenzenes are very different (see Fig. 1.7). The *E* isomer has a strong UV absorption band at approximately 300-350 nm and a weaker visible absorption band at approximately 400-500 nm, which causes azobenzenes to have a distinctive red/orange colour. The *Z* isomer lacks the strong UV band, but has a visible absorption band, similar to the *E* isomer. Irradiation of the *E* isomer by wavelengths within its UV absorption band causes a $\pi \rightarrow \pi^*$ transition to an excited state.[16] This excited state is flexible to structural change by an inversion or rotation mechanism[17] and thus can relax to either the *E* or *Z* isomer. Relaxation is most likely to give the more stable *E* isomer, but any *E* isomer formed can then be excited by further irradiation, while any *Z* isomer formed is less likely to be excited by light of these wavelengths. Continuous irradiation of an azobenzene thus eventually leads to an equilibrium photostationary state (PSS) that is enriched in *Z* isomer, usually in the order of 60-90% *Z*. Irradiation by visible light excites both isomers, and since the excited state is most likely to relax to the more stable *E* isomer, visible irradiation gives a PSS of mainly *E* isomer, usually close to 80% *E*. In normal ambient lighting conditions (i.e. sunlight or indoor lighting) a PSS is obtained that is similar to that obtained by visible irradiation.[1, 5] The *Z* isomer is less thermally stable than the *E* isomer and in the absence of light isomerises to the *E* isomer at room temperature.

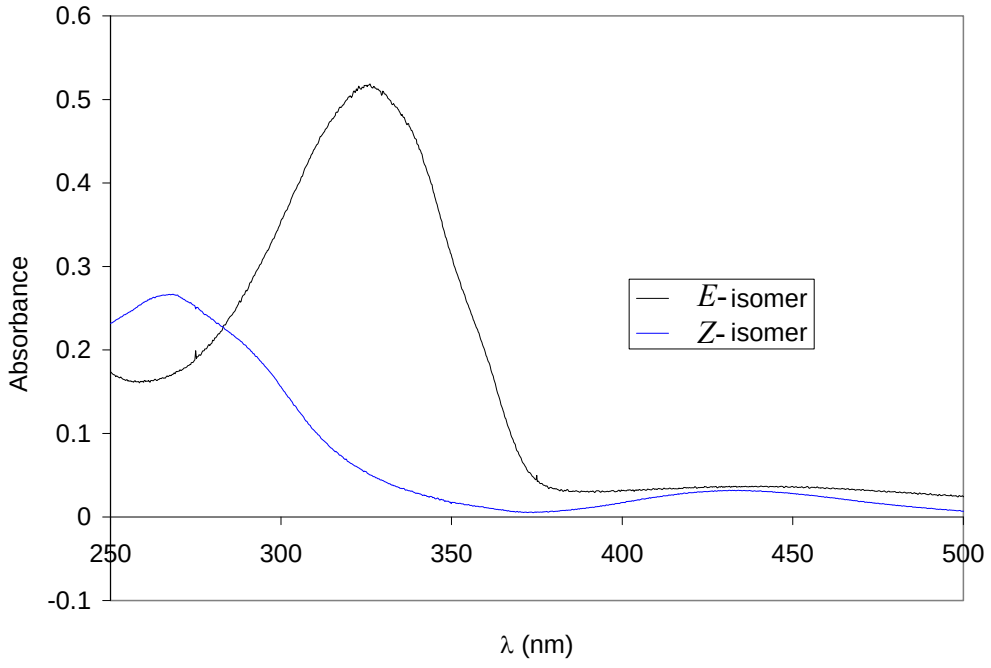

Fig. 1.7. UV/visible spectra of *E* and *Z* azobenzene.

As a photoswitch, azobenzene has several favourable properties: a large difference in shape between isomers, fast photoisomerisation with high quantum yield, no significant photodecomposition and relatively easy synthesis of derivatives. The drawbacks of azobenzene are the thermal instability of the *Z* isomer and the incomplete photoisomerisation that is usually obtained. Despite these problems, azobenzene is an effective photoswitch, especially in laboratory studies where complete switching and thermal stability are not necessarily required, and has been applied to a variety of photoswitching experiments, some of which will be discussed later in this chapter.

1.2.3 Biophotoswitching

One of the most interesting applications of photoswitching is photocontrol of biological systems. Important natural processes such as photosynthesis and vision involve photoreactions, and natural photoswitch proteins have been discovered.[18] In order to mimic these natural processes or to modify biological activity in new ways, it is of interest to incorporate photoswitches into biomolecules such as peptides[19] and proteins.[20] Alternatively, activity of biomolecules can be modulated using external photoswitches such as photoisomerisable enzyme inhibitors or polymers.[21] Most examples of biophotoswitching use azobenzene as photoswitch, as it is relatively easy to incorporate into biological systems.

A recent example of the modification of a biological structure to introduce photoswitching involved the cross linking of collagen with an azobenzene unit.[22] Collagen consists of three polypeptide chains in a triple helix structure. The azobenzene group was attached to these chains as a cross-linking clamp (Fig. 1.8) that was expected to disrupt the peptide structure in the *Z* form, but not affect the structure in the *E* form. As expected, a triple helix was formed from the *E*-azobenzene form of the modified collagen, then UV photoisomerisation to the *Z*-isomer disrupted the structure of the polypeptide chains, causing the helix to partially unfold. Subsequent visible photoisomerisation returned the structure to the triple helix form. As in many cases, the *E* to *Z* photoisomerisation did not proceed to completion, so only a small percentage of the collagen molecules unfolded.

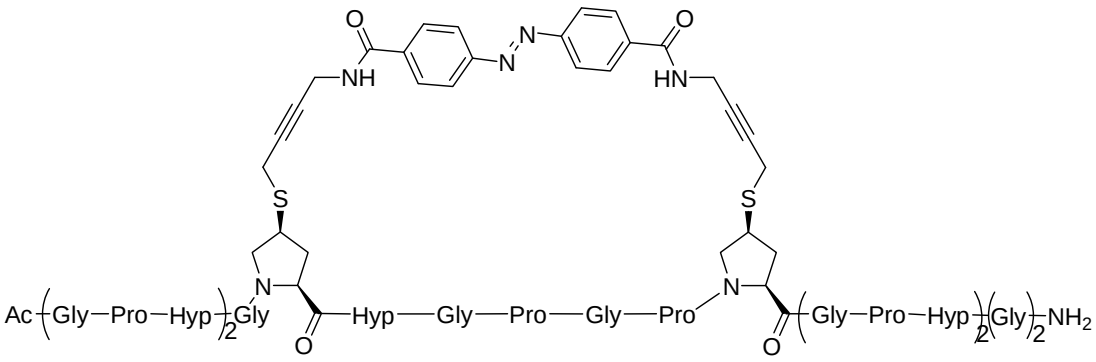

1.17

Fig. 1.8. An azobenzene modified collagen peptide for photoregulated helix folding and unfolding.[22]

Azobenzene photoisomerisation has been used to control enzyme activity in many studies, generally by incorporation of azobenzene into the enzyme or an inhibitor of the enzyme. The former approach has been performed, for example, by the covalent attachment of an azobenzene compound to the exterior lysine residues of papain.[23] Photoisomerisation of the modified enzyme led to 2.75 fold decrease in enzyme activity, presumably due to a change in the protein tertiary structure that affected the shape of the active site. A more ambitious variation on this approach involved the genetic modification of a bacteria to biosynthesise proteins containing a non-natural azobenzene amino acid.[20] Photoisomerisation of this bacteria modulated the biological activity of the modified protein. Recently, the thiooxopeptide bond has been used as an alternative photoswitch.[24] This group is nearly isosteric with a normal peptide bond but is easily photoisomerised between cis and trans forms. Replacement of a normal peptide bond in Ribonuclease S with a thiooxopeptide bond gave an enzyme which retained activity in its normal form, but became inactive on photoisomerisation.

The approach of most interest to our group is the incorporation of the azobenzene group into enzyme inhibitors. This indirect approach may lead to useful molecular devices and applications, such as those that this work begins to investigate. The first photoswitch enzyme inhibitor, 4-azophenyldiphenylcarbamyl chloride **1.18**[14] (Fig. 1.9), was developed in 1969, by modification of known irreversible α-chymotrypsin inhibitor diphenylcarbamyl chloride **1.19**. The *E* and *Z* isomers of **1.18** were isolated, assayed, and

photoisomerisation was studied. The *E* isomer was found to inactivate chymotrypsin 5 times faster than the *Z* isomer, and *in situ* photoisomerisation during an assay was found to change the rate accordingly.

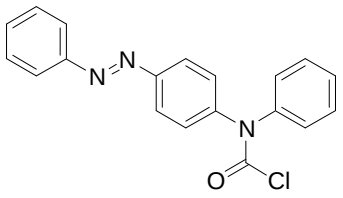

1.18

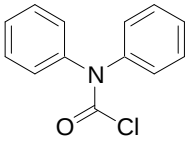

1.19

Fig. 1.9. Photoswitch α-chymotrypsin inhibitor **1.18**[14] and related inhibitor **1.19**.

Since this first example, a variety of photoswitch inhibitors for different enzymes have been developed. The approach used in development of **1.18** (modification of previously known inhibitors) led to the development of photoswitchable irreversible inhibitors for acetylcholine esterase[25] and photoswitchable substrates for trypsin.[26] Photoswitchable reversible inhibitors were later developed, such as those for papain and chymotrypsin[27] consisting of an azobenzene group linked to an aldehyde (**1.20**) and a boronic acid warhead[†] (**1.21**), respectively, as shown in Fig. 1.10. Both inhibitors showed a significant difference in activity between the *E* and *Z* forms. *In situ* photoisomerisation of the papain inhibitor gave a reversible 6 fold decrease in enzyme activity, while only a 13% decrease in activity was observed for the α-chymotrypsin inhibitor. This study was the initial basis for our group's work, which has mainly involved making systematic structural changes to increase the enzyme inhibition, photoswitching and practical use of photoswitch α-chymotrypsin inhibitors.

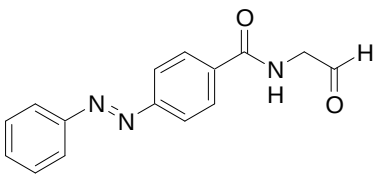

1.20

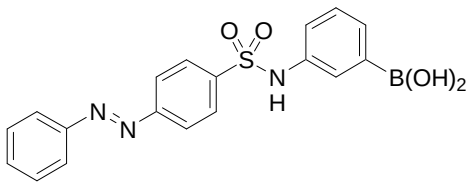

1.21

Fig. 1.10. Photoswitch reversible inhibitors of papain and α-chymotrypsin.[27]

[†] 'Warhead' in this context refers to an electrophilic group that is able to bind to the nucleophilic amino acid residue in the enzyme active site.

In a recent study, a photoswitch inhibitor of mitochondrial complex I was designed to mimic the structure of an effective known inhibitor in the *E* form (**1.22**, Fig. 1.11) and an ineffective known inhibitor in the *Z* form (**1.23**).[28] Despite containing two azobenzene groups, this compound isomerised remarkably well to the *Z*,*Z* form. An initial state of 100% *E*,*E* (obtained by thermal *Z* to *E* reaction in the dark) was isomerised to 95% *Z*,*Z* and 5% *E*,*Z* by UV irradiation. However, visible irradiation of the *Z*,*Z* isomer with visible light only returned 60% *E*,*E* isomer (and 35% *E*,*Z*, 5% *Z*,*Z*). This suggests that the *Z* isomer of these azobenzene groups has high stability, possibly due to hydrophobic interactions of the alkyl substituents. Photoisomerisation and enzyme assays showed that the *E*,*E* enriched state resulting from visible irradiation inhibited the enzyme twice as strongly as the *Z*,*Z* enriched state.

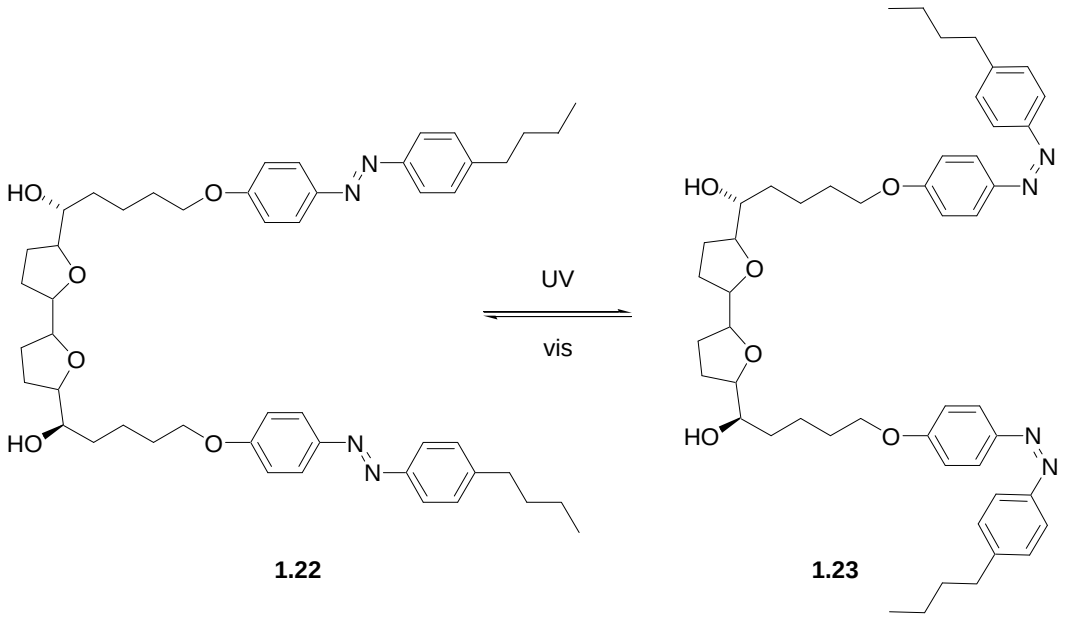

Fig. 1.11. Photoswitch inhibitor of mitochondrial complex I.[28]

1.3 Proteases

In this thesis, photoswitch inhibitors for the serine protease α-chymotrypsin were studied. This enzyme was chosen for study as it is a simple, well characterised enzyme that was expected to be relatively easy to work with, and because proteases are an important class of enzymes that are of much significance in modern medicinal chemistry.

Proteases are enzymes that catalyse the hydrolysis of amide bonds in peptides and proteins. They are involved in many important physiological processes such as digestion, growth, immune response and blood coagulation.[29, 30] As a result, proteases are also involved in a variety of diseases such as cancers, malaria and HIV. Inhibition of proteases has been found to be an effective treatment for some medical conditions. As such, protease inhibitors have been developed into useful drugs.[31, 32]

1.3.1 Serine proteases

α-Chymotrypsin belongs to the serine protease family, the most widely studied family of proteases. These enzymes cleave peptide bonds by the attack of an activated serine residue on the carbonyl group of the bond.[29] Serine proteases are usually classified into several major groups according to their substrate specificity. 'Chymotrypsin-like' serine proteases, the largest group, contain a deep hydrophobic pocket in the S_1 position (by the notation of Schechter and Berger[33]), which results in the enzymes specifically binding to substrates/inhibitors containing an aromatic group that can fit into this pocket, such as the side chains of the amino acids phenylalanine and tryptophan. Other types of serine protease require a positively charged or small hydrophobic group in this position.[30] As a result of these specificities, serine proteases cleave peptides in a position adjacent to a certain type of amino acid residue. α-Chymotrypsin is present in the pancreas and plays a role in digestion by cleaving peptides adjacent to aromatic amino acids.

The generally accepted mechanism of serine protease catalysed amide bond hydrolysis is as follows (Scheme 1.1):[29, 30] Starting from structure **1.24**, first the hydroxyl group of the Ser195 residue attacks the carbonyl group of the substrate amide bond. This step is aided by the 'catalytic triad' of the Ser195, His57, and Asp102 residues. The His57 residue acts as a base to deprotonate the Ser195 hydroxyl group and increase its nucleophilicity. The Asp102 residue hydrogen-bonds to His57, in order to orient it with the Ser195 hydroxyl and the substrate. After nucleophilic attack (structure **1.25**), the negatively charged oxygen atom of the substrate is stabilised by hydrogen bonding to the 'oxyanion hole' – the NH groups of the Ser195 and Gly193 residues. The next step is the cleavage of the C-N bond of the substrate with loss of an amine and the formation of an acyl-enzyme intermediate, shown in structure **1.26**. This step is aided by the His57 residue, this time

acting as an acid to protonate the amine and increase its leaving group ability. Next, a water molecule attacks the newly formed acyl group, activated by deprotonation by the His57 residue. Similar to the first attack, the oxyanion hole stabilises the negatively charged oxygen atom, and the His57 residue acts a base. The enzyme-substrate C-O bond is cleaved, and a carboxylic acid is formed. This is aided again by the His57 residue, acting as an acid to protonate the Ser195 hydroxyl group in order to improve its leaving group ability. The overall result of the reaction is the cleavage of the amide substrate into an amine and a carboxylic acid, with restoration of the enzyme catalyst, as shown in structure **1.27**.

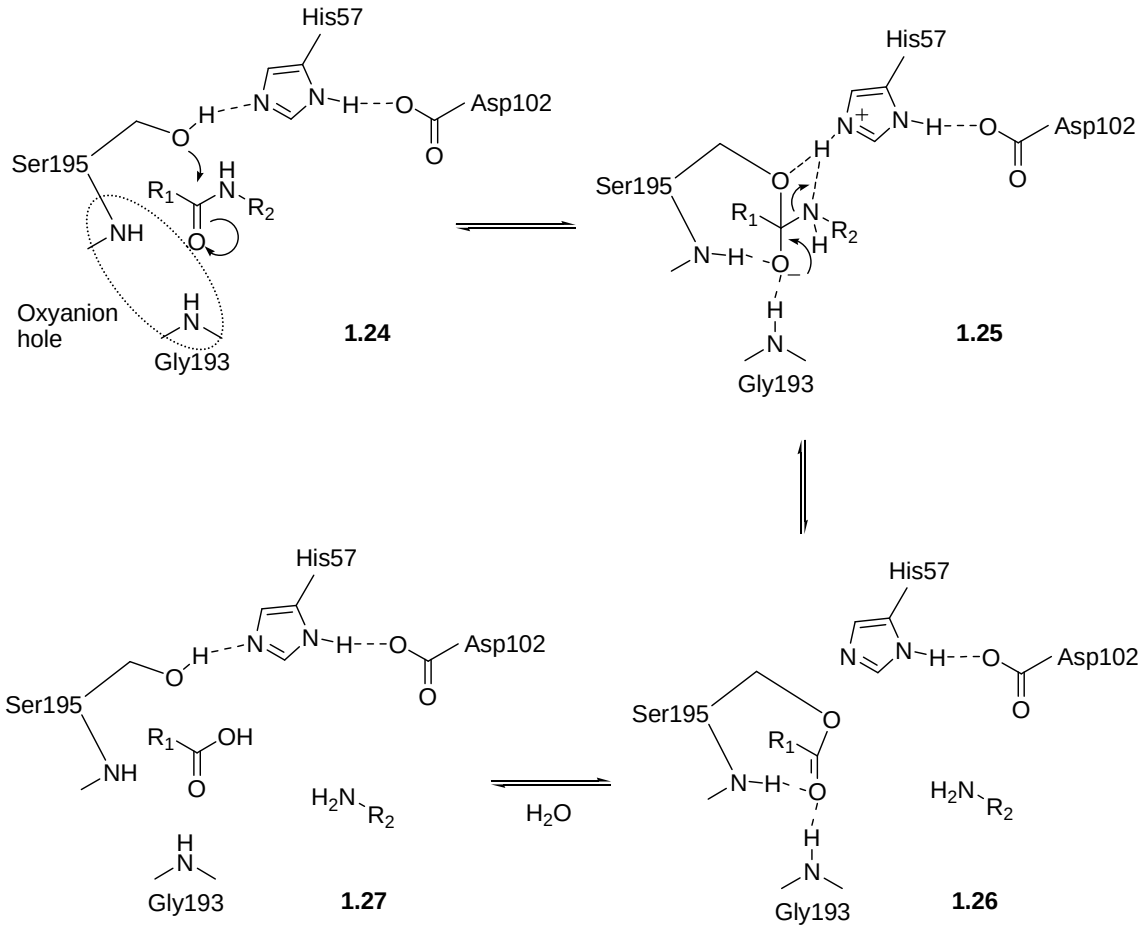

Scheme 1.1. Mechanism of chymotrypsin catalysed amide hydrolysis.

1.3.2 Reversible chymotrypsin inhibitors

The inhibition of α-chymotrypsin has been studied extensively, and a range of reversible and irreversible inhibitors have been designed. This project involves the study of reversible inhibitors only, so these will be the focus of this discussion.

Usually, there are two major components of reversible chymotrypsin inhibitors:

i) The 'warhead' group – This is an electrophilic group that covalently (but reversibly) binds to the highly nucleophilic Ser195 residue, in place of the amide bond of substrates that normally bind to the enzyme (see sections 1.3.3-1.3.5 for examples). While it is preferable not to use a warhead group due to potential selectivity and reactivity problems, the use of a warhead significantly improves enzyme binding affinity.

ii) The active site recognition domain – The remainder of the molecule is required to fit well into the active site, in particular the S_1 and S_2 subsites. This can be carried out by mimicking the structure of substrates that are known to be hydrolysed by α-chymotrypsin.

As mentioned above, α-chymotrypsin binds to substrates and inhibitors containing an aromatic group in the P_1 position. It also contains a large hydrophobic S_2 pocket, which preferentially binds large hydrophobic groups such as the side chains of the amino acids leucine and valine. Beyond the S_2 subsite, α-chymotrypsin has little selectivity,[29] although extended peptidic inhibitors containing four amino acids improve binding over compounds that bind only to the S_1 pocket,[34] possibly due to hydrogen bonding interactions.

There are several major types of reversible chymotrypsin inhibitors, including boronic acids, trifluoromethylketones and α-ketoesters. These, and an example of a group of effective non-warhead inhibitors, will be summarised in the following sections.

1.3.3 Boronic acid and boronate ester based inhibitors

Boronic acids are a class of compounds that are used extensively in synthetic organic chemistry;[35] however, they are also effective as electrophilic enzyme binding groups.

Boron groups are naturally electron deficient, as boron has three valence electrons and can normally form only three covalent bonds in a neutral state. As a result, these groups are electrophilic and can be attacked by nucleophiles such as the activated hydroxyl group of the α-chymotrypsin Ser195 residue. As such, an α-chymotrypsin inhibitor can be produced by combination of a boronic acid or boronate ester† and appropriate active site recognition groups.

The earliest boronic acid inhibitor of α-chymotrypsin was 2-phenylethaneboronic acid,[36] which inhibits α-chymotrypsin with a K_i of 40 μM. This compound is probably the simplest possible boronic acid inhibitor, containing only the boronic acid group and a phenyl group to bind to the S_1 subsite. It was proposed to bind well to the enzyme as it mimics of the transition state of substrate hydrolysis, as shown in Fig. 1.12. When the boron is covalently bound to the enzyme, it is thought that a hydroxyl group of the boronic acid hydrogen bonds to the oxyanion hole. This theory is supported by the crystal structure of the enzyme-inhibitor complex.[37]

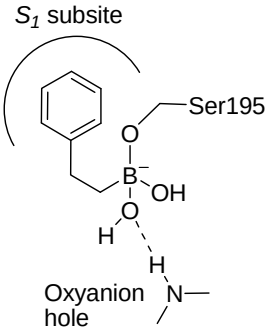

Fig. 1.12. Transition state inhibition by 2-phenylethaneboronic acid.[36]

Since report of this compound, more sophisticated boronic acid inhibitors have been developed. The compounds of most interest here are those designed by replacement of the carboxylic acid group of phenylalanine by a boronic acid. First synthesised by Matteson, these compounds are effective inhibitors of α-chymotrypsin, the simplest (**1.28,** Fig. 1.13) having a K_i of 2.1 μM.[38] Extension of this compound to short peptides such as **1.29** was carried out to obtain more potent inhibitors,[34] the best having a K_i of 3.4 nM due to more

† Boronic acids are compounds of the formula $RB(OH)_2$, where R is any group. Boronate esters are compounds of the formula RBOR′OR″, where R is any group, R′ and R″ are alkyl groups.

effective binding to the extended active site domain. Other work has produced boronic acid analogues of other amino acids, to inhibit different proteases.[31]

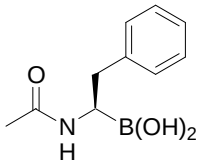

1.28

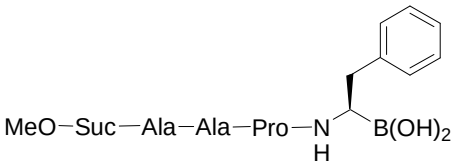

1.29

Fig. 1.13. Peptidomimetic boronic acid inhibitors of α-chymotrypsin.[34, 38]

Boronate esters are a protected form of boronic acids, and in many cases inhibit proteases with similar inhibition constants to the corresponding boronic acids.[34, 39] These compounds were studied in this project, because it was expected that they might be more stable and easier to synthesise than boronic acids and inhibitors containing electrophilic ketone groups.

1.3.4 Trifluoromethylketone based inhibitors

Similar to boronic acids, trifluoromethylketones are electrophilic compounds that can form reversible covalent bonds to the α-chymotrypsin Ser195 hydroxyl, as shown in Fig. 1.14. α-Fluorinated ketones are highly electrophilic due to the electron withdrawing effect of the electronegative fluorine atoms. As such, they are effective protease inhibitiors. Various mono-, di-, and tri- fluorinated ketones have been synthesised and assayed.[6, 40, 41] As would be expected, trifluoromethylketones are the most active of these fluorinated ketones, due to the greater electron withdrawing effect imparted by a larger number of fluorine atoms. On the other hand, α-difluorinated ketones are of interest as they can be extended in the *S′* direction to improve enzyme binding. This approach has been used to produce very potent α-chymotrypsin inhibitors.[41] Trifluoromethylketones containing the azobenzene group have been found to be effective photoswitch inhibitors of α-chymotrypsin.[5]

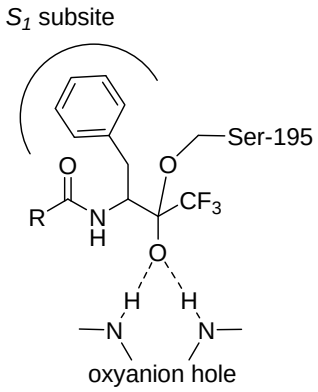

Fig. 1.14. Transition state inhibition by peptidyl trifluoromethylketones.

1.3.5 α-Ketoester based inhibitors

α-Ketoesters bind to serine proteases in a similar manner to trifluoromethylketones, as the electron withdrawing ester group increases the electrophilicity of the ketone. These compounds have been found to exhibit very potent inhibition of α-chymotrypsin. For example, compound **1.30** (Fig. 1.15) has a K_i of 150 nM.[4]

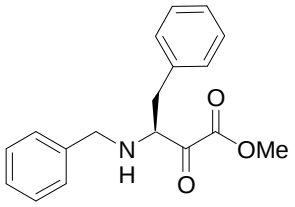

1.30

Fig. 1.15. α-Ketoester α-chymotrypsin inhibitor.[4]

A range of α-ketoesters containing the azobenzene group have been found to be effective photoswitch inhibitors of α-chymotrypsin.[1-3]

1.3.6 Non-covalent inhibitors

Inhibitors containing an electrophilic warhead group can often bind to a range of similar enzymes and other biomolecules, reducing specificity and biostability. Consequently, it is preferable to develop non-covalent inhibitors lacking an electrophilic group. α-Chymotrypsin accepts a range of peptide substrates with specificity primarily relying on

interaction with the S_1 subsite. This creates difficulties in the design of non-covalent inhibitors; however, important exceptions have been reported using a *D*-Leu, *L*-Phe, benzylamine sequence.[42] These peptides bind to chymotrypsin in an unusual inhibitory conformation, with the *D*-Leu and *L*-Phe side chains both placed in the large S_2 subsite and the benzylamine group in the narrow hydrophobic S_1 pocket, as shown in Fig. 1.16. This binding is proposed to be stabilised by hydrophobic interactions between the *D*-Leu and *L*-Phe side chains, and is observed in the crystal structure of the enzyme-inhibitor complex.[43]

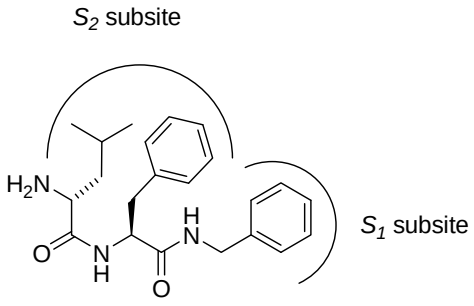

Fig. 1.16 Binding of a non-covalent inhibitor to the chymotrypsin active site.[42]

We envisaged that the benzylamine group of this inhibitor could be replaced by an azobenzene to create a simple photoswitch inhibitor.

1.4 Surface modification for development of functional surfaces

In this thesis, photoswitch inhibitors of α-chymotrypsin were attached to surfaces to generate functional surfaces for photoregulated enzyme binding. The attachment of organic molecules to surfaces is currently an important area of research with potential applications in areas such as sensor science, medicine, and the development of nanoscale devices. As a result, the modification of a variety of surfaces has been studied, in particular carbon,[44, 45] silicon,[46, 47] and gold.[48, 49] Gold surfaces have received the most attention in studies of biological interactions and the development of complex molecular devices. This is due to the relative ease of attachment of a variety of compounds to SAMs on gold, and the use of techniques such as SPR that can be used to monitor interactions of molecules at gold surfaces.

1.4.1 Modification of gold surfaces

The formation of SAMs of alkyl thiols/disulfides on gold was chosen for use in this project for surface attachment of photoswitch enzyme inhibitors. SAMs have been extensively studied and excellent reviews are available,[50] so only aspects most relevant to the work in this thesis are reviewed here. SAMs spontaneously form on immersion of a gold surface in a solution of an alkyl thiol or disulfide, and are relatively stable and ordered structures due to:

a) The covalent bond that is formed between sulfur and gold atoms.[51]

b) Hydrophobic interactions between alkyl groups. These groups are found to pack together, standing upright on an angle of 20-30º from perpendicular to the surface (Fig. 1.17).[52] This well ordered structure requires a long alkyl chain; short chains (less than 9 methylene groups) tend to form less ordered assemblies.

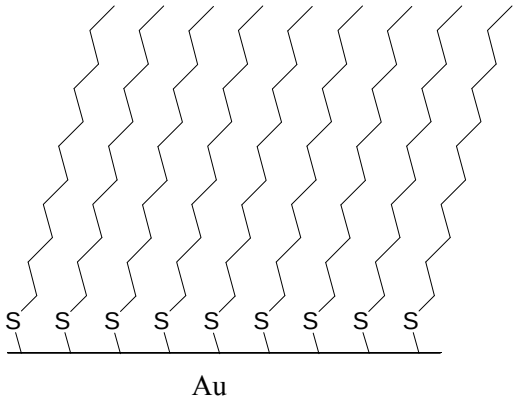

Fig. 1.17. Structure of an alkyl thiol SAM on a gold surface.

As these SAMs are densely packed and ordered such that the thiol 'head' group is bound to the gold, the 'tail' end of the alkyl chain is presented at the surface of the SAM. The properties of the tail group thus have a large impact on the character of the modified surface. However, this group generally has little impact on the formation or stability of the SAM unless sterically bulky and therefore is able to be freely derivatised to modify the properties of the surface.

An example of a surface property that can be controlled through the use of SAMs is wettability. Alkyl thiols with a range of tail groups have been used to form surfaces of varying hydrophilicities.[53] Surface hydrophilicity is measured using contact angles, the angles that droplets of water (or other liquids) make at a surface (see Fig. 1.18). Small water contact angles (<50º) are obtained on hydrophilic surfaces, as the droplets spread out to maximise contact with the surface. Very hydrophobic surfaces give high contact angles (>100º), as the water droplets bead on the surface to minimise contact with the surface. SAMs with hydrophobic tail groups such as CH_3 and CF_3 give very high contact angles, whereas hydrophilic tail groups such as OH and $CONH_2$ give low contact angles. Modification of this type is of interest for the development of highly water resistant surfaces (hydrophobic), and surfaces that resist adsorption of biomolecules (hydrophilic).

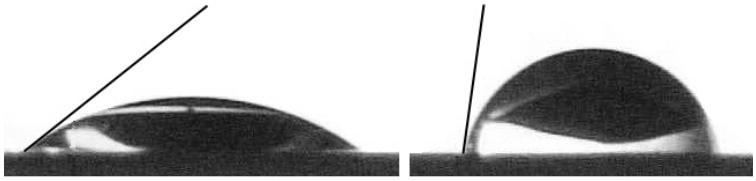

Fig. 1.18. Contact angles: low at hydrophilic surfaces (left) and high at hydrophobic surfaces (right).

In order to produce SAMs presenting complex structures at the surface, molecules can be linked to the tail groups of alkyl thiols. There are two general approaches used:

a) Synthesis of a thiol with the complex structure attached to the alkyl group. This approach has the advantage that the desired SAM can be directly formed from this thiol; the disadvantage is that it can be synthetically challenging. This approach has been used for a variety of systems such as the surface attachment of ferrocenes[54] and calixarenes.[55]

b) Formation of a SAM containing a reactive linker tail group, followed by attachment of the complex structure to this SAM. This approach is potentially more versatile; however, carrying out a reaction at a surface can be difficult due to steric crowding and the difficulties of establishing the yield and identity of products. Several linker groups have been used for this approach, including carboxylic acids,[56] biotin,[57] and azides/alkynes.[58]

In this thesis, both approaches were used to attach photoswitch enzyme inhibitors to surfaces.

1.4.2 Photoswitching at surfaces

The final goal of this thesis was to achieve photoswitching of azobenzene-containing inhibitors at a surface. Photoisomerisation of surface modifiers has been extensively studied; however, most previous studies used simpler systems designed for optical information storage or control of the physical properties of the surface.

SAMs of azobenzene-containing alkyl thiols on gold have been studied. In many of these studies the azobenzene group was used for structural studies only and photoisomerisation was not attempted.[59-61] These structural studies generally found that the azobenzene groups tend to pack tightly together in SAMs in a similar way to alkyl chains, as shown in Fig. 1.19, structure **1.31**. This suggests that photoisomerisation would be difficult in these type of SAMs, as there is little free space for the isomerisation. A detailed study of photoswitching in densely packed azobenzene SAMs using UV/vis and electrochemistry found that only a small proportion of the azobenzene groups was isomerised by UV irradiation.[62] In other studies, successful photoisomerisation was obtained by increasing the free volume in the SAM using asymmetrical disulfides.[63, 64] These disulfides contain two different alkyl chains, one containing an azobenzene group. SAMs formed from these compounds contain space for the azobenzene isomerisation, as shown in structure **1.32**. Photoisomerisation has been obtained more easily on silicon surfaces,[65] which are presumably less densely packed than SAMs on gold. In one example, light was used to switch an azobenzene-modified surface between hydrophilic (contact angle <5º) and super hydrophobic (contact angle 153º).[66]

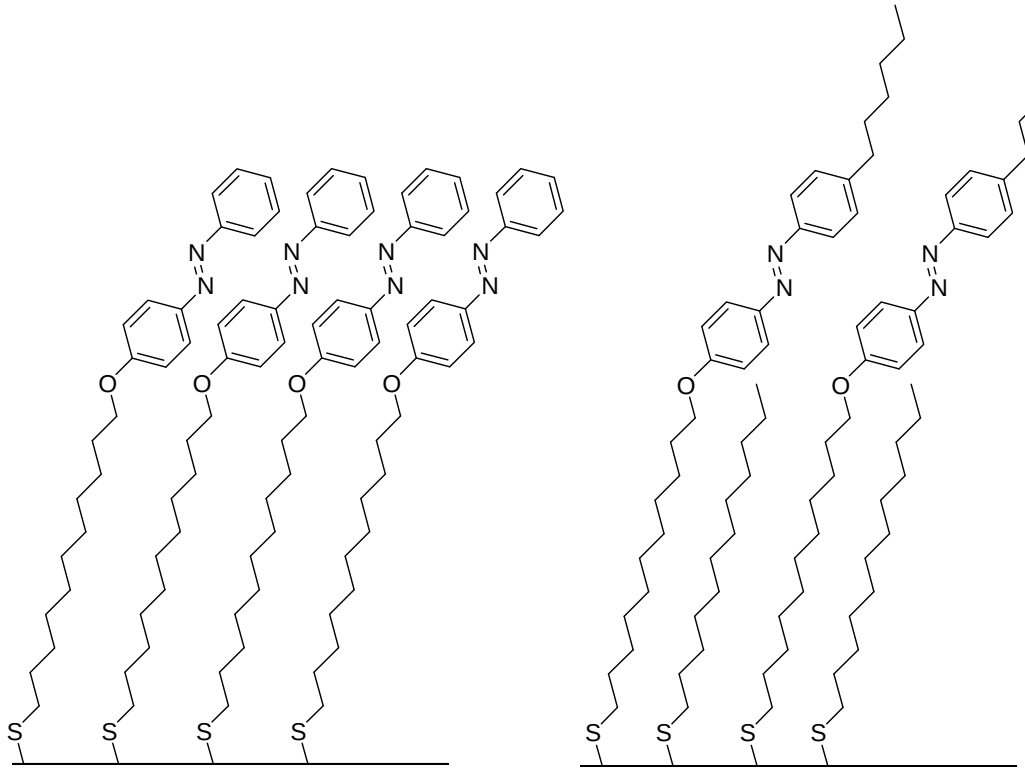

1.31 **1.32**

Fig. 1.19. Comparison of structures of azobenzene SAMs formed from a thiol (**1.31**) and an asymmetrical disulfide after cleavage of the disulfide bond (**1.32**)

Some work has been carried out towards more complex photoisomerisable surfaces. For example, a light controlled molecular shuttle has been developed.[67] This system contains a surface-attached rotaxane-like structure, similar to the pH switching shuttle mentioned previously in section 1.3. The 'ring' of the rotaxane, a cyclodextrin molecule, is associated with the azobenzene group as the *E* isomer and moves to a different location on *E* to *Z* photoisomerisation.

1.4.3 Studies of biological interactions at surfaces using SPR and QCM

The recently developed SPR and QCM technologies were used in this thesis for the detection of enzyme binding to photoswitch surfaces. These methods allow direct label-free monitoring of the binding of biomolecules to surfaces, and are currently of much interest for use in advanced biological assays.

SPR detects binding of molecules to a surface by monitoring changes in the absorption of light at a gold surface.[68] A light beam is directed at the underside of a surface consisting of a gold layer on a glass substrate, as shown in Fig. 1.20, and an electrical field (the evanescent wave) is formed at the interface between the glass and the gold. This field interacts with the gold surface by the excitation of surface plasmons, leading to absorption of the incident light. A solution is flowed over the gold surface, and the absorbance is measured at a range of incident angles, θ. The angle of maximum absorbance (the resonance angle) is dependent on the refractive index of the interface between the gold and the solution, which is in turn dependent on the properties of the gold surface. When molecules attach to the surface, the resonance angle changes. Monitoring the resonance angle thus allows detection of surface binding events. SPR is relatively easy to use in study of biomolecular interactions, partly due to the commercial availability of surfaces with a dextran polymer layer attached to the gold. This polymer layer contains carboxylic acid groups for binding of biomolecules and resists non-specific protein adsorption.[69]

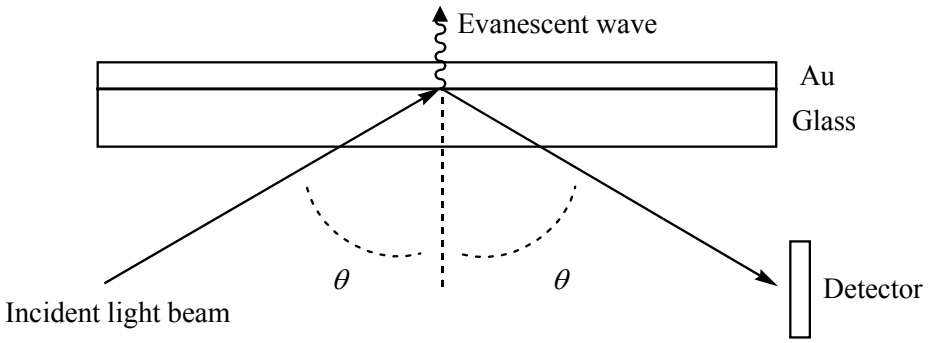

Fig. 1.20. Surface plasmon resonance apparatus involving the reflection of a light beam from a gold/glass surface interface.

QCM utilises the piezoelectric effect of AT-cut quartz crystals.[70] When an alternating current is applied to such a crystal, it vibrates. The resonance frequency of this vibration depends on the mass of the crystal, so changes in the mass of the crystal can be detected by changes in the resonance frequency. Very small mass changes in the order of ng cm^{-2} can be detected in this way, which allows attachment of molecules to the surface of the crystal to be studied. The Sauerbrey equation[71, 72] can be used to calculate the mass change from the observed frequency change:

$$\Delta f = \frac{-2\Delta m f_0^2}{A\sqrt{\rho_q \mu_q}} = -\frac{2 f_0^2}{A\sqrt{\rho_q \mu_q}} \Delta m$$

Where Δf is the change in frequency, Δm is the change in mass, and f_0, A, ρ_q, μ_q, and υ_q are constants. While this equation is not strictly correct for non-rigid surfaces such as a layer of enzyme, it was considered sufficiently accurate for the mass changes studied in this work. Commercially available crystals for use in QCM usually have a layer of gold on the surface for formation of SAMs. QCM has been used in some studies of biological interactions.[73, 74]

Studies of enzyme binding to SAMs have been carried out using SPR. A simple example involved monitoring of non-specific protein adsorption to surfaces.[68, 75] Non-specific binding occurs when proteins in aqueous solutions come into contact with hydrophobic surfaces. As the interior of proteins is hydrophobic, proteins can denature and spread out on surfaces to maximise hydrophobic interactions. These studies measured this binding to SAMs comprising of two components - an ethylene glycol compound known to block non-specific adsorption and a hydrophobic compound that was expected to promote non-specific adsorption. It was found that SAMs with a low proportion of small hydrophobic groups (CH_3) completely resist protein adsorption, whereas SAMs with a low proportion of large hydrophobic groups (CPh_3) only partially resist adsorption. As would be expected, larger amounts of non-specific adsorption were measured for SAMs with greater proportions of either hydrophobic group.

A more complex study involved measurement of specific enzyme binding to a SAM containing an enzyme inhibitor.[76] Mixed SAMs were formed using two components – a diluent thiol containing a triethylene glycol group to block non-specific binding and a thiol containing a known inhibitor of carbonic anhydrase, as shown in Fig. 1.21. The SAMs were able to selectively bind carbonic anhydrase from solution but effectively block non-specific adsorption of other proteins.

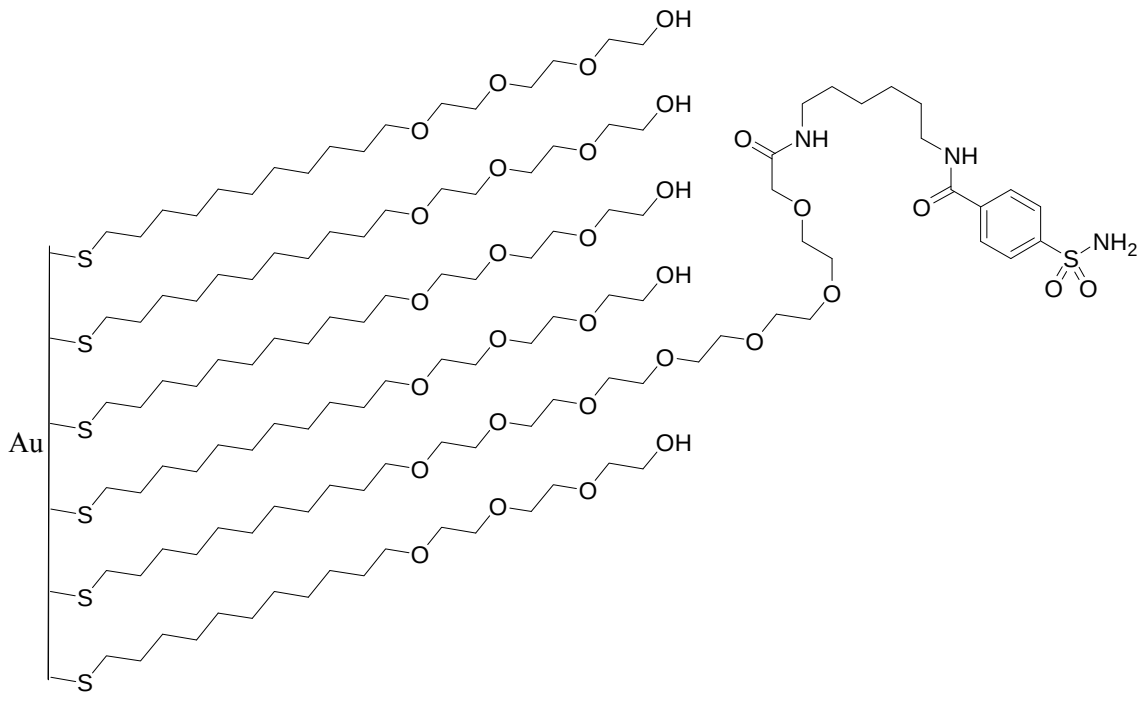

Fig. 1.21. A SAM for biospecific adsorption of carbonic anhydrase.[76]

Some studies of photoregulated binding of biomolecules to surfaces have been carried out. For example, an antibody sensor has been developed using the spiropyran photoswitch.[77] This system contains a spiropyran attached to a gold surface by a thiol linker, as shown in Fig. 1.22. The spiropyran was derivatised to bind anti-dinitrophenyl antibody, and can be converted between isomers **1.33** and **1.34** by UV/vis photoisomerisation. QCM and SPR analysis was used to monitor binding of the antibody to the surface-attached ligand. The antibody attaches to surface **1.33**, but can be washed off the surface after UV photoisomerisation to **1.34**. Visible irradiation returns the active form **1.33** and antibody again binds to the surface.

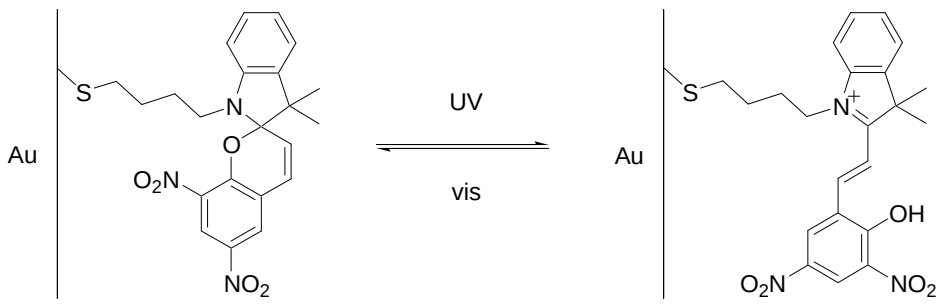

1.33 **1.34**

Fig. 1.22. A SAM for photocontrolled antibody binding.[77]

More recently, a study has reported photocontrolled cell binding to a surface using an azobenzene-containing integrin-binding peptide attached to a polymer surface.[78] The *E* isomer of this peptide binds to integrin, an enzyme which promotes cell growth to the surface. UV photoisomerisation to the *Z* isomer reduces the rate of cell growth to the same as that observed at an unmodified surface.

1.5 Work described in this thesis

The major goal of this thesis was to develop photoswitch protease inhibitors for attachment to surfaces, with a secondary goal being to improve knowledge of biological photoswitching.

This work was carried out to as a step towards the development of functional surfaces that bind and release a range of biomolecules in a controlled manner. Study of such surfaces may lead to the development of new technologies such as reversible biosensors, advanced medical implants and biomolecular computers. The initial development of these functional surfaces requires approaches for the controlled binding of families of biomolecules to surfaces. Towards this goal, a modular approach was developed here for photoregulated surface binding of the protease family of enzymes, initially targeting the serine protease α-chymotrypsin.

This approach involved the synthesis and surface attachment of photoswitch inhibitors containing an azobenzene photoswitch core with substituent surface linker and enzyme binding groups, as shown schematically in Fig. 1.23 below. Photoisomerisation of the photoswitch group then allows modulation of the enzyme binding properties of the surface. The modular system allows a variety of groups to be used as each of the three components, in order to evaluate the best for each function. Enzyme binding groups known to bind α-chymotrypsin were used in this thesis. Modification to target other proteases should be possible by use of alternative enzyme binding groups specific to these enzymes.

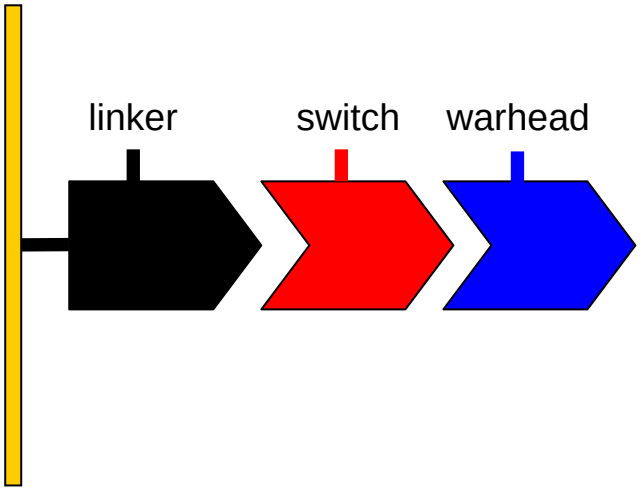

Fig. 1.23. Modular design of photoswitch inhibitors for surface attachment.

More specifically, the inhibitors developed in this thesis can be represented as compound **1.35**, Fig. 1.24. The 4-position of the azobenzene group contains an electrophilic enzyme binding warhead group W, and the 4′ position contains a surface linker group R.

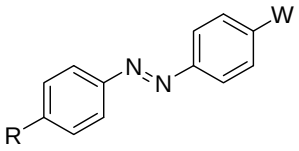

1.35

R = a group for surface attachment, W = an electrophilic enzyme binding warhead group.

Fig. 1.24. General structure of photoswitch inhibitors.

There were several major components of this work:

a) Synthesis of azobenzenes containing a range of electrophilic enzyme binding groups and a range of surface attachment groups. Boronic acids (chapter 2), trifluoromethylketones (chapter 4) and α-ketoesters (chapter 4) were studied as enzyme binding groups. Potential inhibitors lacking an electrophilic enzyme binding group were also synthesised (chapter 3). Primary amines and alkynes were studied as surface attachment groups.

b) Evaluation of the photoswitching and enzyme binding properties of the azobenzenes by photoisomerisation studies and enzyme assays (chapter 6).

c) Synthesis of alkyl disulfides for surface modification (chapter 5), surface attachment of the inhibitors, and photoregulated enzyme binding to the modified surfaces (chapter 7).

1.6 References

1. Harvey, A. J. PhD thesis. University of Canterbury, **2000**.
2. Harvey, A. J.; Abell, A. D., *Tetrahedron* **2000**, 56, (50), 9763.
3. Harvey, A. J.; Abell, A. D., *Bioorg. Med. Chem. Lett.* **2001**, 11, (18), 2441.
4. Angelastro, M. R.; Mehdi, S.; Burkhart, J. P.; Peet, N. P.; Bey, P., *J. Med. Chem.* **1990**, 33, 11.
5. Alexander, N. A. PhD thesis. University of Canterbury, **2006**.
6. Imperiali, B.; Abeles, R. H., *Biochemistry* **1986**, 25, 3760.
7. Ashton, P. R.; Ballardini, R.; Balzani, V.; Baxter, I.; Credi, A.; Fyfe, M. C. T.; Gandolfi, M. T.; Gomez-Lopez, M.; Martinez-Diaz, M.-V.; Piersanti, A.; Spencer, N.; Stoddart, J. F.; Venturi, M.; White, A. J. P.; Williams, D. J., *J. Am. Chem. Soc.* **1998**, 120, 11932.
8. Badjic, J. D.; Ronconi, C. M.; Stoddart, J. F.; Balzani, V.; Silvi, S.; Credi, A., *J. Am. Chem. Soc.* **2006**, 128, 1489.
9. Waldeck, D. H., *Chem. Rev.* **1991**, 91, 415.
10. Irie, M., *Chem. Rev.* **2000**, 100, 1685.
11. Yokoyama, Y., *Chem. Rev.* **2000**, 100, 1717.
12. Robertson, J. M., *J. Chem. Soc.* **1939**, 232.
13. Hartley, G. S., *J. Chem. Soc.* **1938**, 633.
14. Kaufman, H.; Vratsanos, S. M.; Erlanger, B. F., *Science* **1968**, 162, (861), 1487.
15. Hartley, G. S.; Le Fevre, R. J. W., *J. Chem. Soc.* **1939**, 531.
16. Griffiths, J., *Chem. Soc. Rev.* **1972**, 1, 481.
17. Asano, T.; Okada, T., *J. Org. Chem.* **1986**, 51, (23), 4454.
18. Fron, E.; Flors, C.; Schweitzer, G.; Habuchi, S.; Mizuno, H.; Ando, R.; Schryver, F. C. D.; Miyawaki, A.; Hofkens, J., *J. Am. Chem. Soc.* **2007**, 129, 4870.
19. Renner, C.; Moroder, L., *ChemBioChem* **2006**, 7, 868.

20. Bose, M.; Groff, D.; Xie, J.; Brustad, E.; Schultz, P. G., *J. Am. Chem. Soc.* **2006**, 128, 388.

21. Willner, I.; Rubin, S.; Shatzmiller, R.; Zor, T., *J. Am. Chem. Soc.* **1993**, 115, 8690.

22. Kusebauch, U.; Cadamuro, S. A.; Musiol, H.-J.; Lenz, M. O.; Wachtveitl, J.; Moroder, L.; Renner, C., *Angew. Chem. Int. Ed.* **2006**, 45, 7015.

23. Willner, I.; Rubin, S.; Riklin, A., *J. Am. Chem. Soc.* **1991**, 113, 3321.

24. Wildemann, D.; Schiene-Fischer, C.; Aumueller, T.; Bachmann, A.; Kiefhaber, T.; Luecke, C.; Fischer, G., *J. Am. Chem. Soc.* **2007**, 129, 4910.

25. Bieth, J.; Vratsanos, S. M.; Wassermann, N.; Erlanger, B. F., *Proc. Natl. Acad. Sci. U.S.A.* **1969**, 64, 1103.

26. Wainberg, M. A.; Erlanger, B. F., *Biochemistry* **1971**, 10, (21), 3816.

27. Westmark, P. R.; Kelly, J. P.; Smith, B. D., *J. Am. Chem. Soc.* **1993**, 115, 3416.

28. Fujita, D.; Murai, M.; Nishioka, T.; Miyoshi, H., *Biochemistry* **2006**, 45, 6581.

29. Hedstrom, L., *Chem. Rev.* **2002**, 102, 4501.

30. Leung, D.; Abbenante, G.; Fairlie, D. P., *J. Med. Chem.* **2000**, 43, (3), 305.

31. Adams, J.; Behnke, M.; Chen, S. W.; Cruickshank, A. A.; Dick, L. R.; Grenier, L.; Klunder, J. M.; Ma, Y. T.; Plamondon, L.; Stein, R. L., *Bioorg. Med. Chem. Lett.* **1998**, 8, 333.

32. Ghosh, A. K. In *Darunavir, a new protease inhibitor to combat drug-resistance: Structure-based design targeting protein backbone.*, Abstracts of Papers, 233rd ACS National Meeting, March 25-29, 2007.

33. Schechter, I. B., A., *Biochem. Biophys. Res. Commun.* **1967**, 27, 157.

34. Kettner, C. A.; Shenvi, A. B., *J. Biol Chem.* **1984**, 259, (24), 15106.

35. Littke, A. F.; Dai, C.; Fu, G. C., *J. Am. Chem. Soc.* **2000**, 122, 4020.

36. Koehler, K. A.; Lienhard, G. E., *Biochemistry* **1971**, 10, 2477.

37. Tulinsky, A.; Blevins, R. A., *J. Biol Chem.* **1987**, 262, (16), 7737.

38. Matteson, D. S.; Sadhu, K. M.; Lienhard, G. E., *J. Am. Chem. Soc.* **1981**, 103, 5241.

39. Weber, P. C.; Lee, S.-L.; Lewandowski, F. A.; Schadt, M. C.; Chang, C.-H.; Kettner, C. A., *Biochemistry* **1995**, 34, 3750.

40. Brady, K.; Abeles, R. H., *Biochemistry* **1990**, 29, 7608.

41. Imperiali, B.; Abeles, R. H., *Biochemistry* **1987**, 26, 4474.

42. Shimohigashi, Y.; Maeda, I.; Nose, T.; Ikesue, K.; Sakamoto, H.; Ogawa, T.; Ide, Y.; Kawahara, M.; Nezu, T.; Terada, Y.; Kawano, K.; Ohno, M., *J. Chem. Soc. Perkin Trans 1* **1996**, 2479.

43. Kashima, A.; Inoue, Y.; Sugio, S.; Maeda, I.; Nose, T.; Shimohigashi, Y., *Eur. J. Biochem.* **1998**, 255, (1), 12.

44. Allongue, P.; Delamar, M.; Desbat, B.; Fagebaume, O.; Hitmi, R.; Pinson, J.; Saveant, J.-M., *J. Am. Chem. Soc.* **1997**, 119, 201.

45. Brooksby, P. A.; Downard, A. J., *Langmuir* **2004**, 20, 5038.

46. Perring, M.; Dutta, S.; Arafat, S.; Mitchell, M.; Kenis, P. J. A.; Bowden, N. B., *Langmuir* **2005**, 21, 10537.

47. Sieval, A. B.; Linke, R.; Zuilhof, H.; Sudhoelter, E. J. R., *Adv. Mater.* **2000**, 12, (19), 1457.

48. Finklea, H. O.; Avery, S.; Lynch, M., *Langmuir* **1987**, 3, 409.

49. Nuzzo, R. G.; Allara, D. L., *J. Am. Chem. Soc.* **1983**, 105, 4481.

50. Ulman, A., *Chem. Rev.* **1996**, 96, 1533.

51. Langry, K. C.; Ratto, T. V.; Rudd, R. E.; McElfresh, M. W., *Langmuir* **2005**, 21, 12064.

52. Porter, M. D.; Bright, T. B.; Allara, D. L.; Chidsey, C. E. D., *J. Am. Chem. Soc.* **1987**, 109, 3559.

53. Sigal, G. B.; Mrksich, M.; Whitesides, G. M., *J. Am. Chem. Soc.* **1998**, 120, 3464.

54. Lee, L. Y. S.; Sutherland, T. C.; Rucareanu, S.; Lennox, R. B., *Langmuir* **2006**, 22, 4438.

55. Zhang, S.; Song, F.; Echegoyen, L., *Eur. J. Org. Chem.* **2004**, 2936.

56. Lahiri, J.; Isaacs, L.; Tien, J.; Whitesides, G. M., *Anal. Chem.* **1999**, 71, 777.

57. Riepl, M.; Enander, K.; Liedberg, B.; Schaeferling, M.; Kruschina, M.; Ortigao, F., *Langmuir* **2002**, 18, 7016.

58. Collman, J. P.; Devaraj, N. K.; Chidsey, C. E. D., *Langmuir* **2004**, 20, 1051.

59. Han, S. W.; Kim, C. H.; Hong, S. H.; Chung, Y. K.; Kim, K., *Langmuir* **1999**, 15, 1579.

60. Caldwell, W. B.; Campbell, D. J.; Chen, K.; Herr, B. R.; Mirkin, C. A.; Malik, A.; Durbin, M. K.; Dutta, P.; Huang, K. G., *J. Am. Chem. Soc.* **1995**, 117, 6071.

61. Yu, H.-Z.; Ye, S.; Zhang, H.-L.; Uosaki, K.; Liu, Z.-F., *Langmuir* **2000**, 16, 6948.

62. Wang, R.; Iyoda, T.; Jiang, L.; Tryk, D. A.; Hashimoto, K.; Fujishima, A., *J. Electroanal. Chem.* **1997**, 438, 213.

63. Sortino, S.; Petralia, S.; Conocib, S.; Bella, S. D., *J. Mater. Chem.* **2004**, 14, 811.

64. Tamada, K.; Akiyama, H.; Wei, T. X., *Langmuir* **2002**, 18, 5239.

65. Hamelmanna, F.; Heinzmanna, U.; Siemelingb, U.; Bretthauerb, F.; Brueggen, J. V. d., *App. Surf. Sci.* **2004**, 222, 1.

66. Lim, H. S.; Han, J. T.; Kwak, D.; Jin, M.; Cho, K., *J. Am. Chem. Soc.* **2006**, 128, 14458.

67. Willner, I.; Pardo-Yissar, V.; Katz, E.; Ranjit, K. T., *J. Electroanal. Chem.* **2001**, 497, 172.

68. Mrksich, M.; Sigal, G. B.; Whitesides, G. M., *Langmuir* **1995**, 11, 4383.

69. Loefas, S.; Johnsson, B., *J. Chem. Soc., Chem. Commun.* **1990**, 1526.

70. Buttry, D. A.; Ward, M. D., *Chem. Rev.* **1992**, 92, 1355.

71. Sauerbrey, G., *Phys. Verh.* **1957**, 8, 113.

72. Sauerbrey, G., *Z. Phys.* **1959**, 155, 206.

73. Baltus, R. E.; Carmon, K. S.; Luck, L. A., *Langmuir* **2007**, 23, 3880.

74. Höök, F.; Rodahl, M.; Kasemo, B.; Brzezinski, P., *Proc. Natl. Acad. Sci. USA* **1998**, 95, 12271.

75. Ostuni, E.; Grzybowski, B. A.; Mrksich, M.; Roberts, C. S.; Whitesides, G. M., *Langmuir* **2003**, 19, 1861.

76. Mrksich, M.; Grunwell, J. R.; Whitesides, G. M., *J. Am. Chem. Soc.* **1995**, 117, 12009.

77. Kaganer, E.; Pogreb, R.; Davidov, D.; Willner, I., *Langmuir* **1999**, 15, 3920.

78. Auernheimer, J.; Dahmen, C.; Hersel, U.; Bausch, A.; Kessler, H., *J. Am. Chem. Soc.* **2005**, 127, 16107.

Chapter Two

Synthesis of Boronate Esters

Synthesis of boronate esters

2.1 Introduction

The first major goal of this thesis was the development of photoswitch enzyme inhibitors for surface attachment. Azobenzene-containing boronate esters were initially prepared for this purpose. The boronate ester group (see chapter 1, section 1.3.3) was chosen due to its apparent ease of synthesis and thus potential for use in complex disubstituted azobenzenes for surface attachment. For example, the related azobenzene-containing boronic acid **1.21** (Fig. 2.1) exhibits photoregulated inhibition of α-chymotrypsin and was prepared in a relatively simple synthesis[1] compared to other reported photoswitch α-chymotrypsin inhibitors. Extension of this compound in the 4′-position of the azobenzene group was considered a simple method to obtain a photoswitch inhibitor for surface attachment.

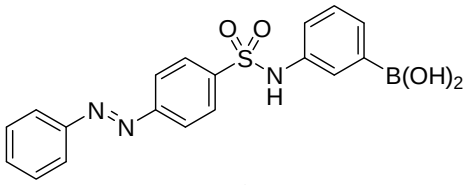

1.21

Fig. 2.1. Reported photoswitch inhibitor of α-chymotrypsin **1.21.**

This chapter describes the synthesis of a range of boronate esters **2.1**-**2.11** (figs. 2.2 and 2.3) designed to act as photoswitch inhibitors of α-chymotrypsin. These compounds contain the azobenzene photoswitch group and an enzyme binding group containing a boronate ester. The boronate esters **2.10**-**2.11** additionally contain a group for surface attachment. Compounds **2.1**-**2.9** lacking a surface attachment group were synthesised so that the best enzyme binding structures could be identified without the added complication of an additional substituent.

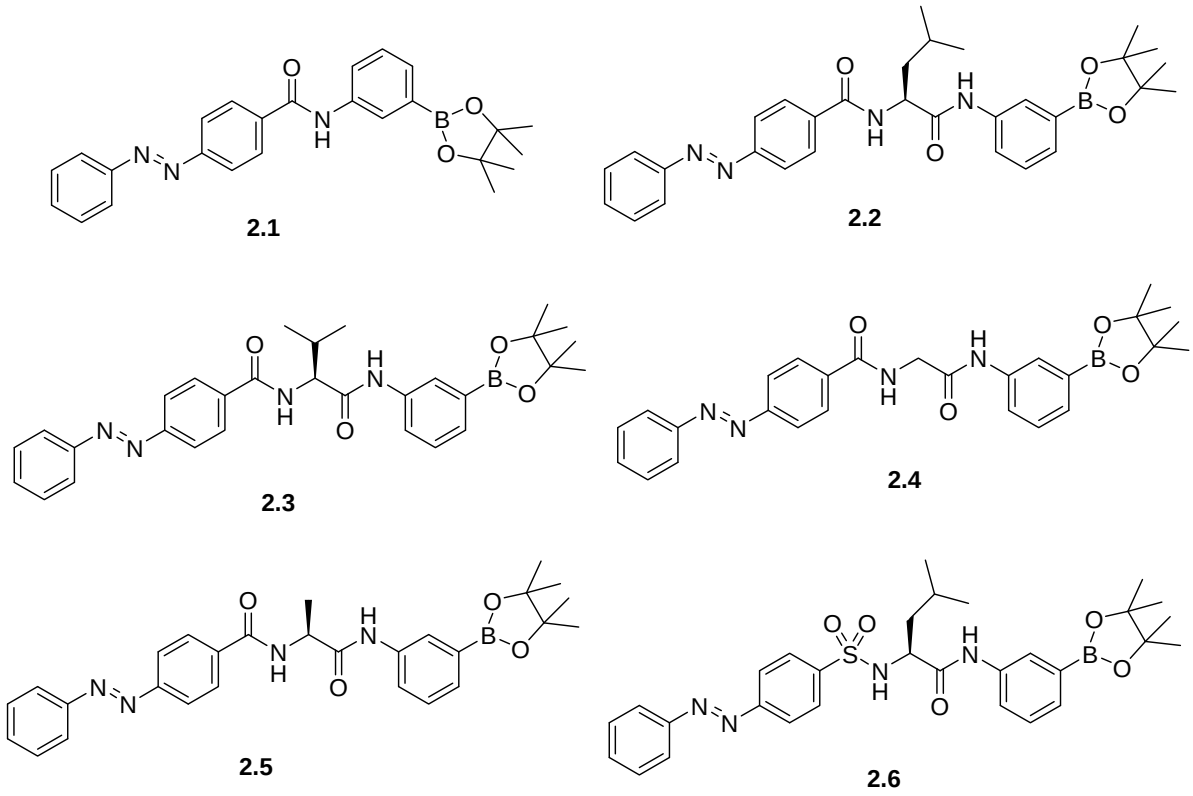

Fig. 2.2. Azobenzenes **2.1**-**2.6** containing aminophenylboronate ester for enzyme binding.

The aminophenylboronate compounds **2.1**-**2.6** are based on known photoswitch inhibitor **1.21**. The simplest, **2.1**, is structurally very similar to **1.21**, differing only in the replacement of the sulphonamide group by an amide and the use of a boronate ester rather than a boronic acid group. While sulfonamides are generally more stable than amides, they are comparatively difficult to introduce synthetically. The amide group was chosen as it is formed in a simple, versatile coupling reaction between an amine and a carboxylic acid. Synthetic versatility is highly important here, as more complex syntheses were required for the preparation of inhibitors for surface attachment, such as amine **2.11**. Derivatives **2.2**-**2.6** contain a hydrophobic amino acid adjacent to the aminophenylboronate group, designed to improve enzyme binding by targeting the S_2 subsite of the α-chymotrypsin active site. Assuming that the aminophenylboronate group binds to the S_1 subsite, this amino acid side chain should bind to the S_2 site, which is known to accommodate large hydrophobic groups.[2] Compounds **2.2**, **2.3** and **2.6** contain amino acids that are known to have affinity for the S_2 site (Val, Leu). A smaller hydrophobic amino acid was used in compounds **2.4** and **2.5** to partially fill the S_2 pocket so that free space remains in this pocket that might be filled by part of the azobenzene

group. Compound **2.6** contains a sulphonamide group in place of the amide group of analogue **2.2**, in order to compare the effects of these groups on enzyme binding and photoswitching.

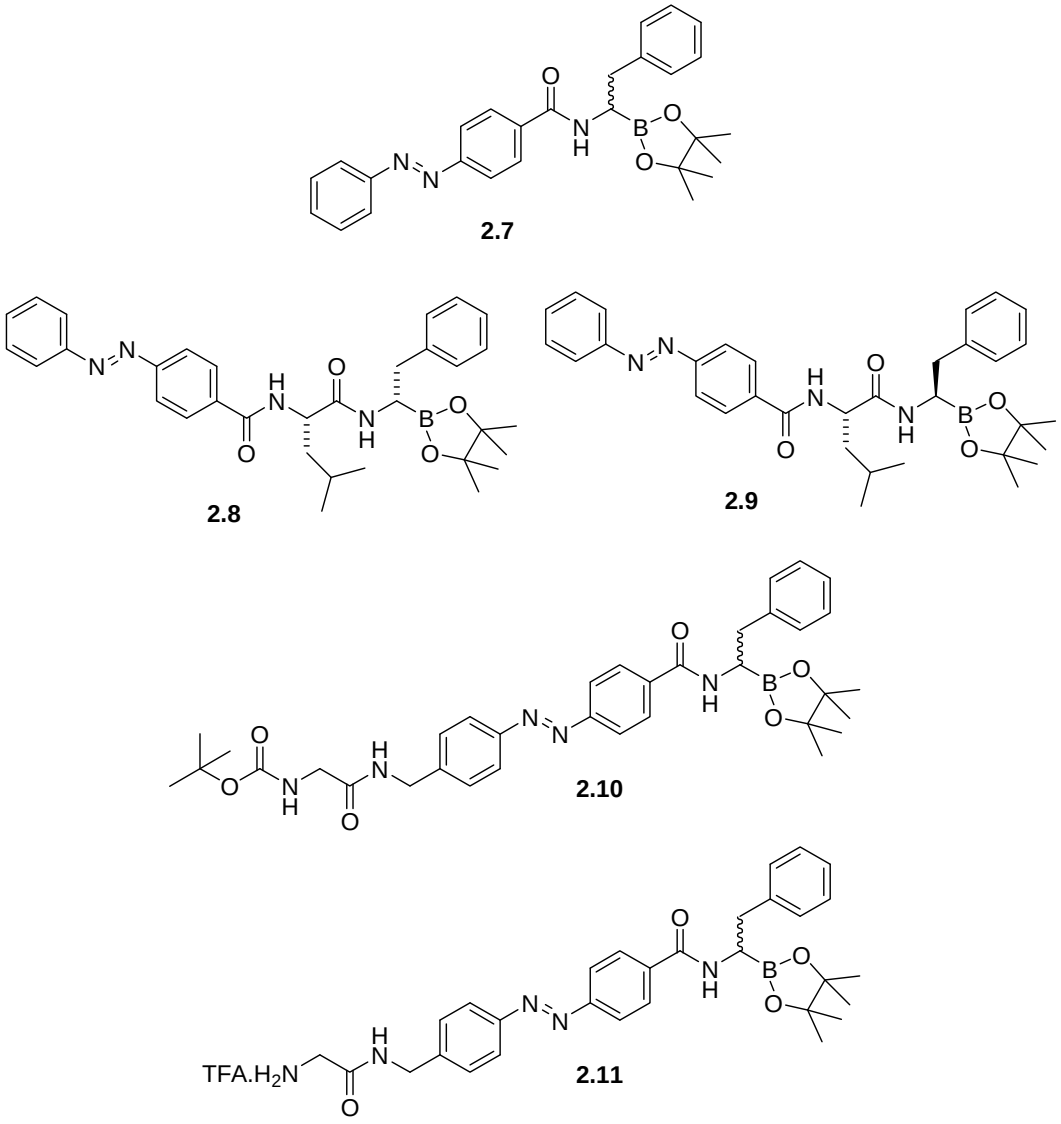

Fig. 2.3. Azobenzenes **2.7**-**2.11** containing borophenylalanine for enzyme binding.

Compounds **2.7**-**2.11** (Fig. 2.3) contain the peptidomimetic borophenylalanine group for enzyme binding. This group has been used successfully in inhibitors of α-chymotrypsin,[3, 4] as discussed in chapter 1, but has not previously been used in photoswitch inhibitors. Compounds **2.7**-**2.11** contain similar design features to the aminophenylboronate compounds. As previously, amide bonds are used to link the enzyme binding group to the azobenzene photoswitch, due to the synthetic versatility of the amide coupling reaction. The simplest analogue, **2.7**, contains borophenylalanine

directly attached to the azobenzene group. Derivatives **2.8** and **2.9** contain the amino acid leucine between these two groups to investigate the influence of an amino acid in the P_2 position, as above for compounds **2.2**-**2.6**. In this case, the chiral centre of the amino acid leads to the formation of two separable diastereomers instead of a racemic mixture of enantiomers. The azobenzenes **2.10** and **2.11** contain an amine group for surface attachment and a Gly residue to increase peptidic character for improved enzyme binding.

In addition, the synthesis of the previously reported α-chymotrypsin inhibitor **2.12**[4] (Fig. 2.4) for assay validation is described. This compound is an acetylated derivative of the borophenylalanine peptidomimetic group used in azobenzenes **2.7**-**2.11**.

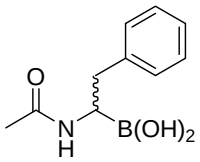

2.12

Fig. 2.4. Compound **2.12**, a reported inhibitor of α-chymotrypsin.

2.2 Synthesis of aminophenylboronate based compounds

*Synthesis of boronate ester **2.1***

The boronate ester **2.1** was prepared as shown in Scheme 2.1. Following a reported synthesis,[5] nitrosobenzene **2.13** was condensed with 4-aminobenzoic acid **2.14** in AcOH to give azobenzene **2.15** in 53% yield. The azobenzene **2.15** was then coupled to aminophenylboronate ester **2.16** in the presence of HATU to give **2.1** in 53% yield.

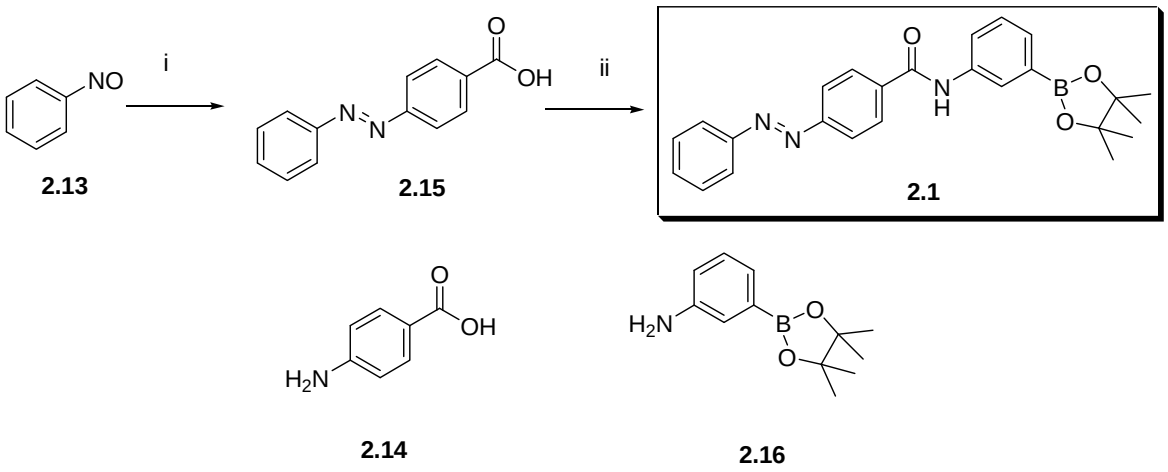

Reagents and conditions: i) **2.14**, AcOH, 53% ii) **2.16**, HATU, DIEA, DMF, 53%

Scheme 2.1. Synthesis of compound **2.1**.

*Synthesis of boronate esters **2.2-2.5***

The boronate esters **2.2**-**2.5** were prepared as shown in Scheme 2.2. First, azobenzene **2.15** was coupled to an amino acid methyl ester (glycine, alanine, valine or leucine) in the presence of HATU to give **2.17**-**2.20** in 85-96% yields. The esters were then deprotected by basic hydrolysis to give carboxylic acids **2.21**-**2.24**. Coupling of **2.21** to amine **2.16** in the presence of HATU was initially attempted, but a colour change from orange to black was observed on mixing of the reactants, and the desired product **2.2** could not be detected in a ^{1}H NMR spectrum of the reaction products after 16 h. However, coupling of amine **2.16** to carboxylic acids **2.21**-**2.24** in the presence of EDCI did give **2.2**-**2.5** in 32-43% yields.

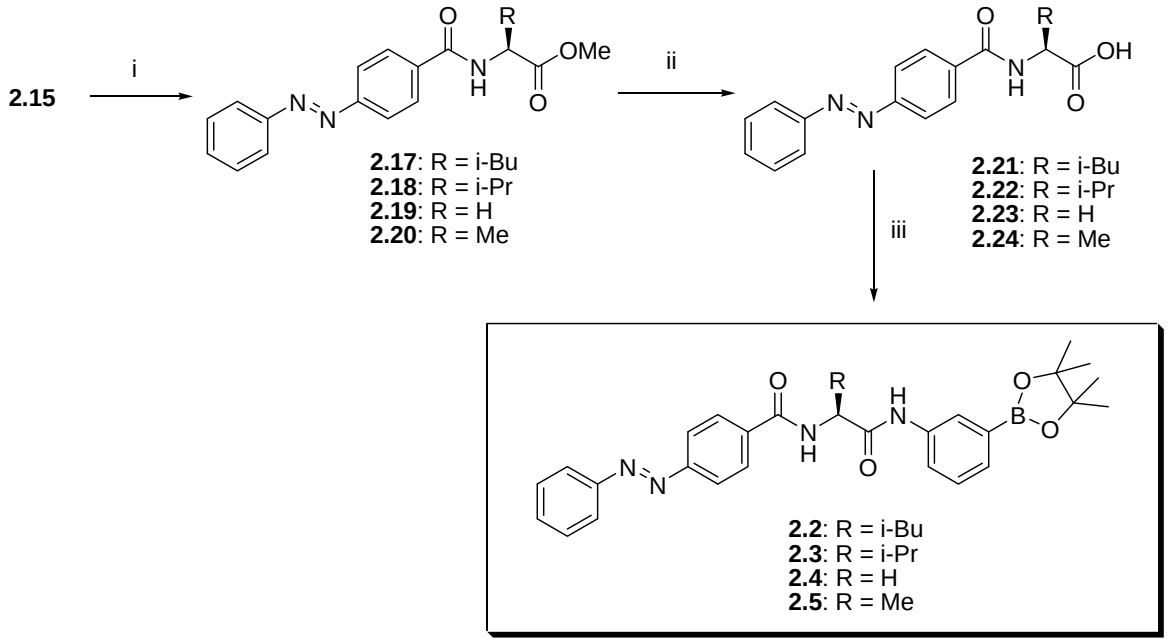

Reagents and conditions: i) Amino acid methyl ester, HATU, DIEA, DMF, 85-96% ii) LiOH, THF, H_2O, 63-100% iii) **2.16**, EDCI, HOBt, DCM, 32-43%

Scheme 2.2. Synthesis of compounds **2.2**-**2.5**.

*Synthesis of sulfonamide **2.6***

The boronate ester **2.6** was synthesised by a similar route, as shown in Scheme 2.3. Initially sulfonyl chloride **2.25**[6] (obtained from Nathan Alexander[7]) was coupled to H-Leu-OMe in the presence of base (DIEA) to give sulphonamide **2.26**. This compound was deprotected by basic hydrolysis with LiOH to give carboxylic acid **2.27**, which was then coupled to amine **2.16** in the presence of HATU to give **2.6**. Interestingly, the use of HATU in this reaction was successful, but caused problems in the synthesis of the close analogue **2.2**.

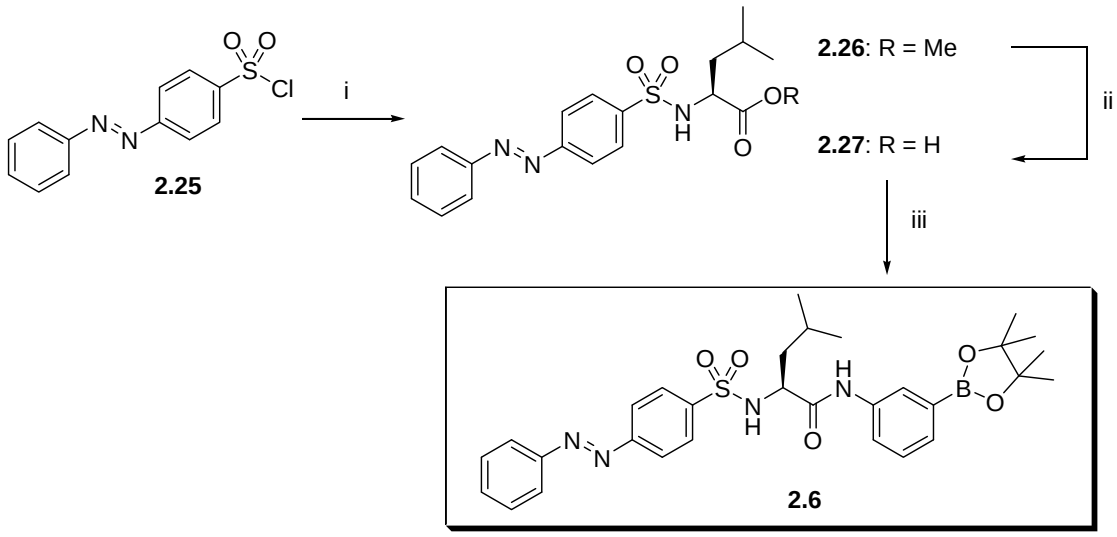

Reagents and conditions: i) H-Leu-OMe, DIEA, DCM, 91% ii) LiOH, THF, H_2O, 63% iii) **2.16**, HATU, DIEA, DMF, 28%.

Scheme 2.3. Synthesis of compound **2.6**.

2.3 Synthesis of borophenylalanine based compounds

*Synthesis of borophenylalanine precursor **2.33***

The synthesis of boronate esters **2.7**-**2.11** required borophenylalanine **2.33** as key precursor, which was synthesised following a reported route (Scheme 2.5).[3] Initially, benzyl chloride **2.28** was reacted with Mg in ether to form the Grignard reagent benzylmagnesium chloride. This reagent was added to trimethylborate to give a methyl boronate intermediate, which was hydrolysed by the addition of sulphuric acid to give boronic acid **2.29**. Next, **2.29** was stirred with pinacol in ether to give the boronate ester **2.30**. A 63% yield was obtained over these first two steps. The boronate ester was then reacted with dichloromethyllithium (formed in situ from DCM and LDA) to give chloride **2.31** as an impure (by TLC and ^{1}H NMR) brown oil. This material was reportedly purified by spinning band distillation, but this was not available. Fractional distillation using a packed column was attempted without success and column chromatography resulted in decomposition. Thus, the next reaction was attempted using crude **2.31**, with the intention of purifying after further reaction steps. The chloride **2.31** was reacted with LiHMDS to give protected amine **2.32**, which was detected in the reaction products by ^{1}H NMR, but again the crude material

could not be purified by distillation or column chromatography. Again a further step was carried out before purification. The crude amine **2.32** was treated with TFA to give borophenylalanine trifluoroacetate **2.33**. This compound precipitated from the reaction solution and was collected as a white solid, pure by ^{1}H NMR. An acceptable yield (19%) was obtained for these three steps.

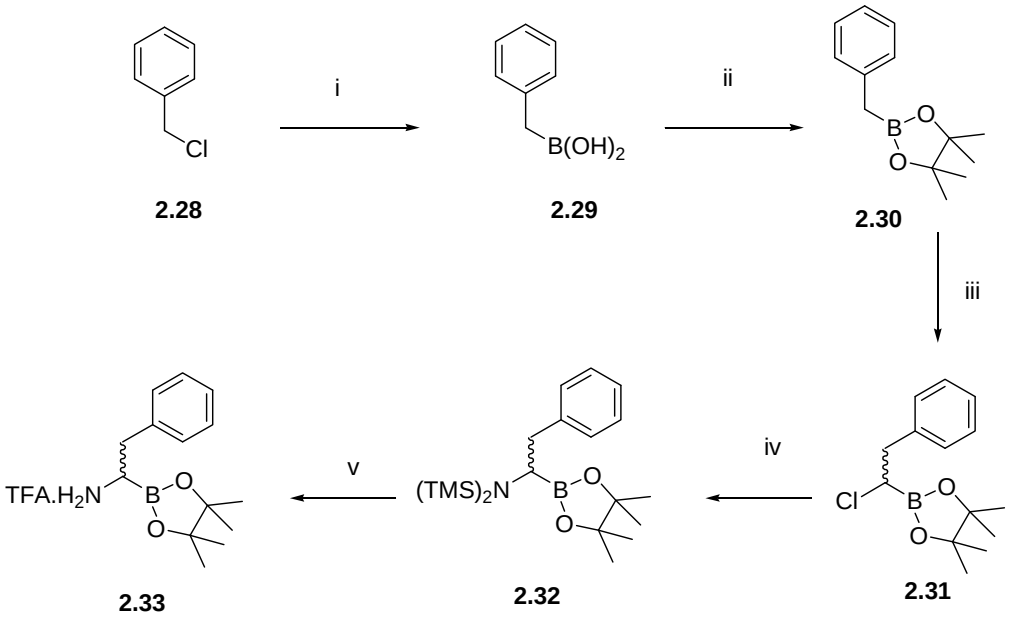

Reagents and conditions: i) 1. Mg, ether, 0ºC → r.t. 2. $B(OMe)_3$, -30ºC → r.t. 3. H_2SO_4 0ºC → r.t. ii) pinacol, ether, 63% over 2 steps iii) LDA, DME, DCM, -78ºC → r.t. iv) LiHMDS, THF, -78ºC → r.t. v) TFA, ether, 0ºC, 19% over 3 steps.

Scheme 2.5. Synthesis of borophenylalanine **2.33**.

*Synthesis of boronate ester **2.7***

The boronate ester **2.7** was prepared from precursor **2.33**, as shown in Scheme 2.6. Initially, coupling of carboxylic acid **2.15** and amine **2.33** in the presence of EDCI was attempted, but a mixture of compounds was formed from which **2.7** could not be identified by ^{1}H NMR. The reaction was repeated using BOP coupling reagent, but the same result was obtained. Finally, the mixed anhydride coupling method with isobutyl chloroformate was carried out to give **2.7** in 51% yield.

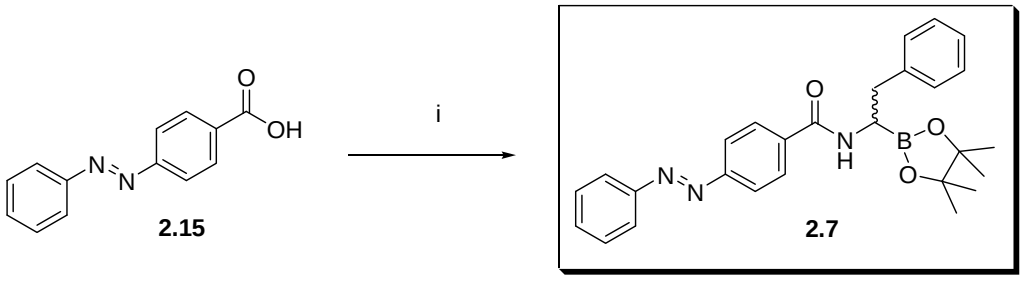

2.15 **2.7**

Reagents and conditions: **2.33**, i-BuOCOCl, NMM, THF, 51%

Scheme 2.6. Synthesis of boronate ester **2.7**.

While the mixed anhydride method is not often used in modern amide coupling reactions, good results have been previously reported in the synthesis of peptides containing borophenylalanine.[3] It is known that the free base form of amine **2.33** is unstable,[4] so it is likely that decomposition of this amine occurs during reaction with EDCI or BOP. However, in the mixed anhydride method, the carboxylic group is initially converted to an anhydride, then the amine is added to react with this activated intermediate. Presumably the unstable amine **2.33** is able to react rapidly with the intermediate before decomposition occurs.

*Synthesis of diastereomeric boronate esters **2.8** and **2.9***

The boronate esters **2.8** and **2.9** were synthesised as shown in Scheme 2.7. The carboxylic acid **2.21** was coupled to amine **2.33** using the mixed anhydride method to give diastereomers **2.8** and **2.9** in 76% combined yield. These compounds were separable by chromatography, but are partially unstable to silica gel. As such, poor recovery was obtained at each purification step. After several chromatography attempts using normal silica, satisfactory separation was obtained using deactivated silica (consisting of 30% H_2O and 70% silica). Each isomer was purified to 86% diastereomeric excess (de, measured by ^{1}H NMR), but with poor recovery (3% and 5%). The observed decomposition may involve cleavage of the boronate ester to form the free boronic acid, which would have eluted very slowly from the silica gel.

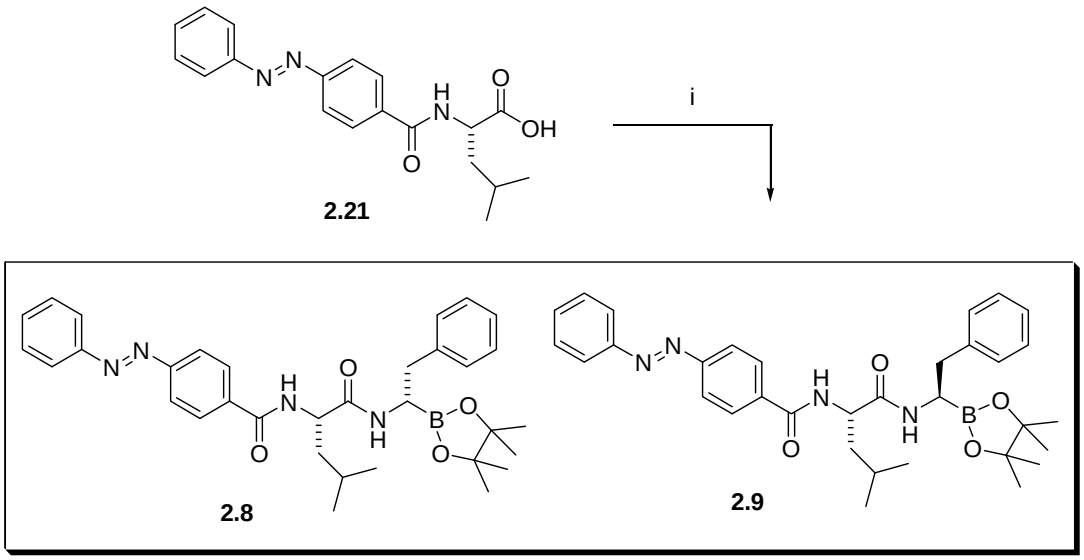

Reagents and conditions: i) **2.33**, iBuOCOCl, NMM, THF, 76% combined yield

Scheme 2.7. Synthesis of diastereomeric boronate esters **2.8** and **2.9**.

*Synthesis of boronate esters **2.10** and **2.11** for surface attachment*

The boronate esters **2.10** and **2.11** were synthesised by a more complex method, as shown in Scheme 2.8. Initially, the amine salt **2.34** was reacted with Fmoc-Cl to give protected amine **2.35**, which was then reduced to aniline **2.36** by catalytic hydrogenation with PtO_2 in 86% yield. Next, ethyl-4-aminobenzoate **2.37** was oxidised using catalyst $Mo(O_2)_2O(H_2O)HMPA$ and hydrogen peroxide to give nitrosobenzene **2.38**, which was condensed with aniline **2.36** in AcOH to give azobenzene **2.39**. This compound was treated with 20% piperidine in DMF to give deprotected amine **2.40**, which was then coupled to Boc-Gly-OH in the presence of HATU to give **2.41** in 88% yield (over two steps). The deprotection of ester **2.41** was carried out by basic hydrolysis to give carboxylic acid **2.42**. This step was initially attempted under mild hydrolysis conditions (LiOH, THF/H_2O, 0 ºC, 16 h) but no reaction was observed by TLC. The reaction was repeated at an elevated temperature (50 ºC) and compound **2.42** was obtained in quantitative yield. Next, carboxylic acid **2.42** was coupled to amine **2.33** using the mixed anhydride method to give boronate ester **2.10** in 60% yield. Finally, **2.10** was treated with TFA to give trifluoroacetate salt **2.11** in 49% yield.

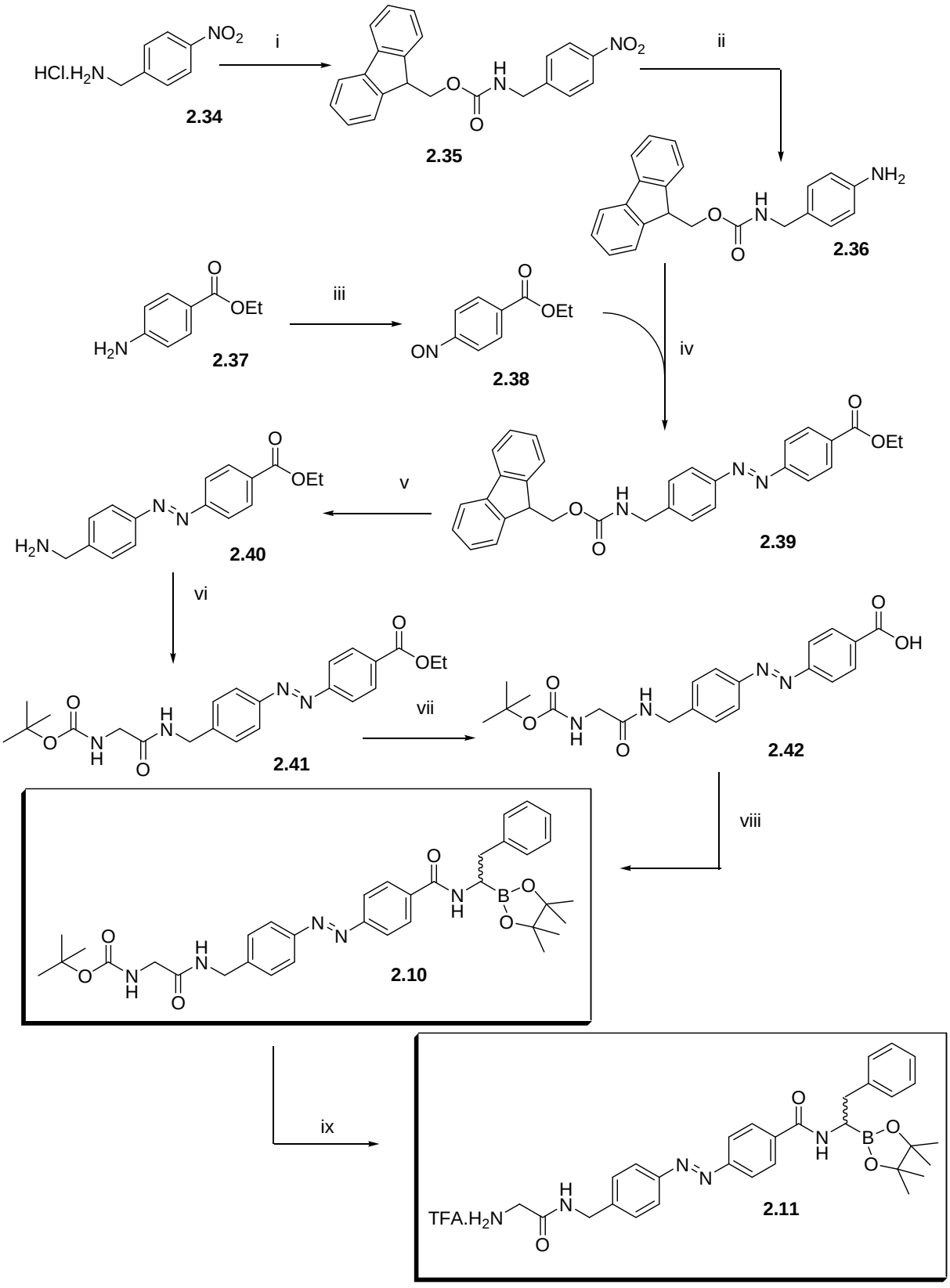

Reagents and conditions: i) Fmoc-Cl, DIEA, DCM, 0ºC → r.t., 52% ii) H_2, PtO_2, EtOAc, 86% iii) $Mo(O_2)_2O(H_2O)HMPA$, DCM, H_2O_2 iv) HOAc, 100ºC, 22% over 2 steps v) DMF, piperidine vi) Boc-Gly, HATU, DIEA, DMF, 88% over 2 steps vii) LiOH, THF, H_2O, 50 ºC, qu viii) **2.33**, ^{i}BuOCOCl, NMM, DMF, 0 ºC → r.t., 60% ix) TFA, DCM, 49%

Scheme 2.8. Synthesis of compounds **2.10** and **2.11**.

*Synthesis of known inhibitor **2.12** for validation of assays*

The boronic acid **2.12** was synthesised as shown in Scheme 2.9, following a reported method.[4] The amine **2.32** was acetylated with acetic anhydride to obtain amide **2.43**, which was then deprotected using boron trichloride to give boronic acid **2.12**. This inhibitor was purified by recrystallisation to obtain a pure sample for assay.

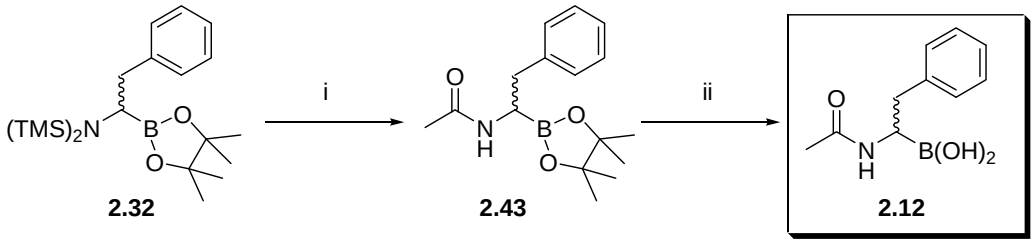

2.32 **2.43** **2.12**

Reagents and conditions: i) Ac_2O, AcOH, THF, -78 ºC → r.t., 47% over 3 steps (see Scheme 2.5) ii) BCl_3, DCM, -78 ºC → r.t., 23%

Scheme 2.9. Synthesis of **2.12**.

2.4 Summary

The azobenzene containing boronate esters **2.1**-**2.11** designed as photoswitch inhibitors of α-chymotrypsin were synthesised. An amine group was included in compounds **2.10** and **2.11** for surface attachment.

Aminophenylboronate based compounds **2.1**-**2.6** were synthesised using peptide coupling methods. The boronate esters **2.1** and **2.6** were successfully prepared using the HATU coupling reagent, but the final step in the synthesis of **2.2**-**2.5** was unsuccessful using this reagent, so instead EDCI was used with acceptable results. For the synthesis of borophenylalanine derivatives, precursor **2.33** was prepared according to a literature method.[3] However, some purification steps could not be carried out successfully, so the purification of two intermediates was omitted. Using this precursor, boronate esters **2.7**-**2.9** were synthesised by the coupling of **2.33** to carboxylic acids **2.15** and **2.21**. The use of standard coupling reagents (EDCI or BOP) was unsuccessful in these reactions, but the mixed anhydride method was successful. The diastereomers **2.8** and **2.9** were somewhat unstable on silica gel, but were successfully separated by chromatography on deactivated silica. Disubstituted azobenzenes **2.10** and **2.11** were synthesised by a more complex route,

involving the key step of condensation of a nitrosobenzene containing a protected amine substituent with an aniline containing an ester substituent.

Enzyme assays of selected boronate esters from this chapter (**2.1**-**2.2** and **2.6**-**2.12**) are described in chapter 6.

2.5 References

1. Westmark, P. R.; Kelly, J. P.; Smith, B. D., *J. Am. Chem. Soc.* **1993**, 115, 3416.
2. Hedstrom, L., *Chem. Rev.* **2002**, 102, 4501.
3. Kettner, C. A.; Shenvi, A. B., *J. Biol. Chem.* **1984**, 259, (24), 15106.
4. Matteson, D. S.; Sadhu, K. M.; Lienhard, G. E., *J. Am. Chem. Soc.* **1981**, 103, 5241.
5. *Organic Syntheses*. Vol. 25, p 86.
6. Desai, R. D.; Mehta, C. V., *Indian J. Pharm.* **1951**, 13, 211.
7. Alexander, N. A. PhD thesis. University of Canterbury, **2006**.

Chapter Three

Synthesis and Stability Studies of Derivatives of a Noncovalent α-Chymotrypsin Inhibitor

Synthesis and stability studies of derivatives of a noncovalent α-chymotrypsin inhibitor

3.1 Introduction

Development of α-chymotrypsin photoswitch inhibitors lacking a warhead group was attempted as an alternative to the boronate esters prepared in chapter 2 and in order to improve inhibitor stability and selectivity (see chapter 1, section 1.3.6 for a discussion of noncovalent inhibitors). Modification of known noncovalent inhibitors **3.1** and **3.2**[1] was carried out in an attempt to introduce photoswitching and allow surface attachment.

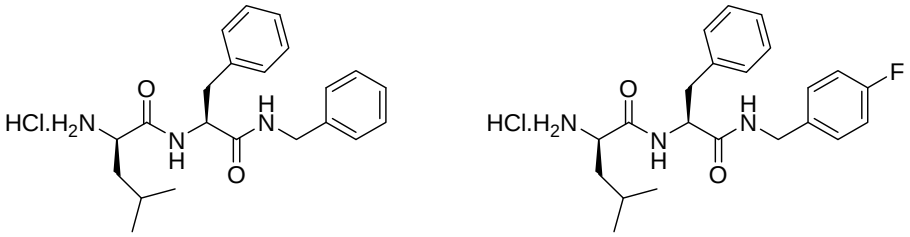

3.1 **3.2**

Fig. 3.1. Noncovalent dipeptide inhibitors of α-chymotrypsin **3.1** and **3.2**.

It was considered that photoswitching activity could be introduced by replacement of the *C*-terminal phenyl group by azobenzene and that surface attachment could be carried out by extension of the *N*-terminal amine group. In order to test these predictions, model compounds **3.3**-**3.5** (Fig. 3.2) containing either a *C*-terminal azobenzene or an *N*-terminal amide were synthesised and assayed (assays described in chapter 6). The crystal structure of a complex of known inhibitor **3.2** with chymotrypsin shows that the amine group of **3.2** appears to form a hydrogen bond to the Gly216 carbonyl group of the enzyme. As modification of this amine group is required for surface attachment, it was important to determine its importance in enzyme binding. The amine group of **3.1** was replaced by a simple acetamide group in **3.3**, and by an extended amino acid group (Boc-Gly) in **3.4**, in order to investigate whether or not the replacement of the amine group by an amide alters the enzyme affinity of the inhibitor. The extended peptide functionality of **3.4** was additionally designed for use in surface attachment and to improve enzyme binding by

targeting the α-chymotrypsin S_3 subsite. The amine **3.5** containing a *C*-terminal azobenzene group was investigated to determine if the large azobenzene group is accommodated in the S_1 subsite, and whether or not a significant difference in activity is observed between the *E* and *Z* isomers of **3.5**, as is required for enzyme photoswitching.

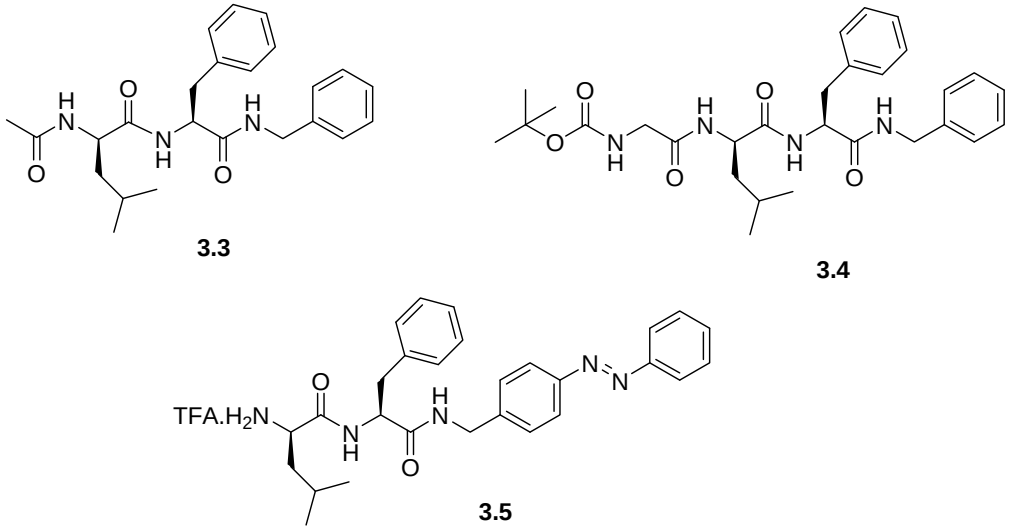

Fig. 3.2. *N*- and *C*-terminally extended derivates of **3.1** for surface attachment and photoswitching.

The inhibitors **3.1** and **3.2** were observed to show high stability to α-chymotrypsin catalysed hydrolysis,[1] a feature not normally observed in simple peptides. This stability is presumably due to the presence of the *D*-Leu residue in the P_2 position, which is unlikely to bind well to the S_2 subsite in the normal substrate conformation (where phenylalanine binds to S_1). As discussed in chapter 1, an unusual enzyme binding conformation is observed instead. For the use of compounds **3.3**-**3.5** as inhibitors, similar stability is required. The stability of these compounds to enzymatic hydrolysis was assessed by incubation of each compound with α-chymotrypsin, monitored by HPLC.

3.2 Synthesis of 3.3-3.5

Compounds **3.3**-**3.5** were synthesised using solution peptide coupling methods, as shown in Scheme 3.1 (compounds **3.3** and **3.4**) and Scheme 3.2 (compound **3.5**).

*Synthesis of **3.3** and **3.4***

The syntheses of **3.3** and **3.4** (Scheme 3.1) were carried out in a similar manner to the reported synthesis of **3.1**, which involved coupling of H-Phe-benzylamine **3.8**[2, 3] with Boc-*D*-Leu-OH, followed by acidic cleavage of the Boc group.

Initially, Boc-Phe-OH **3.6** was coupled to benzylamine in the presence of HATU to give amide **3.7**[4, 5] in 41% yield. This compound was then treated with TFA to give the free amine **3.8**, which was separately coupled to Ac-*D*-Leu-OH and Boc-*D*-Leu-OH to give amides **3.3** and **3.9**, respectively. The Boc group of **3.9** was removed on treatment with TFA to give amine **3.10**, the free base equivalent of **3.1**, in 65% yield. This amine was then coupled to Boc-Gly-OH to give **3.4**.

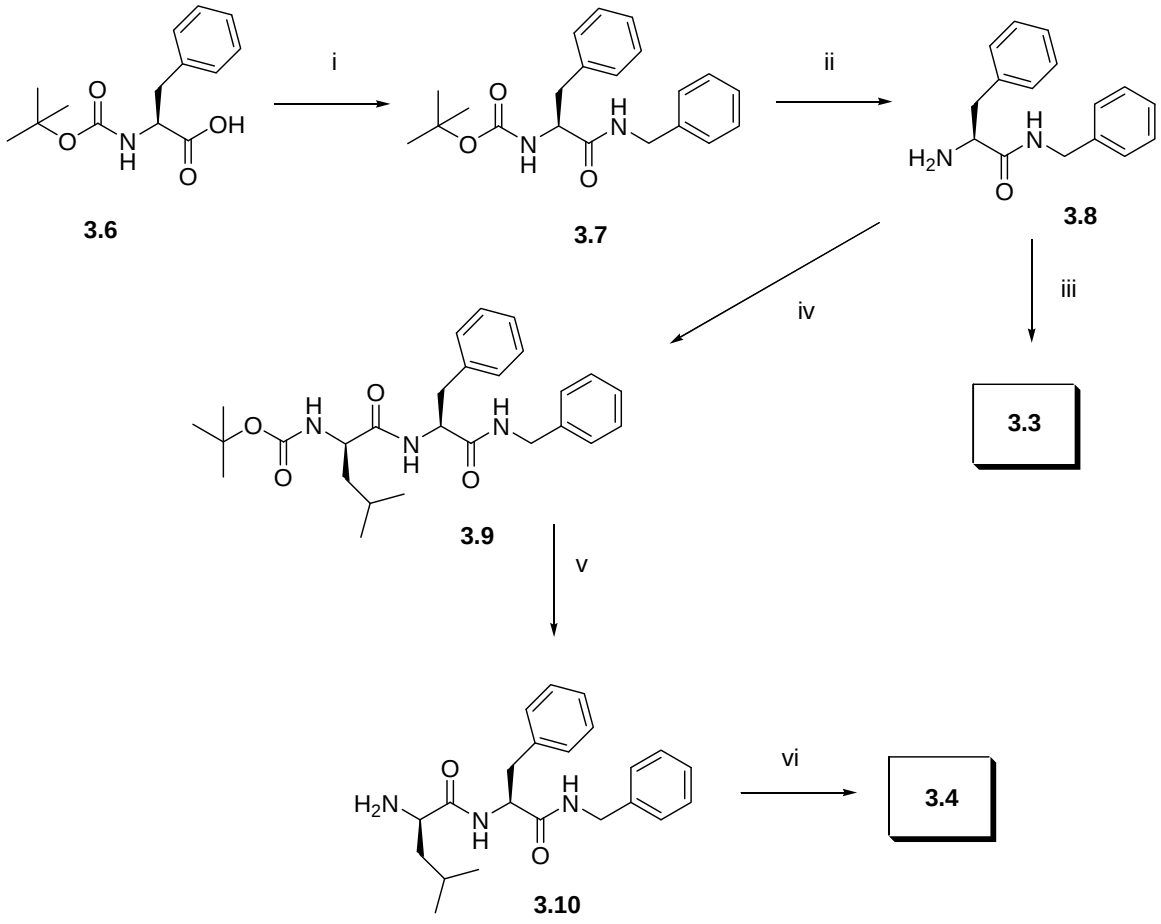

Reagents and conditions: i) benzylamine, HATU, DIEA, DMF, 41% ii) TFA, DCM, 65% iii) Ac-*D*-Leu-OH, HATU, DIEA, DMF, 72% iv) Boc-*D*-Leu-OH, HATU, DIEA, DMF, 76% v) TFA, DCM, 65% vi) Boc-Gly-OH, HATU, DIEA, DMF, 55%.

Scheme 3.1. Synthesis of compounds **3.3** and **3.4**.

Synthesis of ***3.5***

The azobenzene **3.5** was synthesised using a different route, involving the attachment of the *C*-terminal azobenzene group in the final stages of the synthesis, as shown in Scheme 3.2. This convergent route was used with the aim of improving the overall yield. Here, reported carboxylic acid **3.15**[6] and amine **3.12**[7] were the key precursors.

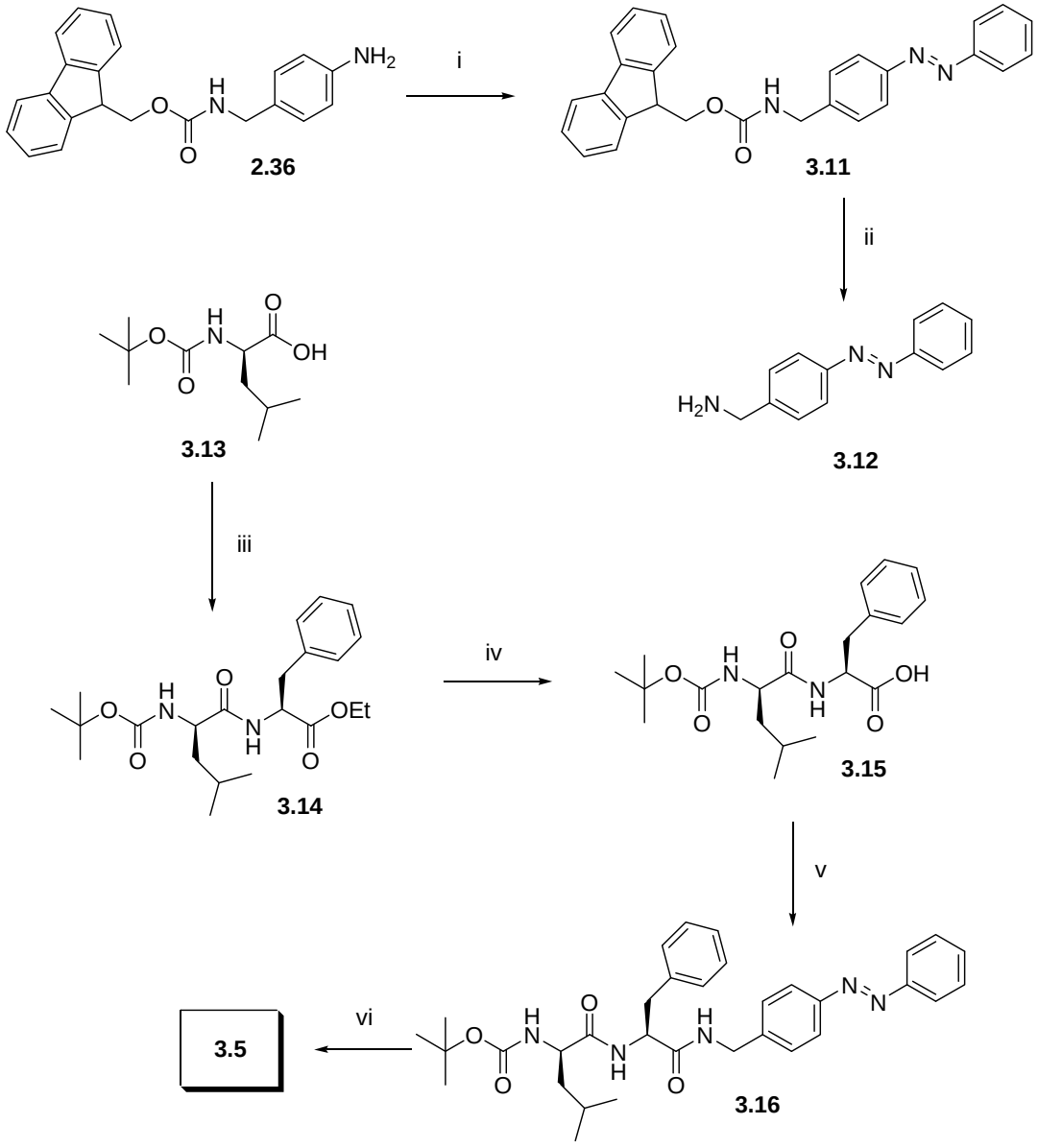

Reagents and conditions: i) nitrosobenzene **2.13**, AcOH, 71% ii) piperidine, DMF, 76% iii) H-Phe-OEt, HATU, DIEA, DMF, 92% iv) LiOH, THF, H_2O, 43% v) **3.12**, HATU, DIEA, DMF, 72% vi) TFA, DCM, 89%.

Scheme 3.2. Synthesis of compound **3.5**.

The aniline **2.36** (used in the synthesis of azobenzenes **2.10** and **2.11**) was condensed with nitrosobenzene **2.13** in AcOH to give azobenzene **3.11**[8] in 71% yield. This Fmoc-protected amine was then treated with 20% piperidine in DMF to give amine **3.12**. Boc-*D*-Leu-OH **3.13** was coupled to H-Phe-OEt in the presence of HATU to give amide **3.14**, which was then deprotected by basic hydrolysis to give carboxylic acid **3.15** in 43% yield. The acid **3.15** was coupled to amine **3.12** to give amide **3.16**, which was then treated with TFA to give **3.5** in 89% yield.

3.3 Stability studies

HPLC studies were carried out to investigate the stability of **3.3**-**3.5** on incubation with α-chymotrypsin, to ensure that these peptides are sufficiently stable for use as inhibitors.

Solutions of **3.3**-**3.5** in acetonitrile (1 mg mL^{-1}) were initially injected onto a reverse phase HPLC column to check purity and determine the retention time for each compound. Using solvent A: water with 0.05% TFA, and solvent B: acetonitrile, and the following elution gradient: 0-1 min 20% solvent B, 1-10 min gradient 20-100% B, 10-12 min 100% B, 12-14 min gradient 100-20% B, 14-20 min 20% B, good chromatograms were obtained (Fig. 3.3). Two peaks are evident in the chromatogram of compound **3.5**, corresponding to the *Z* isomer (minor peak) and *E* isomer (major peak), as determined by UV/vis spectra.

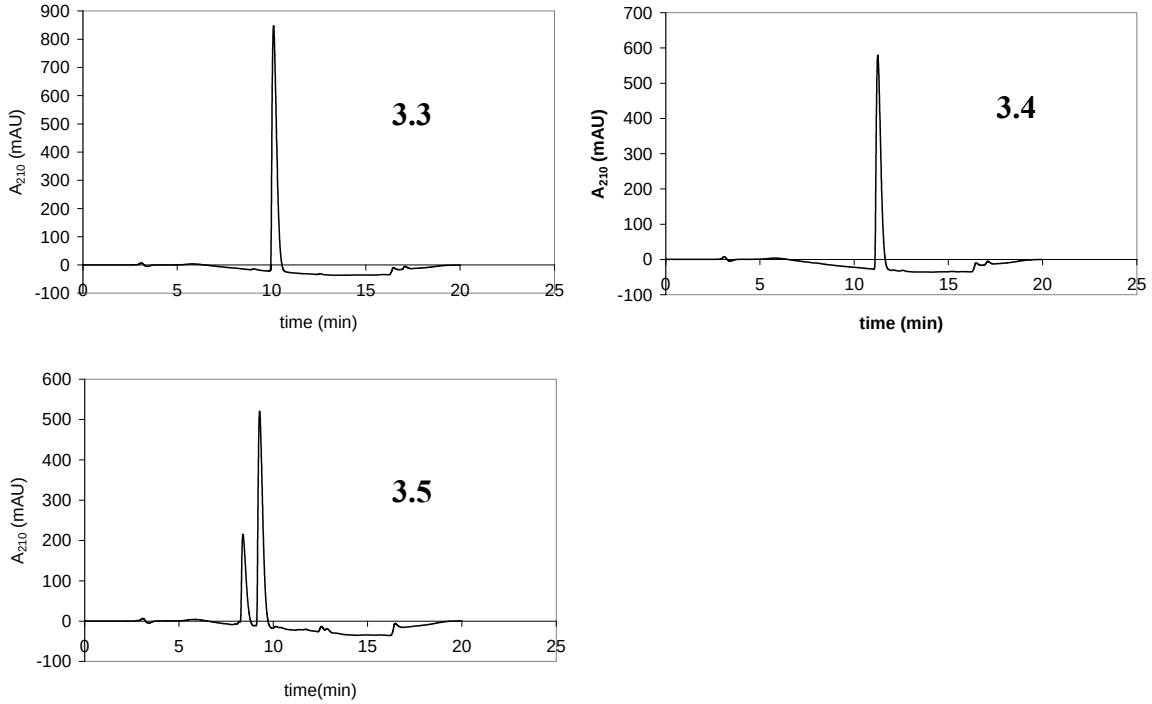

Fig. 3.3. HPLC of compounds **3.3**-**3.5**.

Next, an aliquot from each solution (50 μL) was diluted with Tris buffer (1020 μL) and α-chymotrypsin (30 μL of a 0.24 μM solution) was added.[†] HPLC of these solutions was immediately carried out, then the solutions were incubated for 24 h at 25 ºC and HPLC was repeated in order to determine whether or not enzyme catalysed hydrolysis had

[†] The Tris buffer and enzyme solutions were as used in assays described in chapter 6, and in the experimental chapter, section 9.6.

occurred. Peaks for compounds **3.3**-**3.5** were observed in the chromatograms obtained, at similar retention times to those recorded in acetonitrile. Representative chromatograms for compound **3.4** are shown in Fig. 3.4, and the integrals of the peaks for all compounds are shown in Table 3.1.

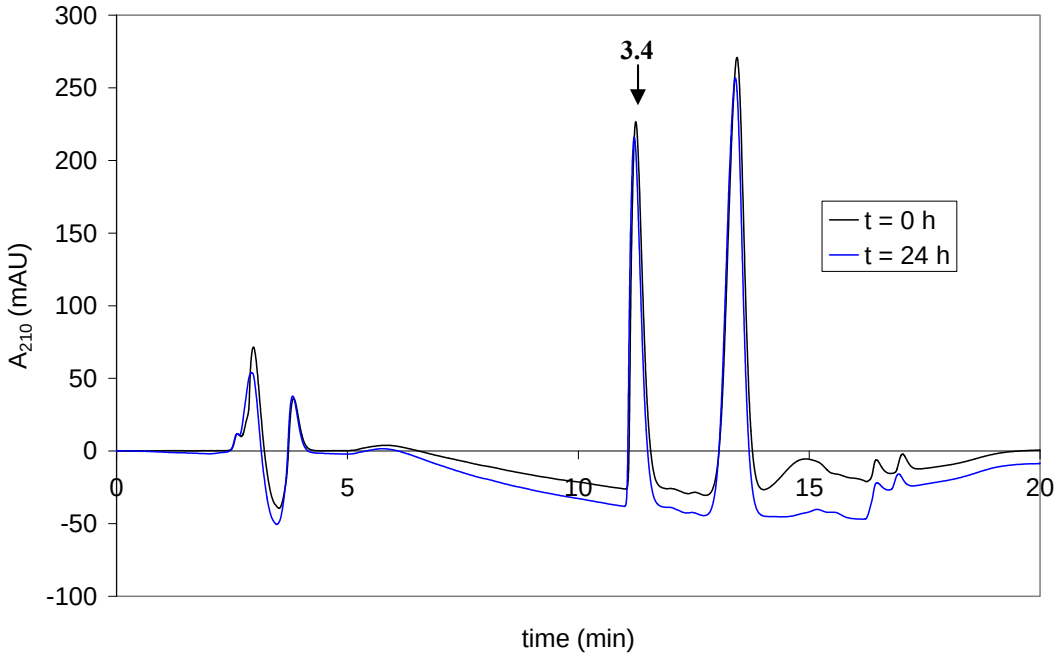

Fig. 3.4. HPLC chromatograms for a solution of **3.4** and α-chymotrypsin in Tris buffer, before and after 24 h incubation.

Table 3.1. HPLC retention times and integrals for compounds **3.3**-**3.5**.

Compound	Retention time (min)	Peak integral at t = 0 h (mAU min)	Peak integral at t = 24 h (mAU min)
3.3	10.1	66.1	66.8
3.4	11.2	71.5	71.6
Z-**3.5**	8.4	7.3	8.4
E-**3.5**	9.3	44.3	53.2

A comparison of the peak integrals in Table 3.1 reveals no significant decrease in the amounts of **3.3**-**3.5** present after 24 h. Therefore, these compounds are stable to α-chymotrypsin catalysed hydrolysis and thus are appropriate for use as inhibitors. The integrals for **3.5** appear to increase slightly after 24 h, probably due to evaporation of solvent or slow dissolution of **3.5**.

3.4 Summary

The peptidomimetics **3.3**-**3.5**, derivatives of known non-covalent α-chymotrypsin inhibitor **3.1**, were synthesised for initial studies towards the development of non-covalent photoswitch inhibitors of α-chymotrypsin. Compounds **3.3**-**3.4** contain an *N*-terminal amide group to investigate extension for surface attachment and **3.5** contains a *C*-terminal azobenzene group for photoswitching.

HPLC stability studies showed that peptidomimetics **3.3**-**3.5** are stable to α-chymotrypsin catalysed hydrolysis, so are appropriate for inhibition studies.

Enzyme assays of **3.3**-**3.5** are described in chapter 6.

3.5 References

1. Shimohigashi, Y.; Maeda, I.; Nose, T.; Ikesue, K.; Sakamoto, H.; Ogawa, T.; Ide, Y.; Kawahara, M.; Nezu, T.; Terada, Y.; Kawano, K.; Ohno, M., *J. Chem. Soc. Perkin Trans. 1* **1996**, 2479.

2. Conley, J. D.; Kohn, H., *J. Med. Chem.* **1987**, 30, (3), 567.

3. Zhang, D.; Xing, X.; Cuny, G. D., *J. Org. Chem.* **2006**, 71, 1750.

4. Hagiwara, D.; Miyake, H.; Morimoto, H.; Murai, M.; Fujii, T.; Matsuo, M., *J. Med. Chem.* **1992**, 35, 3184.

5. Ramalingam, B.; Neuburger, M.; Pfaltz, A., *Synthesis* **2007**, 4, 572.

6. Sakamoto, H.; Shimohigashi, Y.; Maeda, I.; Nose, T.; Nakashima, K.-i.; Nakamura, I.; Ogawa, T.; Ohno, M.; Kawano, K., *J. Mol. Recognit.* **1993**, 6, (2), 95.

7. Oshita, S.; Matsumoto, A., *Chem. Lett.* **2003**, 32, (8), 712.

8. Harvey, A. J. PhD thesis. University of Canterbury, **2000**.

Chapter Four

Synthesis of Trifluoromethylketones and α-Ketoesters

Synthesis of trifluoromethylketones and α-ketoesters

4.1 Introduction

The photoisomerisable boronate esters described in chapter 2 for attachment to surfaces were found to be partially unstable to photoisomerisation and the dipeptide derivatives described in chapter 3 were found to be inactive against α-chymotrypsin (see chapter 6). Consequently, alternative photoswitch inhibitors were required. Trifluoromethylketones and α-ketoesters were chosen for this purpose, since stable photoswitch inhibitors containing these groups are known.[1, 2] Both classes of inhibitor contain a ketone activated by an adjacent electrophilic group that binds to the active site serine of chymotrypsin (see chapter 1). However, α-ketoesters generally exhibit much stronger binding affinities (usually high nM inhibition constants)[3] than do trifluoromethylketones (low μM)[4]. In addition, trifluoromethylketones often exhibit slow-tight binding characteristics,[5] whereas α-ketoesters usually exhibit simple competitive binding. Trifluoromethylketones linked to azobenzenes also tend to exhibit a greater difference in activity between the *E* and *Z* isomers than do related α-ketoesters,[1, 6] although this observation is yet to be systematically studied. Given these differences, we chose to investigate the potential of each for use as surface attached photoswitch inhibitors.

A linker group for surface attachment was included in these inhibitors. Two such groups were studied. Firstly, the primary amine group, as in boronate ester **2.11** (see chapter 2), which is commonly used for surface attachment using the simple and versatile amide coupling reaction. Secondly, the alkyne group, which reacts with azides in a copper(I) catalysed 3 + 2 cycloaddition reaction. This reaction was chosen as recent studies show that it is unaffected by the presence of most functional groups,[7] and has been used successfully in various systems, including surface attachment.[8]

The copper catalysed azide-alkyne cycloaddition has been labelled a 'click chemistry' reaction due to its simple reaction conditions, high yields, and broad applicability.[9] Cycloaddition of alkynes and azides to form triazoles can occur either thermally or with Cu(I) catalysis (Scheme 4.1). Thermal reaction requires high temperatures and gives rise

to a mixture of 1,4- and 1,5-regioisomers, whereas the recently reported copper catalysed reaction proceeds efficiently at room temperature and forms only the 1,4 isomer.

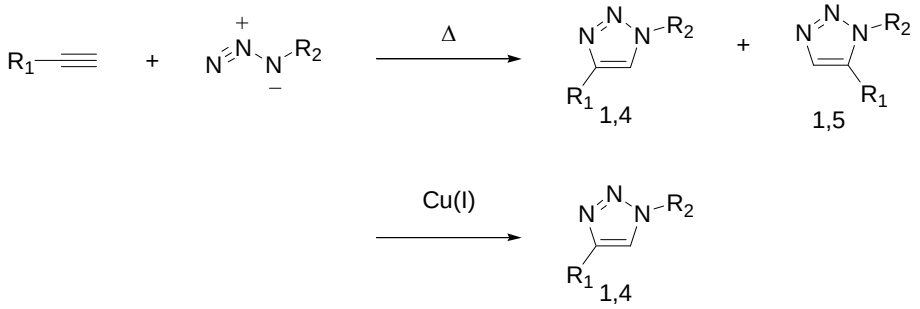

Scheme 4.1. Azide-alkyne cycloaddition.

This chapter describes the synthesis of a series of trifluoromethylketones **4.1**-**4.4** (Fig. 4.1) and α-ketoesters **4.5**-**4.7** (Fig. 4.2) designed to act as photoswitch inhibitors of α-chymotrypsin. These compounds contain an enzyme binding group, an azobenzene photoswitch core, and a linker for surface attachment. A range of compounds was synthesised in order to identify the most effective groups for photoswitch enzyme binding and surface attachment. The enzyme binding groups are phenylalanine derivatives containing an electrophilic ketone, synthesised from reported trifluoromethylalcohol **4.8** or α-hydroxyester **4.9** (Fig. 4.3). The phenylalanine structure was used since it is known to bind strongly to the α-chymotrypsin active site.[11] The surface attachment linker consists of an alkyne (compounds **4.2**-**4.4** and **4.6**-**4.7**) or protected amine (compounds **4.1** and **4.5**) and an appropriate scaffold to attach this functional group to the azobenzene core. The protected amines are designed for surface attachment by amide coupling after liberation of the free amine group, and are analogous in structure to boronate ester **2.10**. A long chain oligoethylene glycol (OEG) group was included in compounds **4.2**, **4.4** and **4.7** as a spacer to separate the enzyme binding group from the surface, to improve α-chymotrypsin binding. Two different groups were used to link the OEG group to the azobenzene group, amide (in compound **4.2**) and internal alkyne (in compounds **4.4** and **4.7**) to compare the impact of these groups on enzyme activity and photoswitching.

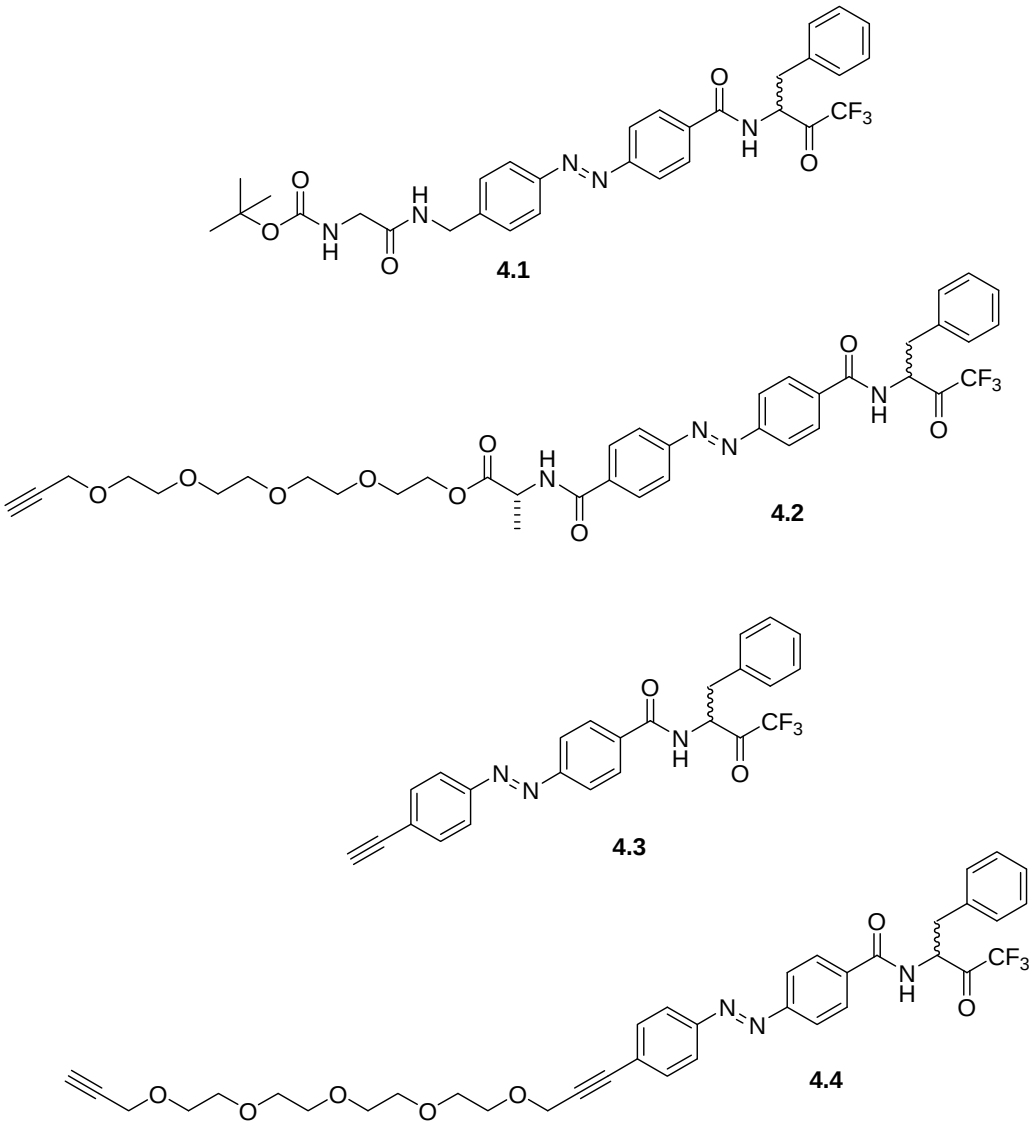

Fig. 4.1. Trifluoromethylketones **4.1**-**4.4** described in this chapter.

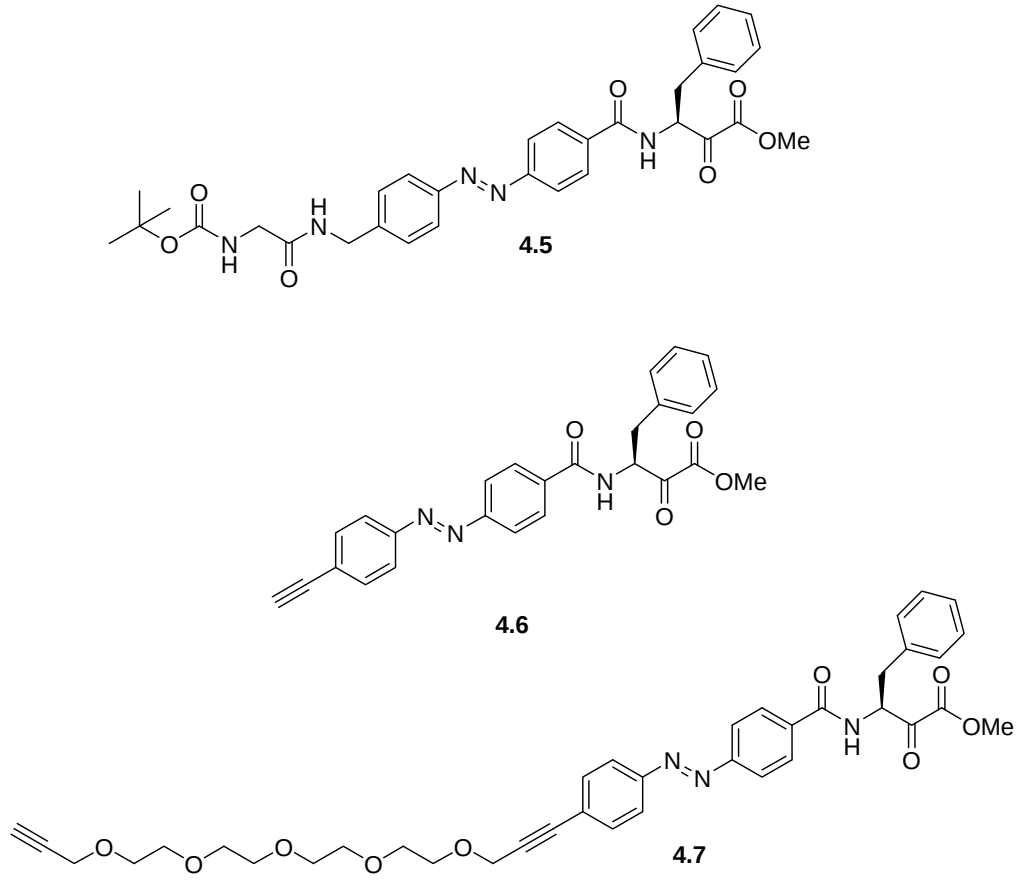

Fig. 4.2. α-Ketoesters **4.5-4.7** described in this chapter.

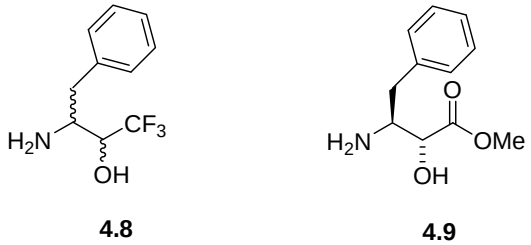

Fig. 4.3. Alcohols **4.8** and **4.9**, precursors to trifluoromethylketones and α-ketoesters.

4.2 Synthesis of precursor 4.9

Compound **4.9** was prepared by modification of reported syntheses,[12-17] involving acidic hydrolysis of a cyanohydrin to the key α-hydroxyester group, as shown in Scheme 4.2. Initially Cbz-Phe-OMe **4.10** was reduced to aldehyde **4.11** in 90% yield using DIBAL. The aldehyde **4.11** was then reacted with $NaHSO_3$ and KCN to give cyanohydrin **4.12** as an inseparable mixture of diastereomers, obtained in a 3:2 ratio (by ^1H NMR) after purification by column chromatography. Hydrolysis of the mixture of cyanohydrins was carried out by stirring in a solution of HCl in MeOH/ether for 70 h, with addition of water after 24 h. The resulting diastereomeric α-hydroxyesters were separated by column chromatography to give **4.13** (33%) and **4.14** (19%). However, much poorer yields were obtained in repeats of this reaction (8% then 11% combined yield of **4.13** and **4.14**). Finally, the Cbz group of **4.13** was removed by catalytic hydrogenolysis to give **4.9** in quantitative yield.

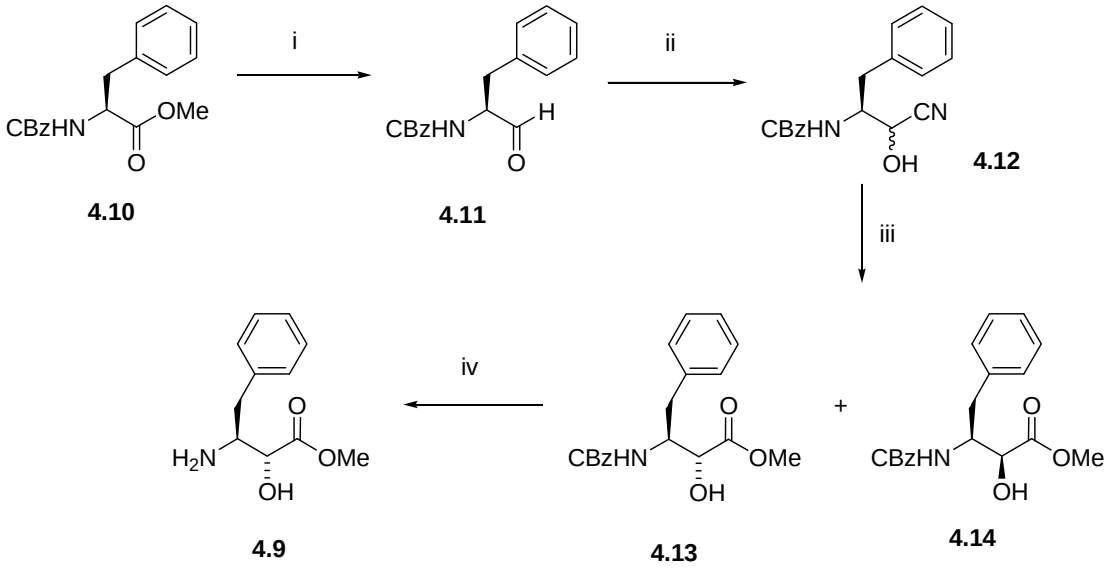

Reagents and conditions: i) DIBAL, toluene, -78ºC, 90% ii) KCN, $NaHSO_3$, EtOAc, H_2O, 0ºC → 4ºC → r.t., 79% iii) HCl, MeOH, ether, H_2O, 0ºC → 4ºC, 8-52% combined yield iv) Pd/C, H_2, EtOAc, qu.

Scheme 4.2. Synthesis of α-hydroxyester **4.9**.

4.3 Synthesis of trifluoromethylketone and α-ketoester derivatives of boronate ester 2.10

Trifluoromethylketone **4.1** and α-ketoester **4.5** were synthesised as shown in Scheme 4.3. The carboxylic acid **2.42** was separately coupled to **4.9** and trifluoromethylalcohol **4.8**[18] (obtained from Nathan Alexander[1]) in the presence of EDCI to give **4.15** and **4.16**, respectively. The alcohols **4.15** and **4.16** were then oxidised using Dess-Martin periodinane to give ketone **4.5** in 83% yield and **4.1** in 44% yield. Dess-Martin periodinane was used since it has been reported to be the most reliable reagent for oxidation of trifluoromethylalcohols to ketones, when used in a 3.7 equivalent excess.[19] Therefore, 3.7 equivalents were used in the oxidation of trifluoromethyl alcohol **4.16**. Two equivalents were used in the oxidation of α-hydroxyester **4.15**. Treatment of **4.1** with TFA gave the amine salt **4.17** which was unstable to chromatography, presumably due to the conflicting reactivities of the electrophilic trifluoromethylketone group and the nucleophilic amine group. This is surprising, as the related boronate ester **2.11** was successfully isolated by chromatography. As this reaction was unsuccessful, deprotection of related ketone **4.5** was not carried out.

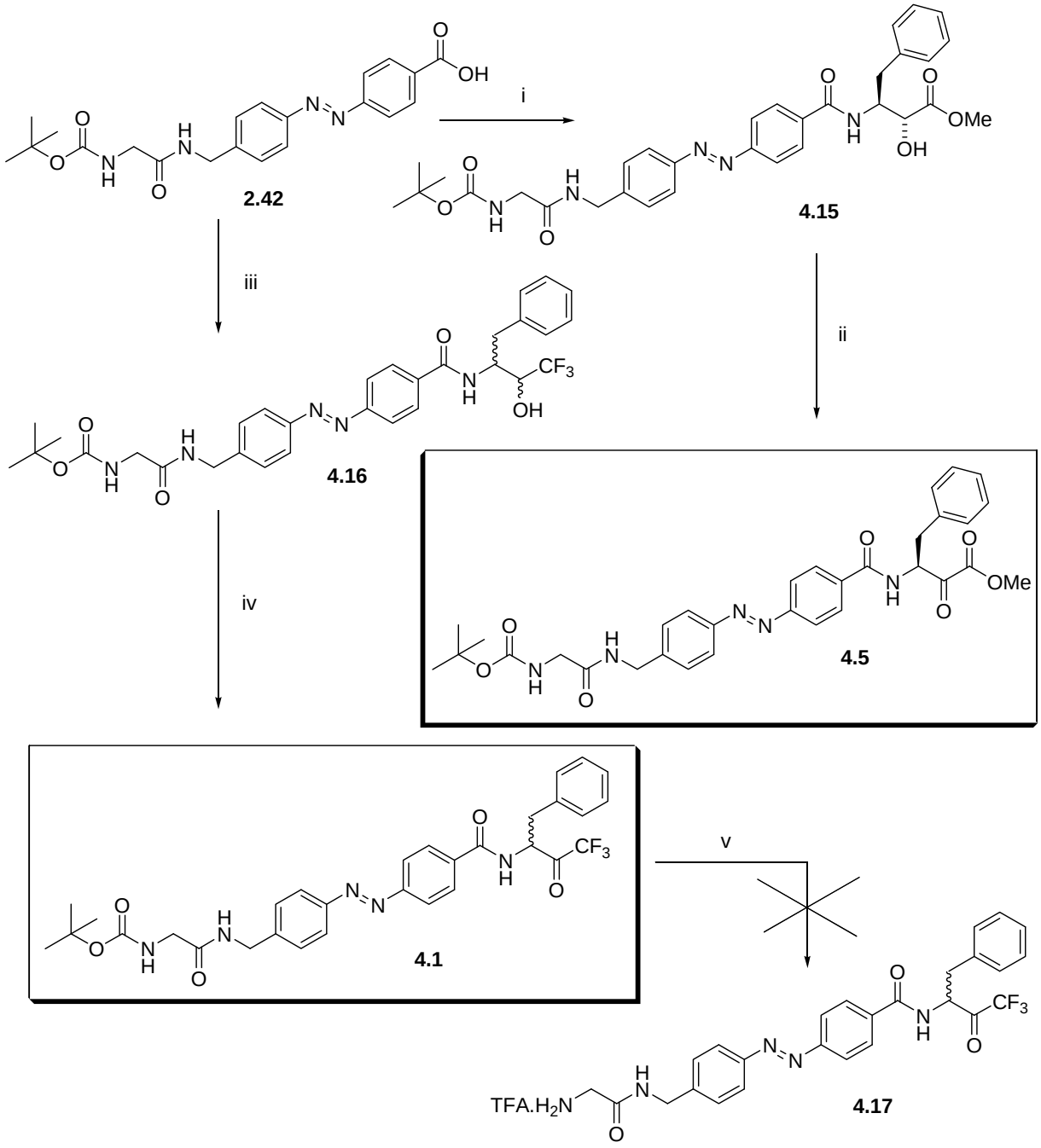

Reagents and conditions i) **4.9**, EDCI, HOAt, DIEA, DMF, 69% ii) Dess-Martin periodinane, DCM, 83% iii) **4.8**, EDCI, HOBt, DIEA, DMF, 50% iv) Dess-Martin periodinane, DCM, 44% v) TFA, DCM

Scheme 4.3. Synthesis of **4.1** and **4.5**, and attempted synthesis of **4.17**.

4.4 Synthesis of azobenzenes with alkyne substituents for surface attachment by 'click' chemistry

Two different approaches were carried out to synthesise azobenzenes containing terminal alkyne substituents, as detailed in sections 4.4.1 and 4.4.2, below.

4.4.1 Synthesis of photoswitch inhibitor 4.2 from a symmetrical azobenzene precursor

Azobenzene **4.2** was synthesised by the sequential reaction of symmetrical azobenzene **4.21**[20] (Scheme 4.4) with trifluoromethylalcohol **4.8** and alkyne **4.28** followed by oxidation (Schemes 4.5-4.8). Initially, synthesis of the related trifluoromethylketone **4.18** lacking the alanine residue (Fig. 4.4) was also attempted (schemes 4.5-4.6). These syntheses were carried out without use of protecting groups in order to eliminate protection/deprotection steps and thus decrease the number of reaction steps.

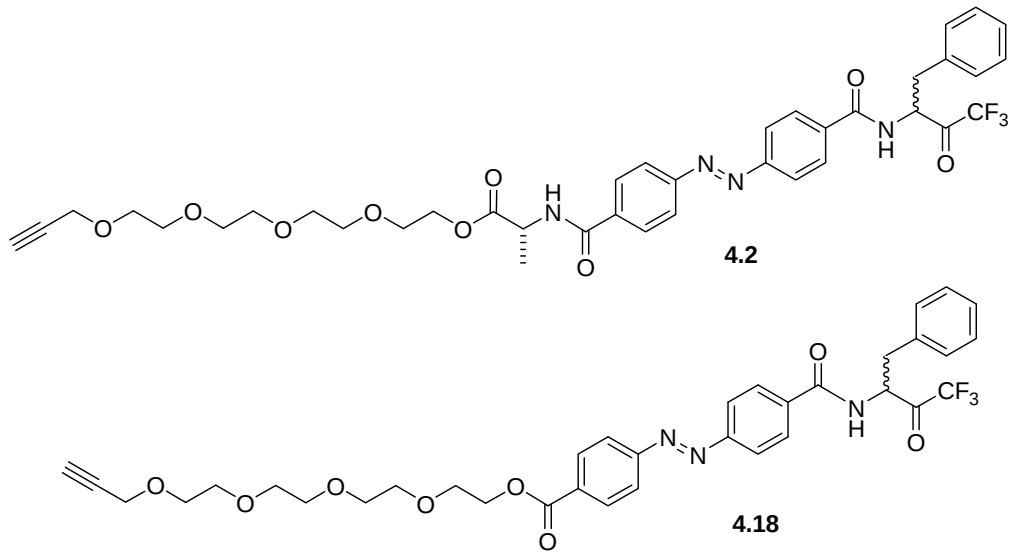

Fig. 4.4. Trifluoromethylketone **4.2** and the related target, trifluoromethylketone **4.18**.

*Synthesis of symmetrical azobenzene **4.21***

Following reported syntheses of **4.21**,[20, 21] nitrosobenzoic acid **4.19** was reduced with glucose to azobenzene **4.20** in 33% yield, followed by reaction with PCl_5 to give acid chloride **4.21** in 47% yield (scheme 4.4).

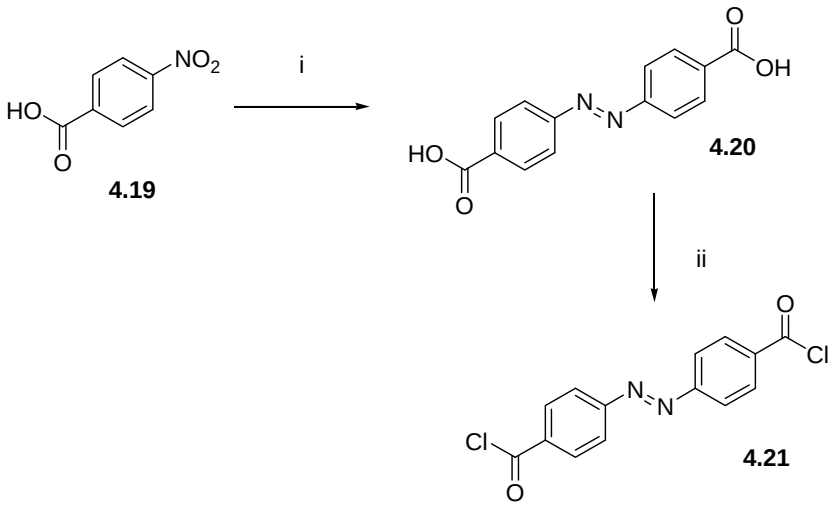

Reagents and Conditions: i) glucose, NaOH, H_2O, 50ºC, 33% ii) PCl_5, 1,2-dichloroethane, reflux, 47%

Scheme 4.4. Synthesis of symmetrical azobenzene **4.21**.

*Synthesis of alkyne **4.23** and attempted reaction with **4.21***

The alkyne **4.23** was prepared in 38% yield by reaction of propargyl bromide with a large excess of tetraethylene glycol **4.22** (scheme 4.6). The alcohol **4.23** was then reacted with acid chloride **4.21** in the presence of base (TEA) in an attempt to obtain ester **4.24**, a precursor to **4.18**, but this product was not obtained. The ^{1}H NMR of the crude product instead suggested the formation of a symmetrical disubstituted derivative resulting from reaction of two equivalents of alcohol **4.23** with both acid chloride groups of **4.21**.

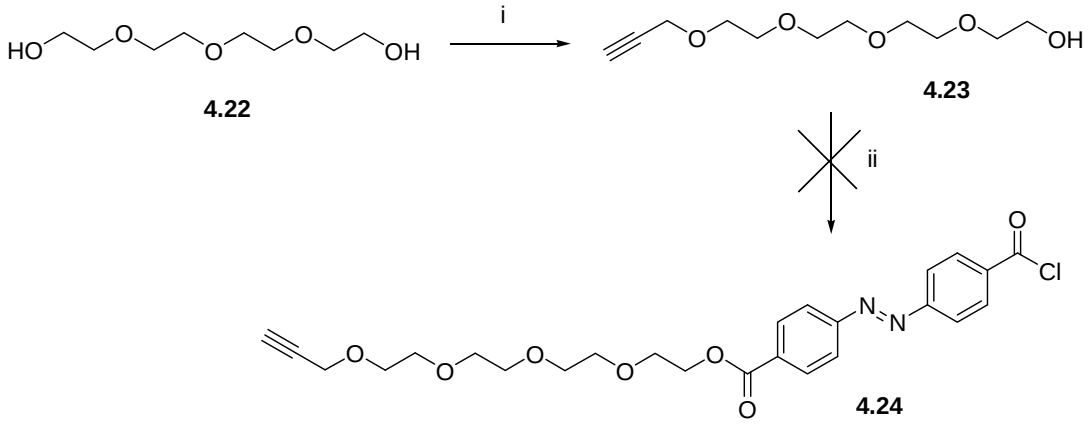

Reagents and Conditions i) propargyl bromide, NaH, THF, 0ºC → r.t., 38% ii) **4.21**, THF, TEA

Scheme 4.5. Synthesis of alkyne **4.24** and attempted synthesis of azobenzene **4.24**.

*Reaction of **4.21** with trifluoromethylalcohol **4.8** and subsequent attempted reaction with alkyne **4.23***

As an alternative approach for the synthesis of **4.18**, the reaction of amine **4.8** with **4.21** was carried out (Scheme 4.6) in order to attach the enzyme binding substituent (**4.8**) to the azobenzene core before attachment of the alkyne substituent (**4.23**). The amine **4.8** and acid chloride **4.21** were reacted in the presence of base (DIEA) to give amide **4.25** in acceptable yield (38%). However, subsequent reaction of acid chloride **4.25** with alcohol **4.23** gave returned starting material only.

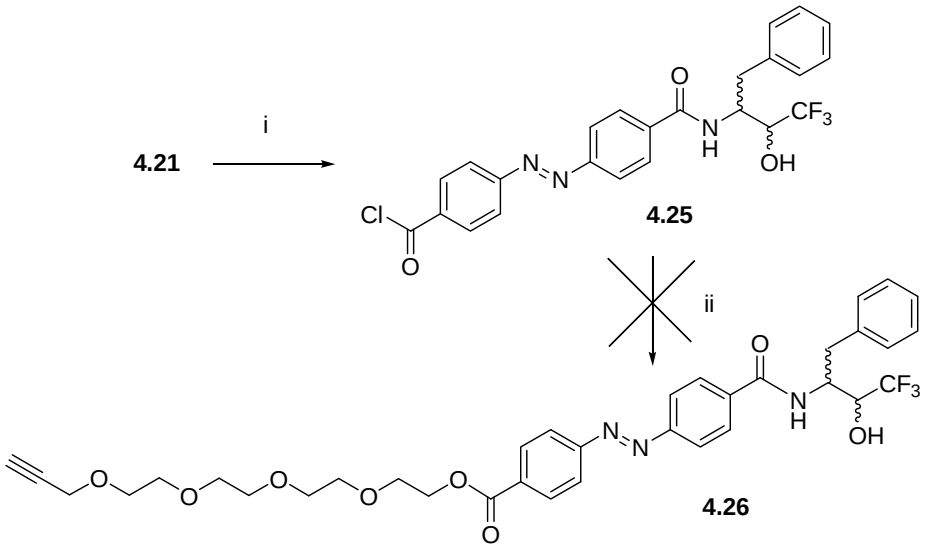

Reagents and conditions: i) **4.8**, DIEA, DCM, 38% ii) **4.23**, DIEA, DCM

Scheme 4.6. Synthesis of azobenzene **4.25** and attempted reaction with alkyne **4.23**.

*Synthesis of alkyne **4.28** and attempted reaction with **4.21***

Efforts were then focused towards synthesis of trifluoromethylketone **4.2** rather than **4.18**. The primary amine **4.28** was synthesised, which was expected to be more reactive than alcohol **4.23** for nucleophilic attack on acid chloride **4.21** or **4.25**.

The alcohol **4.23** was coupled to Boc-Ala-OH to obtain amide **4.27** in 94% yield, which was then treated with TFA to give amine **4.28** (scheme 4.7). This amine was reacted with acid chloride **4.21** in the presence of base (DIEA). Again, products were formed but analysis of these compounds by TLC, ^{1}H NMR, and MS showed only traces of the desired product **4.29**.

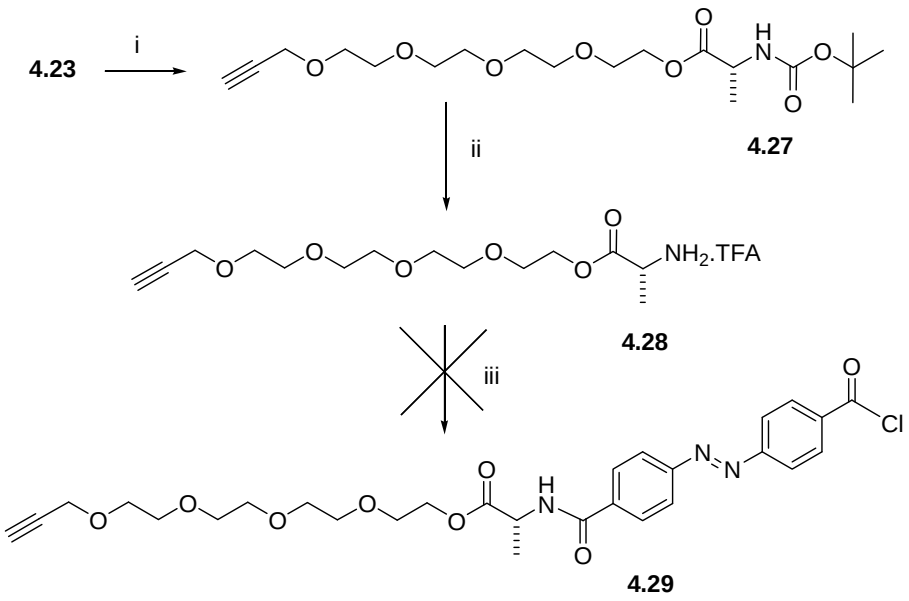

Reagents and conditions: i) Boc-Ala-OH, EDCI, DMAP, DCM, 94% ii) TFA, DCM iii) **4.21**, DIEA, DCM.

Scheme 4.7. Synthesis of alkyne **4.28** and attempted reaction with azobenzene **4.21**.

*Synthesis of **4.2** involving reaction of alkyne **4.28** and azobenzene **4.25***

The amine **4.28** was reacted with acid chloride **4.25** to successfully obtain disubstituted azobenzene **4.30** (Scheme 4.8). This compound was then oxidised by Dess-Martin periodinane to give trifluoromethylketone **4.2** in quantitative yield.

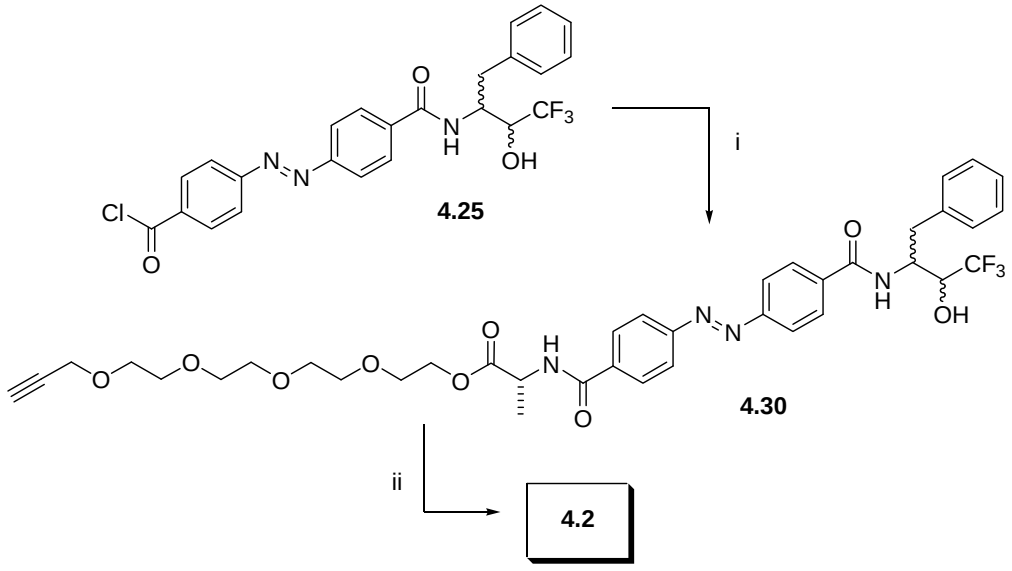

Reagents and Conditions: i) **4.28**, DIEA, DCM, 70% over 2 steps ii) Dess-Martin periodinane, DCM, qu.

Scheme 4.8. Successful synthesis of trifluoromethylketone **4.2**.

It is unclear why the reactions of amine **4.28** with acid chloride **4.25** (Scheme 4.8) and of amine **4.8** with acid chloride **4.21** (Scheme 4.6) were successful but the reaction of amine **4.28** with **4.21** (Scheme 4.7) was not. However, as a result the synthesis of trifluoromethylketone **4.2** requires the use of key precursor **4.8** at an early stage of the synthesis. As precursors **4.8** and **4.9** are difficult to obtain in large quantities, it is preferable to introduce these compounds at a late stage of synthesis. Consequently, an α-ketoester analogue of **4.2** was not synthesised.

4.4.2 Synthesis of alkyne substituted azobenzenes utilising Pd catalysed coupling

The alkynes **4.3**, **4.4**, **4.6**, and **4.7** were synthesised by palladium catalysed coupling of an alkyne to an azobenzene with a halide substituent. This synthetic method has been previously reported for a simple bromobenzoate structure, as shown in Scheme 4.9.[22] First, bromide **4.31** was reacted with the alkyne 2-methyl-3-butyn-2-ol and catalysts $PdCl_2(PPh_3)_2$ and CuI to give aryl alkyne **4.32**. Deprotection was then carried out by reflux with NaOH to give terminal alkyne **4.33**.

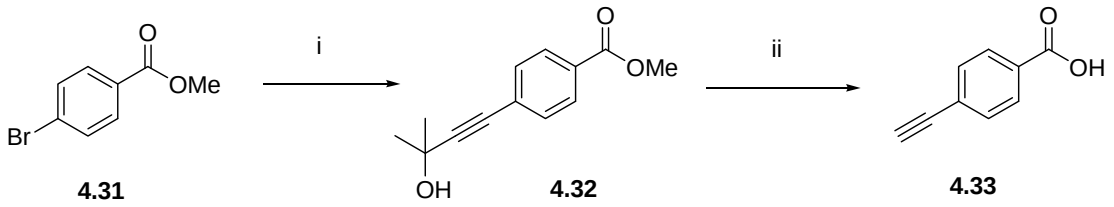

4.31 **4.32** **4.33**

Reagents and conditions: i) 2-methyl-3-butyn-2-ol, $PdCl_2(PPh_3)_2$, PPh_3, CuI, TEA, 98% ii) NaOH, BuOH, 99%

Scheme 4.9. Reported synthesis of an aryl alkyne utilising Pd catalysis.

A directly analogous synthesis was used here in the synthesis of ketones **4.3** and **4.6**, involving reaction of known bromoazobenzene **4.36** with 2-methyl-3-butyn-2-ol followed by deprotection to give alkynylazobenzene **4.40** (Schemes 4.10-4.11).

*Synthesis and Pd-catalysed coupling of **4.36***

The azobenzene **4.36** was initially prepared following a reported method[23] (Scheme 4.10). Methyl aminobenzoate **4.34** was oxidised with Oxone to the corresponding nitrosobenzene **4.35** in 62% yield. Next, condensation of **4.35** with bromoaniline in AcOH was carried out

to give **4.36** in 30% yield. This is surprising, since the reported yield for this reaction is 98%.

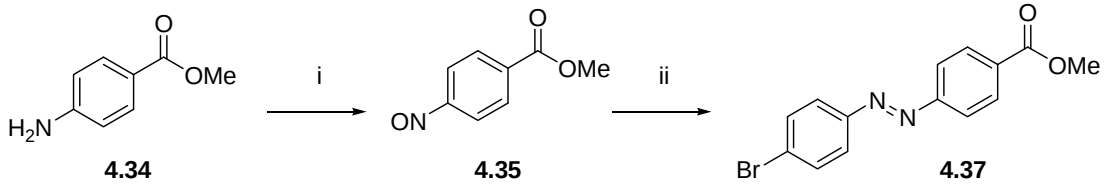

Reagents and conditions: i) Oxone, DCM, H_2O, 90% ii) bromoaniline **4.36**, AcOH, 98%

Scheme 4.10. Synthesis of **4.37** following a reported method.

An alternative route to **4.37** was carried out to improve yields, as shown in Scheme 4.11. Bromoaniline **4.36** was oxidised to bromonitrosobenzene **4.38** in 98% yield, which was then condensed with methyl aminobenzoate **4.34** in AcOH to give azobenzene **4.36** in improved yield (52%). The azobenzene **4.36** was then reacted with the protected alkyne 2-methyl-3-butyn-2-ol in the presence of $PdCl_2(PPh_3)_2$ and CuI to give alkyne **4.39** in 93% yield. Finally, both protecting groups were removed by basic hydrolysis to give terminal alkyne **4.40**.

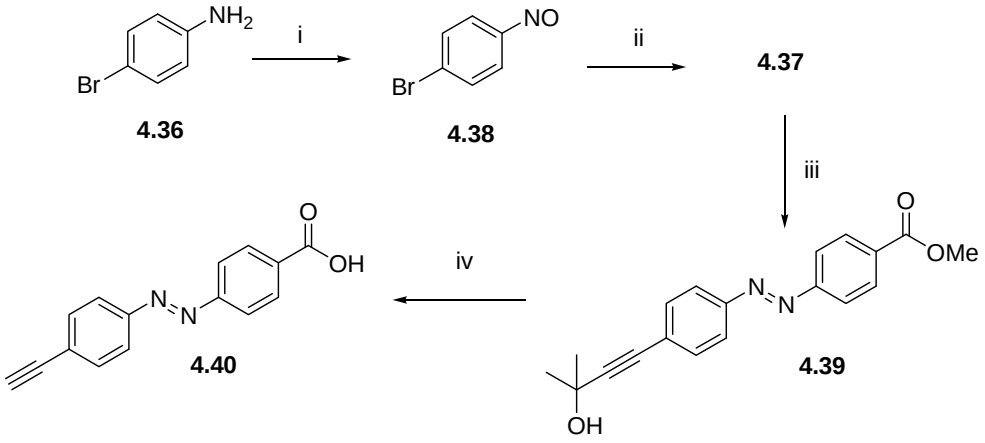

Reagents and conditions i) Oxone, H_2O, DCM, 98% ii) **4.34**, AcOH, 52% iii) 2-methyl-3-butyn-2-ol, $PdCl_2(PPh_3)_2$, PPh_3, CuI, TEA, reflux, 93% iv) NaOH, BuOH, reflux, 71%

Scheme 4.11. Synthesis of azobenzene **4.40** containing an alkyne substituent.

*Synthesis of ketones **4.3** and **4.6***

The ketones **4.3** and **4.6** were then synthesised from compound **4.40**, as shown in Scheme 4.12. The carboxylic acid **4.40** was separately coupled to amines **4.8** and **4.9** to give **4.41** and **4.42**, respectively. The alcohols **4.41** and **4.43** were then oxidised using Dess-Martin periodinane to obtain trifluoromethylketone **4.3** and α-ketoester **4.6**, respectively.

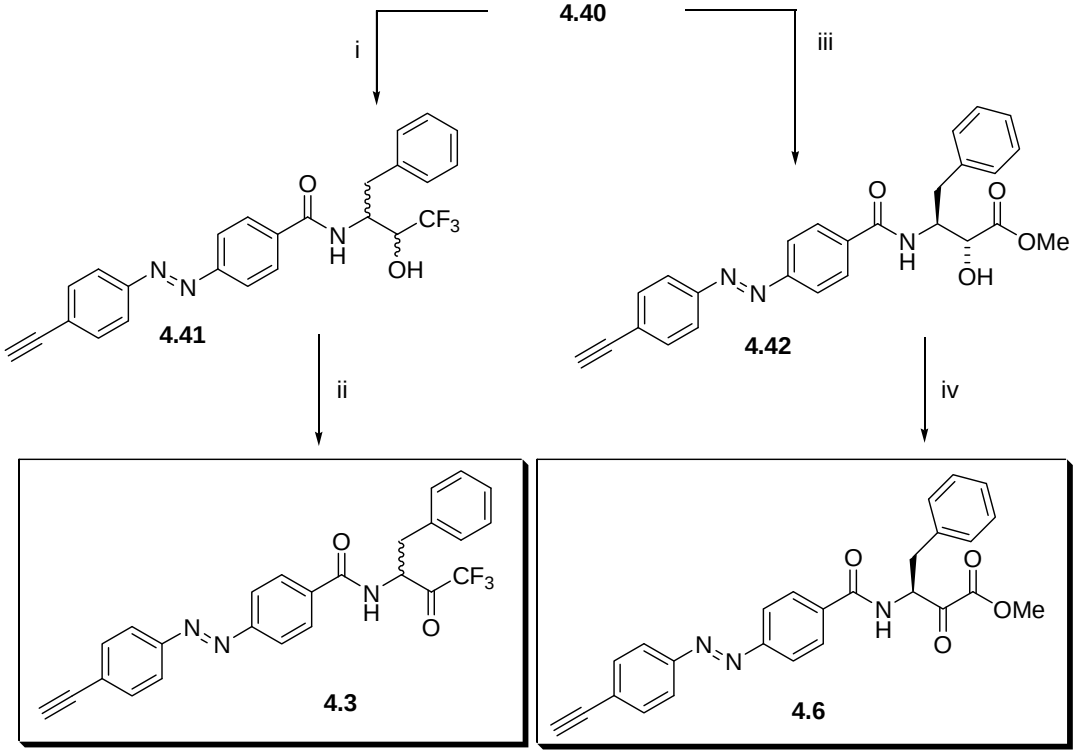

Reagents and conditions i) **4.8**, EDCI, HOAt, DIEA, DMF, 56% ii) Dess-Martin periodinane, DCM, 91% iii) **4.9**, EDCI, HOBt, DIEA, DMF, 61% iv) Dess-Martin periodinane, DCM, 91%.

Scheme 4.12. Synthesis of **4.3** and **4.6**.

*Synthesis of ketones **4.4** and **4.7***

Derivatives **4.4** and **4.7** containing a long chain OEG group were synthesised in a similar manner to **4.3** and **4.6**, using alkyne **4.47** as the key precursor in place of compound **4.40**. The alkyne **4.47** was synthesised by Andrew Muscroft-Taylor[24] (Scheme 4.13). In brief, alkyne **4.44** was coupled to iodide **4.45** to give **4.46**, which was deprotected to obtain carboxylic acid **4.47**.

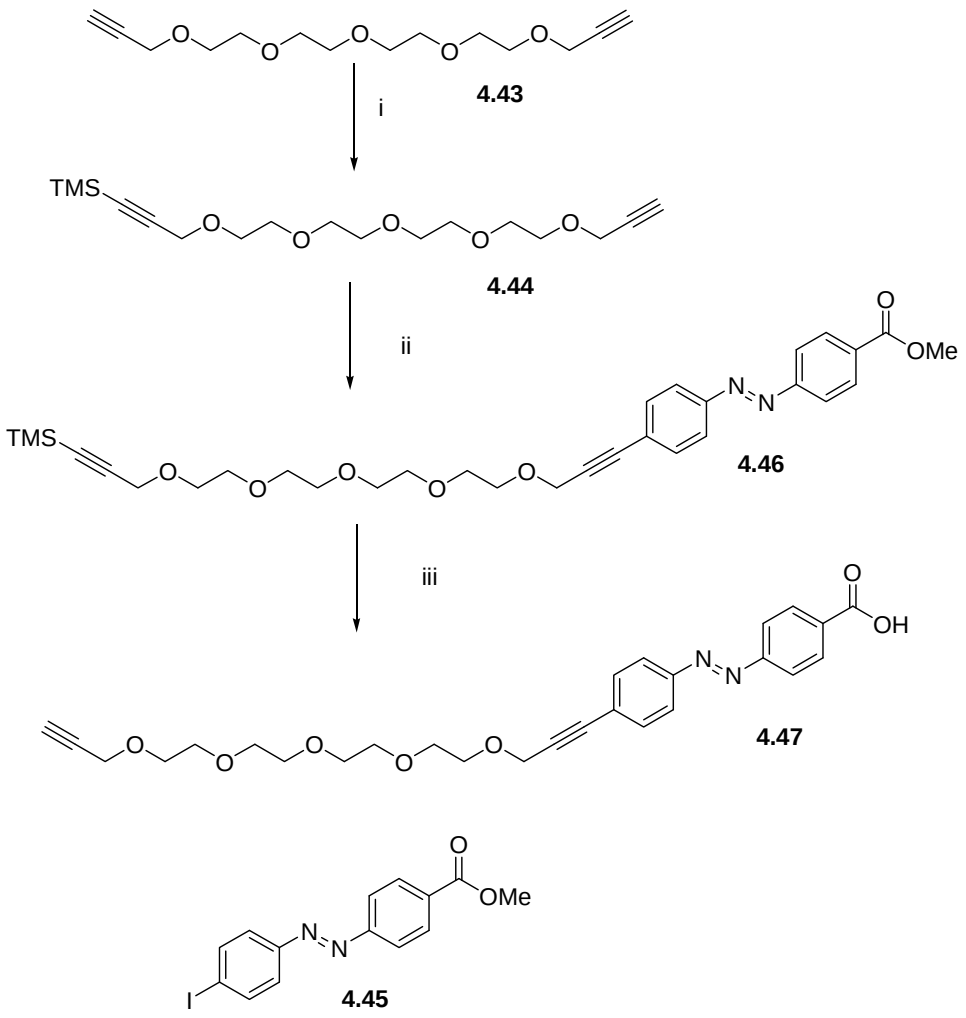

Reagents and conditions: i) *n*-BuLi, TMS-Cl ii) $PdCl_2(PPh_3)_2$, DMF, TEA iii) NaOH, THF, H_2O, MeOH

Scheme 4.13. Synthesis of alkyne **4.47** (carried out by Andrew Muscroft-Taylor).

Using this precursor, trifluoromethylketone **4.4** was synthesised (Scheme 4.14) by the coupling of carboxylic acid **4.47** and amine **4.8** using EDCI coupling reagent to give **4.48** in 80% yield, followed by Dess-Martin periodinane oxidation to give **4.4** in 90% yield. Similarly, α-ketoester **4.7** was synthesised by the coupling of carboxylic acid **4.47** and amine **4.9** to give **4.49** in 58% yield, followed by oxidation to give **4.7** in 51% yield.

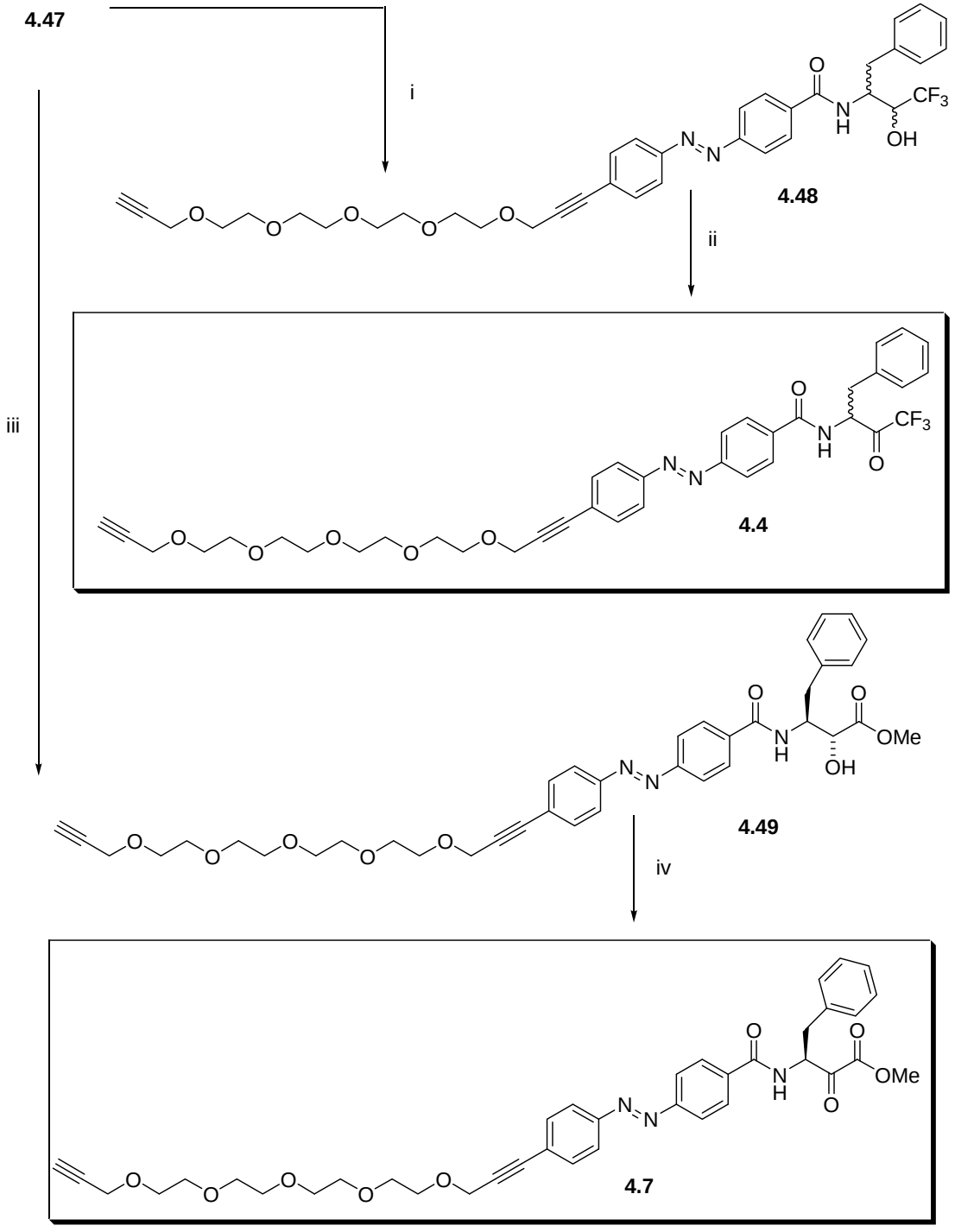

Reagents and conditions: i) **4.8**, EDCI, HOBt, DIEA, DMF, 80% ii) Dess-Martin periodinane, DCM, 90% iii) **4.9**, EDCI, HOBt, DIEA, DMF, 58% iv) Dess-Martin periodinane, DCM, 51%

Scheme 4.14. Synthesis of **4.4** and **4.7**.

4.5 Summary

Azobenzene-containing trifluoromethylketones **4.1**-**4.4** and α-ketoesters **4.5**-**4.7** were synthesised as photoswitch inhibitors of α-chymotrypsin. A terminal alkyne group for surface attachment by azide-alkyne cycloaddition was included in compounds **4.2**-**4.4** and **4.6**-**4.7**.

Precursor **4.9** was synthesised following previously reported methods.[12, 13, 18] While poor yields were obtained, sufficient material was obtained for use in synthesis of inhibitors **4.5**-**4.7**. The protected amines **4.1** and **4.5** were readily synthesised by coupling of carboxylic acid **2.42** to amines **4.8** and **4.9**, respectively, followed by oxidation with Dess-Martin periodinane. Acidic hydrolysis of **4.1** gave amine **4.17**, which was unstable to chromatography. The alkyne **4.2** was synthesised from symmetrical azobenzene precursor **4.21** by direct reaction of the desired substituent groups with **4.20** without use of protecting groups. Several synthetic routes to **4.2** and alternative target **4.18** were attempted, with the coupling of acid chloride **4.21** to amine **4.8** followed by coupling of the product to amine **4.28** to give **4.2** being successful. Alkynes **4.3**-**4.4** and **4.6**-**4.7** were synthesised by Pd-catalysed coupling of an alkyne to an azobenzene with a halide substituent, followed by deprotection, amide coupling to **4.8** or **4.9** then oxidation.

Enzyme assays and photoisomerisation studies carried out on the trifluoromethylketones and α-ketoesters described in this chapter (**4.1**-**4.7**) are described in chapter 6. Surface attachment and SPR studies of photoregulated surface enzyme binding to surface-attached trifluoromethylketone **4.4** are described in chapter 7.

4.6 References

1. Alexander, N. A. PhD thesis. University of Canterbury, **2006**.
2. Harvey, A. J.; Abell, A. D., *Tetrahedron* **2000**, 56, (50), 9763.
3. Angelastro, M. R.; Mehdi, S.; Burkhart, J. P.; Peet, N. P.; Bey, P., *J. Med. Chem.* **1990**, 33, 11.
4. Imperiali, B.; Abeles, R. H., *Biochemistry* **1986**, 25, 3760.
5. Brady, K.; Abeles, R. H., *Biochemistry* **1990**, 29, 7608.

6. Harvey, A. J. PhD thesis. University of Canterbury, **2000**.

7. Rostovtsev, V. V.; Green, L. G.; Fokin, V. V.; Sharpless, K. B., *Angew. Chem. Int. Ed.* **2002**, 41, (14), 2596.

8. Sun, X.-L.; Stabler, C. L.; Cazalis, C. S.; Chaikof, E. L., *Bioconjugate Chem.* **2006**, 17, 52.

9. Kolb, H. C.; Finn, M. G.; Sharpless, K. B., *Angew. Chem. Int. Ed.* **2001**, 40, 2004.

10. Himo, F.; Lovell, T.; Hilgraf, R.; Rostovtsev, V. V.; Noodleman, L.; Sharpless, K. B.; Fokin, V. V., *J. Am. Chem. Soc.* **2005**, 127, 210.

11. Martichonok, V.; Jones, J. B., *J. Am. Chem. Soc.* **1996**, 118, 950.

12. Akahoshi, F.; Ashimori, A.; Sakashita, H.; Yoshimura, T.; Imada, T.; Nakajima, M.; Mitsutomi, N.; Kuwahara, S.; Ohtsuka, T.; Fukaya, C.; Miyazaki, M.; Nakamura, N., *J. Med. Chem.* **2001**, 44, 1286.

13. Foulds, G. PhD thesis. University of Canterbury, **1996**.

14. Harvey, A. J. PhD thesis. University of Canterbury, **2000**.

15. Herranz, R.; Castro-Pichel, J.; Vinuesa, S.; Garcia-Lopez, M. T., *J. Org. Chem.* **1990**, 55, 2232.

16. Kashima, C.; Harada, K.; Fujioka, Y.; Maruyama, T.; Omote, Y., *J. Chem. Soc. Perkin Trans. 1* **1988**, 3, 535.

17. Yuan, W.; Munoz, B.; Wong, C.-H.; Haeggstriim, J. Z.; Wetterholm, A.; Samuelsson, B., *J. Med. Chem.* **1993**, 36, 211.

18. Peet, N. P.; Burkhart, J. P.; Angelastro, M. R.; Giroux, E. L.; Mehdi, S.; Bey, P.; Kolb, M.; Neises, B.; Schirlin, D., *J. Med. Chem.* **1990**, 33, (1), 394.

19. Linderman, R. J.; Graves, D. M., *J. Org. Chem.* **1989**, 54, 661.

20. Tomlinson, M. L., *J. Chem. Soc.* **1946**, 756.

21. Ameerunisha, S.; Zacharias, P. S., *J. Chem. Soc. Perkin Trans. 2* **1995**, 1679.

22. Melissaris, A. P.; Litt, M. H., *J. Org. Chem.* **1992**, 57, 6998.

23. Priewisch, B.; Ruck-Braun, K., *J. Org. Chem.* **2005**, 70, 2350.

24. Pearson, D.; Downard, A. J.; Muscroft-Taylor, A.; Abell, A. D., *J. Am. Chem. Soc.* **2007**, 129, 14862-14863.

Chapter Five

Synthesis of Sulfur-Containing Surface Linkers

Synthesis of sulfur-containing surface linkers

5.1 Introduction

The formation of SAMs of alkyl thiols/disulfides on gold was chosen for the surface attachment of photoswitch enzyme inhibitors (see chapter 1, section 1.4). However, as the inhibitors described in chapters 2-4 do not contain thiol or disulfide groups, linker molecules containing a sulfur group for surface attachment and a carboxylic acid or azide group for attachment to inhibitors were used, as shown in Fig. 5.1. This chapter describes the synthesis of these linkers.

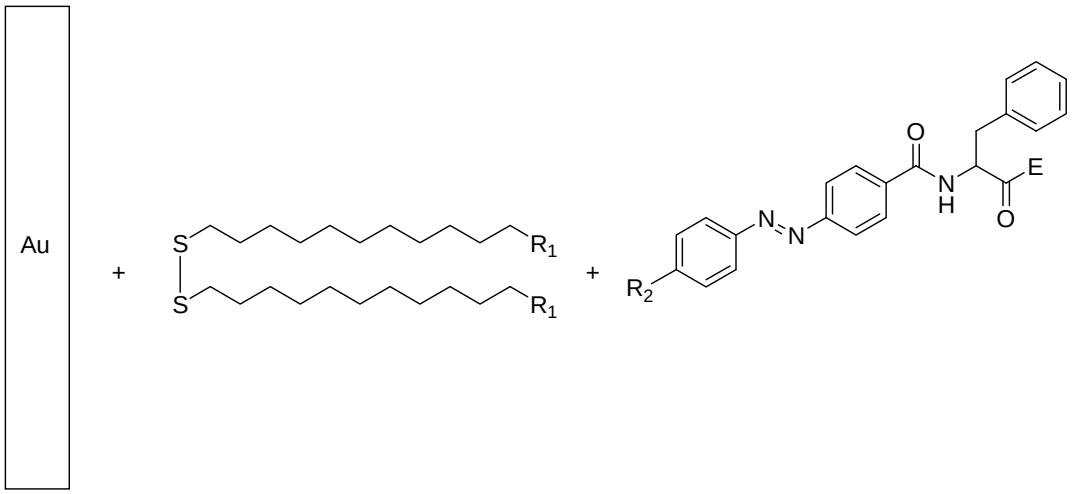

Key: R_1 and R_2 are groups that can be linked together e.g. amine and carboxylic acid, E is an electrophilic group for enzyme binding

Fig. 5.1. Molecular components used to attach photoswitch inhibitors to gold surfaces.

Various thiol/disulfide linkers have been used similarly for the surface attachment of complex molecules. Here, lipoic acid derivatives, acetyl protected alkyl thiols and symmetrical alkyl disulfides were synthesised, in order to obtain a range of surface linker groups for evaluation of the most appropriate for use in surface attachment of photoswitch inhibitors.

Lipoic acid **5.1**[1] (Fig. 5.2) has been used previously as a linker for attachment to surfaces and nanoparticles,[2-4] and was chosen for use here due to its apparent synthetic versatility. In particular, the disulfide group of **5.1** is part of a 5-membered dithiolane ring, and hence both alkyl groups attached to the disulfide group converge into a single chain. Consequently, syntheses involving lipoic acid do not require complex transformations to derivatise both alkyl chains, as can be required in the syntheses of other disulfides.

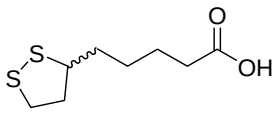

5.1

Fig. 5.2. Lipoic acid **5.1**.

Longer chain alkyl thiols containing carboxylic acid groups are also used often as surface linkers, such as compounds **5.2** and **5.3**[5] (Fig. 5.3). It was considered that these linkers would form higher quality SAMs on gold than lipoic acid derivatives, as they consist of more symmetrical, longer chain molecules that should pack well in a SAM. The thiol **5.2** was chosen for use here as a precursor to protected thiols and symmetrical disulfides for surface attachment.

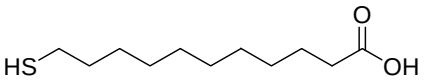

5.2

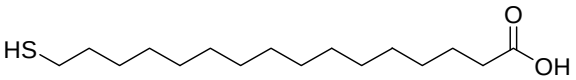

5.3

Fig. 5.3. Alkyl thiols **5.2** and **5.3**.

Non-specific protein binding to hydrophobic surfaces (discussed in chapter 1, section 1.4.3) can be problematic in the study of specific enzyme binding to surface-attached ligands. To reduce this problem, studies of specific binding usually use hydrophilic surface components that block non-specific attachment. In particular, mixed SAMs can be formed containing an enzyme binding component and a hydrophilic diluent that blocks non-specific binding.[6, 7] This inert diluent may have the additional beneficial function of spacing out ('diluting') the active functionality on the surface, improving accessibility for enzyme binding. Here, OEG diluents were used as the hydrophilic component.

This chapter describes the design and synthesis of surface linkers and diluents **5.4**-**5.11** (figs. 5.4 and 5.5), model compounds **5.12**-**5.13** for photoswitching studies (Fig. 5.6), photoswitch inhibitors **5.14**-**5.16** for surface attachment (Fig. 5.7) and inhibitors **5.17**-**5.18** for enzyme assay that mimic surface-attached inhibitors (Fig. 5.8). A range of linkers (amide, triazole) and sulfur groups (protected thiol, disulfide) were used in order to obtain compounds with varying properties for surface attachment studies.

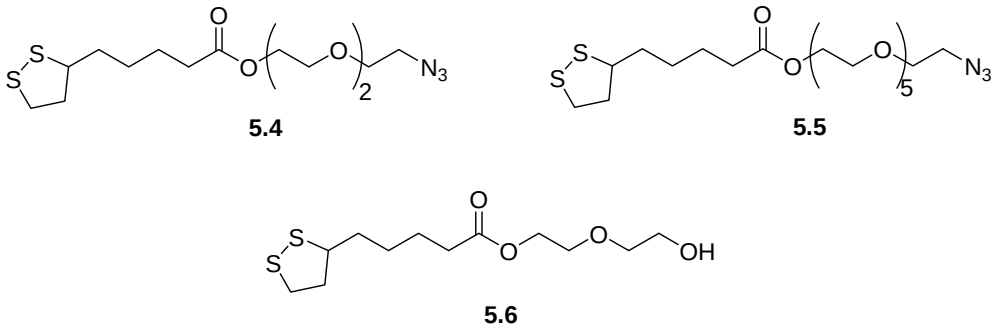

Fig. 5.4. Lipoic acid based surface linkers **5.4**-**5.5** and diluent **5.6**.

The disulfides **5.4**-**5.6** (Fig. 5.4) were synthesised from lipoic acid **5.1**. The surface linkers **5.4**-**5.5** contain an azide group for inhibitor attachment, and the diluent **5.6** contains a terminal OEG group to block non-specific enzyme binding. Longer OEG groups are included in surface linkers **5.4**-**5.5**, so that these compounds can form mixed SAMs with diluent **5.6** but extend further into solution for optimum enzyme binding. Azides **5.4** and **5.5** contain OEG groups of differing lengths, in order to investigate the influence of chain length on enzyme binding.

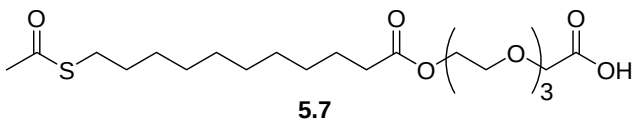

5.7

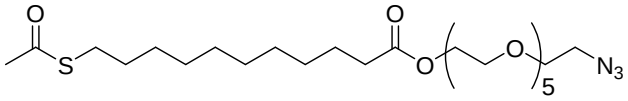

5.8

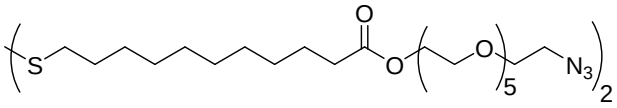

5.9

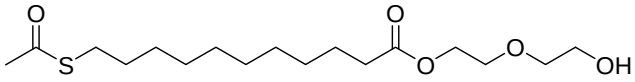

5.10

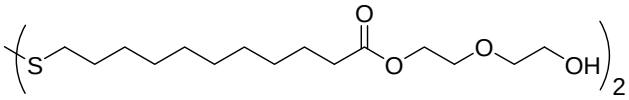

5.11

Fig. 5.5. Surface linkers and diluents synthesised from thiol **5.2**.

The surface linkers **5.7**-**5.9** and diluents **5.10**-**5.11** (Fig. 5.5) are synthesised from alkyl thiol **5.2**. These compounds are similar in structure to lipoic acid derivatives **5.4**-**5.6**, but contain longer alkyl chains and symmetrical disulfides or protected thiols for surface attachment. In addition, **5.7** contains a carboxylic acid group for inhibitor attachment rather than an azide group. While the protected thiols **5.7**, **5.8** and **5.10** may form SAMs on gold,[8] disulfides **5.9** and **5.11** are expected to be more reliable for SAM formation.

Azobenzenes **5.12** and **5.13** (Fig. 5.6) were designed for use in photoswitching studies to assess the potential of the surface linkers for use in surface photoswitching. Both compounds consist of a surface linker (lipoic acid **5.1** or protected thiol **5.7**) attached to an azobenzene.

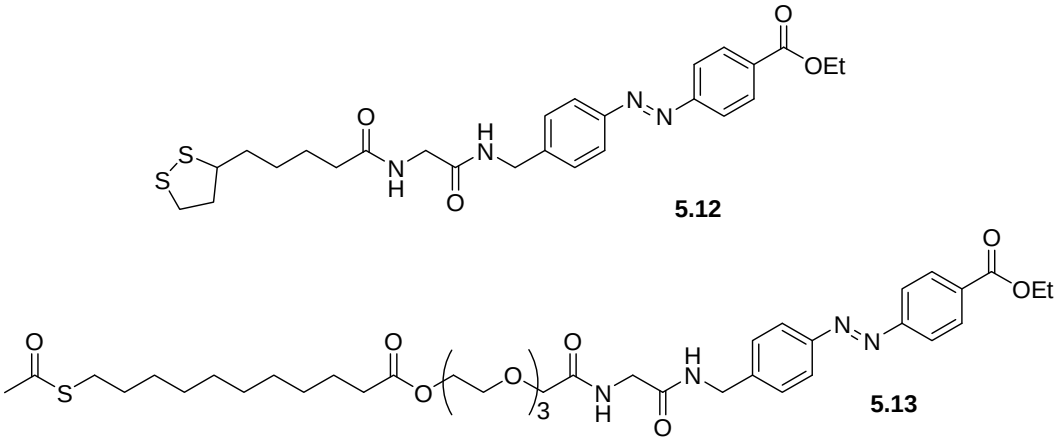

Fig. 5.6. Model compounds **5.12** and **5.13** for photoswitching studies of surface linkers.

Compounds **5.14-5.16** (Fig. 5.7) consist of photoisomerisable trifluoromethylketones attached to selected surface linkers, for use in surface attachment and photoswitching studies.

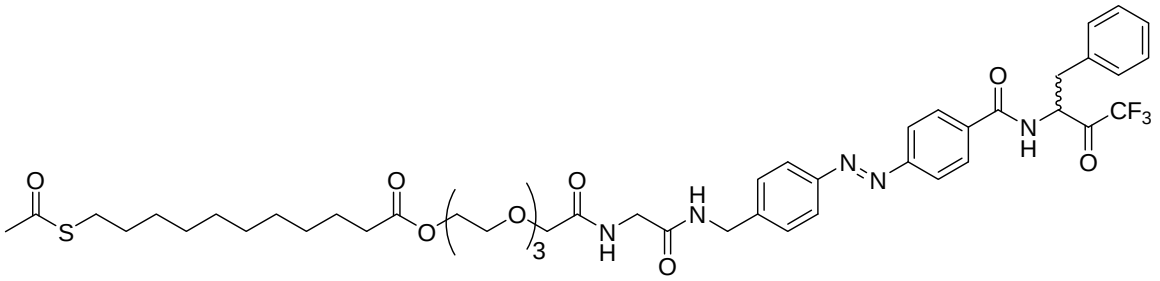

5.14

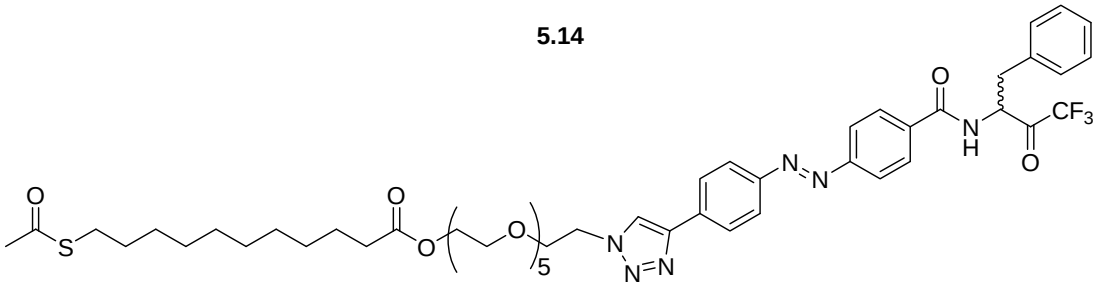

5.15

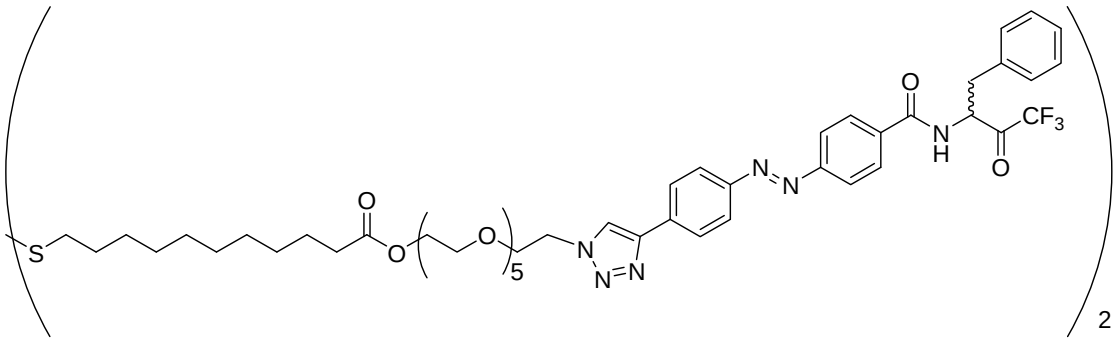

5.16

Fig. 5.7. Surface-attachable photoswitch inhibitors **5.14-5.16**.

Many of the inhibitors that were synthesised in chapter 4 and found to be excellent photoswitch inhibitors (see chapter 6 for photoisomerisation and assay results) were not attached to surface linkers. This is simply due to the chronological order in which this research was performed, since later studies involved SPR, which does not require thiol/disulfide linkers for surface attachment.

Compounds **5.15-5.16** contain triazole groups linking the azobenzene to the alkyl disulfide group. As the azobenzene group is expected to bind to the S_2 subsite of the α-chymotrypsin active site, these triazole groups should be associated with the S_2 and/or S_3 subsites. Consequently, the triazole group is likely to affect the binding and photoswitching properties of inhibitors **5.15-5.16**. To test this prediction, it was of interest to carry out enzyme assays for compounds **5.15-5.16** to assess their enzyme binding and photoswitching properties. However, these compounds are insufficiently water soluble for assays to be carried out, so water soluble model compounds **5.17** and α-ketoester analogue **5.18** (Fig. 5.8) were synthesised by cycloaddition of an OEG azide to alkynes **4.3** and **4.6**, respectively. These compounds mimic the structure of surface-attached alkynes **4.3** and **4.6**, and thus assay and photoisomerisation of these compounds provides information about surface binding and photoswitching of **4.3** and **4.6** (and **5.15-5.16**).

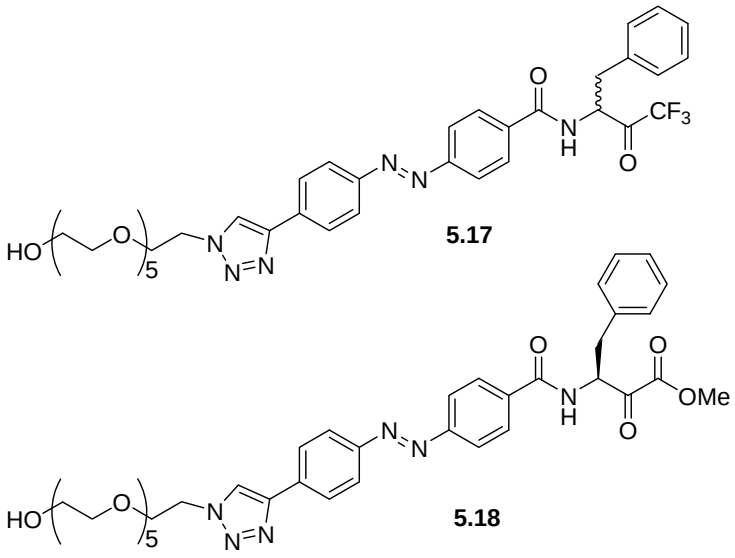

Fig. 5.8. Photoswitch inhibitors **5.17-5.18** designed to mimic surface attached **4.3** and **4.6**.

5.2 Synthesis of lipoic acid derivatives

*Synthesis of **5.4***

The azide surface linker **5.4** was prepared by coupling of known azide **5.21**[9] to lipoic acid **5.1**, as shown in Scheme 5.1. Triethylene glycol **5.19** was reacted with mesyl chloride in the presence of silver oxide to give mesylate **5.20**[5], which was then reacted with sodium azide to give azide **5.21** in quantitative yield. Finally, **5.21** was coupled to lipoic acid **5.1** in the presence of HATU to give **5.4** in 38% yield.

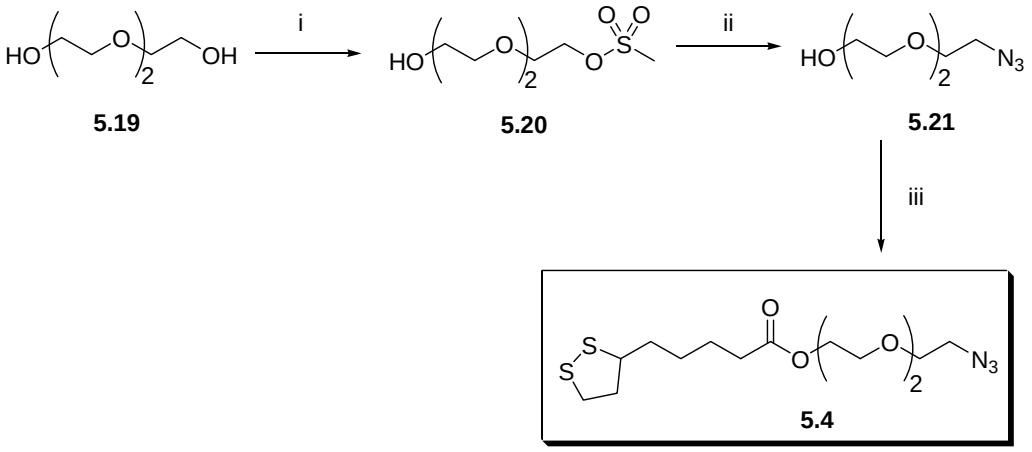

5.19 **5.20** **5.21** **5.4**

Reagents and conditions: i) MsCl, Ag_2O, DCM, 65% ii) NaN_3, DMF, 110ºC, qu. iii) **5.1**, HATU, DIEA, DMF, 38%

Scheme 5.1. Synthesis of azide surface linker **5.4**.

*Synthesis of **5.5***

The azide **5.5** was prepared as shown in Scheme 5.2. Initially, hexaethylene glycol **5.22** was reacted with mesyl chloride to give mesylate **5.23,** using alternative reaction conditions (NaH, THF) to those used to prepare **5.20**. Poorer yield was obtained than in the synthesis of **5.20**; however, the reaction time was much shorter (16 h rather than 68 h). The mesylate **5.23** was then reacted with sodium azide to obtain **5.24** in 81% yield. Finally, azide **5.24** was coupled to **5.1** to give **5.5** in 77% yield. Here, EDCI coupling reagent was used, since use of HATU gave a poor yield in the synthesis of **5.4**.

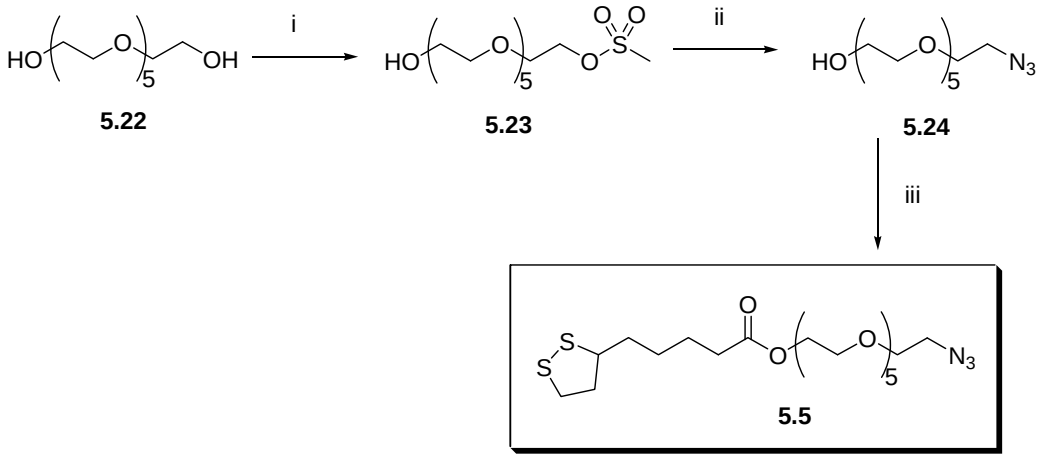

Reagents and conditions: i) MsCl, NaH, THF, 0ºC → r.t., 45% ii) NaN_3, DMF, 110ºC, 81% iii) **5.1**, EDCI, DMAP, DCM, 77%

Scheme 5.2. Synthesis of azide surface linker **5.5**.

Synthesis of ***5.6***

The diluent **5.6** was synthesised as shown in Scheme 5.3. Lipoic acid **5.1** was coupled to diethylene glycol in the presence of EDCI and DMAP to give ester **5.6** in 78% yield.

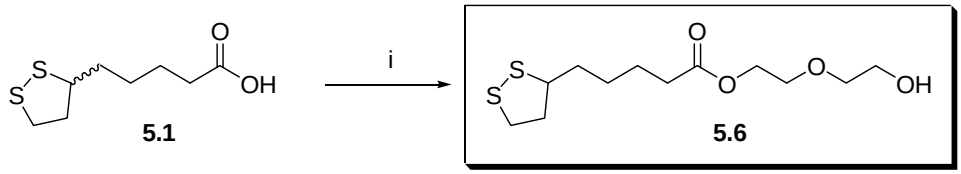

Reagents and conditions: i) diethylene glycol, EDCI, DMAP, DCM, 78%

Scheme 5.3. Synthesis of surface diluent **5.6**.

5.3 Synthesis of thiols and symmetrical disulfides

Surface linkers and diluents **5.7**-**5.11** were synthesised from thiol **5.2**, which was initially protected as a thioester to reduce the reactivity of this group for amide coupling reactions.

Synthesis of ***5.7***

The carboxylic acid **5.7** was synthesised as shown in Scheme 5.4. Thiol **5.2** was reacted with acetyl chloride to give thioester **5.25**. Bromide **5.26** was coupled to triethylene glycol **5.19** in the presence of base (NaH) to give alcohol **5.27** in 38% yield, which was then coupled to carboxylic acid **5.25** in the presence of EDCI and DMAP to give ester **5.28** in 64% yield. This ester was treated with TFA to give carboxylic acid **5.7**.

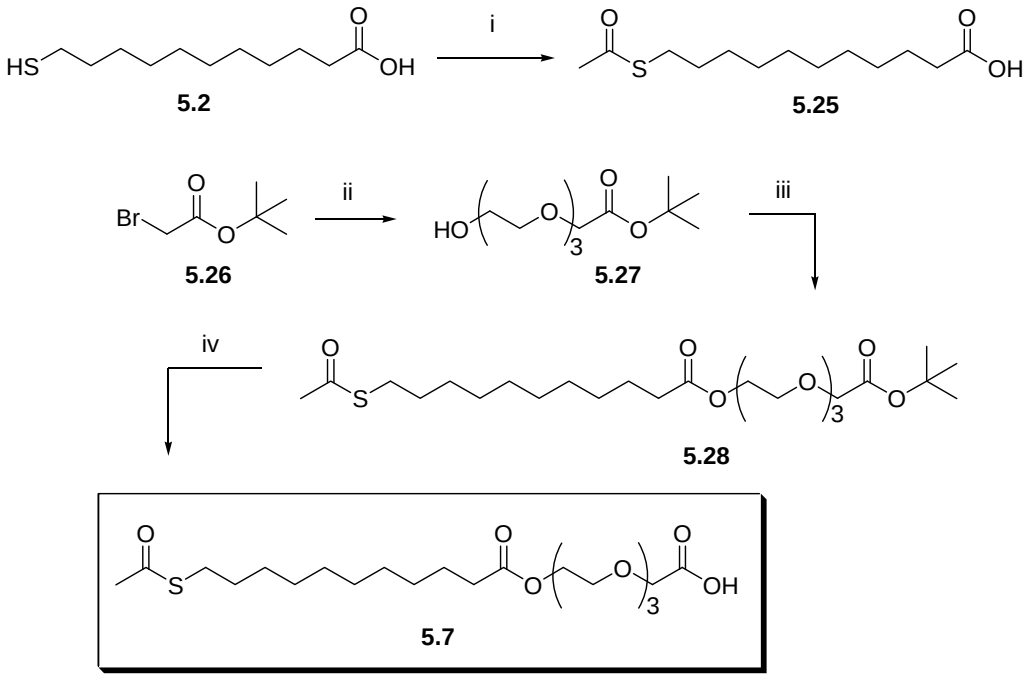

Reagents and conditions: i) AcCl, AcOH, DCM, 0ºC → r.t., 63% ii) triethylene glycol **5.19**, NaH, THF, 0ºC → r.t., 38% iii) **5.25**, EDCI, DMAP, DCM, 63% iv) TFA, DCM, 74%

Scheme 5.4. Synthesis of carboxylic acid surface linker **5.7**.

Synthesis of ***5.8*** *and* ***5.9***

The azides **5.8** and **5.9** were prepared as shown in Scheme 5.5. First, carboxylic acid **5.25** was reacted with azide **5.24** to give **5.8** in 38% yield. The thioacetate **5.8** was then treated

with hydrazine acetate to give disulfide **5.9** in quantitative yield. Hydrazine acetate was used since mild hydrolysis conditions were required to avoid cleavage of the ester group. Deprotection of a similar thioester has been reported using this reagent.[10]

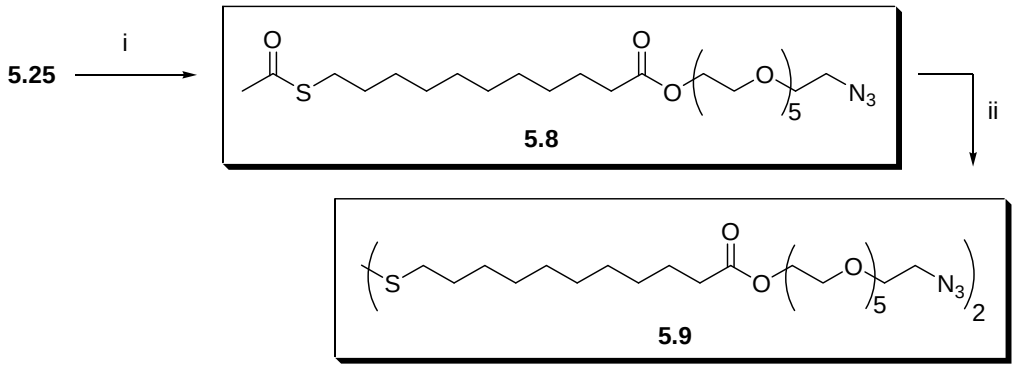

Reagents and conditions: i) **5.24**, EDCI, DMAP, DCM, 38% ii) N_2H_4.AcOH, DMF, qu.

Scheme 5.5. Synthesis of azide surface linkers **5.8** and **5.9**.

*Synthesis of **5.10** and **5.11***

The diluents **5.10** and **5.11** were prepared as shown in Scheme 5.6. First carboxylic acid **5.25** was reacted with diethylene glycol in the presence of EDCI and DMAP to obtain **5.10** in 63% yield. The thioester **5.10** was then treated with hydrazine acetate to give disulfide **5.11** in 67% yield.

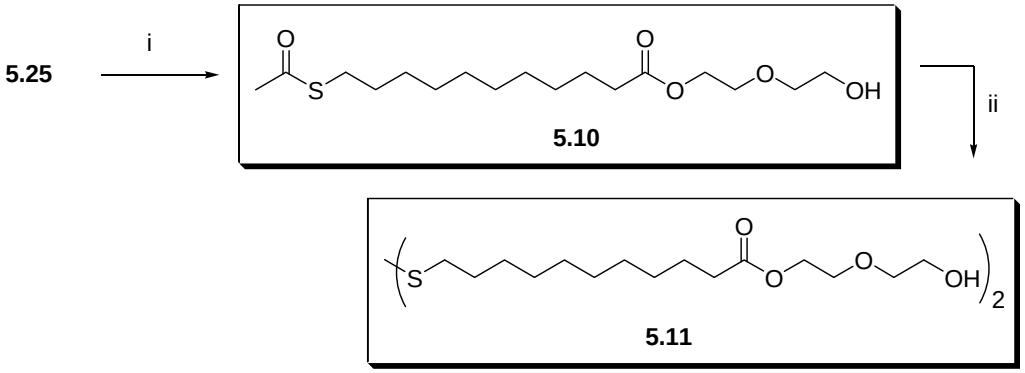

Reagents and conditions: i) diethylene glycol, EDCI, DMAP, DCM, 63% ii) N_2H_4.AcOH, DMF, 67%

Scheme 5.6. Synthesis of surface diluents **5.10** and **5.11**.

5.4 Attachment of azobenzenes to thiol/disulfide linkers

*Synthesis of **5.12***

Compound **5.12** was synthesised as shown in Scheme 5.7. Initially, azobenzene **2.41** was treated with TFA to give amine **5.29** in 99% yield. This amine was then coupled to lipoic acid **5.1** in the presence of EDCI to give amide **5.12** in 36% yield.

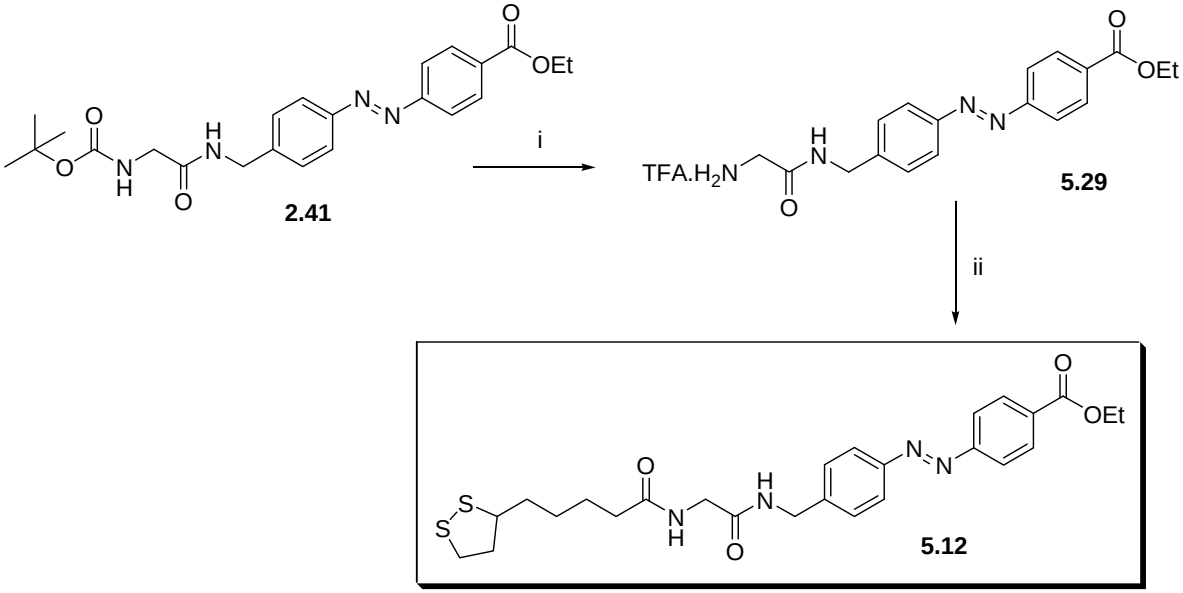

Reagents and conditions: i) TFA, DCM, 99% ii) **5.1**, EDCI, HOBt, DIEA, DMF, 36%

Scheme 5.7. Synthesis of azobenzene **5.12** for photoswitching studies.

*Synthesis of **5.13***

The azobenzene **5.13** was synthesised as shown in Scheme 5.8, by coupling of amine **5.29** and carboxylic acid **5.7** in the presence of EDCI to give **5.13** in 53% yield.

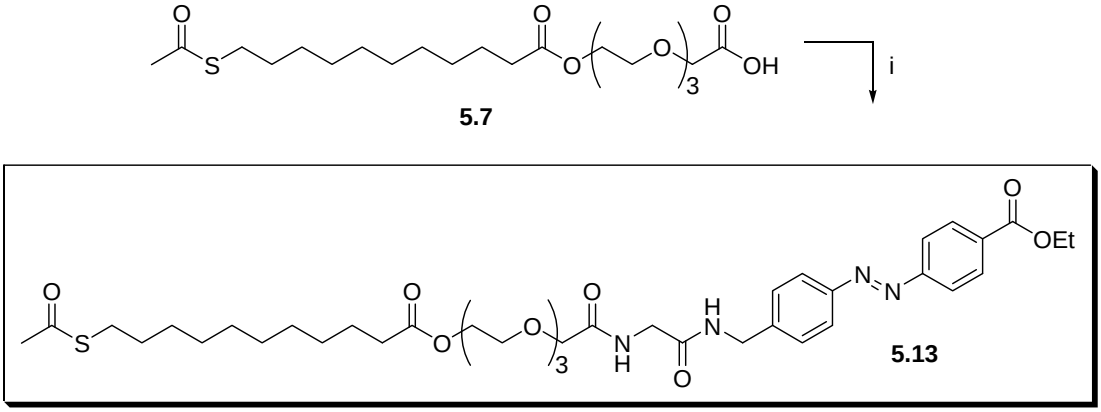

Reagents and conditions: i) **5.29**, EDCI, HOBt, DIEA, DCM, 53%

Scheme 5.8. Synthesis of model azobenzene **5.13** for photoswitching studies.

5.5 Attachment of photoswitch inhibitors to surface linkers

*Synthesis of **5.14***

The protected thiol **5.14** was prepared as shown in Scheme 5.9. Trifluoromethylalcohol **4.16** was treated with TFA to obtain amine **5.30**, which was then coupled to carboxylic acid **5.7** in the presence of EDCI to give amide **5.31** in 99% yield. Finally, **5.31** was oxidised to trifluoromethylketone **5.14** using Dess-Martin periodinane.

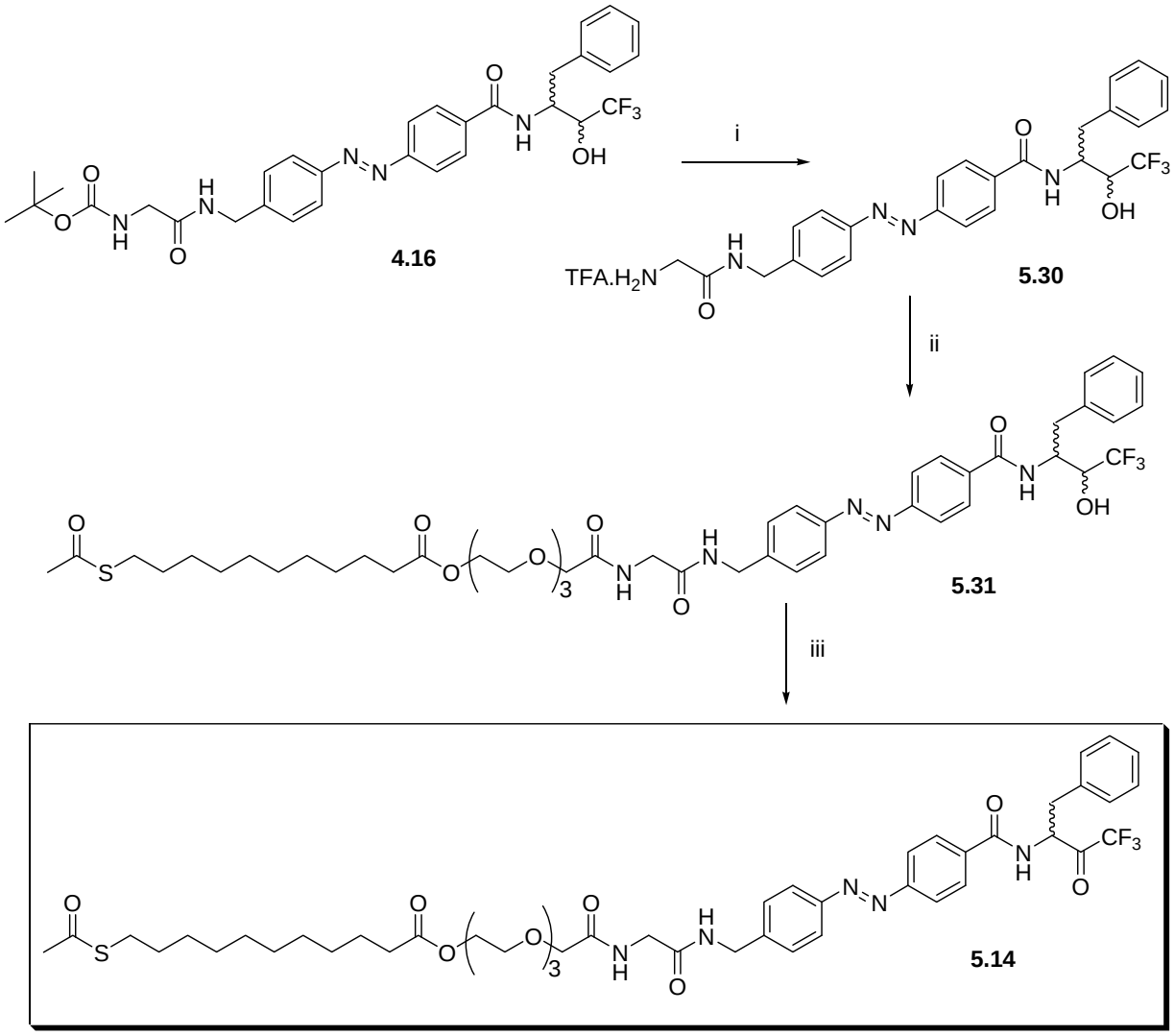

Reagents and conditions: i) TFA, DCM, 60% ii) **5.7**, EDCI, HOAt, DIEA, DMF, 99% iii) Dess-Martin Periodinane, 38%

Scheme 5.9. Synthesis of azobenzene **5.14** for enzyme binding and photoswitching at surfaces.

*Synthesis of **5.15***

The azobenzene **5.15** was prepared by azide-alkyne cycloaddition of alkyne **4.3** and azide **5.8**, as shown in Scheme 5.10. The reaction was initially carried out using the conditions shown in Table 5.1, entry (i). Very poor yield of **5.15** (4%) was obtained, which was surprising considering the reported ease of this reaction. Normally, t-BuOH is used as solvent, but EtOH was used here since it would be the preferred solvent for use in attachment of alkyne **4.3** to an azide SAM. Furthermore, higher reactant concentrations are normally used. However, as relatively low amounts of reactants were available for use here, and practical solvent volumes were required (> 1 mL), the resulting concentrations were low. The reactants dissolved poorly in the first attempt, so the reaction was repeated using an increased solvent volume and a greater proportion of ethanol, as shown in table 5.1, entry (ii). A greater amount of reactants dissolved under these conditions and triazole **5.15** was obtained in 26% yield.

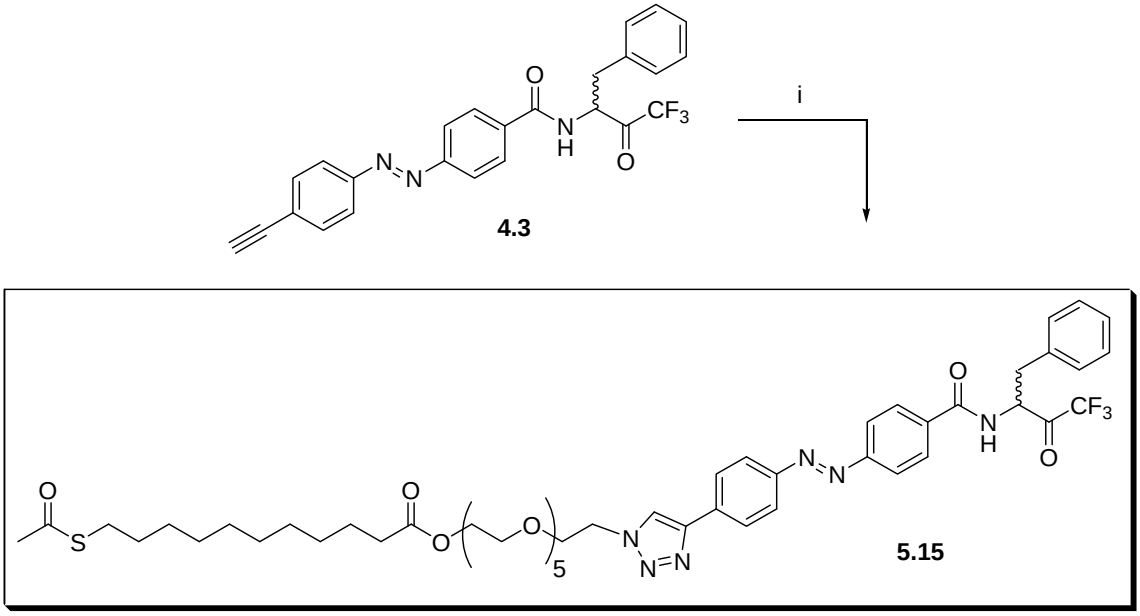

Reagents and conditions: i) **5.8**, $CuSO_4$, sodium ascorbate, EtOH, H_2O, 35%

Scheme 5.10. Synthesis of azobenzene **5.15** for enzyme binding and photoswitching at surfaces.

Table 5.1. Reaction conditions† and yields for reaction of alkyne **4.3** with azide **5.8**.

Entry	Concentrations of alkyne **4.3** and azide **5.8** (mM)	Solvent	Yield of **5.15**
i	11	1:1 EtOH/H_2O	4%
ii	2.0	9:8 EtOH/H_2O	26%

†All reactions were carried out in the presence of catalysts $CuSO_4$ (1 mol%) and sodium ascorbate (5 mol%) at r.t. for 16 h.

Optimisation of azide-alkyne cycloadditions using a model system

As the cycloaddition gave a maximum yield of 26%, reaction conditions were optimised using a model system. The reaction of benzyl azide **5.32** with nitrophenyl propargyl ether **5.34** (see Scheme 5.12 below) was chosen as a model reaction, since it has been previously reported as a simple azide-alkyne cycloaddition.[11] The alkyne starting material **5.34** was synthesised as shown in Scheme 5.11. Nitrophenol **5.33** was reacted with propargyl bromide and base (K_2CO_3) to give **5.34** in 40% yield.

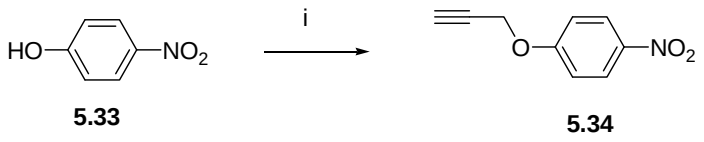

5.33 **5.34**

Reagents and conditions: i) propargyl bromide, K_2CO_3, DMF, 40%

Scheme 5.11. Synthesis of alkyne **5.34**.

Cycloaddition of **5.32** and **5.34** to give triazole **5.35** (scheme 5.12) was then carried out under previously reported conditions,[11] as shown in Table 5.2, entry (i), to give **5.35** in 78% yield. The elevated temperature and high concentration in this reaction are undesirable for reactions of the surface linkers and inhibitors used here, so the reaction was repeated at lower concentration and temperature and with a longer reaction time, as shown in Table 5.2, entry (ii). Under these conditions ^{1}H NMR of the reaction mixture after 16 h showed only 11% product present. To improve yield, the reaction was repeated using stoichiometric amounts of $CuSO_4$ and sodium ascorbate (instead of catalytic amounts), as shown in Table 5.2, entry (iii). ^{1}H NMR of the reaction mixture after 16 h showed 80% product, a significant improvement.

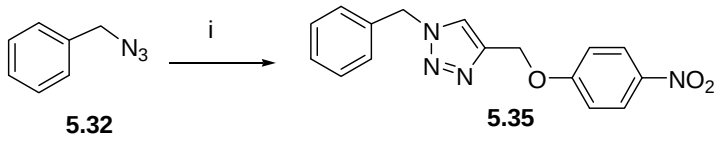

5.32 **5.35**

Reagents and conditions: i) **5.34**, t-BuOH, H_2O, 60ºC, 78%

Scheme 5.12. Model azide-alkyne cycloaddition.

Table 5.2. Reaction conditions† and yields for reaction of alkyne **5.34** with azide **5.32**.

Entry	Concentration of alkyne **5.34** and azide **5.32** (mM)	Catalysts	Temperature (ºC)	Reaction time (h)	Yield of **5.35**
i	500	5 mol% $CuSO_4$, 10 mol% sodium ascorbate	60	1.25	78%
ii	50	5 mol% $CuSO_4$, 10 mol% sodium ascorbate	r.t.	16	11
iii	50	1 eq $CuSO_4$, 1 eq sodium ascorbate	r.t.	16	80

†All reactions were carried out in 1:1 tBuOH/H_2O.

*Synthesis of **5.16***

Having determined an acceptable method using this model system, similar conditions were used in the reaction of surface linker **5.9** with photoswitch inhibitor **4.3**, as shown in Scheme 5.13. The alkyne **4.3** was reacted with azide **5.9** in the presence of 2.2 equivalents of $CuSO_4$ and sodium ascorbate to give triazole **5.16** in 82% yield.

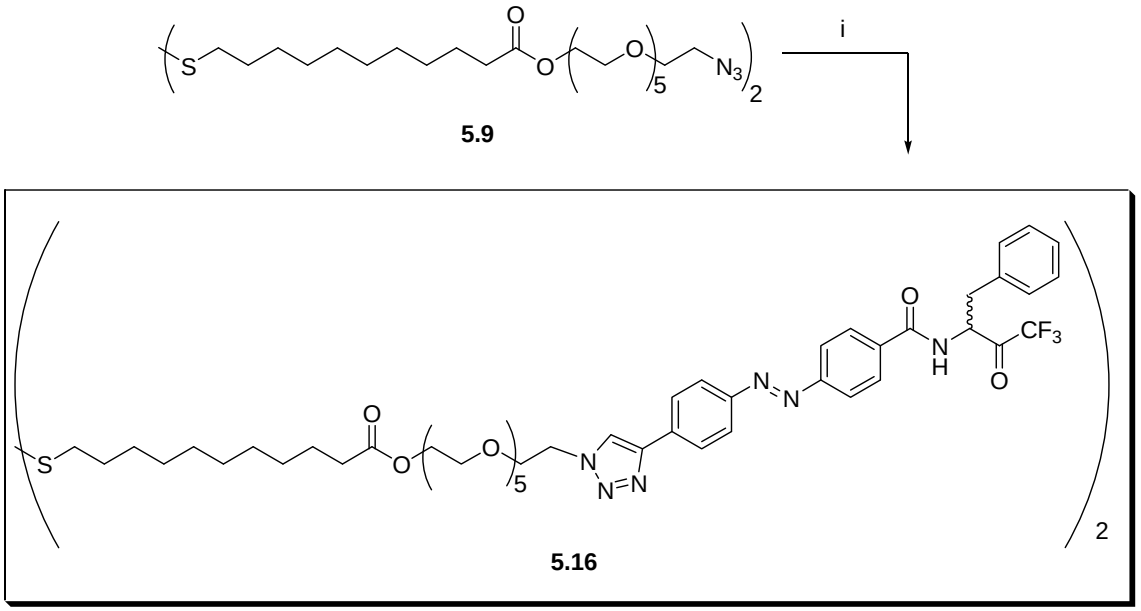

Reagents and conditions: i) **4.3**, $CuSO_4$, sodium ascorbate, t-BuOH, H_2O, 82%

Scheme 5.13. Synthesis of azobenzene **5.16** for enzyme binding and photoswitching at surfaces.

5.6 Synthesis of analogues of surface-attached inhibitors for assay

*Synthesis of **5.17***

The alkyne **4.3** was reacted with azide **5.24** in the presence of 1.1 equivalents of $CuSO_4$ and sodium ascorbate to give triazole **5.17** in 68% yield (Scheme 5.13).

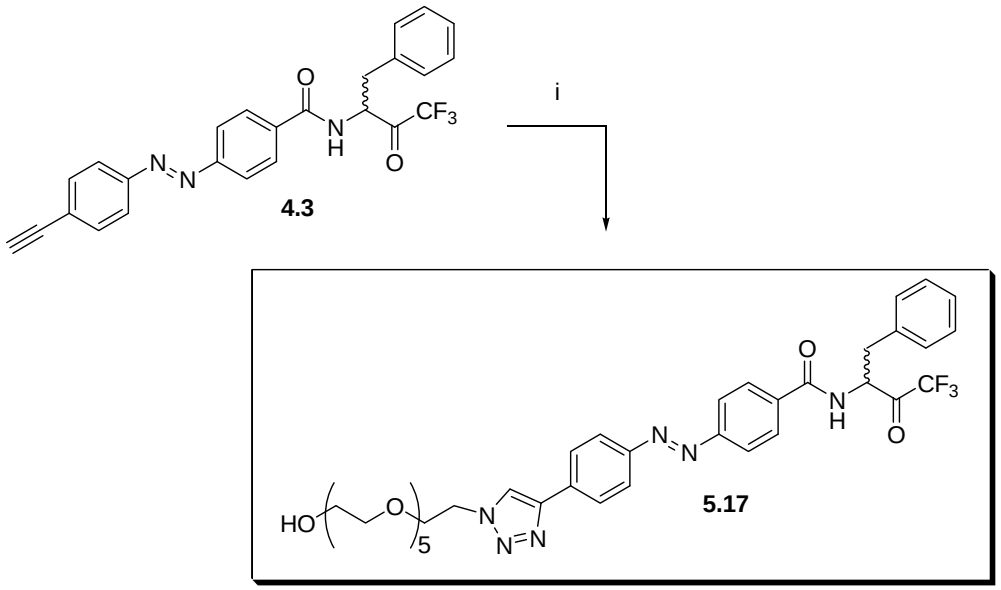

Reagents and conditions: i) **5.24**, $CuSO_4$, sodium ascorbate, t-BuOH, H_2O, 68%

Scheme 5.13. Synthesis of model triazole **5.17** for enzyme assay.

*Synthesis of **5.18***

The alkyne **4.6** was reacted with azide **5.24** in the presence of 1.1 equivalents of $CuSO_4$ and sodium ascorbate to give triazole **5.18** in 37% yield (Scheme 5.14).

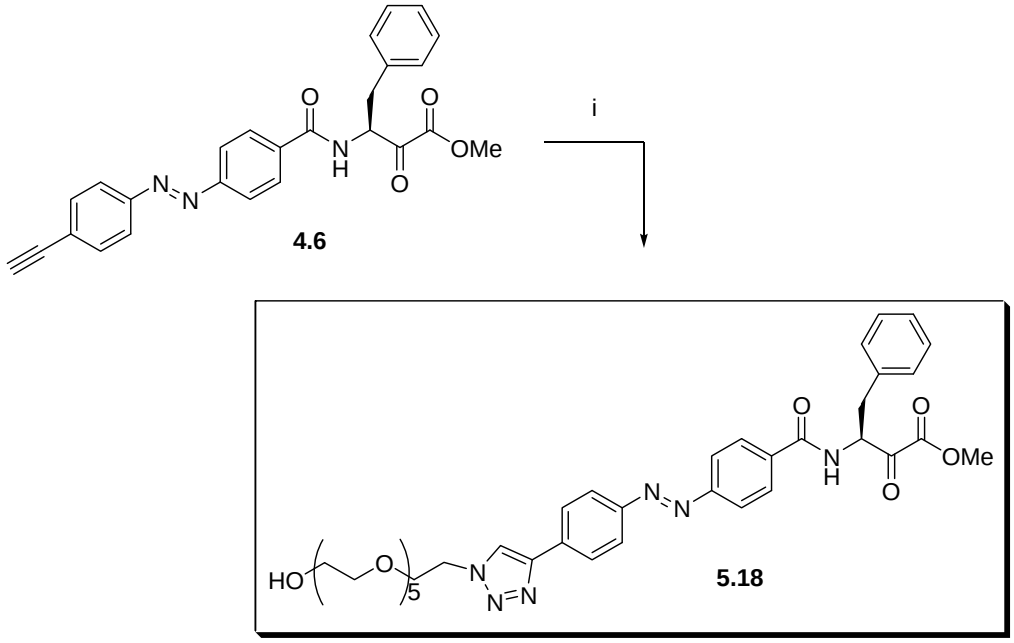

Reagents and conditions: i) **5.24**, $CuSO_4$, sodium ascorbate, t-BuOH, H_2O, 37%

Scheme 5.14. Synthesis of model triazole **5.18** for enzyme assay.

5.7 Summary

A range of thiol/disulfide surface linkers was synthesised for surface attachment of photoswitch enzyme inhibitors. The disulfides **5.4**-**5.5** containing azide groups for surface attachment of inhibitors and diluent **5.6** for blocking of non-specific protein adsorption were synthesised from lipoic acid **5.1**. Analogous protected thiols **5.7**-**5.8** containing carboxylic acid or azide groups and diluent **5.10** were synthesised from thiol **5.2**. The symmetrical disulfides **5.9** and **5.11** were prepared by deprotection of thioesters **5.8** and **5.10**.

The azobenzene **5.29** was coupled to lipoic acid **5.1** and to protected thiol **5.7** to give azobenzenes **5.12** and **5.13** for photoswitching studies. The trifluoromethylalcohol **4.16** was attached to surface linker **5.7** by deprotection and amide coupling to give **5.14** for enzyme binding and photoswitching studies, and trifluoromethylketone **4.3** was attached to

surface linkers **5.8** and **5.9** by azide-alkyne cycloaddition to give **5.15** and **5.16** for the same purpose. The trifluoromethylketone **4.3** and α-ketoester **4.6** were reacted with OEG azide **5.24** to form model compounds **5.17** and **5.18** for enzyme assay that mimic the structure of surface-attached **4.3** and **4.6**.

Photoisomerisation studies of azobenzenes **5.12**-**5.13** and **5.17**-**5.18** and enzyme assays of trifluoromethylketone **5.17** and α-ketoester **4.18** are described in chapter 6. Surface attachment of disulfides **5.9**, **5.11** and **5.16** and QCM studies of enzyme binding to surface-attached trifluoromethylketone **5.16** are described in chapter 7.

5.8 References

1. Gruzman, A.; Hidmi, A.; Katzhendler, J.; Haj-Yehiec, A.; Sassona, S., *Bioorg. Med. Chem.* **2004**, 12, 1183.

2. Kim, K.; Yang, H.; Jon, S.; Kim, E.; Kwak, J., *J. Am. Chem. Soc.* **2004**, 126, 15368.

3. Schiller, S. M.; Naumann, R.; Lovejoy, K.; Kunz, H.; Knoll, W., *Angew. Chem. Int. Ed.* **2003**, 42, (2), 208.

4. Uyeda, H. T.; Medintz, I. L.; Jaiswal, J. K.; Simon, S. M.; Mattoussi, H., *J. Am. Chem. Soc.* **2005**, 127, 3870.

5. Svedhem, S.; Hollander, C.-A.; Shi, J.; Konradsson, P.; Liedberg, B.; Svensson, S. C. T., *J. Org. Chem.* **2001**, 66, 4494.

6. Mrksich, M.; Grunwell, J. R.; Whitesides, G. M., *J. Am. Chem. Soc.* **1995**, 117, 12009.

7. Sigal, G. B.; Bamdad, C.; Barberis, A.; Strominger, J.; Whitesides, G. M., *Anal. Chem.* **1996**, 68, 490.

8. Lau, K. H. A.; Huang, C.; Yakovlev, N.; Chen, Z. K.; O'Shea, S. J., *Langmuir* **2006**, 22, 2968.

9. Rensen, P. C. N.; Leeuwen, S. H. v.; Sliedregt, L. A. J. M.; Berkel, T. J. C. v.; Biessen, E. A. L., *J. Med. Chem.* **2004**, 47, 5798.

10. Tinazli, A.; Tang, J.; Valiokas, R.; Picuric, S.; Lata, S.; Piehler, J.; Liedberg, B.; Tamp, R., *Chem. Eur. J.* **2005**, 11, 5249.

11. Sharpless, W. D.; Wu, P.; Hansen, T. V.; Lindberg, J. G., *J. Chem. Ed.* **2005**, 82, (12), 1833.

Chapter Six

Photoisomerisation and Enzyme Inhibition Studies

Photoisomerisation and enzyme inhibition studies

6.1 Introduction

Photoregulated enzyme binding to a surface required a surface-bound enzyme inhibitor that exhibits a significant change in potency on photoisomerisation. This chapter describes UV/visible photoisomerisation experiments and enzyme assays that were carried out on the compounds described in chapters 2-5 to assess their photoswitching and enzyme inhibition properties, in order to select the best compounds for surface photoswitching studies.

As discussed in chapter 1, the *E* and *Z* isomers of azobenzenes are excited by UV/visible irradiation, allowing controlled *E*/*Z* isomerisation. Methods were thus required to irradiate azobenzenes and to characterise and quantify the isomers obtained from irradiation. Irradiation was carried out using a Hg arc lamp with filters to select UV or visible light and characterisation of *E* and *Z* isomers was performed by analysis of ^{1}H NMR spectra, based on reported methods.[1-3]

Inhibition of α-chymotrypsin was measured using a spectrophotometric assay that measures the rate of hydrolysis of substrate MeO-Suc-Ala-Ala-Pro-Phe-4-nitroanilide,[4] as shown in Scheme 6.1. The increase in the visible absorption of released 4-nitroaniline was measured at 405 nm and plotted against reaction time to obtain a linear graph with slope proportional to the rate of hydrolysis. Determining hydrolysis rates at a range of substrate and/or inhibitor concentrations then allowed calculation of kinetic parameters K_m and V_{max} and/or inhibition constants IC_{50} or K_i.[†]

[†] The IC_{50} inhibition constant represents the concentration of inhibitor required to halve the rate of reaction, and the K_m, V_{max} and K_i parameters are constants in the following Michaelis-Menten equation for the initial rate of an enzymatic reaction with competitive inhibition:

$$V_0 = \frac{V_{\max}[S]}{\left(1+\frac{[I]}{K_i}\right)K_m + [S]}$$

Where V_0 is the initial rate, [S] is the concentration of substrate and [I] is the concentration of inhibitor. Here V_{max} represents the maximum possible rate of enzyme hydrolysis at saturation of all enzyme sites, K_m represents the substrate concentration that gives rise to a rate equal to half of V_{max}, and K_i represents the concentration of inhibitor required to give an apparent doubling of K_m.

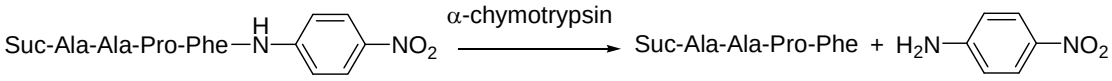

Scheme 6.1. α-Chymotrypsin catalysed hydrolysis of MeO-Suc-Ala-Ala-Pro-Phe-pNA.

6.2 Optimisation of photoisomerisation studies

Photoisomerisation of model azobenzene ***2.26***

Initially, photoisomerisation of simple azobenzene **2.26** (Fig. 6.1) was carried out to optimise irradiation conditions. A solution of *E*-**2.26** (2 mg) in d_3-acetonitrile (500 μL) was placed in a quartz NMR tube and a ^{1}H NMR spectrum of the sample was obtained. The spectrum (Fig. 6.2) shows only *E* isomer. This sample was then irradiated with UV light to induce *E* to *Z* photoisomerisation.

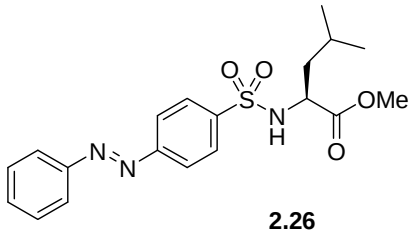

2.26

Fig. 6.1. Azobenzene **2.26** for initial photoisomerisation studies.

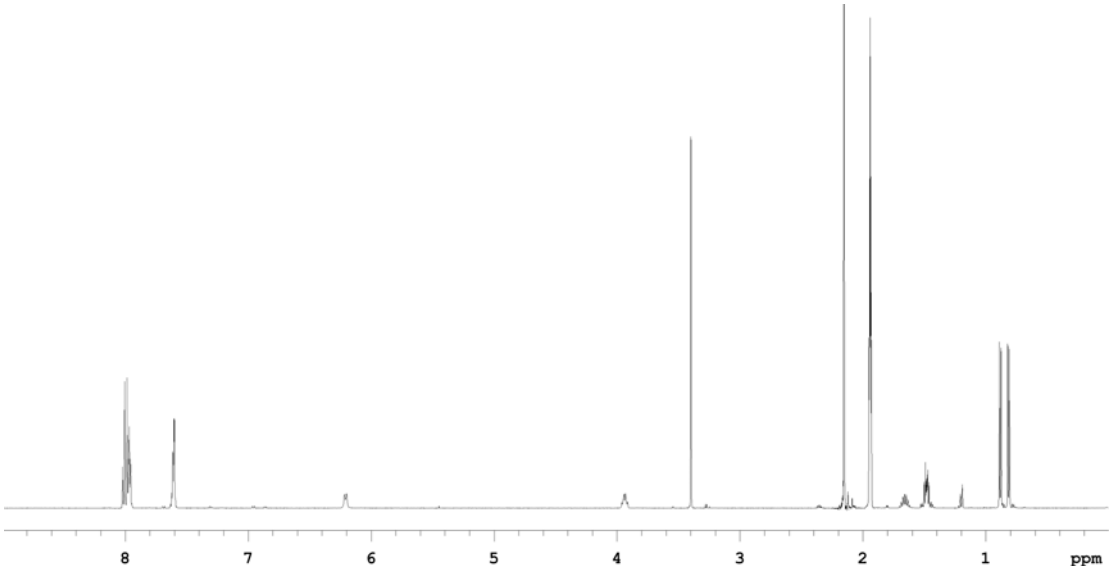

Fig. 6.2. ^{1}H NMR spectrum of *E*-**2.26**.

Irradiation was initially carried out using a Schott UG11 UV filter to select UV wavelengths from a Hg arc lamp and a water filter to remove heat from the UV beam. The NMR tube containing *E*-**2.26** was irradiated for 90 min, obtaining ^{1}H NMR spectra after 30, 60 and 90 min. The spectrum obtained after 30 min irradiation is given in Fig. 6.3, showing a series of new upfield peaks assigned to the *Z* isomer. The sample was then irradiated with visible light (using a Corning 0-51 visible filter) for 60 min to induce *Z* to *E* isomerisation. A further ^{1}H NMR spectrum was obtained (not shown), which revealed a decrease in the integrals of peaks corresponding to the *Z* isomer. Finally, the sample was left in ambient lighting conditions (fluorescent indoor lighting) for 24 h in order to reach an ambient light PSS, and a ^{1}H NMR spectrum was obtained. *E*/*Z* isomeric proportions were determined from each spectrum by comparison of the integrals of peaks corresponding to the amide protons at 6.1 ppm (*Z*) and 6.2 ppm (*E*), as shown in Table 6.1.

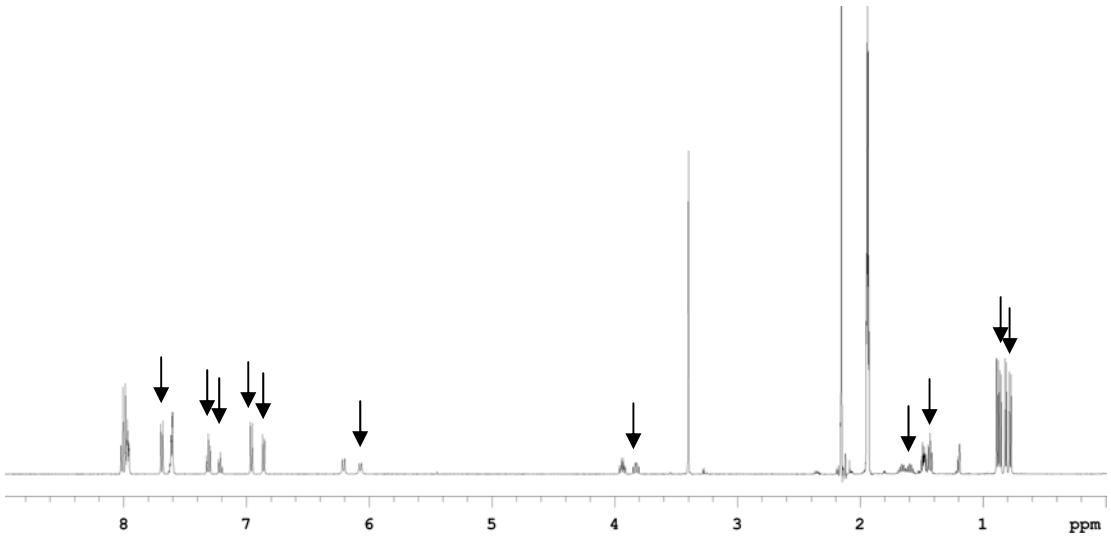

Fig. 6.3. ^{1}H NMR spectrum of *Z*-enriched azobenzene **2.26** (44% *Z*) resulting from 30 min UV irradiation. Arrows show new peaks assigned to *Z*-**2.26**.

Table 6.1. *E*:*Z* ratios for azobenzene **2.26** before/after UV/vis irradiation.

Irradiation(s) carried out	***E:Z* ratio determined by ^{1}H NMR**
None	>95 : <5
UV 30 min	56 : 44
UV 60 min	54 : 46
UV 90 min	53 : 47
UV 90 min, visible 60 min	85 : 15
UV, visible, ambient lighting 16 h	80 : 20

A maximum *Z* isomer enrichment of 47% was obtained from UV irradiation (after 90 min). This represents relatively poor photoisomerisation compared to previous studies, which generally report 70-90% *Z* isomer after UV irradiation.[2, 3] Visible irradiation gave 15% *Z*, similar to previous studies. The PSS obtained in ambient lighting contained 20% Z, similar to that obtained by visible irradiation. This is as expected, since ambient indoor lighting should contain similar wavelengths to the visible light produced by the lamp. To improve the *E* to *Z* photoswitching, experimental conditions (solvent, substrate, wavelength filter) were systematically modified:

*Photoisomerisation of **2.26** in DMSO*

First, solvent was varied, since use of a solvent that stabilises the *Z* isomer over the *E* isomer would improve *E* to *Z* photoswitching. A sample of *E*-**2.26** was dissolved in d_6-DMSO and irradiated with UV. NMR analysis showed *Z*-enrichment to 49% *Z* isomer after 30 min, and no further enrichment after 60 or 90 min. This result is similar to the maximum *Z* enrichment obtained in acetonitrile (47%). Therefore, the change in solvent does not significantly improve photoswitching.

*Photoisomerisation of alternative model azobenzene **2.41***

It was considered that azobenzene **2.26** might simply be a poor photoswitch, due to possible instability of the *Z* isomer. A solution of alternative azobenzene **2.41** (Fig. 6.4) in d_3-acetonitrile was irradiated with UV for 90 min, obtaining ^{1}H NMR spectra after irradiation times of 30, 60 and 90 min. 58% *Z* isomer was obtained after 30 min, and no

further enrichment was observed after 60 or 90 min. Visible irradiation of this sample for 60 min then gave 14% *Z* isomer. This azobenzene gave improved *Z* enrichment on UV irradiation as compared to **2.26** (58% vs. 47%), but the amount of *Z* isomer obtained was still not as high as desired (preferably > 70%).

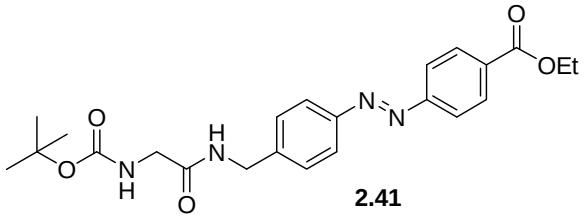

2.41

Fig. 6.4. Alternative azobenzene **2.41** for optimisation of photoisomerisation studies.

Assessment of UV filters used in irradiation

Next, the UV filter was assessed, in order to determine whether or not selective excitation of azobenzene could be performed at the wavelengths transmitted by the UG11 filter. To give selective *E* to *Z* isomerisation, the transmittance wavelengths of the UV filter are required to coincide with absorbance bands of the *E* azobenzene isomer, but not with those of the *Z* isomer (in order to excite the *E* isomer only). A UV/vis transmittance spectrum of the filter was obtained, and absorbance spectra of ethanol solutions of the *E* and *Z* isomers of azobenzene **2.7**[†] were measured for comparison. All three spectra are shown in Fig. 6.5. The absorbance spectra of *E*- and *Z*-**2.7** are not to scale with the transmittance spectrum of the UV filter, but allow comparison of the wavelength ranges of the major absorbance and transmittance bands. The spectrum of the UV filter shows transmittance over a large wavelength range (at least 250-400 nm). This range overlaps the major absorbance band of *E*-**2.7** (~260-370 nm), as is required for *E* to *Z* isomerisation. However, the transmittance range also significantly overlaps the major absorbance bands of the *Z* isomer (< 320 nm and ~370-500 nm). This is undesirable, as the UV irradiation may also excite the *Z* isomer, leading to the reverse *Z* to *E* isomerisation. The overlap may explain why relatively poor *Z* enrichment was obtained on UV irradiation using this filter.

[†] See section 6.3, below, for details of the chromatographic separation of *E*- and *Z*-**2.7**

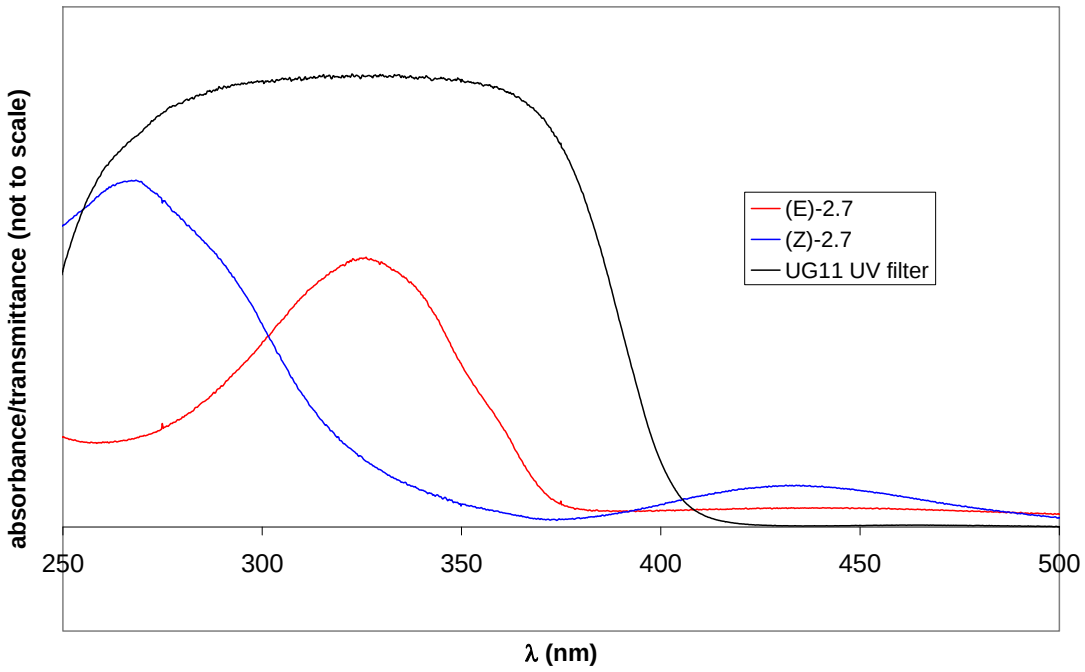

Fig. 6.5. UV/vis spectra of the UG11 UV filter and *E*- and *Z*-**2.7**.

Irradiation of ***2.41*** *using the alternative Corning 7-37 UV filter*

A UV filter that only transmits light in the narrow range 320-380 nm (Corning 7-37 UV filter) was obtained with the aim of improving photoisomerisation. A sample of **2.41** in d_3-acetonitrile was irradiated with UV using this filter to give 65% *Z* after 30 min and 90% *Z* after 60 min, with no further enrichment after 90 min. The NMR spectra of *E*-**2.41** and the *Z*-enriched PSS resulting from 60 min irradiation are shown in Fig. 6.4. This photoswitching is a significant improvement on the result obtained using the UG11 filter (maximum 58% *Z*). Consequently, the Corning 7-37 filter was used in the enzyme photoswitching studies.

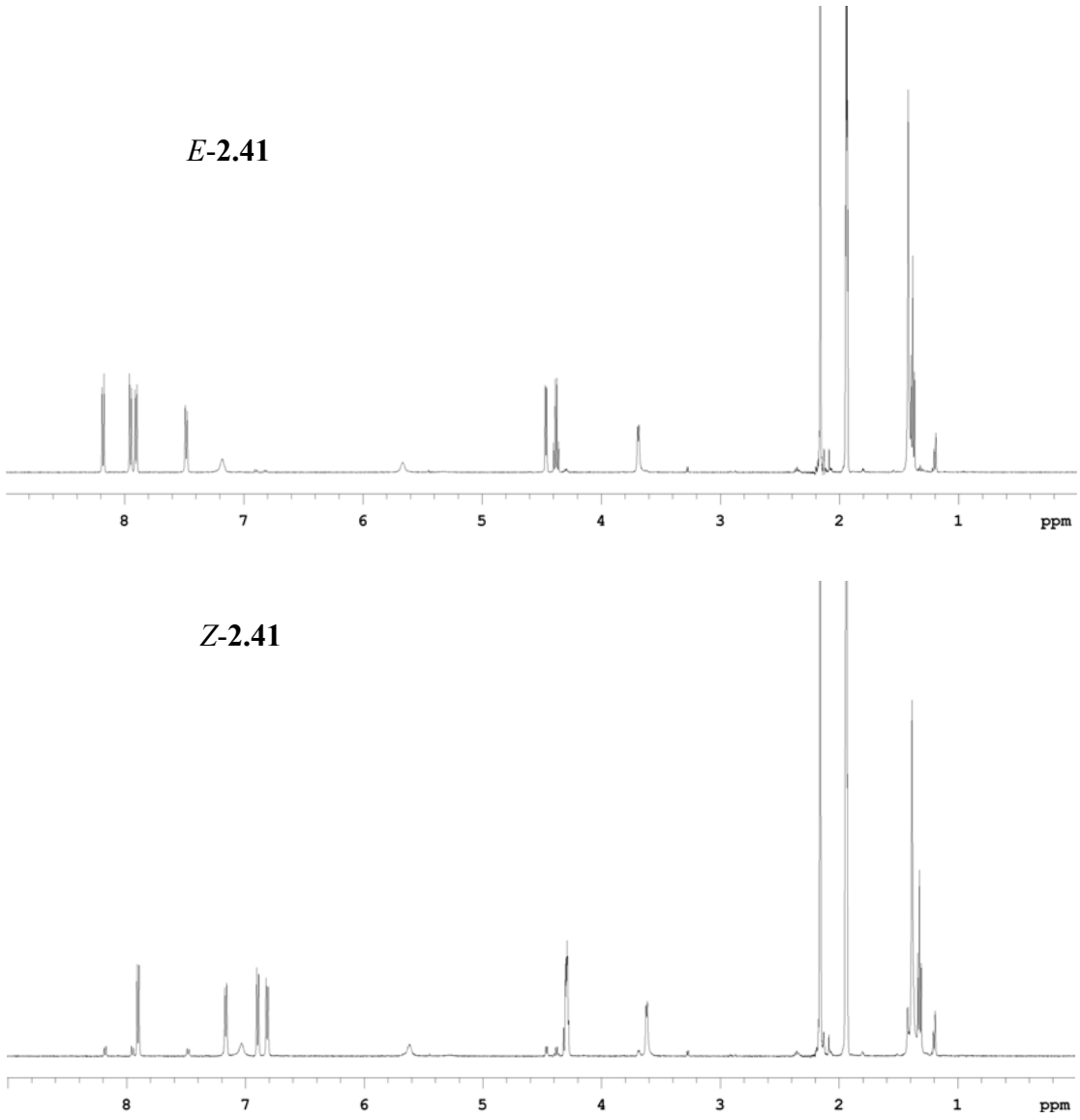

Fig. 6.6. NMR spectra of *E*-**2.41** and a sample of *Z*-**2.41** obtained by UV irradiation. Integrals of peaks at 4.38, 4.46, 7.48, 7.95, 8.18 ppm (*E*) and 4.26-4.33, 6.82, 6.90 ppm (*Z*) were used to determine *E*/*Z* compositions.

6.3 Photoisomerisation of inhibitors and surface linkers

Photoisomerisation of boronate ester ***2.7***

The potential photoswitch inhibitor **2.7** (Fig. 6.7) was photoisomerised using the 7-37 UV filter. A solution of **2.7** in d_3-acetonitrile was irradiated with UV light for 30 min to give 50% *Z* isomer. However, the NMR spectrum showed an usually large peak at 1.20 ppm

(Fig. 6.8), suggesting decomposition. The peaks at 1.18 and 1.20 ppm correspond to the pinacol group of *E*-**2.7**, and the upfield peaks at 1.14 and 1.16 correspond to the *Z* isomer. However, the integral of the *E* peak at 1.20 ppm appears slightly larger than the peak at 1.18 ppm. The sample was irradiated for a further 60 min, after which the peak at 1.20 ppm was clearly larger than the peak at 1.18 ppm (see Fig. 6.8), and appeared to be a doublet. The large size and unexpected structure of the peak at 1.20 ppm suggest that this peak corresponds to a new compound formed by irradiation. TLC of the irradiated sample was carried out. A spot was observed on the TLC plate that was not present in a pure sample of *E* and *Z*-**2.7**, confirming the presence of a new compound formed from irradiation. This decomposition product was not further characterised.

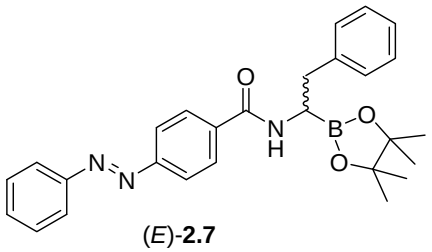

(*E*)-**2.7**

Fig. 6.7. Boronate ester **2.7** for photoswitching and enzyme assays.

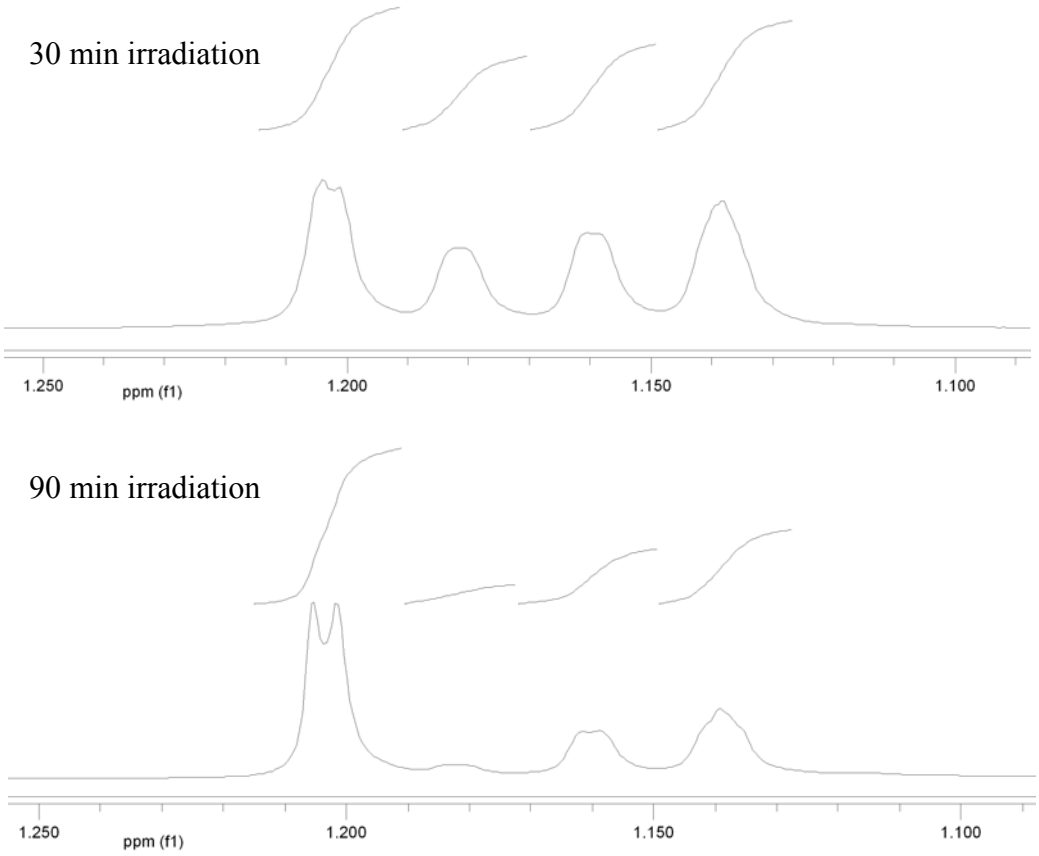

Fig. 6.8. Observed changes to the pinacol peaks of **2.7** on UV irradiation.

A third UV filter was used (Edmund Optics 340 nm interference filter) in an attempt to reduce the apparent decomposition. This filter transmits a narrower range of wavelengths than the 7-37 filter, so allows irradiation at lower intensity and greater selectivity for the major absorbance band of *E* azobenzenes. Irradiation of azobenzene **2.7** was carried out for 90 min to give 74% *Z* isomer. Inspection of the pinacol NMR peaks for this sample revealed the presence of the decomposition product peak at 1.20 ppm. However, the relative integral of this peak was less than was observed after irradiation with the 7-37 filter, showing less decomposition.

Samples of **2.7** irradiated with the Edmund Optics filter were assayed to assess the impact of the decomposition on α-chymotrypsin inhibition (see section 6.5 for details and assay results). In addition, a sample of *Z*-**2.7** was obtained by column chromatography to compare with the partially decomposed irradiated samples. A solution of *E*-**2.7** was left in ambient lighting for 24 h, then the resultant mixture of *E*- and *Z*-**2.7** was separated by silica column chromatography in dim lighting conditions to obtain a sample of *Z*-**2.7** (> 95% *Z*).

*Photoisomerisation of boronate ester **2.10***

A solution of boronate ester **2.10** (Fig. 6.9) in d_3-acetonitrile was irradiated with UV light for 120 min using the Edmund Optics filter to give 50% *Z* after 60 min and 68% Z after 120 min. However, ^{1}H NMR spectra revealed decomposition by the appearance of a new peak at 1.20 ppm. Irradiated samples of this compound were assayed to assess the impact of decomposition on α-chymotrypsin inhibition (see section 6.5).

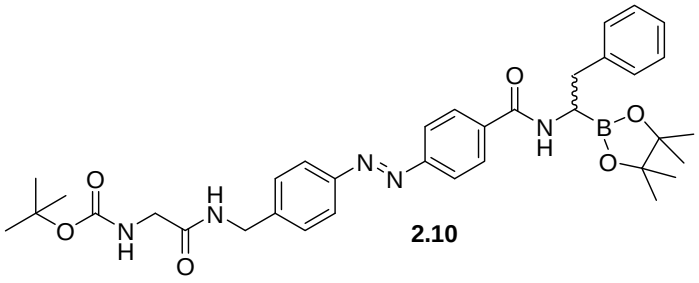

Fig. 6.9. Boronate ester **2.10** for photoswitching and enzyme assays.

Photoisomerisation of trifluoromethylketones and α-ketoesters

The trifluoromethylketone and α-ketoester inhibitors **4.1**-**4.7** and **5.17**-**5.18** were photoisomerised using a fixed set of irradiation conditions (7-37 UV filter, 0-51 visible filter, 90 min UV irradiation followed by 60 min vis irradiation) in order to directly compare the photoisomerisation of these compounds. ^{1}H NMR of these samples after irradiation showed good photoisomerisation (see Table 6.2), from initial states of <10% *Z* isomer to 66-93% *Z* after UV irradiation and back to 8-21% *Z* after visible irradiation, with no observed decomposition.

Table 6.2. Photoisomerisation of trifluoromethylketones and α-ketoesters.

Compound	Structure	Amount of *Z* isomer before irradiation	Amount of *Z* isomer after UV irradiation	Amount of *Z* isomer after visible irradiation
4.1	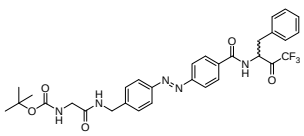	<5%	93%	16%
4.2	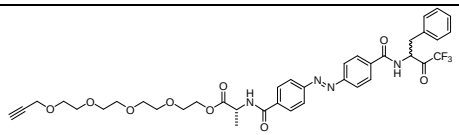	5%	66%	9%
4.3	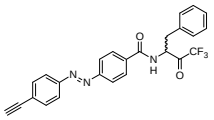	5%	87%	12%
4.4	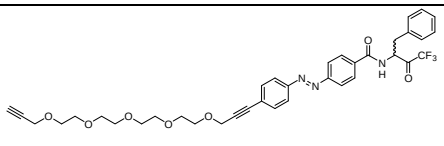	6%	85%	8%
5.17	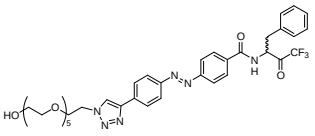	7%	76%	18%
4.5	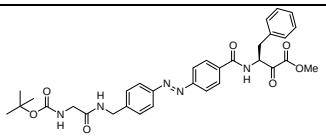	5%	94%	14%
4.6	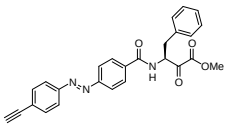	<5%	85%	7%
4.7	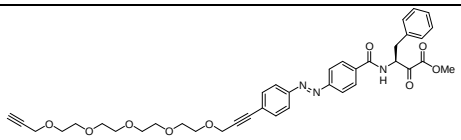	6%	88%	14%
5.18	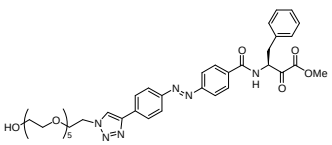	7%	74%	15%

The pairs of compounds containing the same azobenzene 4′-substituent and differing only in the enzyme binding group (**4.1** and **4.5**, **4.3** and **4.6**, **4.4** and **4.7**, **5.17** and **5.18**) exhibit very similar photoswitching properties. This suggests that the electrophilic enzyme binding group does not significantly affect photoswitching. However, the 4′-substituent appears to have a large influence on photoswitching, as can be seen in the difference between the UV PSS compositions of compounds **4.1** and **4.2** (93% and 66%, respectively). The properties of this substituent presumably influence photoisomerisation by affecting one or both of the following factors:

i) The difference between the stability of the *E* and *Z* isomers in solution – i.e. substituents that increase the steric or electronic stability of the *Z* isomer over the *E* isomer are likely to promote *E* to *Z* isomerisation, and substituents that increase the stability of the *E* isomer over the *Z* isomer are likely to promote *Z* to *E* isomerisation.

ii) The UV/visible absorbance of the azobenzene group. Substituents that donate/withdraw electron density to/from the azobenzene group may alter the energy levels involved in electronic excitation of azobenzene to the excited state that allows isomerisation (see chapter 1, section 1.2.2). Changes to these energy levels causes a shift of the corresponding UV/vis absorbance bands of the azobenzene. Assuming irradiation is carried out using a fixed wavelength range, a shift of the azobenzene absorbance bands may lead to increased (or decreased) excitation of either the *E* or *Z* isomer by the irradiation wavelengths, leading to increased (or decreased) isomerisation of this isomer.

Photoisomerisation of model surface linkers

Irradiation experiments were also carried out to assess the photoisomerisation properties of model surface compounds **5.12** and **5.13** (Fig. 6.10). A sample of disulfide **5.12** was irradiated with UV to, unexpectedly, give only trace amounts (< 5%) of *Z* isomer after 90 min. Irradiation was carried out for a further 90 min to give 20% *Z* isomer. This poor photoisomerisation suggests that the UV absorbance of the constituent dithiolane group interferes with the UV absorbance of the azobenzene group. Based on this result, lipoic acid derivatives were not used in surface attachment studies.

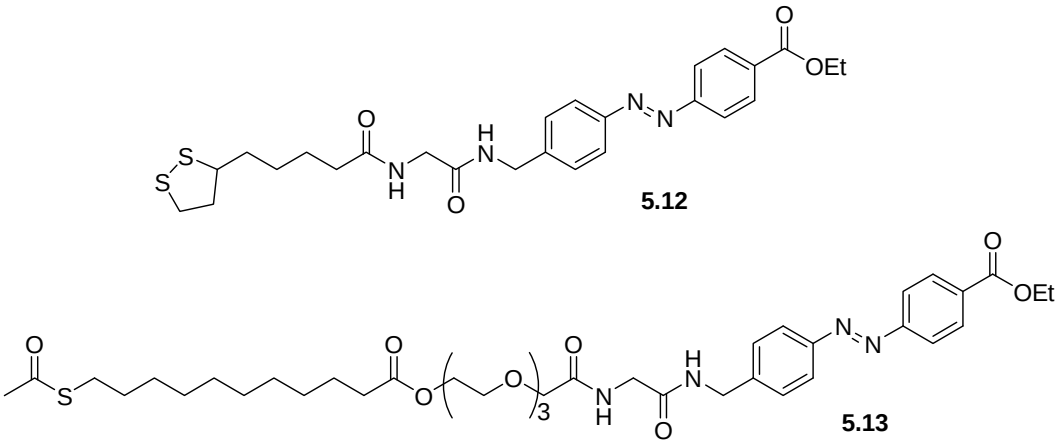

Fig. 6.10. Model azobenzenes **5.12** and **5.13** for photoswitching studies.

A sample of compound **5.13** (initially < 5% *Z* isomer) was irradiated with UV light for 90 min, to obtain 91% *Z* isomer. Visible irradiation for 60 min returned the sample to 15% *Z* isomer. Related compounds were thus used in surface attachment studies (see chapter 7).

6.4 Assay setup and validation

α-Chymotrypsin assays were carried out as described in section 6.1.

Assay conditions

Solutions of Tris buffer (0.1 M, pH 7.8, containing $CaCl_2$ and Triton X-100 surfactant), α-chymotrypsin (in Milli-Q water containing HCl and Triton X-100), substrate (in Tris buffer), and inhibitor (in DMSO or acetonitrile) were made up. Inhibitor and substrate were mixed, incubated for 5 min at 25 ºC, then enzyme was added and the UV/vis absorbance of the solution was monitored at 405 nm for 5 or 10 min. The experiment was repeated over a range of substrate and/or inhibitor concentrations, and the initial or final rate was calculated for each. The uncertainty in affinity constants is estimated at ± 20%, and the uncertainty of affinity increases/decreases on photoisomerisation is estimated at ± 10%. Further details are given in the experimental chapter, section 9.6, and in the descriptions of particular assays in this chapter.

Assay without addition of inhibitor

Initially, assays were carried out without inhibitor to ensure that the enzyme exhibited normal activity. Initial rate data was obtained for a range of substrate concentrations (83-420 μM) and plotted in a double reciprocal plot† (Fig. 6.11) to determine kinetic parameters of K_m = 40 μM and V_{max} = 1.2 μmol s^{-1} mg^{-1}. These results are comparable to previous studies.[5, 6]

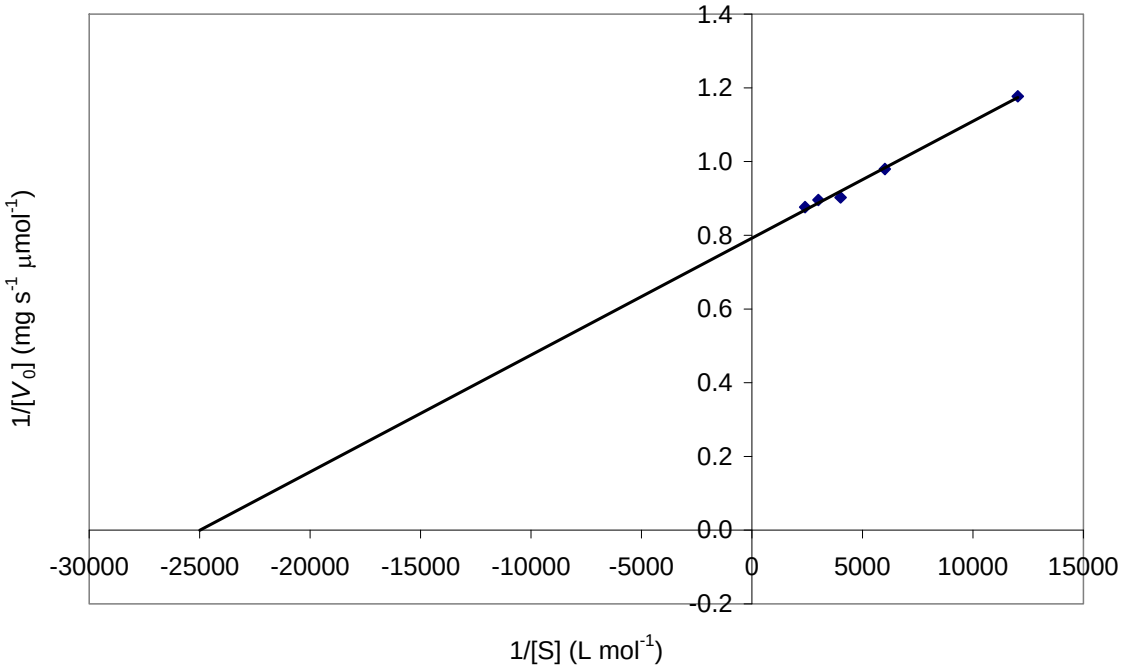

Fig. 6.11. Double-reciprocal plot for calculation of kinetic parameters for α-chymotrypsin.

As inhibitor assays involved addition of acetonitrile or DMSO to the assay solution, preliminary assays with addition of solvent were also carried out. Kinetic constants of V_{max} = 1.2 μmol s^{-1} mg^{-1} and K_m = 19 μM were obtained with the addition of acetonitrile, and V_{max} = 1.1 μmol s^{-1} mg^{-1} and K_m = 33 μM with the addition of DMSO. The K_m in these assays is decreased, as compared to the assay containing no organic solvent. This suggests that acetonitrile and DMSO enhance the rate of α-chymotrypsin catalysed hydrolysis.

† $1/V_0$ vs 1/[S], where [S] is the substrate concentration. The *x*-intercept is equal to $1/K_m$ and the y-intercept is equal to $1/V_{max}$.

Validation of assay with reported inhibitor ***2.12***

The racemic form of reported inhibitor **2.12** (Fig. 6.12) was assayed in order to validate the assay procedure. Assays of both the *L* and *D* enantiomers have been previously reported, with inhibition constant, K_i, of 2.1 μM[7] and 3.8 μM[8] reported for the *L* isomer and 53[7] and 80 μM[8] reported for the *D* isomer.

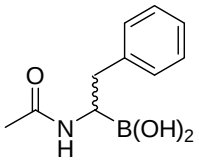

2.12

Fig. 6.12. Known inhibitor **2.12** for assay validation.

Initial rate data was obtained at a range of substrate concentrations (80-410 μM) and inhibitor concentrations (17-69 μM) and a Dixon plot† was used (Fig. 6.13) to obtain a K_i inhibition constant of 7 μM. This result for racemic **2.12** compares well with the literature, where the active *L* enantiomer is reported to give approximately half this value (2-4 μM). As such, this result validates the assay, ensuring that inhibition constants obtained here can be compared with other studies.

† $1/V_0$ vs [I], where [I] is the inhibitor concentration. Lines are drawn through sets of points of the same substrate concentration, the intersection of these lines occurring at ($-K_i$, $1/V_{max}$).

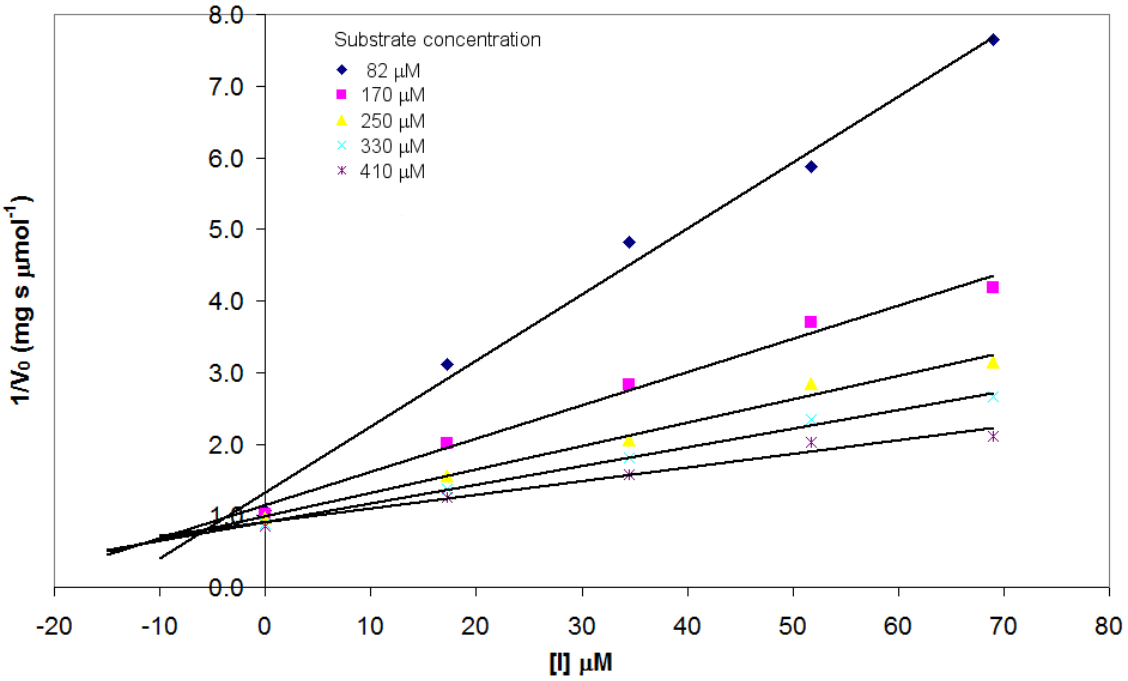

Fig. 6.13. Dixon plot for determining K_i of inhibitor **2.12**.

6.5 Assay of boronate esters described in chapter 2

*Assays of E azobenzenes and chromatographically separated Z-***2.7**

Samples of the *E* isomers (< 5% *Z*) of boronate esters **2.1**-**2.2** and **2.6**-**2.11** and the sample of *Z*-**2.7** obtained by chromatography were assayed at a range of inhibitor concentrations [I] as appropriate for each compound and a fixed substrate concentration [S] of 190 μM, in order to obtain IC_{50} inhibition constants. The percentage inhibition was calculated at each [I] then plotted against log[I]. From these plots, log(IC_{50}) was interpolated at 50% inhibition and used to calculate IC_{50} values. As the plots were found to be non-linear at high and low percentage inhibition, the line of best fit for interpolation was drawn through the linear points, usually in the range 20-80% inhibition. Fig. 6.14 shows a representative IC_{50} plot using data obtained from assay of **2.7**. Here, poor solubility of the inhibitor prevented assay at high inhibitor concentrations (>3.3 μM), but the three linear points were sufficient to obtain an IC_{50} value. The measured IC_{50} values of the boronate esters are shown in Table 6.3, below.

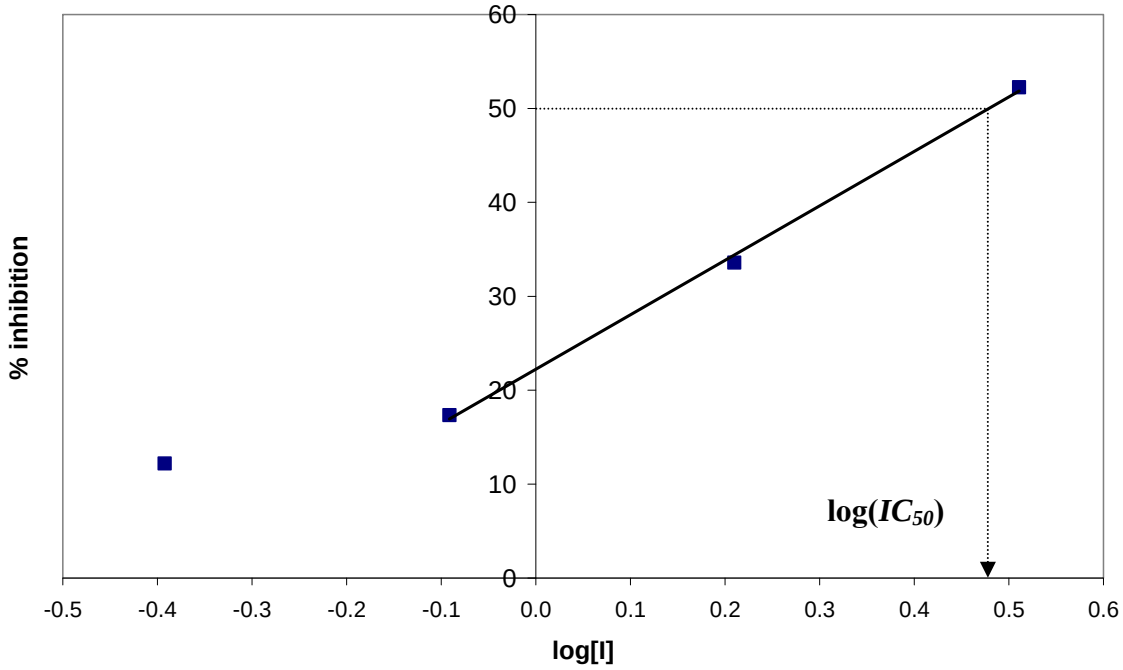

Fig. 6.14. IC_{50} plot for **2.7**.

Table 6.3. IC_{50} inhibition constants for inhibition of α-chymotrypsin by boronate esters.

Compound (< 5% *Z* unless specified)	**Structure**	***IC*$_{50}$ (μM)**
2.1	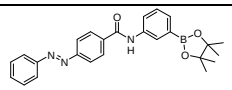	> 15
2.2	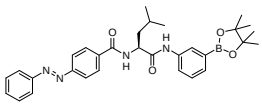	> 25
2.6	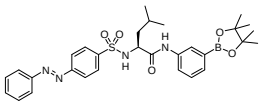	> 200
E-**2.7**	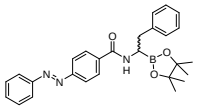	3.0
Z-**2.7** (> 95% *Z*, obtained by chromatography)	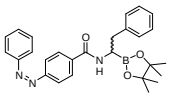	4.7
2.8/**2.9** (92 : 8 ratio)	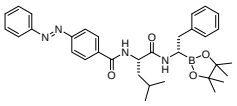	18
2.8/**2.9** (7 : 93 ratio)	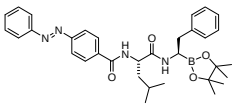	1.3
2.10	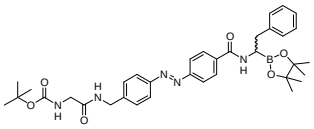	10
2.11	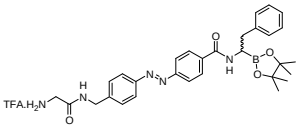	11

The azobenzenes **2.1**-**2.2** and **2.6** containing an aminophenylboronate ester group were found to be inactive against α-chymotrypsin up to their solubility limits (15-200 μM). This is surprising, as these compounds are structurally very similar to the reported photoswitch inhibitor **1.21** (Fig. 6.15), which inhibits α-chymotrypsin with inhibition constant, K_i, of 11 μM.[3] This suggests that the fit of **1.21** into the enzyme active site is significantly enhanced by the shape and/or hydrogen bonding attributable to the sulfonamide group. However, replacing the amide of **2.2** with a sulfonamide to give **2.6** did not replicate this effect, as sulphonamide **2.6** was also inactive. It is possible that the incorporation of the boronate ester group into **2.1**-**2.2** and **2.6** (instead of the boronic acid group) might account for the reduction in potency relative to **1.21**. However, the observed 1.4-18 fold decreases in activity are not consistent with literature, where boronate esters and their corresponding free acids are reported to give very similar activities in enzyme assays.[9, 10] Our results suggest that **1.21**, although an effective photoswitch, cannot be simply extended as a peptide analogue. As such, the related boronate esters **2.3**-**2.5** were not assayed and efforts were focussed on the borophenylalanine derivatives **2.7**-**2.11**, which inhibited α-chymotrypsin with low micromolar IC_{50} values.

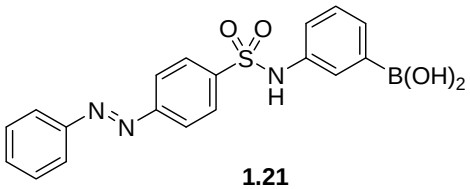

1.21

Fig. 6.15. Known α-chymotrypsin inhibitor **1.21**.

Encouragingly, the potency of compounds **2.7** and **2.9** (3.0 and 1.3 μM, respectively) is similar to the activity of acetylborophenylalanine **2.12** (K_i = 7 μM). This result implies that activity is not significantly impaired by the presence of the azobenzene group or the protection of the boronic acid as the pinacol ester. It is possible that the azobenzene group may even enhance activity by providing either a good fit into the shallow hydrophobic S_2 subsite, or an extended mimic of a β-strand, the preferred conformation of peptide substrates of proteases.[11] This could then offset any possible reduction in activity due to the boronic acid protection. The absolute configuration of diastereomers **2.8** and **2.9** could not be assigned from NMR data. However, the more active isomer **2.9** is tentatively assigned the (*R*) configuration, as this corresponds to (i) the configuration of natural

phenylalanine and (ii) that commonly found in the more active isomers of related inhibitors.[8] Interestingly, the most active diastereomer **2.9** was found to have approximately twice the potency of racemic **2.7**. This suggests that incorporation of leucine into the inhibitor structure does not significantly enhance binding through interaction of leucine with the S_2 subsite. It is, however, possible that any increase in binding conferred by leucine is off-set by the affinity of the hydrophobic azobenzene group for the S_2 subsite (as in **2.7**) rather than the S_3 subsite (as in **2.9**).

The azobenzenes **2.10** and **2.11** containing a surface attachment group in the 4′ position gave inhibition constants that are not significantly different (10 and 11 μM), several times weaker than monosubstituted azobenzene **2.7**, but significantly more potent than **2.1**-**2.2** and **2.6**. This suggests that the extra substitution of the azobenzene group only slightly impairs the fit of the inhibitor into the active site. The extra bulk of the Boc group in **2.10** is tolerated, suggesting that the specificity of the enzyme binding site does not extend further than the glycine in these inhibitors. Consequently, it is likely that the primary amine group of **2.11** protrudes from the active site and thus may be used for surface attachment.

The azobenzene *E*-**2.7** exhibits more potent inhibition than chromatographically separated *Z*-**2.7** (IC_{50} values of 3.0 vs. 4.7 μM). This is consistent with the reported photoswitching of azobenzene **1.21**, where the *E* isomer was also found to be the most active.

*Assay of irradiated boronate esters **2.7** and **2.10***

To compare with the chromatographically separated samples of *E*- and *Z*-**2.7**, assays were carried out on UV/vis irradiated samples. A solution of *E*-**2.7** was irradiated for 90 min, an aliquot was removed and assayed, and the remainder of the solution irradiated with visible light for 60 min with subsequent assay. Two further irradiations (UV then visible) and assays were carried out, with the resulting IC_{50} values after each irradiation shown in Fig. 6.16.

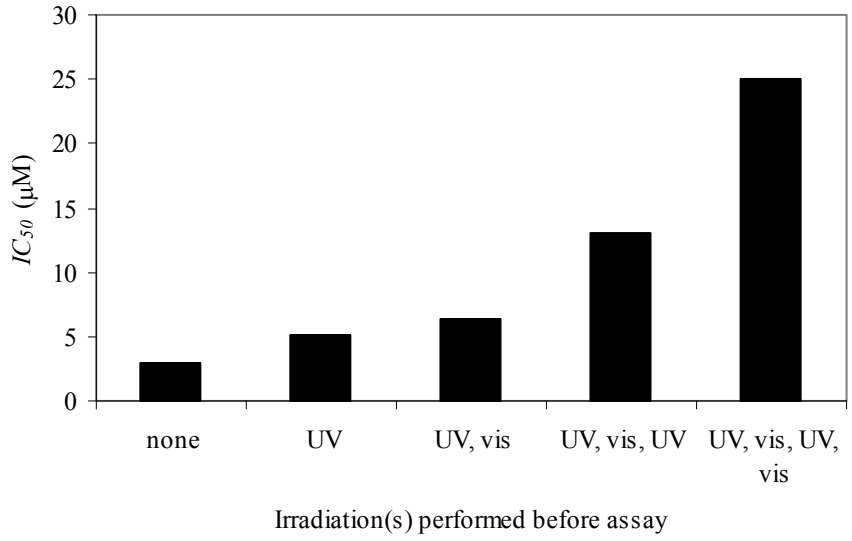

Fig. 6.16. Assay of irradiated **2.7** showing decomposition.

A decrease in inhibition was observed after each irradiation. In addition, the samples irradiated two or more times were less potent than the chromatographically isolated sample of *Z*-**2.7** (4.7 μM). Combined with the NMR and TLC results in section 6.3, these results show that decomposition of **2.7** occurred on irradiation, with a loss of activity.

A similar set of irradiations and assays was carried out for boronate ester **2.10**. Photoswitching was observed with limited decomposition at each cycle. The assay results recorded over three irradiations are shown in Fig. 6.17. The activity increased from 10 μM (for sample containing <5% *Z* isomer) to 7.0 μM after UV isomerisation to give 60% Z isomer. Subsequent visible irradiation reduced activity to 13 μM (85% *E* isomer), and a further UV irradiation increased activity to 10 μM. The *Z* isomer of this boronate ester is the more potent isomer, contrasting with the results obtained for the simpler compounds **2.7** and **1.21,** where the *E* isomer is more potent. Consequently, there appears to be no direct correlation between the nature of the enzyme binding group and the relative activities of the *E* and *Z* isomers. Rather, it is dependent on the shape of the inhibitor and hence the nature of its overall fit into the α-chymotrypsin active site.

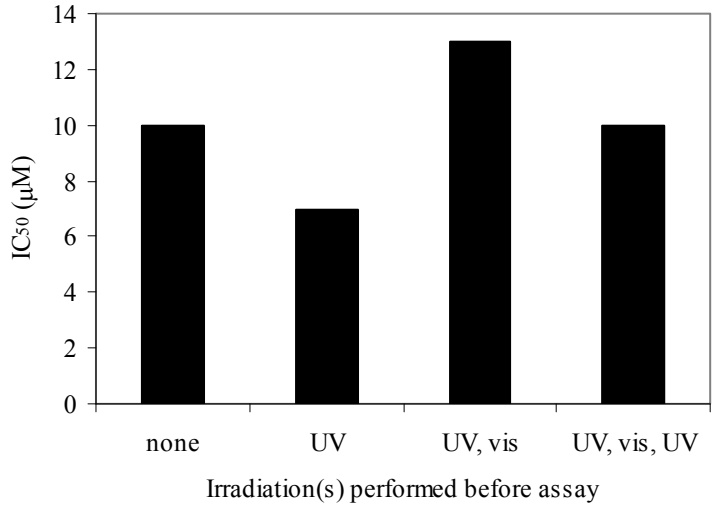

Fig. 6.17. Photoswitching of boronate ester **2.10** with limited decomposition.

As boronate esters **2.7** and **2.10** decomposed on irradiation, these compounds are not sufficiently stable for surface photoswitching, and photoisomerisation of other boronate esters was not carried out.

6.6 Assay of compounds described in chapter 3

Assays were carried out to obtain IC_{50} values for compounds **3.3**-**3.5** (Fig. 6.18), derivatives of reported non-covalent inhibitor **3.1** (see chapter 3) further substituted to introduce photoswitching activity (**3.5**) or a surface attachment group (**3.3** and **3.4**).

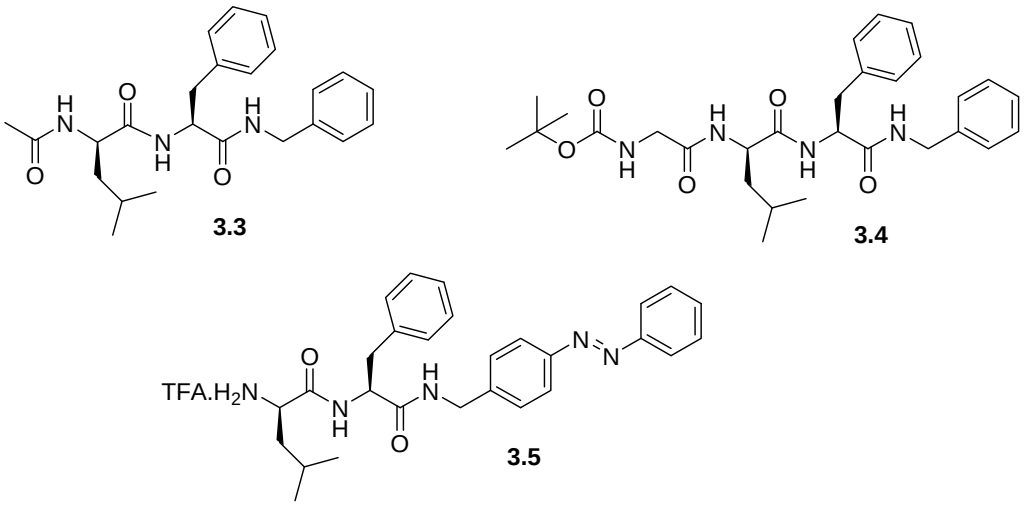

Fig. 6.18. Derivatives **3.3**-**3.5** of a non-covalent α-chymotrypsin inhibitor.

The azobenzene **3.5** was assayed as a mixture of *E* and *Z* isomers (83% *E*, 17% *Z*, determined by HPLC) for an initial screening assay. All compounds **3.3**-**3.5** were found to be inactive against α-chymotrypsin up to their solubility limits (25-91 μM). To confirm the previously reported activity of compound **3.1**,[12] intermediate **3.10** was assayed to obtain a K_i value. This compound is essentially identical to **3.1**, simply lacking the HCl salt. A result of 4 μM was obtained, comparable to the reported value of 3.6 μM for **3.1**.

The reduced potency of compounds **3.3** and **3.4** (compared to **3.1**) suggests that either the amine group of **3.1** is involved in important hydrogen bonding interactions with the active site of α-chymotrypsin or there is simply insufficient space in the active site for the replacement of the amine by the larger amide group. Consequently, inhibitor **3.1** cannot be simply extended at the *N*-terminus for surface attachment. The crystal structure of the enzyme-inhibitor complex of **3.2** with chymotrypsin shows that the *D*-Leu side chain extends from the binding pocket. Modification of this side chain might be a more effective approach for surface attachment.

The inactivity of the mixture of *E*- and *Z*-**3.5** suggests that the azobenzene group is too large to fit into the S_1 subsite of α-chymotrypsin. Consequently, photoswitching activity cannot be introduced to compound **3.1** by replacement of the P_1 phenyl group by azobenzene. As an alternative photoswitching strategy, the P_2 phenyl group (the Phe side chain) could be replaced with azobenzene, as the large azobenzene group is more likely to be tolerated in the shallow S_2 pocket than the deep, narrow S_1 pocket.

6.7 Assay of trifluoromethylketones and α-ketoesters described in chapters 4 and 5

Potential photoswitch inhibitors containing trifluoromethylketone or α-ketoester groups **4.1**-**4.7** and **5.17**-**5.18** were assayed to obtain IC_{50} values. As these compounds all appeared to be stable to UV/visible irradiation (by ^{1}H NMR), all were assayed as: i) the *E* isomer before irradiation ii) the *Z* enriched PSS resulting from UV irradiation iii) the *E* enriched PSS from visible irradiation. The *E*:*Z* compositions are as given previously in Table 6.3, section 6.5.

All compounds were found to be inhibitors of α-chymotrypsin, with IC_{50} values as shown in Table 6.4. While the α-ketoesters exhibited normal inhibition characteristics, the inhibition of the trifluoromethylketones appeared to increase over time. This slow increase in binding strength is consistent with the 'slow-tight' binding mode involving the initial formation of a weakly bound enzyme-inhibitor complex followed by rearrangement to a more tightly bound complex.[13] To record a steady state hydrolysis rate, trifluoromethylketones were allowed to incubate with enzyme and substrate for 8 minutes before rate data was collected. Consequently, the IC_{50} values given for trifluoromethylketones reflect the final 'tight' binding. In all cases, the initial binding of trifluoromethylketones was too weak to obtain an accurate IC_{50} value.

Table 6.4. Inhibition constants (IC_{50}) for trifluoromethylketones and α-ketoesters.

Compound	Structure	IC_{50} before irradiation (μM)	IC_{50} after UV irradiation (μM)	IC_{50} after visible irradiation (μM)
4.1	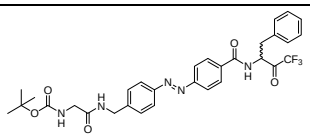	32	13	29
4.2	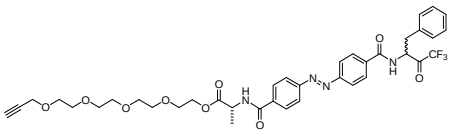	20	17	21
4.3	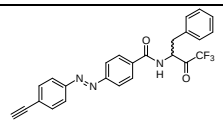	>85	16	>85
4.4	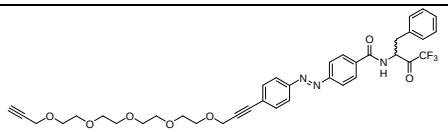	>51	14	>51
5.17	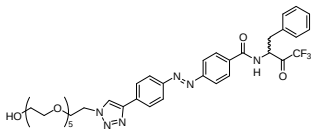	19	12	21
4.5	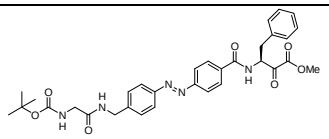	0.71	0.23	0.59
4.6	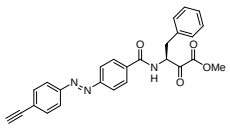	1.0	0.47	0.85
4.7	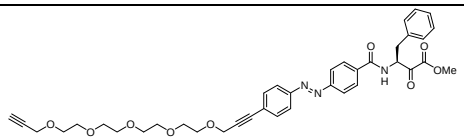	2.0	0.73	2.2
5.18	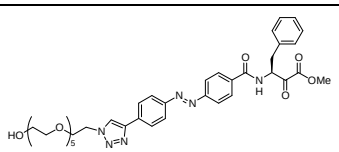	0.47	0.19	0.43

A range of structure-activity-photoswitching comparisons can be drawn from the data in Table 6.4. The α-ketoesters are more potent inhibitors than the trifluoromethylketones, with inhibition constants ranging from 0.23 to 2.2 μM for the α-ketoesters and 12 to 85 μM for the trifluoromethylketones. This suggests that the α-ketoester group binds more rapidly and/or strongly to the Ser195 residue of the active site. Both α-ketoesters and trifluoromethylketones are more active as the *Z*-enriched PSS obtained from UV irradiation, as previously reported for these classes of photoswitch inhibitors,[2, 5] and observed for the related boronate ester **2.10** (see section 6.5).

It is clear that the structural requirements for potent binding of trifluoromethylketones are very different to those of α-ketoesters, despite the close similarity of these classes of inhibitor. For example, the *Z* enriched forms of the trifluoromethylketones exhibit a narrow range of inhibition constants (12-17 μM) and the *E* enriched forms vary considerably (19-85 μM), whereas the inhibition constants of both the *E* and *Z* enriched states of the α-ketoesters vary significantly between compounds. Therefore, it appears that the 4′ substituent has little impact on the potency of *Z*-trifluoromethylketones, but has a major effect on the potency of *E*-trifluoromethylketones and of both *E*- and *Z*-α-ketoesters.

Furthermore, the difference in activity between the *E* and *Z* isomers of an inhibitor (i.e. the extent of enzyme photoswitching) varies more between trifluoromethylketones than it does between α-ketoesters. For example, the best and worst photoswitching results are observed for trifluoromethylketones (**4.3** and **4.2**, respectively), while all of the α-ketoesters exhibit intermediate photoswitching of 2-3 fold changes in activity between isomers.

In comparison of the 4′ azobenzene substituents, the strongest binding is exhibited by triazoles **5.17** and **5.18** and the weakest binding is exhibited by alkynes **4.3**, **4.6**, **4.4** and **4.7**. This suggests that the triazole group fits better into the α-chymotrypsin active site than the alkyne group does. However, the best photoswitching is exhibited by alkynes **4.3** and **4.4**, which give >5.3 and >3.6 fold changes in activity on photoswitching. As the *E* isomers of these compounds were inactive up to their solubility limits, the exact extent of photoswitching may be greater than that reported. As the *Z*-trifluoromethylketones all exhibit similar potencies, the excellent photoswitching of **4.3** and **4.4** is due to the

particularly weak binding of the *E* isomers of these compounds, as compared to other *E*-trifluoromethylketones.

For surface photoswitching, it should be considered that alkynes **4.3** and **4.6** would form triazoles on surface attachment, resembling triazoles **5.17** and **5.18**, respectively. Therefore, the activities of these model triazoles are the best measures of the activity of surface attached **4.3** and **4.6**. While alkyne **4.3** is an excellent photoswitch, triazole analogue **5.17** is a poor photoswitch, which suggests that **4.3** would give poor results after surface attachment. Conversely, alkyne **4.6** and triazole **5.18** give similar photoswitching results. As the best photoswitch (**4.3**) is likely to give poor results after surface attachment, the trifluoromethylketone **4.4** is a better candidate for surface enzyme photoswitching. This alkyne contains an extended OEG group, so reaction to give a triazole is unlikely to significantly affect enzyme binding or photoswitching.

6.8 Summary

Photoisomerisation of azobenzenes **2.26** and **2.41** was carried out to optimise irradiation conditions. The best *E* to *Z* irradiation was obtained using a UV filter with a relatively narrow wavelength range. Subsequently, compounds **2.7**, **2.10**, **4.1**-**4.7**, **5.12**-**5.13** and **5.17**-**5.18** were photoisomerised. Good photoisomerisation was obtained for all azobenzenes except the boronic acids, which partially decomposed on irradiation, and lipoic acid derivative **5.12**, which did not isomerise well.

α-Chymotrypsin assays were carried out, initially for reported inhibitor **2.12** to validate the assay, then for compounds **2.1**-**2.2**, **2.6**-**2.11**, **3.3**-**3.5**, **3.10**, **4.1**-**4.7** and **5.17**-**5.18**. The aminophenylboronate-based compounds **2.1**-**2.2** and **2.6** and dipeptide derivatives **3.3**-**3.5** were inactive, but the borophenylalanine based compounds, trifluoromethylketones, α-ketoesters, and dipeptide **3.10** were all micromolar inhibitors of the enzyme.

Reversible photoswitching of inhibition was obtained for trifluoromethylketones and α-ketoesters, but boronic acids exhibited a decrease in activity on irradiation due to decomposition. α-Ketoesters were found to be the most potent inhibitors, while trifluoromethylketones **4.3** and **4.4** gave the greatest changes in potency on

photoisomerisation. Alkyne **4.4** was determined to be the best inhibitor for surface attachment studies.

6.9 References

1. Dong, S.-L.; Loweneck, M.; Schrader, T. E.; Schreier, W. J.; Zinth, W.; Moroder, L.; Renner, C., *Chem. Eur. J.* **2006**, 12, 1114.

2. Harvey, A. J.; Abell, A. D., *Tetrahedron* **2000**, 56, (50), 9763.

3. Westmark, P. R.; Kelly, J. P.; Smith, B. D., *J. Am. Chem. Soc.* **1993**, 115, 3416.

4. Geiger, R., *Methods of Enzymatic Analysis*. 3 ed.; Verlag Chemie: Weinheim: **1984**; Vol. 5, p 99-129.

5. Alexander, N. A. PhD thesis. University of Canterbury, **2006**.

6. Harvey, A. J. PhD thesis. University of Canterbury, **2000**.

7. Matteson, D. S.; Sadhu, K. M.; Lienhard, G. E., *J. Am. Chem. Soc.* **1981**, 103, 5241.

8. Martichonok, V.; Jones, J. B., *J. Am. Chem. Soc.* **1996**, 118, 950.

9. Kettner, C. A.; Shenvi, A. B., *J. Biol Chem.* **1984**, 259, (24), 15106.

10. Weber, P. C.; Lee, S.-L.; Lewandowski, F. A.; Schadt, M. C.; Chang, C.-H.; Kettner, C. A., *Biochemistry* **1995**, 34, 3750.

11. Tyndall, J. D. A.; Nall, T.; Fairlie, D. P., *Chem. Rev.* **2005**, 105, 973.

12. Shimohigashi, Y.; Maeda, I.; Nose, T.; Ikesue, K.; Sakamoto, H.; Ogawa, T.; Ide, Y.; Kawahara, M.; Nezu, T.; Terada, Y.; Kawano, K.; Ohno, M., *J. Chem. Soc. Perkin Trans. 1* **1996**, 2479.

13. Brady, K.; Abeles, R. H., *Biochemistry* **1990**, 29, 7608.

Chapter Seven

Surface Modification and Study of Photoregulated Enzyme Binding to Surfaces

Surface modification and study of photoregulated enzyme binding to surfaces

7.1 Introduction

The final goals of this thesis were the attachment of photoswitch inhibitors to surfaces and photoregulated enzyme binding to the resultant modified surfaces. The most appropriate inhibitors to use in these studies were selected from those described in chapters 2-5. The trifluoromethylketone-based inhibitors (chapter 4) gave the best enzyme photoswitching, and the symmetrical disulfide surface linkers (chapter 5) gave good photoswitching and are likely to form high quality SAMs. Therefore, the trifluoromethylketone **5.16** containing a disulfide surface linker was chosen for initial surface attachment and enzyme binding studies. In addition, related diluent **5.11** and azide **5.9** were chosen for blocking of non-specific enzyme attachment and initial SAM characterisation, respectively. The trifluoromethylketone **4.4** was chosen for final SPR studies of surface enzyme binding and photoswitching due to its excellent photoswitching properties. These surface compounds are shown in Fig. 7.1.

This chapter describes the formation of SAMs from disulfides **5.9**, **5.11**, and **5.16**, characterisation of these SAMs by cyclic voltammetry (CV) and contact angle measurements, and QCM enzyme binding studies using **5.16**/**5.11** mixed SAMs. Finally, SPR studies of photoregulated enzyme binding to surface-attached inhibitor **4.4** are described.

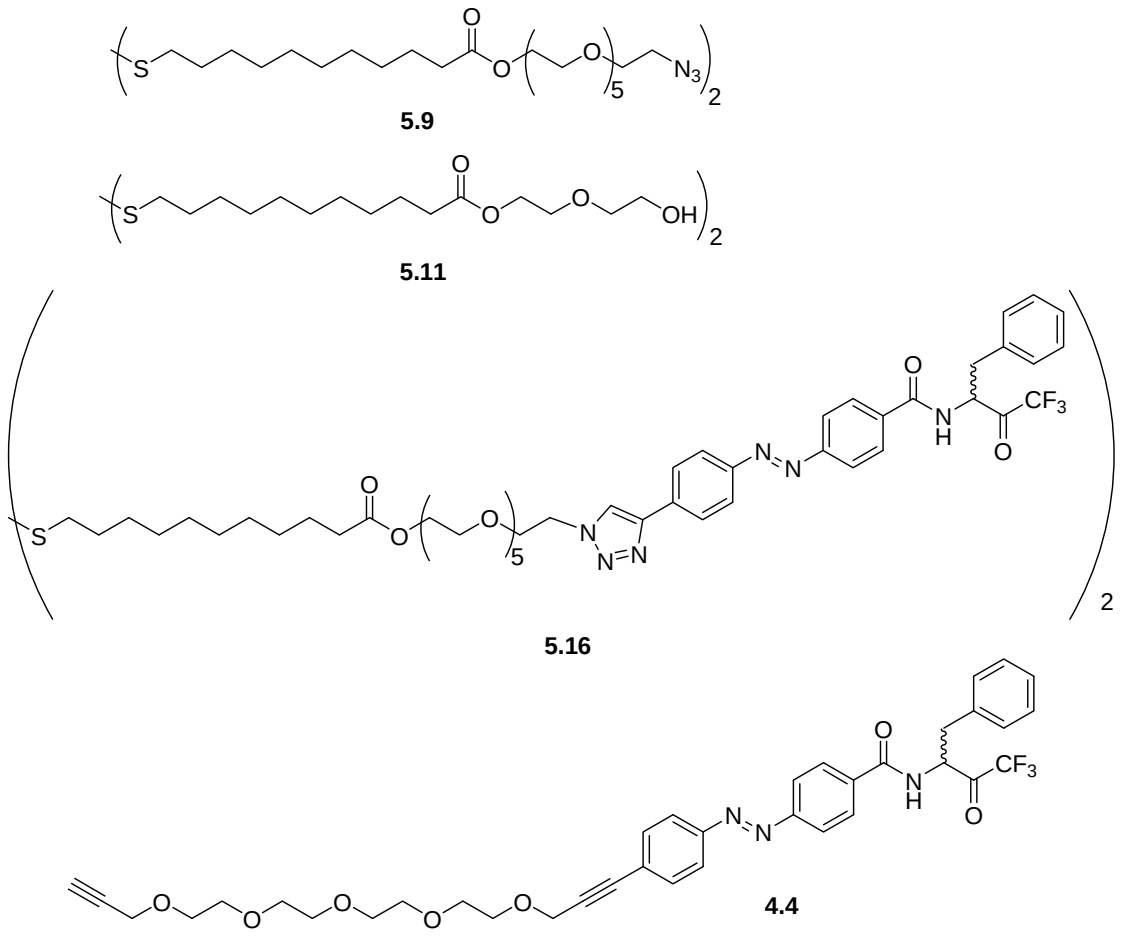

Fig. 7.1. Surface attachment compounds used in this chapter.

7.2 Preparation of SAMs of azide 5.9 and diluent 5.11

*Contact angle measurements at SAMs of disulfides **5.9** and **5.11** on gold films*

SAMs of azide **5.9** and the corresponding OEG diluent **5.11** were formed for initial SAM characterisation studies. Six gold film substrates were immersed in ethanol solutions of each of the disulfides (0.5 mM), and a further six substrates were immersed in ethanol as control samples. After 24 h, three substrates were removed from each solution, rinsed thoroughly with ethanol and dried under a stream of nitrogen gas. After 48 h, the remaining substrates were removed from the solutions as above. Contact angle measurements were made immediately after removal to assess changes in surface hydrophobicity due to SAM formation. The results are listed in Table 7.1. Further details

of the preparation of gold substrates and the procedure used for contact angle measurement are given in the experimental chapter, section 9.7.

Table 7.1. Contact angle measurements† for SAMs of disulfides **5.9** and **5.11**.

Solution	Averaged contact angle after 24 h immersion (º)	Averaged contact angle after 48 h immersion (º)
Control	71	71
Azide **5.9**	59	62
Diluent **5.11**	53	64

† Averaged results obtained using two drops of water on each of three surfaces. All values are ±3º.

First, it is clear that the substrates immersed in disulfide solutions are more hydrophilic than the control substrates, as the water contact angles of these substrates are lower than those of the control surfaces. This indicates the successful formation of SAMs on these substrates, since the disulfides contain hydrophilic OEG groups and polar terminal groups that would be expected to give hydrophilic surfaces.

There was no significant change in the contact angles of the SAM of azide **5.9** between 24 and 48 h, which suggests that this SAM was well formed and stable after 24 h. However, the contact angles for the SAM of diluent **5.11** increased between 24 and 48 h. This increase is unexpected, as the formation of the hydrophilic SAMs initially decreased contact angles. It is tentatively suggested that on the shorter timescale (24 h) a relatively disordered SAM was formed that traps water or ethanol molecules at the surface. Denser packing of such a SAM (after 48 h) could result in a decrease in trapped solvent and thus a decrease in hydrophilicity.

*CV of SAMs of disulfides **5.9** and **5.11** on a gold plug electrode*

SAMs of **5.9** and **5.11** were also formed on a gold plug electrode in order to study these surfaces by electrochemistry. The electrode was immersed in a solution of **5.9** (0.5 mM) or **5.11** (0.25 mM) in ethanol for 40 h, then rinsed with ethanol and dried under a stream of nitrogen gas. CV was then carried out at each electrode in a solution of $K_3Fe(CN)_6$ (1 mM) and $NaClO_4$ (1 M) (Fig. 7.2). A potential scan rate of 300 mVs^{-1} was used for all CVs unless specified otherwise, and all data is reported vs. a saturated calomel electrode

(SCE). As a control, the same experiments were carried out using a gold electrode lacking attached disulfide. The control surface shows an electrochemical response due to the ferricyanide/ferrocyanide redox couple (peaks at 0.18 V and 0.26 V). Both modified surfaces lack this response, with only very small current increases observed below 0 V in the negative scan and above 0.35 V in the positive scan. Clearly, these surfaces are blocking to electron transfer, suggesting that SAMs are formed as expected. Further details of the procedures used for CV are given in the experimental chapter, section 9.7.

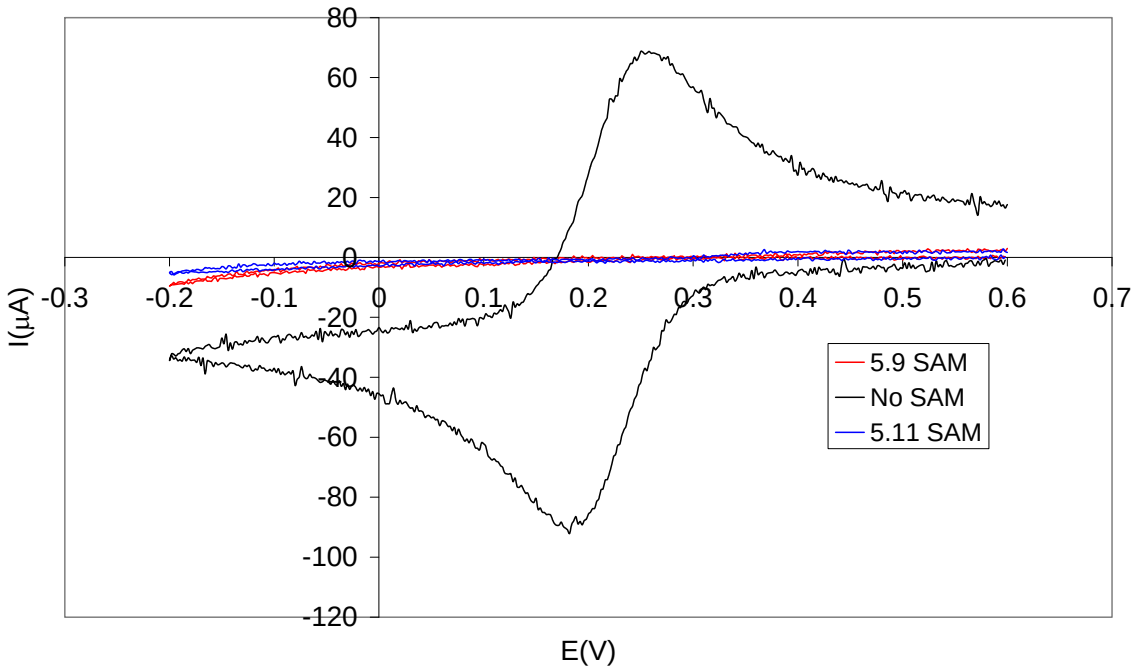

Fig. 7.2. CVs of ferricyanide (1 mM) in $NaClO_4$ (1 M) obtained at a bare gold plug electrode, and at SAMs of **5.9** and **5.11**.

*CV of SAMs of **5.9** and **5.11** on gold films*

The same electrochemical analysis was carried out on SAMs of diluent **5.11** formed on gold film substrates, to ensure that the contact angle results and the electrochemical studies were carried out at comparable surfaces. Two solutions of **5.11** (0.25 mM and 0.025 mM) were prepared, and a substrate was immersed in each for 40 h, then rinsed with ethanol and dried under a stream of nitrogen gas. CVs were recorded for each of these surfaces (Fig. 7.3) in ferricyanide solutions as above. Here, both surfaces are blocking to electron transfer, implying that SAMs are formed from both 0.25 mM and 0.025 mM solutions of **5.11**. This is consistent with the CV obtained for a SAM of **5.11** on a gold plug electrode

(Fig. 7.2) and shows that relatively densely packed SAMs are formed both on the gold plug electrode and the gold films. Thus, the contact angle measurements at gold films and the CV results obtained more conveniently at the gold plug electrode can be assumed to probe essentially the same surfaces. Furthermore, similarly blocking surfaces were formed from 0.25 mM and 0.025 mM solutions, which suggests that changes to the disulfide concentration in this range do not significantly affect the quality of SAMs formed.

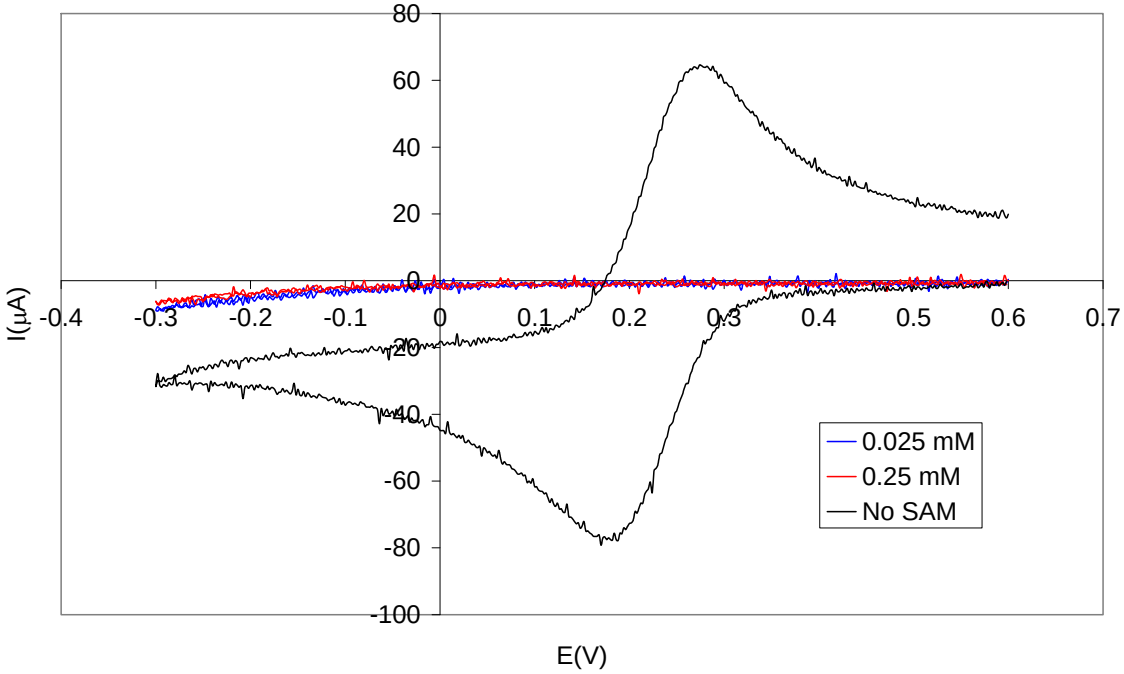

Fig. 7.3. CVs of ferricyanide (1 mM) in $NaClO_4$ (1 M) obtained at a bare gold film electrode, and at SAMs of **5.11** formed from 0.025 or 0.25 mM solutions of the disulfide.

7.3 Preparation of SAMs of 5.16 and 5.11 for enzyme binding

Following the successful formation of simple SAMs on gold, mixed SAMs of photoswitch enzyme inhibitor **5.16** and diluent alcohol **5.11** were formed on gold electrodes and gold coated QCM crystals.

*CV of mixed SAMs of disulfides **5.11** and **5.16** on a gold plug electrode*

Initial studies were carried out on a gold plug electrode to characterise surfaces by CV. The electrode was immersed in a solution of **5.16** and **5.11** (total disulfide concentration 0.25 mM, proportion of **5.16** ($\chi_{5.16}$) = 1, 0.7, 0.4, 0.2, 0.1, 0 in separate experiments) for 40

h, then rinsed with ethanol and dried under a stream of nitrogen. The SAMs were analysed by CV (figs. 7.4-7.8). Fig. 7.4 shows a CV at a SAM with $\chi_{5.16}$ = 1 (i.e. no diluent) in ferricyanide solution. This surface is highly blocking to electron transfer compared to the control surface shown, suggesting that a SAM is present.

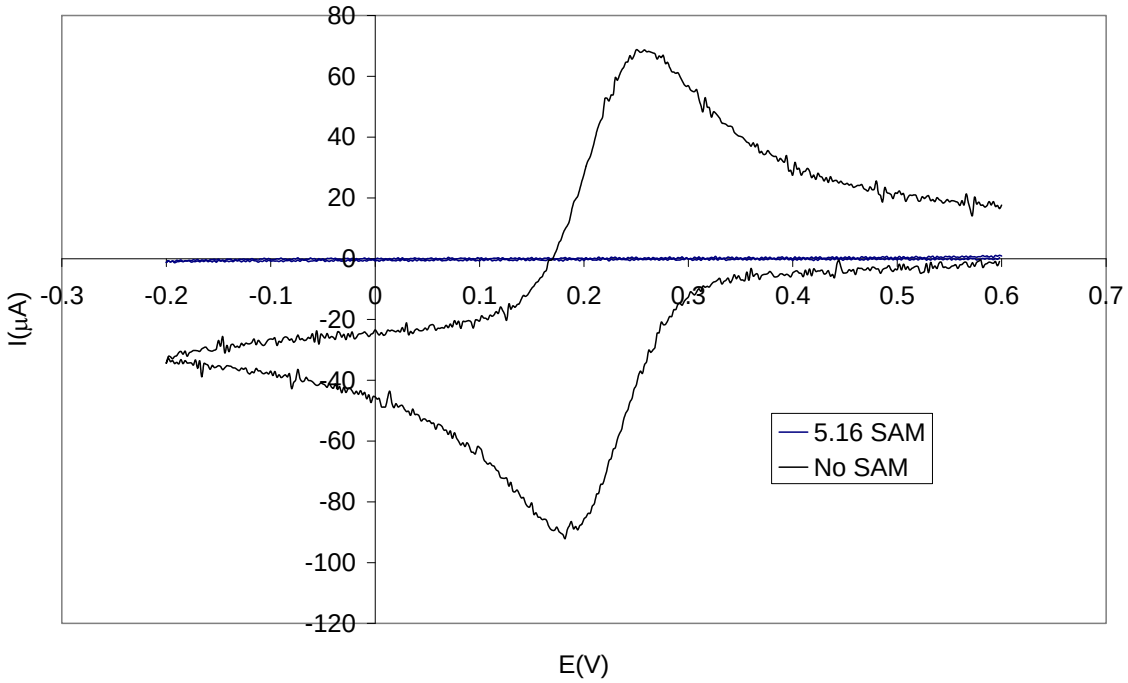

Fig. 7.4. CVs of ferricyanide (1 mM) in $NaClO_4$ (1 M) obtained at a bare gold plug electrode and at a SAM of **5.16**.

Fig. 7.5 shows CVs at the same SAM in a solution of $NaClO_4$ (1 M) lacking ferricyanide, scanning over a wider potential range from 0.4 or 0.5 V to -0.7, -0.8, -0.9 or -1.0 V, then back to the starting potential. Here, a pair of redox peaks are identified at -0.9 and 0.3 V. These peaks are assigned to the reduction of the azobenzene group to hydrazobenzene and the reoxidation process, respectively.[1] The observation of azobenzene redox chemistry might seem surprising given the length of the linker. However, redox chemistry arising from groups at a similar distance from the electrode has been reported previously;[2] the mechanism for electron transfer is not clear. The scan to -1.0 V also shows the beginning of a larger reduction current that is assigned to reductive desorption of disulfide from the surface.[3, 4]

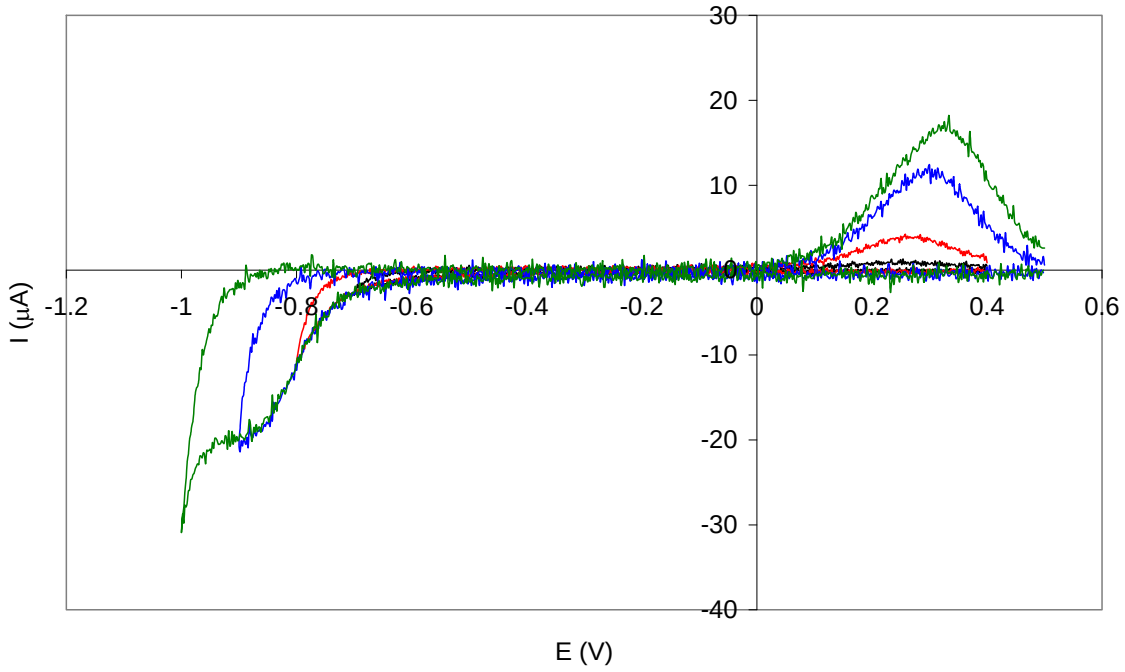

Fig. 7.5 CVs of a SAM of **5.16** in $NaClO_4$ solution (1 M), sequentially scanning to more negative potentials (-0.7, -0.8, -0.9, -1.0 V).

A similar CV experiment was carried out for a SAM of **5.11** ($\chi_{5.16}$ = 0), to compare with the SAM of **5.16**. Fig. 7.6 shows the CVs for both SAMs. As expected, the SAM of **5.11** does not show the redox peaks assigned to azobenzene, but there is an increase in current below -0.8 V that is assigned to disulfide reduction.

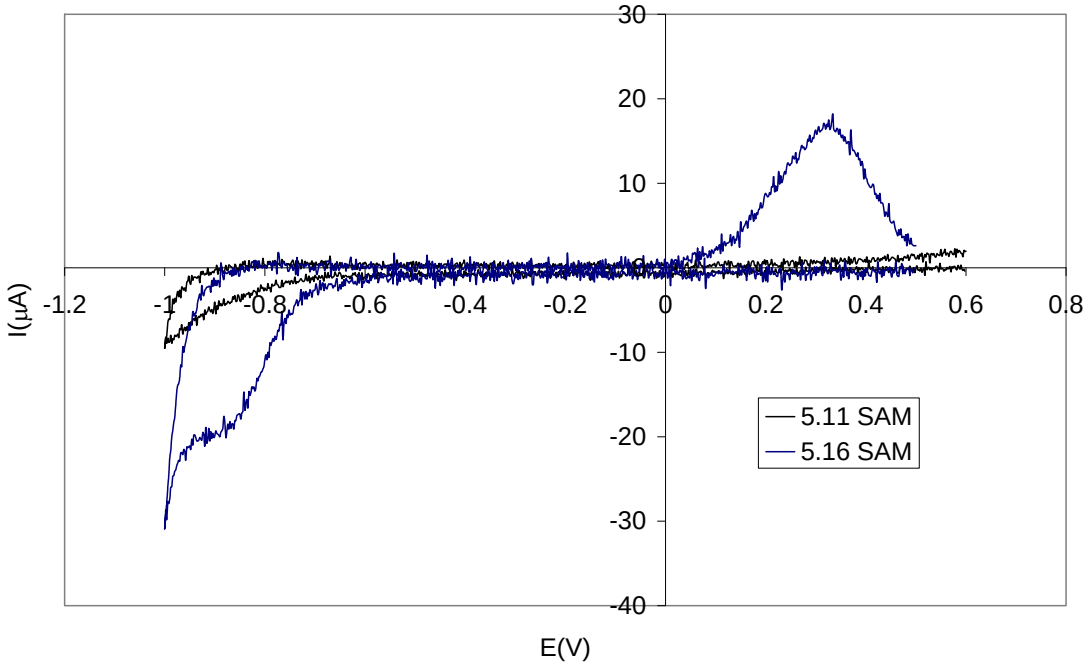

Fig. 7.6. CVs of SAMs of **5.16** and **5.11** in $NaClO_4$ (1 M) solution.

Further CVs of the **5.16** SAM were carried out at scan rates of 100, 200 and 300 mVs^{-1}, scanning first in the negative potential direction from 0.6 to -1.1 V to ensure complete reduction of the azobenzene group, then back to 0.6 V to reoxidise to azobenzene. The integrals of the oxidation peaks were calculated using a curve fitting program[5] and plotted against scan rate (Fig. 7.7). The plot shows a linear relationship between scan rate and peak area, indicating that the same amount of charge is transferred at each scan rate. This is consistent with the redox response of a surface species, because it can be assumed that the surface attached species will be completely oxidised and reduced in each scan, and hence the charge should be independent of scan rate.[6] Therefore, it is confirmed that the observed azobenzene redox peaks arise from the redox reactions of a SAM at the surface.

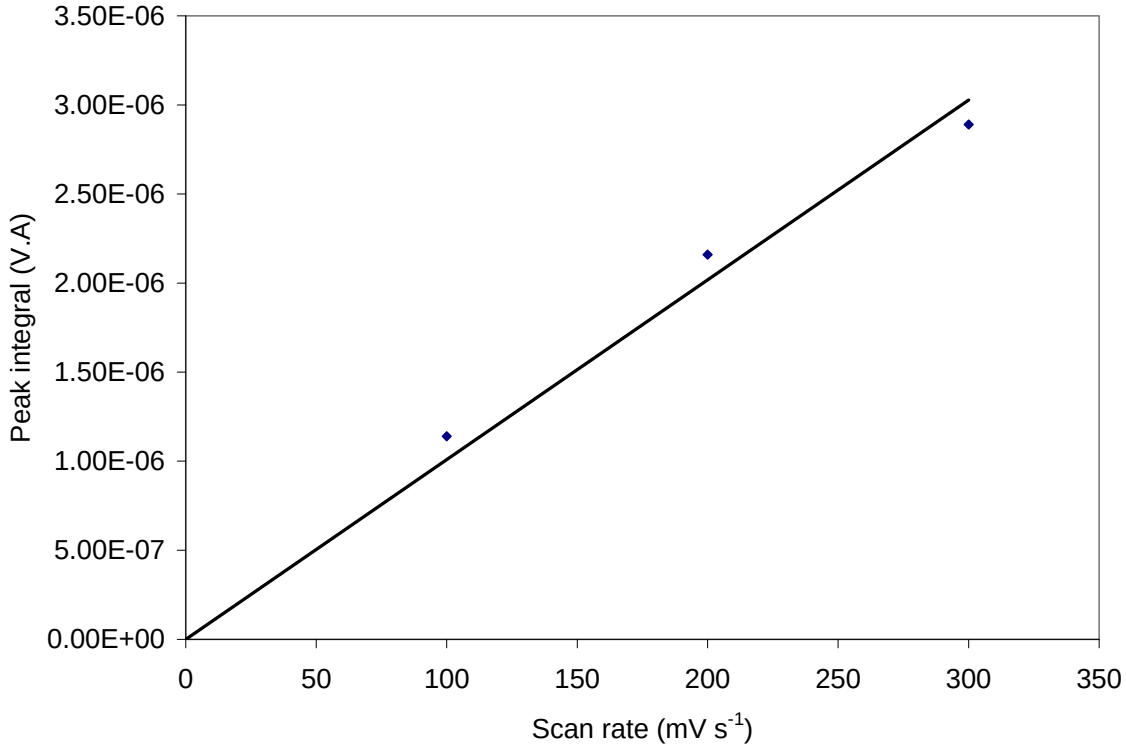

Fig. 7.7. Hydrazobenzene oxidation peak integral vs. scan rate for a SAM of **5.16** in $NaClO_4$ solution (1 M).

The mixed SAMs ($\chi_{5.16}$ = 0.1, 0.2, 0.4 and 0.7) were also analysed. CVs recorded in ferricyanide solutions (not shown) showed that all of these surfaces were highly blocking to electron transfer, suggesting that dense SAMs were formed. CVs were also obtained in $NaClO_4$ solution (1 M) in the absence of ferricyanide, scanning to -1.0 V to reduce the azobenzene group, as described above for the SAMs with $\chi_{5.16}$ = 0 and 1. As previously for $\chi_{5.16}$ = 1, the CVs for these SAMs showed azobenzene redox peaks at -0.9 V and 0.3 V. The integrals of the oxidation peaks were calculated and plotted vs. $\chi_{5.16}$ (Fig. 7.8) to determine the relationship between the proportion of azobenzene disulfide in the SAM formation solution and the proportion attached to the surface. This plot shows a linear relationship between $\chi_{5.16}$ and peak area for hydrazobenzene oxidation. Therefore, the proportions of **5.16** and **5.11** present in a SAM at the surface are the same as the proportions of these compounds present in the solution used to form the SAM. This is surprising, as longer chain length thiols/disulfides normally adsorb preferentially to a shorter chain analogue at a surface.[7] However, both disulfides used here contain an alkyl chain of the same length, which is likely to be the molecular structure most important in stabilisation of the SAM. The major structural difference between **5.16** and **5.11** involves extended OEG chains, which are known to form disordered structures at surfaces and thus may not significantly affect SAM formation.

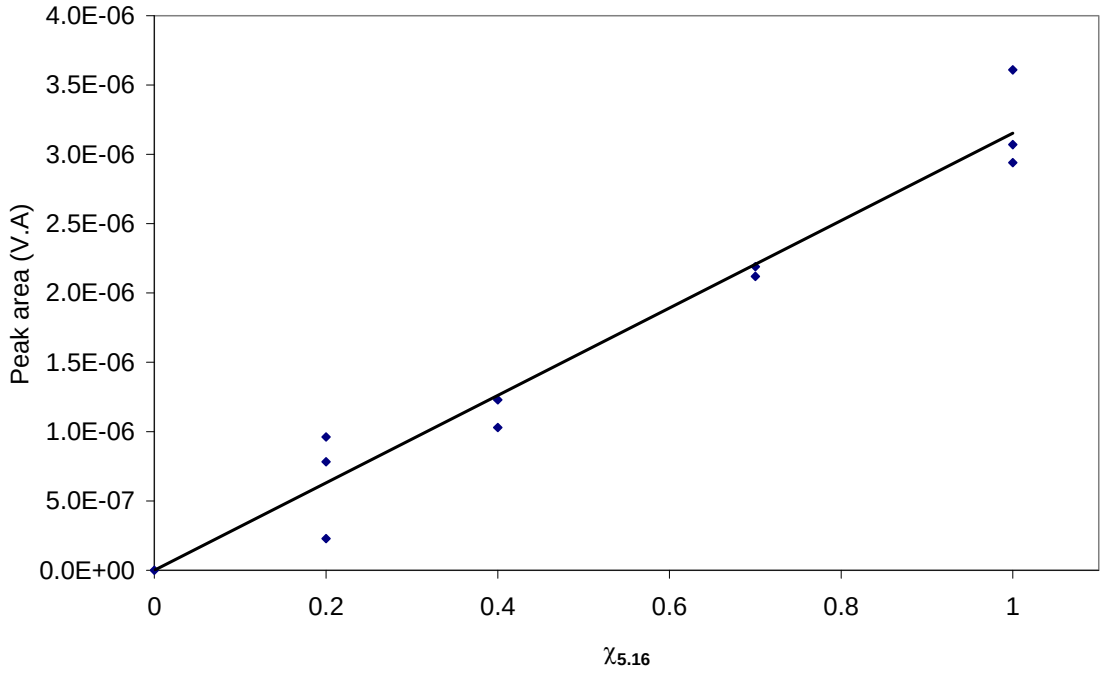

Fig. 7.8. Hydrazobenzene oxidation peak area for mixed SAMs of **5.16** and **5.11** vs. $\chi_{5.16}$. Each data point represents an different SAM.

*CV of mixed SAMs of disulfides **5.11** and **5.16** formed from dilute deposition solutions*

As SAMs formed from 0.25 mM solutions required milligram quantities of disulfides **5.16** and **5.11** for each experiment, it was preferable in some cases to use more dilute solutions for SAM formation. Hence, SAMs of **5.16** and **5.11** were formed from 0.025 mM solutions and compared with those formed from 0.25 mM solutions (a 0.025 mM SAM on gold film was also studied, see section 7.3, Fig. 7.3). A gold plug electrode was immersed in a solution of **5.16** and **5.11** (total disulfide concentration 0.025 mM, $\chi_{\mathbf{5.16}}$ = 0.5 or 1) for 40 h, rinsed with ethanol and dried under a stream of nitrogen. CVs were recorded for these surfaces in ferricyanide solution (not shown). All were highly blocking to electron transfer, indicating that well-packed SAMs were formed. Scans were also carried out in $NaClO_4$ (1 M), giving CVs (Fig. 7.9) with similar shape and oxidation peak areas to SAMs formed from 0.25 mM solutions (see Fig. 7.6). However, the oxidation peaks in Fig. 7.9 are broader and shifted to a higher potential (peak potential, E_p = 0.4 V compared with E_p = 0.3 V for the 0.25 mM SAMs). The broader peaks suggest that the azobenzene group may be present in a range of environments, indicating less ordered SAMs compared to those formed from 0.25 mM solutions.

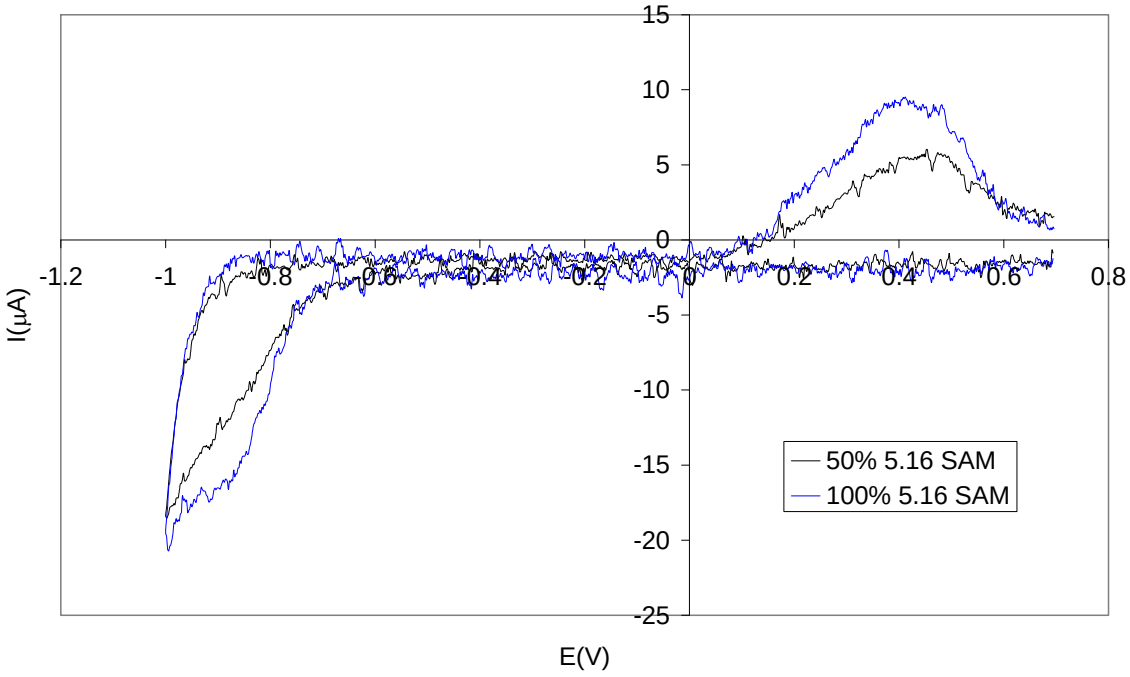

Fig. 7.9. CVs of **5.16**/**5.11** SAMs in $NaClO_4$ (1 M) formed on a gold plug electrode from 0.025 mM disulfide solutions.

*CV of SAMs of disulfide **5.11** on QCM crystals*

As the above results show that SAMs of **5.16** and **5.11** can be successfully formed on gold surfaces, similar SAMs were formed on QCM crystals[†] and briefly studied by CV and contact angle measurements. Initially, a gold-coated QCM crystal was immersed in a solution of **5.11** (0.025 mM) for 40 h, then rinsed with ethanol and dried under a stream of nitrogen gas. A CV was recorded for this SAM in a solution of ferricyanide (1 mM) and $NaClO_4$ (1 M). The crystal was then cleaned with piranha solution[‡], another SAM of **5.11** was formed, and the CV was repeated. To compare, a CV of the same gold surface with no SAM was recorded in the same solution. The three CVs (**5.11** SAM on a new QCM crystal, **5.11** SAM on a piranha cleaned QCM crystal, control) are shown in Fig. 7.10.

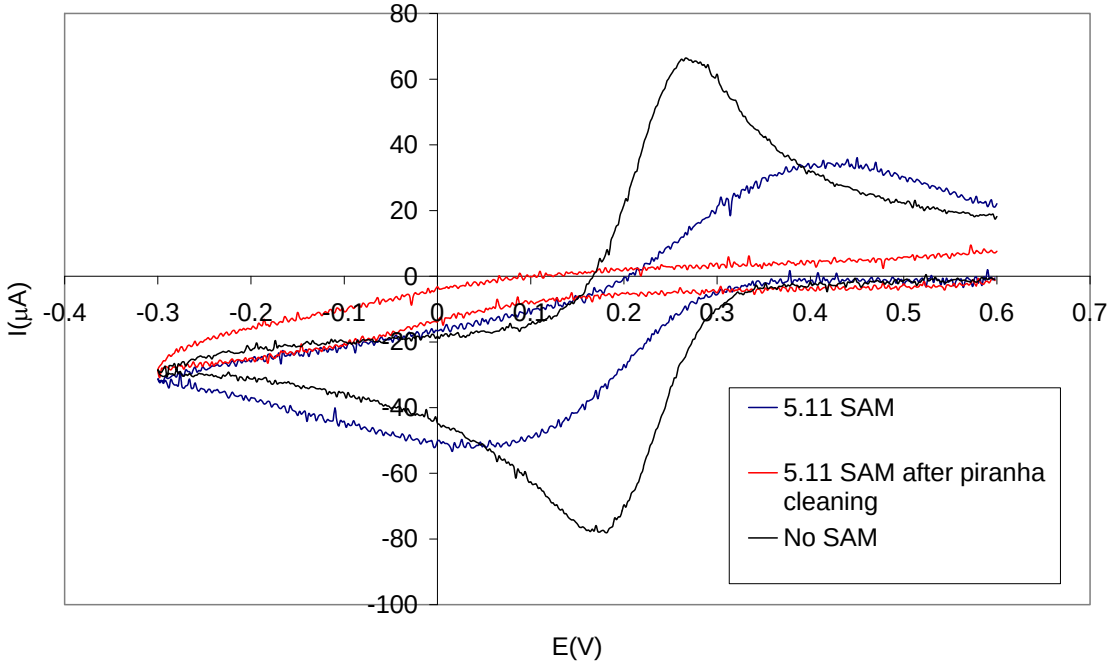

Fig. 7.10. CVs of ferricyanide (1 mM) and $NaClO_4$ (1 M) obtained at SAMs of **5.11** on gold coated QCM crystals prepared before and after piranha cleaning of the surface, and at a control QCM crystal with no SAM.

The control CV shows ferricyanide redox peaks, as expected. At the SAM formed without prior piranha cleaning, the ferricyanide response has lower peak currents and larger potential difference between the reduction and oxidation peaks, compared to the control.

[†] Commercially available crystals designed for use in a Q-sense QCM instrument; further QCM details are given in section 7.4 and the experimental chapter, section 9.7.
[‡] 1:3 H_2O_2/H_2SO_4. Surfaces were cleaned by immersion in piranha solution for several minutes followed by rinsing with water.

This is consistent with slower electron transfer due to the presence of the SAM of **5.11**. The SAM formed after piranha cleaning leads to even slower electron transfer for the ferrocyanide/ferrocyanide redox couple. Neither of the SAMs is as blocking to electron transfer as the SAMs formed on gold film substrates and the gold plug electrode. However, the SAM formed after piranha cleaning is more blocking than that formed without cleaning. Therefore, more densely packed SAMs form on the cleaned surface.

*Contact angle measurements of SAMs of **5.11** on QCM crystals*

Contact angle measurements were also carried out at a SAM of **5.11** on a gold coated QCM crystal. The SAM was formed by soaking the crystal in a solution of **5.11** (0.025 mM, ethanol) for 40 h after cleaning of the gold surface by immersion in piranha solution for 4 minutes and rinsing with water and ethanol. Contact angle measurements were taken, then the surface was again cleaned in piranha solution for 3 min to remove the SAM, rinsed with water and dried under a stream of nitrogen. Contact angle measurements were repeated at the cleaned surface as a control. To confirm that the SAM was removed by this cleaning process, piranha cleaning was repeated for a further 3 min and further contact angle measurements were taken. The averaged measurements are shown in Table 7.2.

Table 7.2. Contact angle measurements[†] at a **5.11** SAM on a gold coated QCM crystal and the same surface after piranha cleaning.

Surface	Averaged contact angle (º)
SAM of **5.11**	38
Au after 3 min piranha soak	86
Au after 2 × 3 min piranha soak	83

[†] Averaged results obtained using three drops of water on one surface. All values are ±3º.

The contact angle after soaking in the **5.11** solution is significantly lower than that of the cleaned surface, suggesting that a SAM of **5.11** has formed on the surface. The results for the piranha treated surfaces are not significantly different, which suggests that soaking in piranha solution for 3 min is sufficient to remove a SAM from the surface. It should be noted that the contact angles here are significantly different to those measured at SAMs of **5.11** on evaporated gold substrates (Table 7.1). In particular, a larger difference between the contact angles of SAMs and bare gold surfaces is observed. This might indicate that

better quality SAMs are formed here, due to the use of piranha treatment to prepare the surfaces. However, this interpretation is inconsistent with the electrochemistry results (compare figs. 7.2 and 7.10), where more blocking SAMs are obtained at evaporated gold substrates. Alternatively, the larger change in contact angles may be attributable to greater surface roughness.[8] Nevertheless, it appears that SAMs are successfully formed on QCM crystals, and the best quality SAMs are obtained after piranha treatment of the surfaces.

7.4 QCM studies of enzyme binding to a surface

Having shown that SAMs with low contact angles can be successfully formed on QCM crystals, QCM experiments were carried out to analyse enzyme binding at these surfaces. Details of the QCM apparatus are given in the experimental chapter, section 9.7.

*QCM study of blocking of enzyme binding to SAMs of **5.11***

Initially, a SAM of **5.11** was formed on a QCM crystal, as described above. This surface was monitored in the QCM instrument, with a solution of Tris buffer flowing at 100 μL min^{-1} over the surface. The QCM frequency response initially drifted significantly over time, but became relatively stable after 2.5 hours of buffer flow. A solution of α-chymotrypsin (4 μM) in Tris buffer was then injected over the surface for 15 min, followed by buffer flow. The calculated mass[†] response vs. time for the enzyme injection is shown in Fig. 7.11.

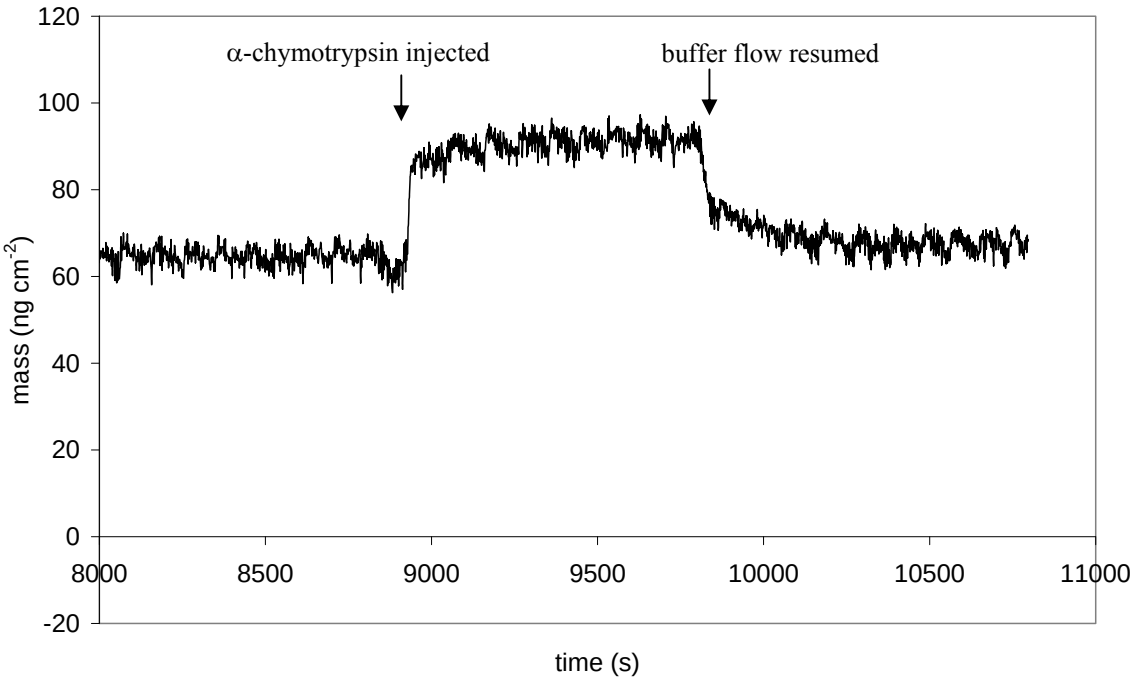

Fig. 7.11. Mass response vs. time for injection of α-chymotrypsin (4 μM in Tris buffer) over a SAM of **5.11** at a flow rate of 100 μL min^{-1}

[†] Calculated using the Sauerbrey equation, as described in chapter 1, section 1.7.3

It can be seen from this plot that the apparent mass increases during injection of enzyme over the surface, then decreases to a level close to the original surface mass when the injection ceases. These results show that very little, if any, enzyme has attached to the surface (<10 ng cm^{-2}). Therefore, the SAM of alcohol **5.11** blocks enzyme attachment to the surface, as expected.

*QCM study of α-chymotrypsin binding to mixed SAMs of **5.16** and **5.11***

In further experiments, mixed SAMs of **5.16** and **5.11** were formed on two QCM crystals (as described above, $\chi_{5.16}$ = 0.05 and 0.1). QCM analysis was then carried out by injection of a solution of α-chymotrypsin over both crystals simultaneously. The mass response vs. time is shown in Fig. 7.12. Here, a significant increase in mass is observed on injection of enzyme, and the mass decreases somewhat when buffer flow is returned. The observed relative mass increases are approximately proportional to the amount of inhibitor **5.16** present in the SAM (i.e. the mass increase at the SAM containing 10% **5.16** is approximately twice that of the SAM containing 5% **5.16**). This suggests that enzyme has attached to the surface-attached inhibitors. The mass increase appears to be largely stable over the timescale of this experiment.

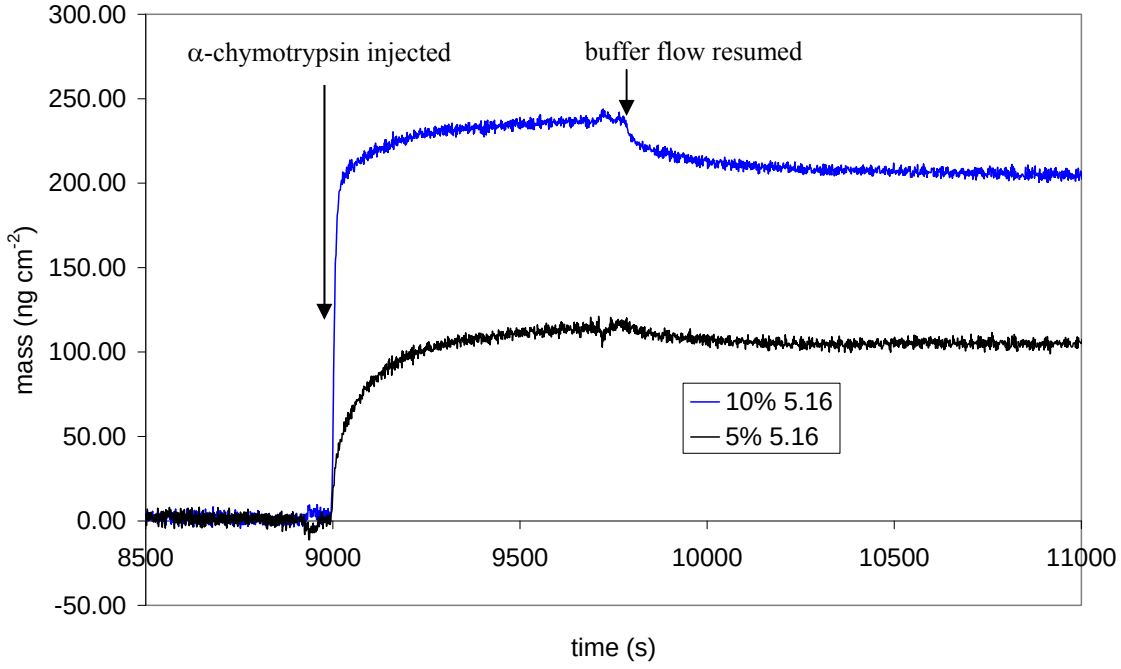

Fig. 7.12. Mass response vs. time for injection of α-chymotrypsin (4 μM) over mixed SAMs of **5.16** and **5.11** at a flow rate of 100 μL min^{-1}.

While enzyme attachment to the surface-bound inhibitor was achieved, the observed stable attachment may arise from denaturation of enzymes and binding of the hydrophobic core residues to the surface, as discussed in chapter 1, section 1.4.3. In this study, enzyme attachment via inhibitor-active site interactions is required for successful photoswitching.

Using the QCM instrument, attached enzyme could not be easily removed for repeated use of a surface in photoswitching studies. In addition, the long equilibration time required to obtain a stable baseline (2.5 h) would be problematic in photoswitching experiments. Consequently, SPR studies were carried out to address these problems.

7.5 SPR studies of enzyme binding and photoswitching at a surface

*Attachment of photoswitch inhibitor **4.4** to a SPR chip*

Gold surfaces are commercially available for SPR that contain a carboxylic acid containing dextran polymer layer which allows attachment of molecules and blocks non-specific enzyme binding. Consequently, these surfaces were appropriate for use in this study, but a different attachment method was required to that used to modify the QCM crystals (described earlier). To link alkyne **4.4** to an SPR chip by azide-alkyne cycloaddition, a surface containing azide groups was required. A carboxylic-acid containing SPR chip was reacted with azide **7.1** (Fig. 7.13) to generate such a surface.

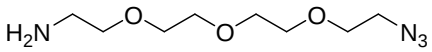

7.1

Fig. 7.13. Azide **7.1** for generation of an azide terminated SPR chip.

This reaction was carried out in an SPR instrument, by activation of the carboxylic acid terminated surface using EDCI/NHS, then coupling of **7.1** to the activated surface.[†] The SPR response increased by 147 RU (resonance units) after injection of **7.1**. While this SPR response is not quantifiable without calibration, this increase represents a significant quantity of **7.1** attached to the surface, by comparison with the increase observed on attachment of NHS to the surface (109 RU).

[†] Full details of SPR procedures and surface modification are given in the experimental chapter, section 9.7.

The azide modified surface was removed from the instrument and reacted with alkyne **4.4**. 150 μL of reaction solution (**4.4**, CuBr, 2,6-lutidine, 2,2'-bipyridine and sodium ascorbate in 1:1 DMF/H_2O) was pipetted onto the surface and left for 1 h at room temperature, then rinsed off by washing sequentially with 1:1 DMF/H_2O, H_2O, 0.1 M EDTA, 1:1 DMF/H_2O, then H_2O. This procedure is adapted from a reported method used to attach alkynes to an azide polymer.[9] The chip was then replaced in the instrument and an SPR sensorgram was obtained while flowing Tris buffer for several hours to allow equilibration of the system.

SPR analysis of α-chymotrypsin binding to surface-attached ***4.4***

After equilibration, α-Chymotrypsin solutions (0, 2.0, 6.0 or 18 μM in Tris buffer, 150 μL) were sequentially injected over the surface for 5 min each, at a flow rate of 30 μL min^{-1}. After each injection, buffer was run for 5 min to monitor dissociation of enzyme from the surface, then the surface was regenerated to remove attached enzyme for the next injection. Regeneration was carried out as per the recommended approach for SPR[10] by the injection of guanidine hydrochloride (6 M, 5 μL) followed by acetic acid (1 M, 10 μL) then Tris buffer for 5 min, all at a flow rate of 5 μL min^{-1}. The SPR curves (response vs. time) for 5 min enzyme injection and 5 min buffer are shown in Fig. 7.14. The response of a control surface not containing inhibitor **4.4** (formed as above except omitting injection of **7.1**) was subtracted from these curves.

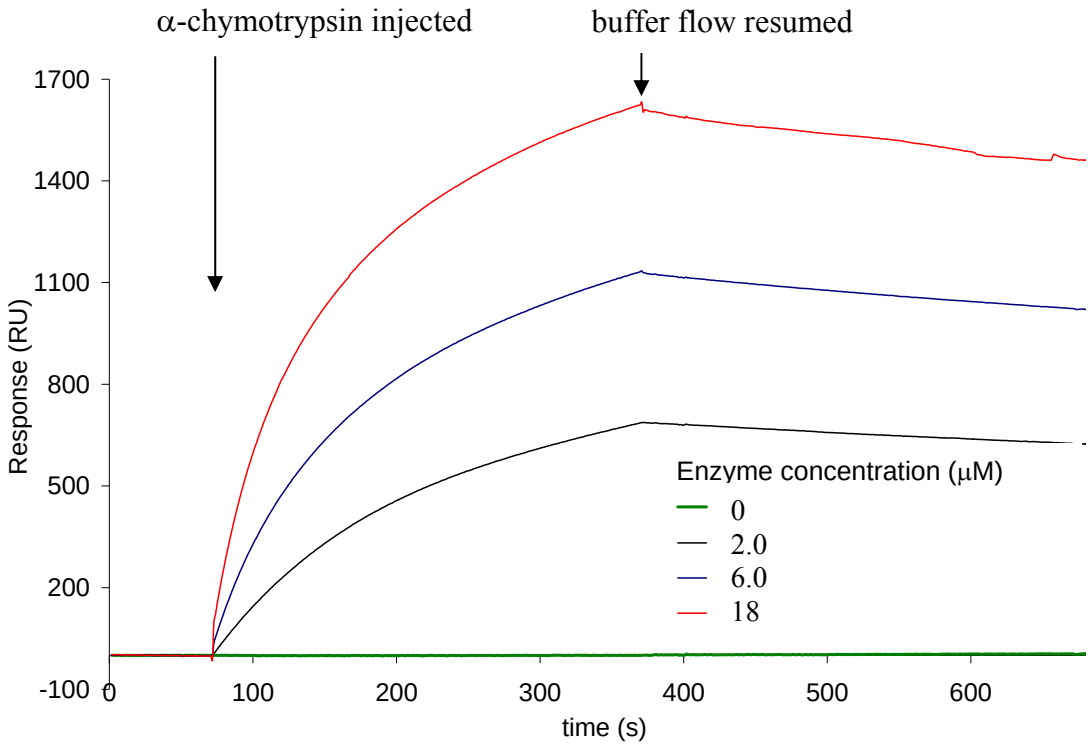

Fig. 7.14. SPR response for 5 min injection of α-chymotrypsin (0-18 μM in Tris buffer) beginning at time = 70 s at 30 μL min^{-1} flow rate over a surface containing attached **4.4**.

An increase in response (proportional to an increase in mass) is observed on injection of enzyme over the surface, suggesting the attachment of enzyme to the surface. The response slowly decreases after enzyme injection ceases, suggesting that enzyme slowly desorbs from the surface, and thus that the attachment is at least partially reversible.

Calculation of the K_D affinity constant for enzyme binding to the surface-bound inhibitor from this data was attempted using a curve-fitting model. However, a good fit could not be obtained by simultaneous modelling of all three concentration curves. Individual modelling of each curve gave calculated k_A, k_D and K_D, values[†] shown in Table 7.3.

[†] K_D is the equilibrium dissociation constant, determined from the equation $K_D = k_D/k_A$, where k_D is the kinetic dissociation constant and k_A is the kinetic association constant.

Table 7.3. Apparent k_A, k_D, and K_D constants for binding of α-chymotrypsin to a surface containing inhibitor **4.4**, calculated by individual curve fitting to SPR data.

Enzyme concentration (μM)	k_A (M^{-1} s^{-1})	k_D (s^{-1})	K_D (μM)
2.0	3260 ± 70	$3.24 \times 10^{-4} \pm 4 \times 10^{-6}$	0.099 ± 0.003
6.0	1400 ± 20	$3.25 \times 10^{-4} \pm 2 \times 10^{-6}$	0.233 ± 0.005
18	590 ± 4	$3.19 \times 10^{-4} \pm 2 \times 10^{-6}$	0.541 ± 0.007

The apparent affinity constant K_D increases with increasing enzyme concentration, corresponding to apparently weaker binding at higher enzyme concentrations. This is surprising, since a constant K_D value should be obtained. The apparent kinetic dissociation rate constant (k_D) is almost constant at all enzyme concentrations, but the apparent kinetic association rate constant (k_A) decreases with increasing enzyme concentration. This shows that the rate of association of α-chymotrypsin with surface-bound **4.4** is decreased at high enzyme concentrations. This trend of a decrease in the apparent association constant with increasing enzyme concentration was also observed in solution-phase studies of the binding of trifluoromethylketones to α-chymotrypsin.[11] The decrease in k_A was attributed to an equilibrium between the active ketone inhibitor and an inactive hydrated form, as shown in the equation:

$$I_h \underset{H_2O}{\rightleftharpoons} I_k \overset{E}{\rightleftharpoons} E\text{-}I$$

where I_h represents hydrated inhibitor, I_k represents ketone inhibitor, E represents α-chymotrypsin and E-I represents the enzyme-inhibitor complex. In aqueous solutions, the hydrated form I_h is known to be present in an approximately 4500-fold excess.[11] At a high concentration of enzyme, the concentration of ketone will be significantly decreased by reaction with the enzyme and it was proposed that a relatively slow rate of hydrate to ketone dehydration would lead to a decrease in the actual concentration of ketone, dependent on the enzyme concentration. This would lead to a decrease in the apparent k_A as the enzyme concentration increases, and thus an increase in the apparent K_D. It seems likely that the surface-attached trifluoromethylketone in the present study is exhibiting the same behaviour.

Photoregulated binding of α-chymotrypsin to surface-attached ***4.4***

To achieve photoswitching of the surface bound inhibitor, enzyme binding was measured before and after irradiation of the surface with a UV lamp, as described in chapter 6 for solution-phase irradiations. The SPR chip, after regeneration, was removed from the instrument and irradiated with UV light for 5 min, then replaced in the instrument and injection of enzyme (0, 2.0, 6.0 or 18 μM) was repeated as previously. The surface was regenerated, removed from the instrument, irradiated with visible light for 5 min, then enzyme injection was repeated. The SPR curves for the 2.0 μM enzyme injections before and after each irradiation are shown in Fig. 7.16, and representative data (maximum response at time = 370 s, apparent k_A, k_D, and K_D) for all enzyme concentrations is given in tables 7.4-7.6.

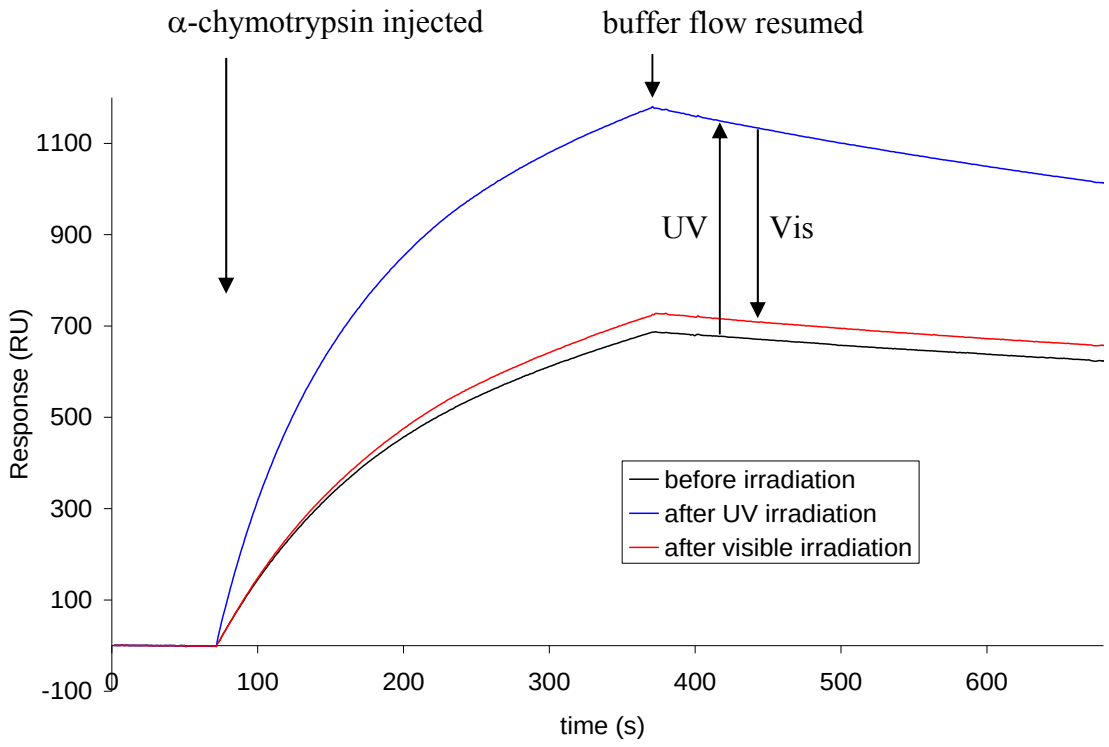

Fig. 7.16. Reversible photoregulation of α-chymotrypsin binding (2.0 μM) to surface attached inhibitor **4.4**.

Table 7.4. Maximum SPR response (RU) for binding of α-chymotrypsin binding to surface attached inhibitor **4.4**, before and after UV/vis irradiations.

Enzyme concentration (μM)	Maximum SPR response before irradiation (RU)	Maximum SPR response after UV irradiation (RU)	Maximum SPR response after visible irradiation (RU)
2.0	690	1200	720
6.0	1100	1700	1200
18	1600	2100	1700

Table 7.5. Apparent k_A, k_D, and K_D constants for binding of α-chymotrypsin to a surface containing inhibitor **4.4** after UV irradiation, calculated by individual curve fitting to SPR data.

Enzyme concentration (μM)	k_A ($M^{-1} s^{-1}$)	k_D (s^{-1})	K_D (μM)
2.0	4220 ± 70	$5.02 \times 10^{-4} \pm 1 \times 10^{-6}$	0.119 ± 0.002
6.0	1890 ± 20	$4.82 \times 10^{-4} \pm 1 \times 10^{-6}$	0.255 ± 0.003
18	748 ± 6	$4.43 \times 10^{-4} \pm 1 \times 10^{-6}$	0.593 ± 0.006

Table 7.6. Apparent k_A, k_D, and K_D constants for binding of α-chymotrypsin to a surface containing inhibitor **4.4** after visible irradiation, calculated by individual curve fitting to SPR data.

Enzyme concentration (μM)	k_A ($M^{-1}s^{-1}$)	k_D (s^{-1})	K_D (μM)
2.0	3060 ± 50	$3.31 \times 10^{-4} \pm 1 \times 10^{-6}$	0.108 ± 0.002
6.0	1330 ± 10	$3.22 \times 10^{-4} \pm 1 \times 10^{-6}$	0.242 ± 0.003
18	533 ± 3	$2.98 \times 10^{-4} \pm 1 \times 10^{-6}$	0.559 ± 0.004

After UV irradiation, a greater amount of enzyme attaches to the surface (see Table 7.4) and the apparent association and dissociation rate constants k_A and k_D are increased (see tables 7.3 and 7.5), as compared to the surface before irradiation. However, only a small increase in the apparent K_D affinity constant is observed after irradiation. After visible irradiation, the binding response is restored to close to that of the surface before UV irradiation (see tables 7.4 and 7.6).

The lack of a large change of the K_D affinity constants after irradiation contrasts with the solution-phase photoswitching studies (see chapter 6), where the *E*- and *Z*-enriched PSS of **4.4** exhibit a > 3.6 fold difference in IC_{50} affinity constants. This difference is attributed to the fact that solution phase studies yield an overall affinity value for binding of both *E*- and *Z*-**4.4**, since the affinity constant is calculated from the total activity and total concentration of both *E* and *Z* isomers. Conversely, the observed SPR response is likely to be predominantly due to binding of α-chymotrypsin to the more potent *Z* isomer of **4.4**, since the activity of the less potent *E*-isomer is unlikely to significantly alter the shape of the SPR curve, and the concentrations of surface-attached *E*- and *Z*-**4.4** are not involved in the affinity calculations. UV irradiation of the surface then gives an increase in the amount of *Z*-**4.4** at the surface, and thus more enzyme is able to bind to the surface (at a given enzyme concentration) with a similar thermodynamic dissociation constant. Visible irradiation restores surface-attached *Z*-**4.4** to *E*-**4.4**, resulting in a reduction to the original enzyme binding capacity. The small increase in the apparent K_D on UV irradiation represents slightly weaker binding, despite a larger amount of enzyme attachment to the surface. This is consistent with the greater apparent K_D values observed on injection of higher enzyme concentrations over the surface, and is also attributed to the ketone-hydrate equilibrium.

7.6 Summary

SAMs of disulfides **5.9** and **5.11** were formed on a gold plug electrode and gold film surfaces and characterised with contact angle measurements and electrochemistry. Surfaces were obtained that blocked electron transfer, and gave lower contact angles than unmodified surfaces. SAMs of photoswitch inhibitor **5.16** and diluent **5.11** were formed on gold electrodes and gold coated QCM crystals, and characterised using the same techniques. The two disulfides were found to bind to the surface in proportions equal to those in the deposition solution. SAMs of **5.11** on QCM crystals exhibited lower contact angles than SAMs of **5.11** on evaporated gold substrates, but were less blocking to electron transfer. α-Chymotrypsin attachment to mixed SAMs of **5.16** and **5.11** was studied by QCM. Enzyme attachment was observed, but was largely irreversible. Photoregulated binding of α-chymotrypsin to surface attached inhibitor **4.4** was studied by SPR. Enzyme attachment to the surfaces was observed, but a single K_D affinity constant could not be

obtained as the apparent affinity decreased as enzyme concentration was increased. This decrease is attributed to the ketone-hydrate equilibrium of the trifluoromethylketone inhibitor. UV/vis irradiation reversibly modified the amount and kinetic rates of enzyme binding to the surface, presumably due to photoisomerisation of surface-attached inhibitor **4.4**.

7.7 References

1. Zhang, W. W.; Ren, X. M.; Li, H. F.; Lu, C. S.; Hu, C. J.; Zhu, H. Z.; Meng, Q. J., *Journal of Colloid and Interface Science* **2002**, 255, (1), 150-157.

2. Yousaf, M. N.; Houseman, B. T.; Mrksich, M., *Angew. Chem. Int. Ed.* **2001**, 40, (6), 1093.

3. Shepherd, J. L.; Kell, A.; Chung, E.; Sinclar, C. W.; Workentin, M. S.; Bizzotto, D., *J. Am. Chem. Soc.* **2004**, 126, 8329.

4. Sumi, T.; Uosaki, K., *J. Phys. Chem. B* **2004**, 108, 6422.

5. Loring, J. S., *Linkfit* **2004**.

6. Bard, A. J.; Faulkner, L. R., *Electrochemical methods : fundamentals and applications*. 2 ed.; **2001**.

7. Laibinis, P. E.; Fox, M. A.; Folkers, J. P.; Whitesides, G. M., *Langmuir* **1991**, 7, 3167.

8. Lim, H. S.; Han, J. T.; Kwak, D.; Jin, M.; Cho, K., *J. Am. Chem. Soc.* **2006**, 128, 14458.

9. Punna, S.; Kaltgrad, E.; Finn, M. G., *Bioconjugate Chem.* **2005**, 16, 1536.

10. *Biacore Sensor Surface Handbook*. **2003**.

11. Brady, K.; Abeles, R. H., *Biochemistry* **1990**, 29, 7608.

Chapter Eight

Conclusions and Future Work

Conclusions and future work

Reversible photoswitching of α-chymotrypsin binding to a surface attached inhibitor was achieved, as shown schematically in Fig. 8.1.

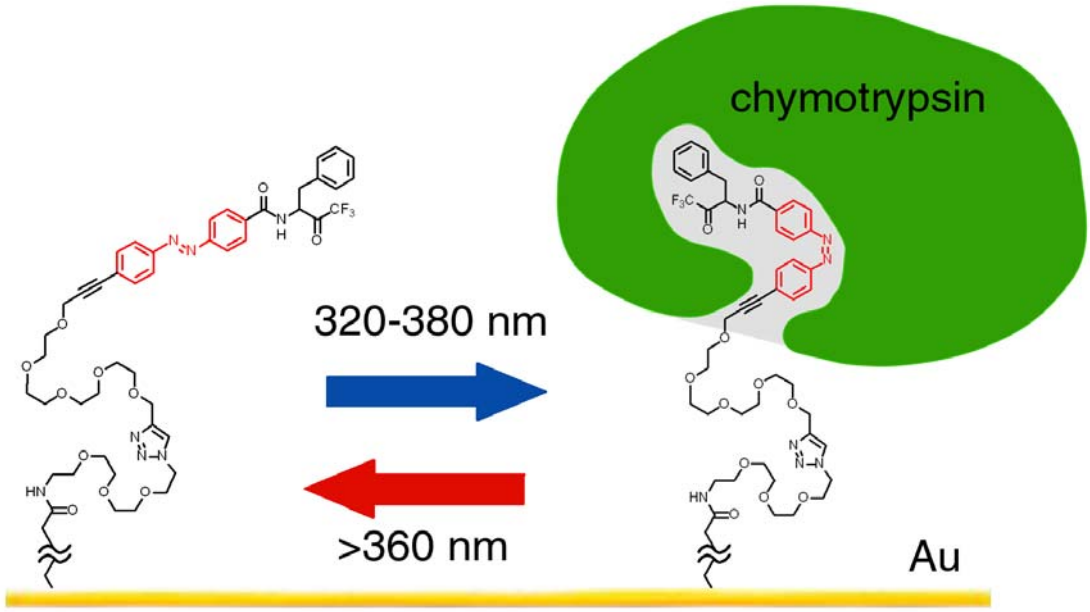

Fig. 8.1. Schematic of photoswitching showing surface attached inhibitor **4.4** with α-chymotrypsin bound to the *Z* isomer.

A range of azobenzene-containing photoswitch inhibitors of α-chymotrypsin with boronic acid, trifluoromethylketone and α-ketoester enzyme binding groups were designed and synthesised (chapters 2 and 4). Photoisomerisation studies and enzyme assays of these inhibitors (chapter 6) found that the trifluoromethylketones and α-ketoesters were effective photoswitch inhibitors, with a best result of a reversible > 5.3 fold increase in activity obtained on UV/vis irradiation. The most promising photoswitch for surface attachment, trifluoromethylketone **4.4**, was attached to a gold surface in a two step process involving amide bonding and 'click chemistry' azide-alkyne cycloaddition. Photoregulated binding of α-chymotrypsin to this surface was studied by SPR (chapter 7). A reversible change in the rate and amount of enzyme binding to this surface was detected on UV/visible irradiation of the surface.

These results represent a preliminary example of photoregulated surface binding of a protease. A modular inhibitor design was developed with an azobenzene photoswitch core containing attached groups for surface attachment and enzyme binding. The system presented here uses a peptidomimetic trifluoromethylketone group specific for α-chymotrypsin as enzyme binding group. Future work will investigate extension of this approach to target other proteases using enzyme binding groups specific to these enzymes.

The photoswitching achieved here is not complete. In particular, the azobenzene group does not completely isomerise to either the *E* or *Z* isomer on irradiation. Consequently, a maximum of approximately 5 fold change in activity is possible with azobenzene inhibitors of this type. Furthermore, it appears that the less active *E* isomer of the inhibitors also binds to the enzyme to some extent. Future work will investigate improvement of photoswitching using a photoswitch group that gives more complete photoisomerisation, or by use of multiple azobenzene groups in a single inhibitor molecule.

In addition, the kinetic dissociation rate for enzyme from surface-attached inhibitor **4.4** is very slow, most likely due to the tight binding mode of the trifluoromethylketone group with α-chymotrypsin. Consequently, a relatively harsh regeneration method (guanidine hydrochloride and acetic acid) was required to rapidly remove enzyme from the surface. For development of technologies such as reversible biosensors, surfaces are required that rapidly dissociate enzyme under mild conditions. Future work will investigate obtaining faster kinetic dissociation using alternative enzyme binding groups, preferably those lacking an electrophilic warhead as investigated in chapter 3.

Chapter Nine

Experimental

Experimental

9.1 General Methods and Experimental Procedures

NMR data reporting for azobenzene derivatives

The azobenzenes reported in this work were synthesised as predominantly the *E* isomer (<5% *Z*), unless specified otherwise, and NMR data is reported for the *E* isomer only. NMR data for the *Z* isomer are reported for selected cases where the amount of *Z* isomer was enriched.

Elemental Analysis

Elemental analyses were performed for carbon, nitrogen and hydrogen at the University of Otago microanalytical laboratory.

Concentrating of solvents

Bulk removal of solvent and volatiles was carried out under reduced pressure using a Büchi rotary evaporator (low vacuum pump). More rigorous drying was achieved under high vacuum (oil pump) for at least 30 min.

Column Chromatography

Column chromatography was performed on silica 60 gel, using either N_2 pressure or gravity to elute solvents from the column. All solvents were distilled before use.

High Performance Liquid Chromatography

Analytical HPLC was performed on a Dionex liquid chromtograph controlled by Chromeleon software, with a Prodigy C18 column (250 x 4.6, 5 μm).

Infrared Spectroscopy

IR spectra were obtained using a Shimadzu 8201PC series FTIR. Spectra were run either neat or as a nujol mull.

Melting points

All melting points were obtained on an Electrothermal apparatus and are uncorrected. Melting points are not reported for diastereomeric or ketone/hydrate mixtures.

Mass Spectrometry

Electrospray ionisation (ES) mass spectroscopy was performed on a Micromass LCT TOF Mass Spectrometer operating with a probe voltage of 3.2 kV at 150 °C and a source temperature of 80 °C.

Nuclear Magnetic Resonance

^{1}H NMR spectra were obtained on either a Varian UNITY 300 or INOVA 500 spectrometer operating at 300 and 500 MHz, respectively. ^{19}F NMR were obtained on the Varian UNITY 300 spectrometer operating at 282 MHz. ^{13}C NMR were obtained on either the Varian UNITY 300 or the INOVA 500 spectrometer operating at 75 and 126 MHz, respectively. All spectra were obtained at 23 °C with a delay (D_1) of at least 1 s. ^{1}H and ^{19}F NMR experiments had an acquisition time (A_t) of 2 s, ^{13}C NMR experiments had an acquisition time of 1-2 s. All two-dimensional NMR experiments, which include COSY, HSQC, and HMBC were run on the INOVA 500 spectrometer.

Chemical shifts are reported in parts per million (ppm) on the δ scale and were referenced to the appropriate residual solvent peaks: $CDCl_3$ referenced to $(CH_3)_4Si$ at δ_H 0.00 ppm (^{1}H) and ($CDCl_3$) at δ_C 77.16 ppm (^{13}C); methanol-d_4 referenced to CHD_2OD at δ_H 3.31 ppm (^{1}H) and CD_3OD at δ_C 49.00 ppm (^{13}C); acetone-d_6 referenced to $(CHD_2)(CD_3)CO$ at δ_H 2.05 ppm (^{1}H) and $(CD_3)_2CO$ at δ_C 29.84 ppm (^{13}C); acetonitrile-d_3 referenced to

C*H*D_2CN at δ_H 1.94 ppm (^{1}H) and *C*D_3CN at δ_C 1.32 ppm; DMSO-d_6 referenced to (C*H*D_2)(CD_3)SO at δ_H 2.50 ppm (^{1}H) and (*C*D_3)$_2$SO at δ_C 39.52 ppm (^{13}C); D_2O referenced to D_2*O* at 4.79 ppm (^{1}H). All ^{19}F NMR spectra were referenced against an internal standard (fluorobenzene C_6H_5*F*) at δ_F –113.15 ppm (^{19}F).

Optical Rotary Dispersion

Optical rotation measurements were performed on a Perkin Elmer polarimeter Model 341 with a 1.00 dm pathlength. Measurements were taken at 20 ºC, at a wavelength of 589 nm. $[\alpha]_D$ values are given in º mL g^{-1} dm^{-1} and the sample concentration given in units of 10 mg mL^{-1}.

Ultraviolet Spectroscopy

UV/Visible spectroscopy was performed on a GBC UV/Vis 918 spectrometer running the default GBC Scientific v 2.01 software package.

Thin Layer Chromatography

Analytical TLC was performed on plastic-backed Merck-Kieselgel KG60F_{254} or Polygram Sil G/UV_{254} plates. Traces were visualised with UV light and/or a suitable dip, typically basic potassium permanganate (general use), ninhydrin (amines), or ammonium molybdate-ceric sulphate dip (azobenzenes, sulfur compounds).

Reagents and solvents

Purchased reagents (primarily from Aldrich, Sigma, Fluka and Acros) were used as supplied. All other reagents and solvents were purified according to well established procedures.[1] Triethylamine, dichloromethane, pyridine and toluene were distilled from calcium hydride powder immediately prior to use. Ether and THF were distilled from sodium benzophenone ketyl immediately prior to use. Anhydrous methanol was distilled

from magnesium ethoxide or magnesium methoxide respectively and stored under argon over 4 Å molecular sieves.

9.2 Experimental for work described in chapter 2

(*E*)-4-phenylazobenzoic acid 2.15:[2]

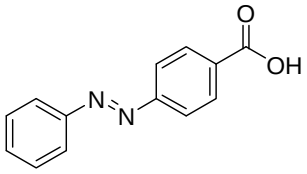

A solution of nitrosobenzene **2.13** (730 mg, 6.8 mmol) and 4-aminobenzoic acid **2.14** (940 mg, 1 eq) in AcOH (5.0 mL) was stirred for 20 h then filtered to collect an orange precipitate, which was washed with AcOH (2 × 5.0 mL) then concentrated. The crude product was recrystallised from EtOH to give **2.15** (820 mg, 53%) as an orange solid:
mp 247-248 ºC (lit 248.5-249.5)[2]
^{1}H NMR (300 MHz, $(CD_3)_2SO$) δ 7.59-7.66 (3H, m), 7.91-8.00 (4H, m), 8.15 (2H, d, J = 8.6 Hz).

(*E*)-4-(Phenylazo)-*N*-(3-(4,4,5,5-tetramethyl-1,3,2-dioxaborolan-2-yl)phenyl) benzamide 2.1:

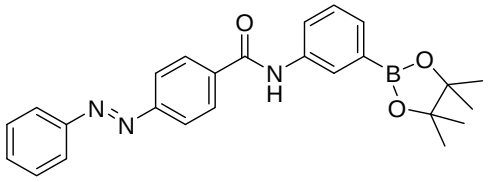

To a mixture of carboxylic acid **2.15** (200 mg, 0.88 mmol), amine **2.16** (190 mg, 1 eq) and HATU (370 mg, 1.1 eq) was added DMF (5.0 mL) then DIEA (340 µL, 2.2 eq). The mixture was stirred for 16 h then diluted with EtOAc (50 mL), washed with water (50 mL × 2), dried over $MgSO_4$ and concentrated. The crude product was purified by flash chromatography, eluting with DCM followed by 1:9 EtOAc/DCM then 1:4 EtOAc/DCM to give **2.1** (200 mg, 53%) as an orange solid:
mp: 162–164 ºC
Elemental analysis: Calcd. for $C_{25}H_{26}BN_3O_3$: C 70.27, H 6.13, N 9.83%, found: C, 70.19; H, 6.04; N, 9.93.

^{1}H NMR (300 MHz, $CDCl_3$) δ 1.32 (12H, s, (C*Me*$_2$)$_2$), 7.37 (1H, t, *J* = 7.8), 7.50 (3H, m), 7.60 (1H, d, *J* = 7.2), 7.87–8.04 (8H, m), 8.23 (1H, s).

^{13}C NMR (75 MHz, $CDCl_3$) δ 24.9, 84.0, 123.1, 123.1, 123.3, 126.2, 128.0, 128.7, 129.2, 131.0, 131.7, 136.5, 137.3, 152.5, 154.3, 164.

HRMS(ES): Calcd. 428.2145 for $C_{25}H_{27}BN_3O_3$ (MH^+), found 428.2162.

(*S*,*E*)-4-Methyl-2-(4-(phenylazo)-benzoylamino)-pentanoic acid methyl ester 2.17:[3, 4]

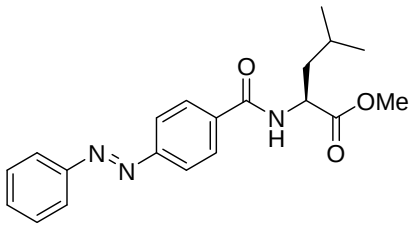

To a solution of carboxylic acid **2.15** (200 mg, 0.88 mmol), H-Leu-OMe.HCl (160 mg, 1 eq), and HATU (370 mg, 1.1 eq) in DMF (3.0 mL) was added DIEA (510 μL, 3.3 eq). The resultant solution was stirred for 16 h then diluted with EtOAc (50 mL), washed with H_2O (50 mL × 2), HCl (50 mL), sat. $NaHCO_3$ (50 mL), brine (50 mL), dried over $MgSO_4$ and concentrated. The crude material was purified by flash chromatography, eluting with 1:19 EtOAc/DCM to give **2.17** (290 mg, 93%) as an orange solid:

mp: 88-90 ºC

$[\alpha]_D^{20}$: +1.5 º (c = 0.65, MeOH)

^{1}H NMR (500 MHz, $CDCl_3$) δ 0.96-1.03 (6H, m, CH*Me*$_2$), 1.65-1.82 (3H, m, C*H*$_2$CHMe$_2$ and CH$_2$C*H*Me$_2$), 3.78 (3H, s, O*Me*), 4.89 (1H, m, NHC*H*), 6.79 (1H, d, *J* = 8.2 Hz, N*H*), 7.47-7.55 (3H, m), 7.92-7.95 (6H, m).

^{13}C NMR (75 MHz, $CDCl_3$) δ 22.1, 23.0, 25.1 (CH$_2$*C*HMe$_2$), 41.9 (*C*H$_2$CHMe$_2$), 51.4 (NH*C*H), 52.6 (O*Me*), 123.0, 123.2, 128.2, 129.3, 131.7, 135.7, 152.6, 154.4, 166.5, 173.8.

HRMS (ES): Calcd. for $C_{20}H_{24}N_3O_3$ (MH^+) 354.1818, found 354.1802.

(*S*,*E*)-3-Methyl-2-(4-(phenylazo)-benzoylamino)-butyric acid methyl ester 2.18:

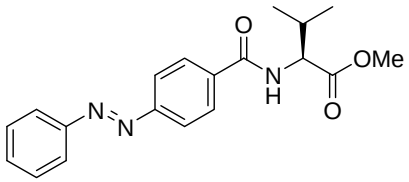

To a solution of **2.15** (200 mg, 0.88 mmol), H-Val-OMe.HCl (150 mg, 1 eq), and HATU (370 mg, 1.1 eq) in DMF (3.0 mL) was added DIEA (510 μL, 380 mg, 3.3 eq). The resulting solution was stirred for 16 h then diluted with EtOAc (50 mL), washed with H_2O (50 mL), HCl (1.0 M, 50 mL), sat. $NaHCO_3$ (50 mL), brine (50 mL), dried over $MgSO_4$ and concentrated. The crude material was purified by flash chromatography, eluting with 1:19 EtOAc/DCM to give **2.18** (270 mg, 89%) as an orange solid:

mp: 139-141 ºC

$[\alpha]_D^{20}$: +17.8 º (c = 0.40, MeOH)

^{1}H NMR (500 MHz, $CDCl_3$) δ 1.01-1.06 (6H, m, CH*Me*$_2$), 2.31 (1H, m, C*H*Me$_2$), 3.80 (3H, s, O*Me*), 4.82 (1H, dd, J = 8.5, 4.9 Hz, C*H*NH), 6.69 (1H, d, J = 8.5 Hz, N*H*), 7.49-7.57 (3H, m), 7.94-8.00 (6H, m).

^{13}C NMR (75 MHz, $CDCl_3$) δ 18.2, 19.2, 31.8, 52.5, 57.7, 123.1, 123.2, 128.2, 129.3, 131.7, 135.9, 152.6, 154.5, 166.7, 172.7.

HRMS(ES): Calcd. 340.1661 for $C_{19}H_{22}N_3O_3$ (MH^+), found 340.1677.

(*E*)-(4-(Phenylazo)-benzoylamino)-acetic acid methyl ester 2.19:

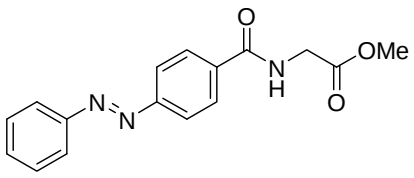

To a solution of **2.15** (200 mg, 0.88 mmol), H-Gly-OMe.HCl (120 mg, 1 eq) HATU (370 mg, 1.1 eq) in DMF (3.0 mL) was added DIEA (510 μL, 380 mg, 3.3 eq). The resulting solution was stirred for 16 h then diluted with EtOAc (50 mL), washed with H_2O (50 mL), HCl (1.0 M, 50 mL), sat. $NaHCO_3$ (50 mL), brine (50 mL), dried over $MgSO_4$ and concentrated. The crude material was purified by flash chromatography, eluting with 1:4 EtOAc/DCM to give **2.19** (250 mg, 96%) as an orange solid:

mp: 123-124 ºC

^{1}H NMR (500 MHz, $CDCl_3$) δ 3.83 (3H, s, *Me*), 4.29 (2H, d, J = 5.0 Hz, C*H*$_2$), 6.73 (1H, s, N*H*), 7.49-7.57 (3H, m), 7.93-8.01 (6H, m).

^{13}C NMR (75 MHz, $CDCl_3$) δ 41.9, 52.7, 123.1, 123.2, 128.2, 129.3, 131.8, 135.4, 152.6, 154.6, 166.9, 170.6.

HRMS(ES): Calcd. 298.1192 for $C_{16}H_{16}N_3O_3$ (MH^+), found 298.1186.

(*S*,*E*)-2-(4-(Phenylazo)-benzoylamino)-propionic acid methyl ester 2.20:

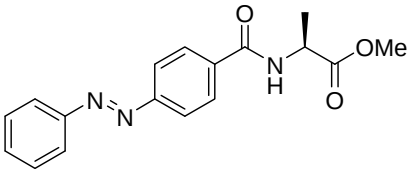

To a solution of **2.15** (200 mg, 0.88 mmol), H-Ala-OMe.HCl (130 mg, 1 eq), HATU (370 mg, 1.1 eq) in DMF (3.0 mL) was added DIEA (510μL, 380 mg, 3.3 eq). The resulting solution was stirred for 16 h, then diluted with EtOAc (50 mL), washed with H_2O (50 mL), HCl (1.0 M, 50 mL), sat. $NaHCO_3$ (50 mL), brine (50 mL), dried over $MgSO_4$ and concentrated. The crude material was purified by flash chromatography, eluting with a gradient from 1:19 to 1:4 EtOAc/DCM to give **2.20** (230 mg, 85%) as an orange solid:

mp: 144-147 ºC

$[\alpha]_D^{20}$: +19.3 º (c = 0.60, MeOH)

^{1}H NMR (500 MHz, $CDCl_3$) δ 1.56 (3H, d, J = 7.2 Hz, CH*Me*), 3.82 (3H, s, O*Me*), 4.84 (1H, p, J = 7.2 Hz, C*H*Me), 6.80 (1H, d, J = 7.0 Hz, N*H*), 7.49-7.57 (3H, m), 7.93-8.00 (6H, m).

^{13}C NMR (75 MHz, $CDCl_3$) δ 18.8, 48.7, 52.8, 123.1, 123.2, 128.2, 129.3, 131.7, 135.7, 152.6, 154.5, 166.2, 173.8.

HRMS(ES): Calcd. 312.1348 for $C_{17}H_{18}N_3O_3$ (MH^+), found 312.1344.

(*S*,*E*)-4-Methyl-2-(4-(phenylazo)-benzoylamino)-pentanoic acid 2.21:[3, 4]

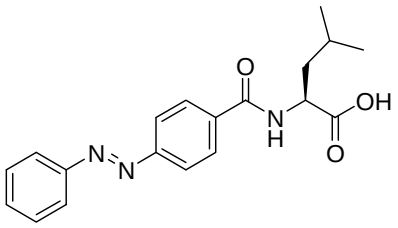

A solution of ester **2.17** (150 mg, 0.42 mmol) in THF (10 mL) was cooled to 0 ºC, then LiOH (0.25 M in 2:1 THF/H_2O, 2.7 mL) was added. The resultant mixture was stirred for 2 h, then diluted with 1:1 DCM/H_2O (50 mL). The aqueous layer was separated, washed with DCM (50 mL), acidified with 10% HCl (50 mL), then extracted with DCM (50 mL × 2). The final organic extracts were combined and concentrated to give **2.21** (140 mg, 97%) as an orange solid:

mp: 122-124 ºC (lit. 115-115.5 ºC)[3]

$[\alpha]_D^{20}$: +5.8 º (c = 0.50, MeOH)

^{1}H NMR (500 MHz, $CDCl_3$) δ 1.01-1.04 (6H, m, CH*Me*$_2$), 1.72-1.92 (3H, m C*H*$_2$CHMe$_2$ and CH$_2$C*H*Me$_2$), 4.88 (1H, m, NHC*H*), 6.58 (1H, d, *J* = 7.9 Hz, N*H*), 7.48-7.56 (3H, m), 7.92-7.99 (6H, m).

^{13}C NMR (75 MHz, $CDCl_3$) δ 22.0, 23.0, 25.2 (CH$_2$C*H*Me$_2$), 41.3 (C*H*$_2$CHMe$_2$), 51.6 (NHC*H*), 123.0, 123.2, 128.4, 129.2, 131.7, 135.3, 152.6, 154.5, 167.5, 177.0.

HRMS (ES): Calcd. for $C_{19}H_{22}N_3O_3$ (MH^+) 340.1661, found 340.1670.

(*S*,*E*)-3-Methyl-2-(4-(phenylazo)-benzoylamino)-butyric acid 2.22:

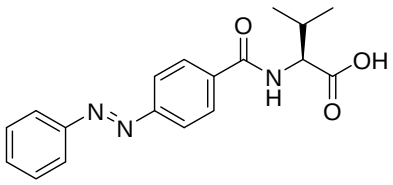

A solution of ester **2.18** (260 mg, 0.75 mmol) in THF (10 mL) was cooled to 0ºC and LiOH (0.25 M in 2:1 THF/H_2O, 4.5 mL) was added. The resulting mixture was stirred for 2 h, then diluted with DCM (50 mL) and H_2O (50 mL) and the layers were separated. The organic layer was concentrated to return starting material **2.18** (77 mg, 30%). The aqueous layer was acidified with HCl (1.0 M) and extracted with DCM (50 mL). The organic extract was washed with brine (50 mL), dried over $MgSO_4$ and concentrated to give **2.22** (150 mg, 63%) as an orange solid:

mp: 159-162 ºC

$[\alpha]_D^{20}$: +30.0 º (c = 0.65, MeOH)

^{1}H NMR (500 MHz, $CDCl_3$) δ 1.05-1.12 (6H, m), 2.40 (1H, m, C*H*Me$_2$), 4.85 (1H, dd, J = 8.2, 4.9 Hz, C*H*NH), 6.71 (1H, d, J = 8.2 Hz, N*H*), 7.49-7.56 (3H, m), 7.93-8.00 (6H, m).

^{13}C NMR (75 MHz, $CDCl_3$) δ 18.0, 19.2, 31.5, 57.8, 123.1, 123.3, 128.3, 129.3, 131.8, 135.5, 152.6, 154.6, 167.5, 175.9.

HRMS(ES): Calcd. 326.1505 for $C_{18}H_{20}N_3O_3$ (MH^+), found 326.1520.

(*E*)-(4-(Phenylazo)-benzoylamino)-acetic acid 2.23:

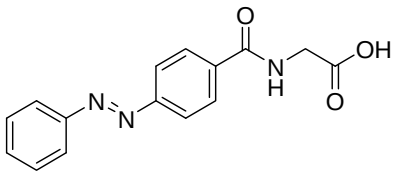

A solution of ester **2.19** (240 mg, 0.81 mmol) in THF (10 mL) was cooled to 0ºC and LiOH (0.25 M in 2:1 THF/H_2O, 5.0 mL) was added. The resulting mixture was stirred for 2 h then diluted with DCM (50 mL) and H_2O (50 mL) and the layers were separated. The aqueous layer was acidified with HCl (1.0 M) and extracted with DCM (50 mL). The final organic extract was washed with brine (50 mL), dried over $MgSO_4$ and concentrated to give **2.23** (190 mg, 83%) as an orange solid:

mp: 224-227 ºC

^{1}H NMR (500 MHz, $(CD_3)_2CO$) δ 4.19 (2H, d, J = 5.9 Hz, C*H*$_2$), 7.57-7.65 (3H, m), 7.96-8.03 (4H, m), 8.14 (2H, d, J = 8.6 Hz), 8.25 (1H, s).

^{13}C NMR (75 MHz, $(CD_3)_2SO$) δ 41.4, 122.5, 122.8, 128.6, 129.6, 132.1, 136.0, 151.9, 153.4, 165.8, 171.3.

HRMS (ES): Calcd. 284.1035 for $C_{15}H_{14}N_3O_3$ (MH^+), found 284.1031.

(*S*,*E*)-2-(4-(Phenylazo)-benzoylamino)-propionic acid 2.24:

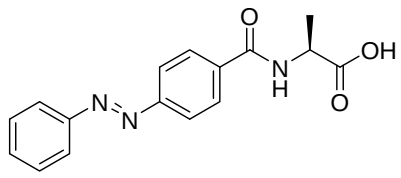

A solution of ester **2.20** (220 mg, 0.71 mmol) in THF (10 mL) was cooled to 0ºC and LiOH (0.25 M in 2:1 THF/H_2O, 4.2 mL) was added. The resulting mixture was stirred for

2 h, then diluted with DCM (50 mL) and H_2O (50 mL) and the layers were separated. The aqueous layer was acidified with HCl (1.0 M) and extracted with DCM (50 mL). The final organic extract was washed with brine (50 mL), dried over $MgSO_4$ and concentrated to give **2.24** (210 mg, qu) as an orange solid:

mp: 213-215 ºC

$[\alpha]_D^{20}$: +35.4 º (c = 0.65, MeOH)

^{1}H NMR (500 MHz, $(CD_3)_2CO$) δ 1.54 (3H, d, J = 7.3 Hz, *Me*), 4.71 (1H, p, J = 7.3 Hz, C*H*Me), 7.57-7.64 (3H, m), 7.95-8.01 (4H, m), 8.07 (1H, d, J = 6.6 Hz, N*H*), 8.14 (2H, d, J = 8.7 Hz).

^{13}C NMR (75 MHz, CD_3OD) δ 17.5, 123.7, 124.0, 129.7, 130.3, 132.9, 137.3, 153.9, 155.6, 169.2, 176.1.

HRMS(ES): Calcd. 298.1192 for $C_{16}H_{16}N_3O_3$ (MH^+), found 298.1196.

(*S*,*E*)-*N*-(4-Methyl-1-oxo-1-(3-(4,4,5,5-tetramethyl-1,3,2-dioxaborolan-2-yl)phenyl amino)pentan-2-yl)-4-(phenylazo)-benzamide 2.2:

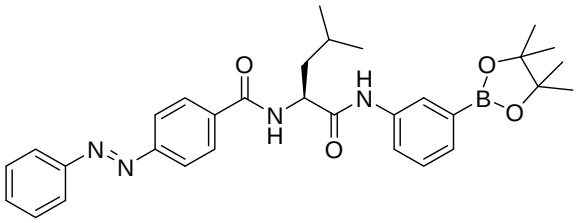

A solution of carboxylic acid **2.21** (170 mg, 0.49 mmol), amine **2.16** (110 mg, 1 eq), EDCI (130 mg, 1 eq) and HOBt (92 mg, 1 eq) in DCM (5.0 mL) was stirred for 16 h then washed with water (50 mL), brine (50 mL), and filtered to give **2.2** (110 mg, 43%) as an orange solid:

mp: 225–227 ºC

$[\alpha]_D^{20}$: +1.0º (c = 0.60, DMSO)

^{1}H NMR (300 MHz, $(CD_3)_2SO$) δ 1.05 (6H, t, *J* = 6.8, CH*Me*$_2$), 1.38 (12H, s, (C*Me*$_2$)$_2$) 1.72 (1H, m), 1.80–2.00 (2H, m), 4.77 (1H, m, COC*H*), 7.42 (2H, m), 7.71 (3H, m), 7.92 (1H, d, *J* = 6.6), 8.05 (5H, m), 8.25 (2H, d, *J* = 8.4 Hz), 8.92 (1H, d, *J* = 7.2), 10.30 (1H, s).

^{13}C NMR (75 MHz, $(CD_3)_2SO$) δ 21.6 (CH*Me*$_2$), 23.2 (CH*Me*$_2$), 24.8 (2C, (C*Me*$_2$)$_2$ and *C*HMe$_2$), 41 (obscured by solvent peak, *C*H$_2$), 53.2 (CO*C*H), 83.8 (*C*Me$_2$)$_2$), 122.4, 122.9, 125.6, 128.5, 129.1, 129.4, 129.7, 132,2, 136.3, 138.8, 152.0, 153.5, 165.9, 171.5.

HRMS (ES): Calcd. 541.2986 for $C_{31}H_{38}BN_4O_4$ (MH^+), found 541.2958.

(*E*)-*N*-((S)-2-Methyl-1-(3-(4,4,5,5-tetramethyl-(1,3,2)dioxaborolan-2-yl)-phenyl carbamoyl)-propyl)-4-(phenylazo)-benzamide 2.3:

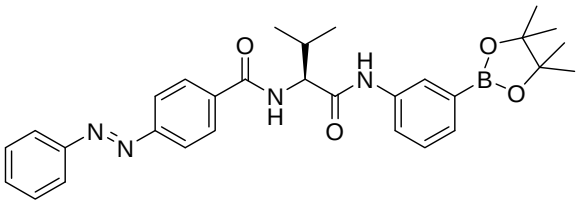

A solution of carboxylic acid **2.22** (100 mg, 0.31 mmol), aminophenylboronic acid **2.16** (68 mg, 1 eq), EDCI (65 mg, 1.1 eq) and HOBt (46 mg, 1.1 eq) in DCM (10 mL) was stirred for 16 h, diluted with DCM (50 mL), washed with H_2O (50 mL × 2), brine (50 mL), dried over $MgSO_4$ and concentrated. The crude product was purified by flash chromatography, eluting with 1:9 EtOAc/DCM to give **2.3** (52 mg, 32%) as an orange solid.

mp: 215-220 ºC

$[\alpha]_D^{20}$: +1.2 º (c = 0.33, MeOH)

^{1}H NMR (500 MHz, $CDCl_3$) δ 1.09 (6H, d, J = 6.1 Hz, CH*Me*$_2$), 1.29 (12H, s, (C*Me*$_2$)$_2$), 2.34 (1H, m), 4.92 (1H, t, J = 7.5 Hz), 7.31 (1H, t, J = 7.5 Hz), 7.47-7.59 (5H, m), 7.79 (1H, d, J = 7.5 Hz), 7.90-8.08 (7H, m), 9.19 (1H, s).

^{13}C NMR (75 MHz, $CDCl_3$) δ 18.9, 19.6, 25.0, 31.9, 60.0, 84.0, 123.1, 123.2, 123.3, 126.3, 128.5, 128.6, 129.3, 131.0, 131.7, 135.7, 137.4, 152.6, 154.5, 167.3, 170.2.

HRMS (ES): Calcd. 527.2830 for $C_{30}H_{36}BN_4O_4$ (MH^+), found 527.2839.

(*E*)-4-(Phenylazo)-*N*-((3-(4,4,5,5-tetramethyl-(1,3,2)dioxaborolan-2-yl)-phenyl carbamoyl)-methyl)-benzamide 2.4:

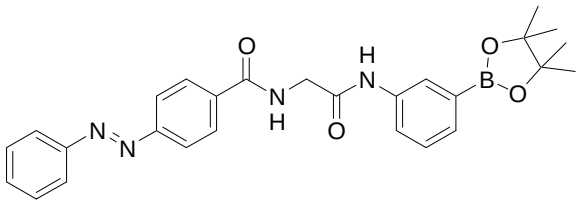

A solution of carboxylic acid **2.23** (100 mg, 0.35 mmol), aminophenylboronic acid **2.16** (72 mg, 1 eq), EDCI (75 mg, 1.1 eq) and HOBt (53 mg, 1.1 eq) in DCM (10 mL) was stirred for 16 h, diluted with DCM (50 mL), washed with H_2O (50 mL × 2), brine (50 mL), dried over $MgSO_4$ and concentrated. The crude product was purified by flash chromatography, eluting with 1:4 EtOAc/DCM to give **2.4** (70 mg, 41%) as an orange solid:

mp: 255-257 ºC

^{1}H NMR (300 MHz, $(CD_3)_2SO$) δ 1.28 (12H, s, $(CMe_2)_2$), 4.09 (2H, d, J = 5.6 Hz, CH_2), 7.29-7.38 (2H, m), 7.57-7.68 (3H, m), 7.75 (1H, d, J = 7.2 Hz), 7.91-8.02 (5H, m), 8.13 (2H, d, J = 8.3 Hz), 9.05 (1H, t, J = 5.6 Hz, N*H*CH_2), 10.10 (1H, s, N*H*$COCH_2$).

^{13}C NMR (300 MHz, $(CD_3)_2SO$) δ 24.7, 43.4, 83.7, 122.2, 122.5, 122.8, 125.3, 128.4, 128.7, 129.3, 129.6, 132.1, 136.2, 138.5, 152.0, 153.4, 166.0, 167.8.

HRMS (ES): Calcd. 485.2360 for $C_{27}H_{30}BN_4O_4$ (MH^+), found 485.2375.

(*E*)-4-(Phenylazo)-*N*-((*S*)-1-(3-(4,4,5,5-tetramethyl-(1,3,2)dioxaborolan-2-yl)-phenyl carbamoyl)-ethyl)-benzamide 2.5:

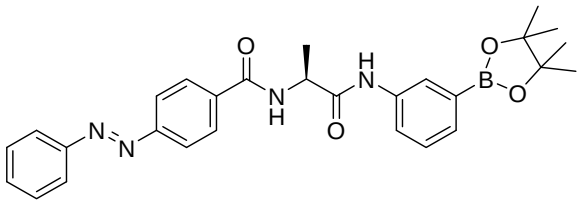

A solution of carboxylic acid **2.24** (100 mg, 0.34 mmol), aminophenylboronic acid **2.16** (74 mg, 1 eq), EDCI (71 mg, 1.1 eq) and HOBt (50 mg, 1.1 eq) in DCM (7.0 mL) was stirred for 16 h, diluted with DCM (50 mL), washed with H_2O (50 mL × 2), brine (50 mL), dried over $MgSO_4$ and concentrated. The crude product was purified by flash chromatography, eluting with a gradient from DCM to 15:85 EtOAc/DCM to give **2.5** (70 mg, 41%) as an orange solid:

mp: 211-213 ºC

$[\alpha]_D^{20}$: +4.4 º (c = 0.50, EtOAc)

^{1}H NMR (300 MHz, $(CD_3)_2SO$) δ 1.28 (12H, s, $(CMe_2)_2$), 1.47 (3H, d, J = 7.1 Hz, CH*Me*), 4.61 (1H, p, J = 7.1 Hz, C*H*Me), 7.33 (2H, m), 7.58-7.66 (3H, m), 7.77 (1H, d, J = 7.1 Hz), 7.91-8.01 (5H, m), 8.15 (1H, d, J = 8.4 Hz), 8.85 (1H, d, J = 6.8 Hz), 10.10 (1H, s).

^{13}C NMR (75 MHz, $(CD_3)_2SO$) δ 18.6, 24.8, 50.1, 83.9, 123.0, 123.1, 126.0, 128.3, 128.5, 129.1, 130.9, 131.6, 135.2, 137.3, 152.5, 154.4, 166.8, 170.6.

HRMS (ES): Calcd. 499.2517 for $C_{28}H_{32}BN_4O_4$ (MH^+), found 499.2495.

(*S*,*E*)-Methyl-4-methyl-2-(4-(phenylazo)phenylsulfonamido)pentanoate 2.26:

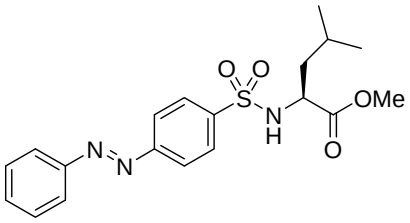

A mixture of 4-(phenylazo)benzenesulfonyl chloride **2.25**[5] (supplied by Nathan Alexander[6], 770 mg, 2.8 mmol) and H-LeuOMe.HCl (500 mg, 1 eq) was dissolved in DCM (15 mL) then DIEA (1.4 mL, 3 eq) was added. The reaction mixture was refluxed for 2 h then cooled, diluted with EtOAc (100 mL), washed with water (100 mL) then brine (100 mL), dried over $MgSO_4$ and concentrated. The crude product was purified by flash chromatography, eluting with DCM then 1:9 EtOAc/DCM to obtain **2.26** (980 mg, 91%) as an orange solid:

mp: 131–134 ºC

$[\alpha]_D^{20}$: +19.0 º (c = 1.0, MeOH)

^{1}H NMR (300 MHz, $CDCl_3$) δ 0.91 (6H, m, CH*Me*$_2$), 1.53 (2H, t, *J* = 7.1, C*H*$_2$), 1.81 (1H, m, C*H*Me$_2$), 3.45 (3H, s, O*Me*), 4.03 (1H, m, COC*H*), 5.39 (1H, d, *J* = 9.6, NH), 7.54 (3H, m), 7.93–8.01 (6H, m).

^{13}C NMR (126 MHz, $CDCl_3$) δ 21.3, 22.7, 24.3, 42.2, 52.3, 54.4, 123.1, 123.2, 128.3, 129.2, 132.1, 141.1, 152.3, 154.6, 172.5.

HRMS(ES): Calcd. 390.1488 for $C_{19}H_{24}N_3O_4S$ (MH^+), found 390.1485.

(*S*)-4-Methyl-2-(4-(phenylazo)phenylsulfonamido)pentanoic acid 2.27:

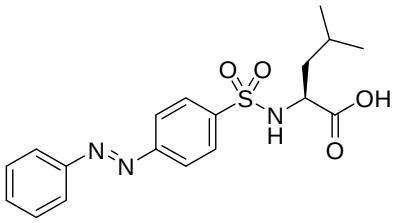

To a solution of ester **2.26** (500 mg, 1.3 mmol) in THF (20 mL) was added a solution of LiOH (8.0 mL; 0.25 M in 2:1 THF/water). The reaction mixture was stirred for 16 h then diluted with water (100 mL), washed with DCM (100 mL), then acidified to pH 3 with HCl (1.0 M) and extracted with DCM (100 mL). The organic layer was dried over $MgSO_4$ and concentrated. The crude material was purified by silica column chromatography,

eluting with 1:1 EtOAc–DCM to give recovered starting material **2.26** (114 mg, 23%) and **2.27** (300 mg, 63%) as an orange solid:

mp: 128–130 ºC

$[\alpha]_D^{20}$: +31.6 º (c = 0.45, MeOH)

^{1}H NMR (300 MHz, $CDCl_3$) δ 0.83 (6H, m, CH*Me*$_2$), 1.48 (2H, m, C*H*$_2$), 1.74 (1H, m, C*H*Me$_2$), 3.97 (1H, m, COC*H*), 5.18 (1H, d, *J* = 9.9, N*H*), 5.35–5.90 (1H, br s, O*H*), 7.54 (3H, m), 7.96 (6H, m).

^{13}C NMR (75 MHz, $CDCl_3$) δ 21.1, 22.7, 24.3, 41.9, 54.1, 123.2, 123.3, 128.3, 129.3, 132.2, 141.0, 152.3, 154.8, 176.6.

HRMS(ES): Calcd. 376.1331 for $C_{18}H_{22}N_3O_4S$ (MH^+), found 376.1345.

(*S*,*E*)-4-Methyl-2-(4-(phenylazo)phenylsulfonamido)-*N*-(3-(4,4,5,5-tetramethyl-1,3,2-dioxaborolan-2-yl)phenyl)pentanamide 2.6:

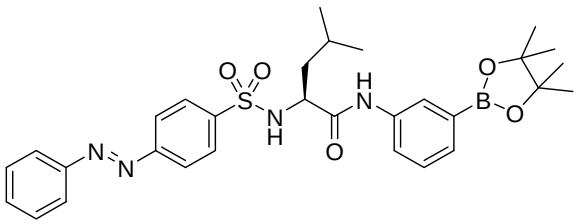

A mixture of amine **2.16** (50 mg, 0.23 mmol), carboxylic acid **2.27** (100 mg, 1 eq) and HATU (95 mg, 1.1 eq) was dissolved in DMF (5.0 mL) and DIEA (87 μL, 2.2 eq) was added. The reaction mixture was stirred overnight then diluted with EtOAc (50 mL), washed with water (50 mL), brine (50 mL), dried over $MgSO_4$ and concentrated. The crude material was purified by flash chromatography, eluting with 1:19 EtOAc/DCM to give **2.6** (43 mg, 28%) as an orange solid:

mp: 75–80 ºC

$[\alpha]_D^{20}$: -17.1 º (c = 0.90, MeOH)

^{1}H NMR (500 MHz, $CDCl_3$) δ 0.75 (3H, d, *J* = 5, CH*Me*$_2$), 0.87 (3H, d, *J* = 5.5, CH*Me*$_2$), 1.31 (12H, m, (C*Me*$_2$)$_2$), 1.54 (1H, t, *J* = 9), 1.65 (2H, m), 3.88 (1H, m, COC*H*), 5.45 (1H, m, N*H*), 7.24 (1H, t, *J* = 7.8), 7.49–7.54 (4H, m), 7.60 (1H, s), 7.64 (1H, d, *J* = 7), 7.86 (1H, s), 7.90–7.96 (4H, m), 8.03 (2H, d, *J* = 7.5).

^{13}C NMR (75 MHz, CDCl3) δ 21.4 (CH*Me*$_2$), 22.9 (CH*Me*$_2$), 24.4 (*C*HMe$_2$), 24.8 ((C*Me*$_2$)$_2$), 42.2 (*C*H$_2$), 56.4 (COCH), 83.9 (*C*Me$_2$)$_2$), 123.1, 123.3, 123.4, 125.9, 128.4,

128.5, 129.2, 131.1, 132.1, 136.4, 140.5, 152.3, 154.8, 169.2.

HRMS (ES): Calcd. 577.2656 for $C_{30}H_{38}BN_4O_5S$ (MH^+), found 577.2665.

2-Benzyl-4,4,5,5-tetramethyl-(1,3,2)dioxaborolane 2.30:[7]

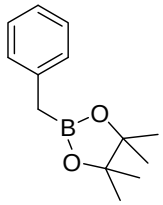

Mg turnings (8.0 g, 0.33 mol) were stirred under a nitrogen atmosphere for 16 h, then ether (100 mL) was added and the mixture was cooled to 0ºC and stirred for 1 h. Benzyl chloride **2.28** (35 mL, 38 g, 0.30 mol) was added and the mixture was warmed to r.t. to initiate the Grignard reaction. After the reaction subsided, ether (100 mL) was added. The Grignard mixture and a solution of trimethyl borate (34 mL, 31 g, 0.30 mol) in ether (150 mL) were then added alternately to cooled (-60 ºC) ether (150 mL), maintaining the temperature below -30ºC. The resulting mixture was then stirred for 16 h, warming to r.t., then was cooled to 0 ºC and H_2SO_4 (40% aqueous, 75 mL) was added slowly, maintaining the temperature below 15 ºC. The mixture was stirred overnight, warming to r.t., then the layers were separated, and the aqueous layer was extracted with ether (70 mL × 4). The organic extracts were combined and the ether solvent was removed by distillation at 60 ºC. The distilland residue was collected to obtain benzylboronic acid **2.29** (56 g) as a pale yellow oil, which was used subsequently without further purification. A solution of the crude benzylboronic acid (30 g, < 0.22 mol) and pinacol (26 g, 0.22 mol) in ether (100 mL) was stirred for 16 h, washed with H_2O (100 mL × 3), dried over $MgSO_4$ and concentrated. The crude product was purified by flash chromatography, eluting with a gradient of pet ether to 1:19 EtOAc/pet ether to obtain **2.30** (20 g, 63% over 2 steps) as a colourless oil:

^{1}H NMR (500 MHz, $CDCl_3$) δ 1.23 (12H, s, (CMe_2)$_2$), 2.29 (2H, s, CH_2), 7.12 (1H, t, J = 7.2 Hz), 7.18 (1H, d, J = 7.2 Hz), 7.24 (2H, m).

2-(1-Chloro-2-phenyl-ethyl)-4,4,5,5-tetramethyl-(1,3,2)dioxaborolane 2.31:[7]

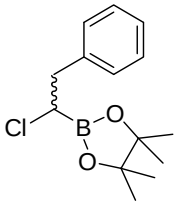

A solution of diisopropylamine (7.7 mL, 5.6 g, 55 mmol) and THF (1.0 mL) was cooled to 0ºC and n-butyllithium (1.6 M in THF, 32 mL, 51 mmol) was added to form LDA *in situ*. A solution of boronate ester **2.30** (10 g, 46 mmol) in DME (80 mL) and DCM (4.7 mL) was cooled to -78ºC and the LDA solution was added slowly. The resulting solution was stirred for 4 d, warming to r.t., then diluted with DCM (100 mL), filtered and concentrated. The residue was then dissolved in pet ether (100 mL), filtered and concentrated to obtain **2.31** (12 g) as a brown oil, which was used subsequently without further purification: selected peaks from ^{1}H NMR (500 MHz, $CDCl_3$) δ 1.22 (12H, m, (C*Me*$_2$)$_2$), 3.09 (1H, dd, J = 13.7, 8.3 Hz), 3.17 (1H, dd, J = 13.7, 8.1 Hz), 3.59 (1H, t, J = 8.2 Hz), 7.20-7.31 (5H, m).

2-(1-(1,1,1,3,3,3-Hexamethyl-disilazan-2-yl)-2-phenyl-ethyl)-4,4,5,5-tetramethyl-(1,3,2)dioxaborolane 2.32:[7]

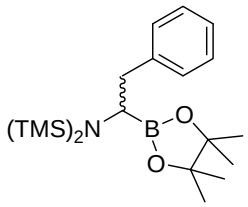

A solution of HMDS (9.0 mL, 6.9 g, 43 mmol) in THF (60 mL) was cooled to -78 ºC and n-BuLi (1.6 M in THF, 27 mL, 43 mmol) was added. The solution was then warmed to r.t., then cooled to -78ºC and a solution of crude **2.31** (10 g, < 38 mmol) in THF (15 mL) was added. The resulting mixture was stirred overnight, warming to r.t., then concentrated to give **2.32** (16 g) as a brown oil which was used subsequently without further purification: selected peaks from ^{1}H NMR (500 MHz, $CDCl_3$) δ 0.05 (18H, s, N(Si*Me*$_3$)$_2$), 1.21 (12H, s, (C*Me*$_2$)$_2$), 2.61 (1H, dd, J = 13.1, 8.2 Hz), 2.73 (1H, dd, J = 8.2, 6.4 Hz), 2.99 (1H, dd, J = 13.1, 6.4 Hz), 7.12-7.26 (5H, m, *Ph*).

2-Phenyl-1-(4,4,5,5-tetramethyl-(1,3,2)dioxaborolan-2-yl)-ethylamine trifluoroacetate 2.33:[7]

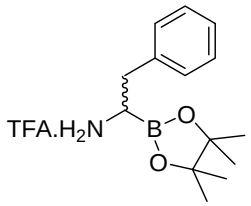

A solution of crude **2.32** (16 g) in ether (100 mL) was cooled to 0ºC and TFA (8.7 mL) was added slowly. The resulting mixture was stirred 10 min then concentrated, dissolved in pet ether, filtered and concentrated. The crude product was recrystallised twice from EtOAc to give **2.33** (2.7 g, 19% over 3 steps) as a white solid:

mp 174-181 ºC (lit.[7] 109-112 ºC)

^{1}H NMR (500 MHz, $CDCl_3$) δ 1.20-1.28 (12H, m, (C*Me*$_2$)$_2$), 3.16-3.33 (3H, m), 4.67 (1H, s), 7.22-7.40 (5H, m, *Ph*), 7.97 (2H, s).

(*E*)-*N*-(2-Phenyl-1-(4,4,5,5-tetramethyl-1,3,2-dioxaborolan-2-yl)-ethyl)-4-(phenylazo) benzamide 2.7:

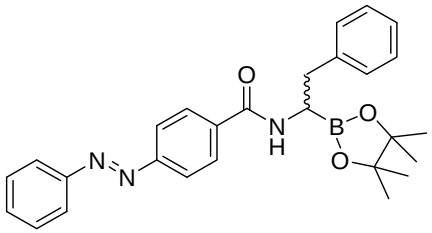

To a solution of carboxylic acid **2.15** (190 mg, 0.84 mmol) in THF (5.0 mL) was added isobutylchloroformate (110 μL, 1 eq) then NMM (180 μL, 2 eq). The reaction mixture was stirred for 10 min, then a solution of amine **2.33** (300 mg, 1 eq) in THF (5.0 mL) was added. The resulting mixture was stirred for 16 h, then diluted with EtOAc (50 mL), washed with water (50 mL) then brine (50 mL) and concentrated. The crude material was purified by flash chromatography, eluting with 3:7 EtOAc/DCM to give **2.7** (190 mg, 51%) as an orange solid:

mp: 205–206 ºC

Elemental analysis: Calcd. for $C_{27}H_{30}BN_3O_3$: C 71.22, H 6.64, N 9.23%, found: C, 71.13; H, 6.55; N, 9.31.

^{1}H NMR (500 MHz, $CDCl_3$) δ 1.31 (6H, s, (C*Me*$_2$)$_2$), 1.32 (6H, s, (C*Me*$_2$)$_2$), 2.83 (1H, dd, *J* = 11.8 and 14.3, CHC*H*$_2$), 3.08 (1H, dd, *J* = 4.3 and 14.3, CHC*H*$_2$), 3.15 (1H, m,

C*H*CH_2), 6.96 (1H, s, N*H*), 7.27 (3H), 7.36 (2H, t, *J* = 7.8), 7.53 (3H), 7.87 (2H, d, *J* = 8.5), 7.94 (4H).

^{13}C NMR (126 MHz, CDCl3) δ 25.0, 25.3, 37.3 (CHC*H*$_2$), 46.3 (*C*HCH_2), 81.0, 122.9, 123.2, 126.3, 128.7, 128.9, 129.0, 129.2, 131.9, 140.8, 152.4, 155.2, 170.4.

HRMS (ES): Calcd. 456.2458 for $C_{27}H_{31}BN_3O_3$ (MH^+), found 456.2451.

(*E*)-(*N*-((*S*)-3-Methyl-1-((*S*)-2-phenyl-1-(4,4,5,5-tetramethyl-(1,3,2)dioxaborolan-2-yl)-ethylcarbamoyl)-butyl)-4-phenylazo-benzamide 2.8

and **(*E*)-(*N*-((*S*)-3-Methyl-1-((*R*)-2-phenyl-1-(4,4,5,5-tetramethyl-(1,3,2)dioxaborolan-2-yl)-ethylcarbamoyl)-butyl)-4-phenylazo-benzamide 2.9:**

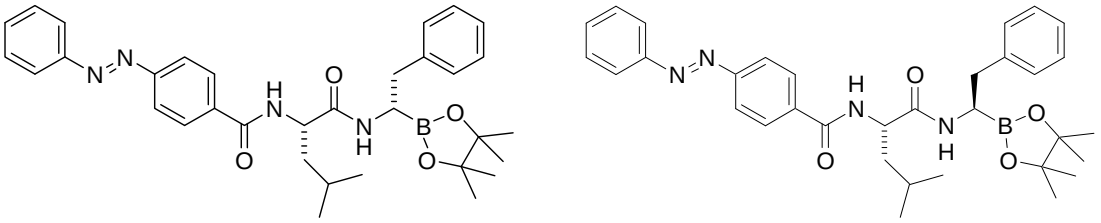

A solution of carboxylic acid **2.21** (100 mg, 0.29 mmol) in THF (4.0 mL) was cooled to 0 ºC, then isobutylchloroformate (40 μL, 1 eq) and NMM (65 μL, 2 eq) were added. The reaction mixture was stirred for 10 min then a solution of amine **2.33** (110 mg, 1 eq) in THF (4.0 mL) was added. The mixture was stirred for 16 h, diluted with EtOAc (50 mL), washed with water (50 mL) then brine (50 mL), dried over $MgSO_4$ and concentrated. The crude material was purified by silica column chromatography on deactivated silica (containing 35% water w/w), eluting with 3:7 EtOAc/DCM to give a mixture of **2.8** and **2.9** (130 mg, 76%) as an orange solid. The mixture of diastereomers was further purified three times by column chromatography to give **2.8** (5.0 mg, 3%, 86% de) as an orange solid:

^{1}H NMR (500 MHz, CD_3OD) δ 0.96 (3H, d, *J* = 6, CH*Me*$_2$), 0.99 (3H, d, *J* = 6.5, CH*Me*$_2$), 1.10 (6H, s, (C*Me*$_2$)$_2$), 1.15 (6H, s, (C*Me*$_2$)$_2$), 1.68 (1H, m), 1.78 (1H, m), 1.87 (1H, m), 2.62 (1H, dd, *J* = 8.5, 12), 2.84 (2H, m), 4.92 (1H, dd, *J* = 5, 10.5), 7.17 (1H,m), 7.26 (4H, m), 7.55 (4H, m), 7.94–8.04 (6H, m).

HRMS(ES): Calcd. 569.3299 for $C_{33}H_{42}BN_4O_4$ (MH^+), found 569.3279.

and **2.9** (8.0 mg, 5%, 86% de) as an orange solid:

^{1}H NMR (500 MHz, CD_3OD) δ 0.98 (3H, d, J = 6.5, CHMe_2), 1.00 (3H, d, J = 5, CHMe_2), 1.14 (12H, m, (CMe_2)$_2$), 1.68–1.87 (3H, m), 2.60 (1H, dd, J = 9.3, 12.8), 2.80–2.88 (2H, m), 4.89 (1H, m, COCH), 7.12– 7.23 (5H, m), 7.55 (3H,m), 7.94–8.03 (6H, m).

HRMS(ES): Calcd. 569.3299 for $C_{33}H_{42}BN_4O_4$ (MH^+), found 569.3307.

(4-Nitro-benzyl)-carbamic acid 9H-fluoren-9-ylmethyl ester 2.35:[3, 8]

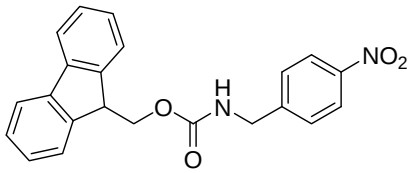

A solution of 4-nitrobenzylamine hydrochloride **2.34** (1.3 g, 8.5 mmol) and 9-fluorenylmethyl chloroformate (2.4 g, 1.1 eq) in DCM (50 mL) was cooled to 0 ºC then DIEA was added (1.6 mL, 1.2 g, 1.1 eq). The resulting solution was stirred for 18 h then concentrated. The crude product was recrystallised from DCM to give **2.35** (1.7 g, 52%) as a white solid:

mp: 141-144 ºC (lit.[3] 155-156 ºC)

^{1}H NMR (500 MHz, $CDCl_3$) δ 4.23 (1H, t, J = 6.5 Hz), 4.46 (2H, d, J = 5.9 Hz), 4.54 (2H, d, J = 6.6 Hz), 5.16 (1H, s), 7.29-7.47 (6H, m), 7.60 (2H, d, J = 7.2 Hz), 7.78 (2H, d, J = 7.2 Hz), 8.18 (2H, d, J = 8.1 Hz).

^{13}C NMR (300 MHz, $CDCl_3$) δ 44.2, 47.3, 66.6, 120.0, 123.8, 124.9, 127.0, 127.7, 127.8, 141.3, 143.6, 146.0, 147.2, 156.4.

HRMS(ES): Calcd. 375.1345 for $C_{22}H_{19}N_2O_4$ (MH^+), found 175.1353.

(4-Amino-benzyl)-carbamic acid 9H-fluoren-9-ylmethyl ester 2.36:[3, 8]

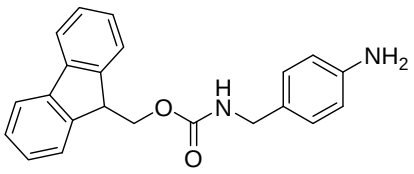

To a solution of **2.35** (1.7 g, 4.4 mmol) in EtOAc (120 mL) was added PtO_2 (50 mg). The reaction vessel was evacuated then filled with H_2 gas. The mixture was stirred under H_2 for 16 h, then filtered through Celite-545 filter aid and concentrated. The crude product

was purified by flash chromatography, eluting with a gradient from DCM to 1:9 EtOAc/DCM to give **2.36** (1.3 g, 86%) as a white solid:

mp: 144-146ºC decomp. (lit.[3] 147-147.5)

^{1}H NMR (300 MHz, $CDCl_3$) δ 3.67 (2H, br s, NH_2), 4.17-4.31 (3H, m), 4.43 (2H, d, J = 6.5 Hz), 4.98 (1H, s), 6.64 (2H, d, J = 8.0 Hz), 7.07 (2H, d, J = 8.0 Hz), 7.24-7.45 (4H, m), 7.59 (2H, d, J = 7.4 Hz), 7.76 (2H, d, J = 7.4 Hz).

(*E*)-Ethyl 4-((4-((((9*H*-fluoren-9-yl)methoxy)carbonylamino)methyl)-phenyl)diazenyl) benzoate 2.39:

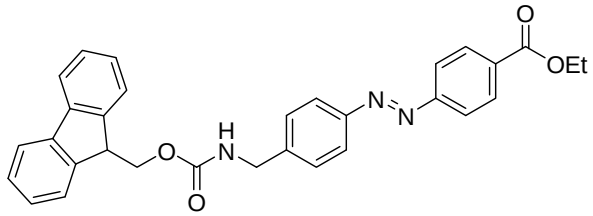

A mixture of ethyl 4-aminobenzoate **2.37** (2.0 g, 12 mmol) and $MoO_5 \cdot H_2O \cdot$HMPA (0.45 g, 0.1 eq) was dissolved in DCM (20 mL) and a solution of H_2O_2 (6.0 mL; 30% in water) was added. The reaction mixture was stirred for 16 h then quenched by addition of excess $MgSO_4$, filtered and concentrated. The crude material was purified by flash chromatography, eluting with 1:9 EtOAc/DCM to obtain ethyl 4-nitrosobenzoate **2.38** as a yellow solid. To this compound was added the aniline **2.36** (1.2 g, 3.49 mmol) then AcOH (25 mL). The resulting mixture was heated to 100 ºC for 1 h, then cooled and filtered to collect an orange precipitate. The filtrate was diluted with DCM (100 mL), washed with sat. $NaHCO_3$ (100 mL × 3) then dried over $MgSO_4$ and concentrated. This crude material was combined with the precipitate and purified by silica column chromatography, eluting with 1:19 EtOAc/DCM to give **2.39** (1.3 g, 22% over 2 steps) as an orange solid:

mp: 191–194 ºC

^{1}H NMR (300 MHz, $CDCl_3$) δ 1.43 (3H, t, J = 7, *Me*), 4.24 (1H, t, J = 6.3, CH_2CH), 4.40–4.53 (6H, m), 5.17 (1H, N*H*), 7.26–7.42 (6H, m), 7.61 (2H, d, J = 6.9), 7.77 (2H, d, J = 7.2), 7.93 (4H, m), 8.20 (2H, d, J = 8.7).

^{13}C NMR (75 MHz, $CDCl_3$) δ 14.3 (*Me*), 44.7, 47.3 (CH_2CH), 61.3, 66.7, 120.0, 122.6, 123.5, 125.0, 127.1, 128.1, 130.6, 132.2, 141.4, 142.3, 143.8, 151.9, 155.0, 156.5, 166.1.

HRMS(ES): Calcd. for $C_{31}H_{28}N_3O_4$ (MH^+) 506.2080, found 506.2120.

(*E*)-Ethyl 4-((4-((2-(*tert*-butoxycarbonylamino)acetamido)methyl)-phenyl)diazenyl) benzoate 2.41:

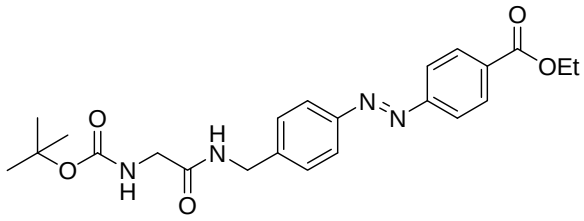

To a solution of **2.39** (900 mg, 1.78 mmol) in DMF (12 mL) was added piperidine (3.0 mL). The reaction mixture was stirred for 15 min then diluted with EtOAc (100 mL), washed with water (100 mL) then brine (100 mL), dried over $MgSO_4$, filtered and concentrated *in vacuo* to give amine **2.40** as an orange solid which was not purified further. To this compound was added Boc-Gly-OH (310 mg, 1 eq), HATU (680 mg, 1 eq) then DMF (10 mL) and DIEA (620 μL, 2 eq). The reaction mixture was stirred for 16 h, diluted with EtOAc (100 mL) and washed with water (100 mL) brine (100 mL), dried over $MgSO_4$, filtered and concentrated. The crude material was purified by silica column chromatography, eluting with 1:1 EtOAc/DCM to give **2.41** (690 mg, 88% over 2 steps) as an orange solid:

mp: 136–139 ºC

^{1}H NMR (500 MHz, $CDCl_3$) δ 1.41–1.47 (12H, C*Me*$_3$ and CH_2*Me*), 3.87 (2H, d, J = 5.5), 4.42 (2H, q, J = 5.4), 4.57 (2H, d, J = 6.0), 5.13 (1H, br, N*H*), 6.56 (1H, br,N*H*), 7.44 (2H, d, J = 8.0), 7.92 (2H, d, J = 8.0), 7.94 (2H, d, J = 8.5), 8.19 (2H, d, J = 8.5).

^{13}C NMR (75 MHz, $CDCl_3$) δ 14.3, 28.2, 42.9, 44.5, 61.2, 80.4, 122.6, 123.4, 128.2, 130.5, 132.1, 141.8, 151.8, 154.9, 156.2, 166.0, 169.6.

HRMS(ES): Calcd. for $C_{23}H_{29}N_4O_5$ (MH^+) 441.2138, found 441.2108.

(*E*)-4-((4-((2-(*tert*-Butoxycarbonylamino)acetamido)methyl)phenyl)-diazenyl)benzoic acid 2.42:

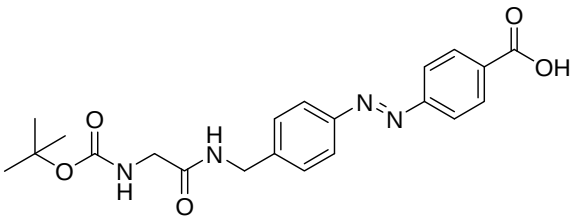

To a solution of **2.41** (68 mg, 0.15 mmol) in THF (5.0 mL) was added a solution of LiOH (1.0 mL; 0.25 M in 2:1 THF/water). The reaction mixture was heated to 50 ºC and stirred for 16 h then concentrated. The crude material was purified by flash chromatography, eluting with 1:99 AcOH/EtOAc to give **2.42** (55 mg, 87%) as an orange solid:

mp > 360 ºC

^{1}H NMR (500 MHz, CD_3OD) δ 1.45 (9H, s, C*Me*$_3$), 3.76 (2H, s), 4.49 (2H, s), 7.47 (2H, d, *J* = 8), 7.87 (4H, m), 8.08 (2H, d, *J* = 8).

^{13}C NMR (75 MHz, CD_3OD) δ 29.0 (C*Me*$_3$), 43.9, 45.1, 81.1 (*C*Me$_3$), 123.4, 124.3, 129.5, 131.5, 141.8, 144.0, 153.5, 155.3, 158.8, 173.1, 174.7.

HRMS(ES): Calcd. for $C_{21}H_{25}N_4O_5$ (MH^+) 413.1825, found 413.1805.

(*E*)-*tert*-Butyl-2-oxo-2-(4-((4-(2-phenyl-1-(4,4,5,5-tetramethyl-1,3,2-dioxaborolan-2-yl)ethylcarbamoyl)phenyl)diazenyl)benzylamino)-ethylcarbamate 2.10:

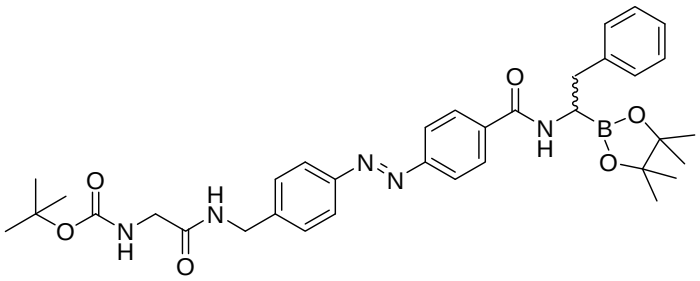

A solution of **2.42** (30 mg, 0.07 mmol) in DMF (3.0 mL) was cooled to 0ºC and isobutylchloroformate (10 μL, 1 eq) and NMM (16 μL, 2 eq) were added. The reaction mixture was stirred for 10 min then a solution of amine **2.33** (26 mg, 1 eq) in DMF (2.0 mL) was added. The resulting mixture was stirred for 16 h, warming from 0 ºC to r.t., then diluted with EtOAc (50 mL), washed with water (50 mL × 2), brine (50 mL), dried over $MgSO_4$, filtered and concentrated. The crude material was purified by silica column

chromatography on deactivated silica (containing 35% water w/w), eluting with EtOAc to give **2.10** (28 mg, 60%) as an orange solid:

mp: 188–191 ºC

^{1}H NMR (500 MHz, $CDCl_3$) δ 1.31 (12H, m, (C*Me*$_2$)$_2$), 1.45 (9H, s, C*Me*$_3$), 2.83 (1H, dd, *J* = 12,14.1, CHC*H*$_2$), 3.08 (1H, dd, *J* = 14.1, 3.80, CHC*H*$_2$), 3.16 (1H, m, C*H*CH$_2$), 3.86 (2H, d, *J* = 6), 4.55 (2H, d, *J* = 5.5), 5.18 (1H, s, N*H*), 6.65 (1H, s, N*H*), 7.13 (1H, s, N*H*), 7.28 (3H, m), 7.37 (2H, t, *J* = 7.8), 7.41 (2H, d, *J* = 8), 7.88 (6H, m).

^{13}C NMR (75 MHz, $CDCl_3$) δ 25.0 (C*Me*$_2$)$_2$), 25.1 (C*Me*$_2$)$_2$), 28.2 (C*Me*$_3$), 37.4 (CH*C*H$_2$), 42.7, 44.2, 46.8 (*C*HCH$_2$), 80.1 (*C*Me$_2$), 80.6 (*C*Me$_2$)$_2$), 122.7, 123.3, 126.0, 127.8, 128.4, 129.0, 129.2, 140.7, 142.1, 151.4, 154.8, 156.2, 169.9, 170.5, 207.0.

HRMS (ES): Calcd. 642.3463 for $C_{35}N_{45}BN_5O_6$ (MH^+), found 642.3488.

(*E*)-4-((4-((2-Aminoacetamido)methyl)phenyl)diazenyl)-*N*-(2-phenyl-1-(4,4,5,5-tetramethyl-1,3,2-dioxaborolan-2-yl)-ethyl)benzamide 2.11:

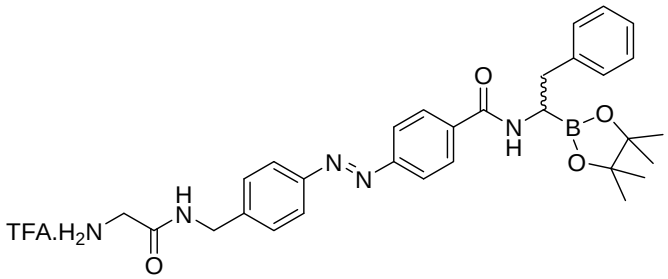

To a solution of **2.10** (17 mg, 0.03 mmol) in DCM (4.0 mL) was added TFA (1.0 mL). The reaction mixture was stirred for 30 min then concentrated. The crude material was purified by flash chromatography, eluting with 1:3 EtOH/DCM to give **2.11** (14 mg, 82%) as an orange solid:

mp 157–160 ºC

^{1}H NMR (500 MHz, CD_3OD) δ 1.15 (12H, m, (C*Me*$_2$)$_2$), 2.73 (1H, dd, *J* = 9.1,13.8), 2.96 (1H, dd, *J* = 6.4, 13.8), 2.99 (1H, dd, *J* = 6.4, 9.1), 3.72 (2H, s), 4.49 (2H, s), 7.16 (1H, m), 7.27 (4H, m), 7.47 (2H, d, *J* = 8.1), 7.89 (2H, d, *J* = 8.1), 7.96 (2H, d, *J* = 8.1), 8.09 (2H, d, *J* = 8.1).

HRMS(ES): Calcd. 542.2938 for $C_{30}H_{37}BN_5O_6$ (M – TFA + H^+), found 542.2965.

1-acetamido-2-phenyl-ethylboronic acid 2.12:[9, 10]

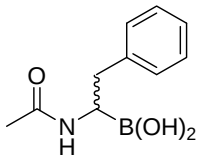

A solution of crude **2.32** (1.5 g, < 3.8 mmol) in THF (10 mL) was cooled to -78 ºC and AcOH (0.3 mL) and Ac_2O (1.4 mL, 3.9 eq) were added dropwise. The resulting mixture was stirred overnight, warming to r.t., then concentrated. The residue was dissolved in EtOAc, washed with H_2O (50 mL), brine (50 mL), dried over $MgSO_4$ and concentrated. The crude product was purified by flash chromatography, eluting with 1:19 EtOH/DCM to obtain boronate ester **2.43** (480 mg) as a yellow solid. A solution of **2.43** (100 mg, 0.35 mmol) in DCM (4.0 mL) was cooled to -78 ºC and BCl_3 (1.0 M in DCM, 1.5 mL, 1.5 mmol) was added. The resulting solution was stirred 1 h, warmed to r.t., stirred 1.5 h and concentrated. The residue was dissolved in MeOH (100 mL) and distilled to remove $B(OH)_3$. The distilland residue was concentrated, then ether (3.0 mL) and H_2O (4.0 mL) were added. The layers were separated and the aqueous layer was washed with ether (3.0 mL × 2) and lyophilized to obtain **2.12** (17 mg, 11% over 4 steps) as a white solid:
^{1}H NMR (500 MHz, D_2O) δ 2.09 (3H, s, *Me*), 2.55 (1H, dd, J = 13.8, 11.0 Hz), 2.82 (1H, dd, J = 11.0, 5.0 Hz), 2.88 (1H, dd, J = 13.6, 4.9 Hz), 7.27-7.34 (3H, m), 7.39 (2H, t, J = 7.6 Hz).

9.3 Experimental for work described in chapter 3

((*S*)-1-Benzylcarbamoyl-2-phenyl-ethyl)-carbamic acid tert-butyl ester 3.7:[11, 12]

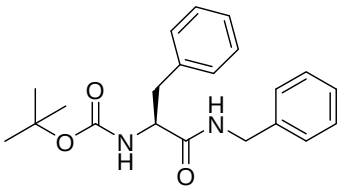

To a solution of Boc-Phe-OH **3.6** (900 mg, 3.4 mmol), benzylamine (360 mg, 1 eq) and HATU (1.3 g, 1 eq) in DMF (10 mL) was added DIEA (1.2 mL, 0.89 g, 2 eq) and the resulting mixture was stirred for 17 h, then diluted with EtOAc (50 mL), washed with H_2O (50 mL × 2), sat. $NaHCO_3$ (50 mL), brine (50 mL), dried over $MgSO_4$ and concentrated.

The crude material was purified by recrystallisation from EtOH to give **3.7** (500 mg, 41%) as a white solid:

mp: 132-133 ºC (lit.[11] 131-132 ºC)

$[\alpha]_D^{20}$: +0.9 º (c = 0.65, MeOH)

^{1}H NMR (500 MHz, $CDCl_3$) δ 1.39 (9H, s, C*Me*$_3$), 3.08 (2H, m), 4.35 (3H, d, J = 5.4 Hz), 5.07 (1H, s), 6.11 (1H, s), 7.04-7.31 (10H, m, 2*Ph*).

HRMS (ES): Calcd. for $C_{21}H_{27}N_2O_3$ (MH^+) 355.2022, found 355.2033.

(*S*)-2-Amino-*N*-benzyl-3-phenyl-propionamide 3.8:[12, 13]

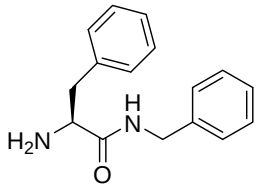

To a solution of **3.7** (350 mg, 0.98 mmol) in DCM (4.0 mL) was added TFA (1.0 mL) and the resulting mixture was stirred for 1 h then concentrated. The residue was dissolved in H_2O (10 mL), washed with DCM (10 mL), basified by addition of sat. $NaHCO_3$ and extracted with DCM (10 mL × 3) to give **3.8** (160 mg, 65%) as a white solid.

mp: 59-66 ºC

$[\alpha]_D^{20}$: +9.7º (c = 0.34, MeOH)

^{1}H NMR (500 MHz, $CDCl_3$) δ 1.34 (2H, br s, N*H*$_2$), 2.74 (1H, dd, J = 13.6, 9.1 Hz), 3.25 (1H, dd, J = 13.6, 3.7 Hz), 3.63 (1H, s), 4.41 (2H, m), 7.16-7.33 (10H, m, 2*Ph*), 7.63 (1H, s).

HRMS (ES): Calcd. for $C_{16}H_{19}N_2O$ (MH^+) 255.1497, found 255.1504.

(*R*)-2-Acetylamino-4-methyl-pentanoic acid ((*S*)-1-benzylcarbamoyl-2-phenyl-ethyl)-amide 3.3:

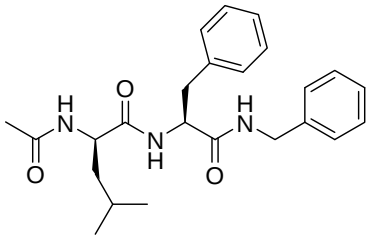

To a solution of **3.8** (50 mg, 0.20 mmol), Ac-*D*-Leu-OH (34 mg, 1 eq) and HATU (82 mg, 1.1 eq) in DMF (2.0 mL) was added DIEA (76 μL, 56 mg, 2.2 eq) and the resulting

mixture was stirred for 16 h, then diluted with EtOAc (50 mL), washed with HCl (1.0 M, 50 mL), sat. $NaHCO_3$ (50 mL), brine (50 mL), dried over $MgSO_4$ and concentrated. The crude material was purified by flash chromatography, eluting with DCM to remove leading impurities, then EtOAc to give **3.3** (59 mg, 72%) as a white solid:

mp 194-197 ºC

$[\alpha]_D^{20}$: -22.7 º (c = 0.30, MeOH)

^{1}H NMR (300 MHz, $(CD_3)_2SO$) δ 0.69 (3H, d, J = 6.1 Hz, CH*Me*Me), 0.75 (3H, d, J = 6.0 Hz, CHMe*Me*), 1.02-1.21 (3H, m), 1.75 (3H, s, O*Me*), 2.75 (1H, dd, J = 13.7, 11.1 Hz), 3.14 (1H, dd, J = 13.6, 3.9 Hz), 4.12 (1H, q, J = 7.4 Hz), 4.30 (2H, dd, J = 5.8, 3.0 Hz), 4.42-4.51 (1H, m), 7.14-7.33 (10H, m, 2*Ph*), 8.04 (1H, d, J = 6.8 Hz), 8.41-8.51 (2H, m).

^{13}C NMR (75 MHz, $(CD_3)_2SO$) δ 22.3, 22.3, 22.5, 23.9, 37.2, 40.5, 42.2, 51.8, 54.5, 126.2, 126.8, 127.2, 128.0, 128.3, 129.2, 138.2, 139.2, 169.8, 171.0, 172.4.

HRMS (ES): Calcd. for $C_{24}H_{32}N_3O_3$ (MH^+) 410.2444, found 410.2454.

((*R*)-1-((*S*)-1-Benzylcarbamoyl-2-phenyl-ethylcarbamoyl)-3-methyl-butyl)-carbamic acid tert-butyl ester 3.9:[14]

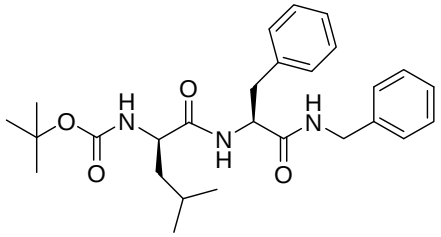

To a solution of amine **3.8** (50 mg, 0.20 mmol), Boc-*D*-Leu-OH (45 mg, 1 eq) and HATU (82 mg, 1.1 eq) in DMF (3.0 mL) was added DIEA (75 µL, 56 mg, 2.2 eq) and the resulting mixture was stirred for 16 h, then diluted with EtOAc (50 mL), washed with H_2O (50 mL), sat. $NaHCO_3$ (50 mL), brine (50 mL), dried over $MgSO_4$ and concentrated. The crude material was purified by flash chromatography, eluting with 1:4 EtOAc/DCM to give **3.9** (70 mg, 76%) as a white solid:

mp: 129-133ºC (lit.[14] 179-181ºC)

$[\alpha]_D^{20}$: -18.2 º (c = 0.55, MeOH)

^{1}H NMR (500 MHz, $CDCl_3$) δ 0.81-0.88 (6H, m, CH*Me*$_2$), 1.33 (11H, m), 1.54 (1H, dt, J = 13.5, 6.8 Hz), 3.12-3.22 (2H, m), 3.81 (1H, m), 4.27 (1H, dd, J = 14.8, 5.4 Hz), 4.50 (1H, dd, J = 14.8, 6.2 Hz), 4.74-4.84 (2H, m), 6.22 (1H, d, J = 7.4 Hz), 7.01 (1H, s), 7.14-7.30 (10H, m, 2*Ph*).

(*R*)-2-amino-*N*-((*S*)-1-(benzylamino)-1-oxo-3-phenylpropan-2-yl)-4-methylpentanamide 3.10:

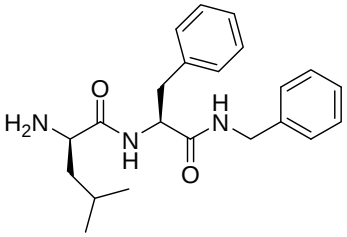

To a solution of **3.9** (55 mg, 0.12 mmol) in DCM (0.8 mL) was added TFA (0.2 mL) and the resulting mixture was stirred for 1 h then concentrated. The residue was dissolved in H_2O (10 mL), washed with DCM (10 mL), basified by addition of sat $NaHCO_3$ and extracted with DCM (10 mL × 3) to give **3.10** (37 mg, 85%) as a white solid:

mp: 130-132 ºC

$[\alpha]_D^{20}$: -20.9 º (c = 0.44, MeOH)

^{1}H NMR (500 MHz, $CDCl_3$) δ 0.84-0.90 (6H, m, CH*Me*$_2$), 1.23 (1H, m), 1.50-1.64 (2H, m), 1.79 (2H, br s, N*H*$_2$), 3.07 (1H, dd, J = 13.8, 7.6 Hz), 3.17 (1H, dd, J = 13.8, 7.6 Hz), 3.34 (1H, dd, J = 9.6, 4.0 Hz), 4.35 (2H, d, J = 5.8 Hz), 4.61 (1H, q, J = 7.6 Hz), 6.55 (1H, s), 7.11 (2H, m), 7.19-7.29 (8H, m), 7.84 (1H, d, J = 7.1 Hz).

^{13}C NMR (75 MHz, $CDCl_3$) δ 21.4, 23.5, 24.9, 38.0, 43.5, 44.0, 53.5, 54.5, 127.0, 127.5, 127.6, 128.7, 128.7, 129.4, 137.0, 138.0, 171.0, 176.2.

HRMS (ES): Calcd. for $C_{22}H_{30}N_3O_2$ (MH^+) 368.2338, found 368.2328.

***tert*-Butyl 2-((*R*)-1-((*S*)-1-(benzylamino)-1-oxo-3-phenylpropan-2-ylamino)-4-methyl-1-oxo pentan-2-ylamino)-2-oxoethylcarbamate 3.4:**

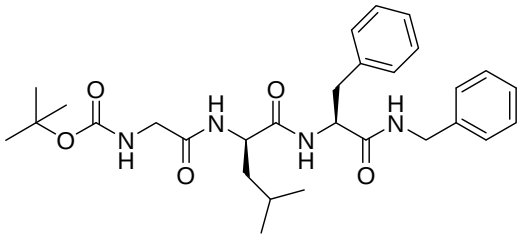

To a solution of **3.10** (100 mg, 0.27 mmol), Boc-Gly-OH (48 mg, 1 eq) and HATU (120 mg, 1.1 eq) in DMF (8.0 mL) was added DIEA (110 μL, 78 mg, 2.2 eq) and the resulting mixture was stirred for 16 h, then diluted with EtOAc (50 mL), washed with sat. $NaHCO_3$ (50 mL), brine (50 mL), dried over $MgSO_4$ and concentrated. The crude material was

purified by flash chromatography, eluting with 2:3 EtOAc/DCM, then by recrystallisation from EtOAc/pet ether to give **3.4** (78 mg, 55%) as white solid:

mp: 174-176 ºC

$[\alpha]_D^{20}$: -5.9 º (c = 0.32, MeOH)

^{1}H NMR (500 MHz, $(CD_3)_2SO$) δ 0.72 (6H, dd, J = 16.5, 5.7 Hz, $CH(CH_3)_2$), 1.12-1.18 (3H, m, $NHCHCH_2CH$ and $NHCHCH_2CH$), 1.36 (9H, s, $C(CH_3)_3$), 2.74 (1H, dd, J = 13.5, 10.9 Hz, $CHCHHPh$), 3.10 (1H, dd, J = 13.5, 4.1 Hz, $CHCHHPh$), 3.51 (2H, d, J = 5.8 Hz), 4.16-4.34 (3H, m), 4.48 (1H, m), 6.90 (1H, t, J = 6.0 Hz), 7.15-7.26 (8H, m), 7.30 (2H, t, J = 7.4 Hz), 7.81 (1H, d, J = 7.3 Hz), 8.42-8.49 (2H, m).

^{13}C NMR (126 MHz, $(CD_3)_2CO$) δ 22.2, 22.7, 23.8, 28.2, 37.4, 40.9, 42.2, 43.1, 51.4, 54.4, 78.1, 126.2, 126.8, 127.3, 128.1, 128.3, 129.3, 138.1, 139.2, 155.8, 169.4, 171.0, 171.9.

HRMS (ES): Calcd. for $C_{29}H_{41}N_4O_5$ (MH^+) 525.3077, found 525.3072

(*E*)-(4-Phenylazo-benzyl)-carbamic acid 9H-fluoren-9-ylmethyl ester 3.11:[3]

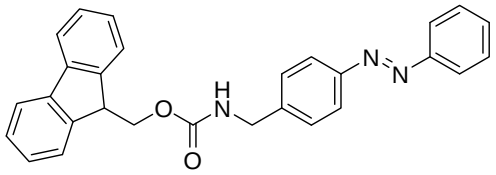

A solution of the aniline **2.36** (1.6 g, 4.7 mmol) and nitrosobenzene **2.13** (600 mg, 1.2 eq) in AcOH (50 mL) was stirred for 2 days, then diluted with DCM (100 mL) and H_2O (100 mL). The mixture was neutralised by addition of solid $NaCO_3$, the layers were separated and the aqueous layer was back extracted with DCM. The combined organic layers were concentrated. The crude product was purified by flash chromatography, eluting with DCM to give **3.11** (1.5 g, 71%) as an orange solid:

mp: 166-168 ºC (lit.[3] 164.5-165.5 ºC)

^{1}H NMR (500 MHz, $CDCl_3$) δ 4.24 (1H, t, J = 6.7 Hz), 4.46 (2H, d, J = 6.0 Hz), 4.51 (2H, d, J = 6.7 Hz), 5.13 (1H, t, J = 5.4 Hz), 7.32 (2H, t, J = 7.2 Hz), 7.37-7.44 (4H, m), 7.45-7.55 (3H, m), 7.61 (2H, d, J = 7.6 Hz), 7.77 (2H, d, J = 7.4 Hz), 7.87-7.94 (4H, m).

HRMS(ES): Calcd. for $C_{28}H_{24}N_3O_2$ (MH^+) 434.1869, found 434.1854.

(*E*)-4-Phenylazo-benzylamine 3.12:[3, 15]

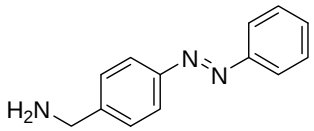

To a solution of **3.11** (100 mg, 0.23 mmol) in DMF (4.0 mL) was added piperidine (1.0 mL). The solution was stirred for 15 min then diluted with EtOAc (50 mL), washed with H_2O (50 mL × 3) then HCl (1.0 M, 50 mL). An orange precipitate formed which was collected, washed with H_2O (5.0 mL) and EtOAc (5.0 mL), then stirred in a mixture of 1:1 EtOAc/sat. $NaHCO_3$ for 10 min. The organic layer was collected, washed with brine, dried and concentrated to give **3.12** as an orange solid (37 mg, 76%):

^{1}H NMR (500 MHz, $CDCl_3$) δ 1.50 (2H, s), 3.92 (2H, s), 7.40-7.52 (5H, m), 7.87-7.93 (4H, m).

(*S*)-2-((*R*)-2-tert-Butoxycarbonylamino-4-methyl-pentanoylamino)-3-phenyl-propionic acid ethyl ester 3.14:

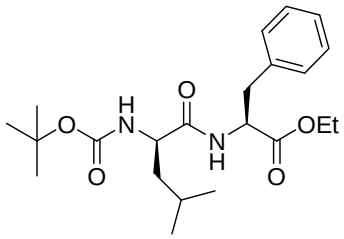

To a solution of Boc-*D*-Leu-OH **3.13** (500 mg, 2.1 mmol), H-Phe-OEt (470 mg, 1 eq), and HATU (900 mg, 1.2 eq) in DMF (8.0 mL) was added DIEA (1.3 mL, 3.6 eq) and the resulting mixture was stirred 16 h, diluted with EtOAc (50 mL), washed with H_2O (50 mL × 2), brine (50 mL), dried over $MgSO_4$ and concentrated. The crude material was purified by flash chromatography, eluting with 1:9 EtOAc/DCM to give **3.14** (760 mg, 92%) as a white solid:

mp: 75-82ºC

$[\alpha]_D^{20}$: +16.0 º (c = 0.75, MeOH)

^{1}H NMR (500 MHz, $CDCl_3$) δ 0.89 (6H, d, J = 6.2 Hz, CH*Me*$_2$), 1.23 (3H, t, J = 7.15 Hz, OCH$_2$*Me*), 1.43 (9H, s, C*Me*$_3$), 1.53-1.64 (2H, m), 3.06-3.16 (2H, m), 4.07-4.20 (3H, m) 4.77-4.86-4.77 (2H, m), 6.56 (1H, m), 7.12 (2H, m), 7.21-7.30 (3H, m).

^{13}C NMR (75 MHz, $CDCl_3$) δ 14.2, 22.0, 23.0, 14.8, 28.4, 38.1, 41.4, 53.2, 61.6, 80.2,

127.2, 128.6, 129.4, 135.9, 155.7, 155.7, 171.4, 172.3.

HRMS(ES): Calcd. for $C_{22}H_{35}N_2O_5$ (MH^+) 407.2546, found 407.2528.

(*E*)-((*R*)-3-Methyl-1-((*S*)-2-phenyl-1-(4-phenylazo-benzylcarbamoyl)-ethylcarbamoyl)-butyl)-carbamic acid *tert*-butyl ester 3.16:

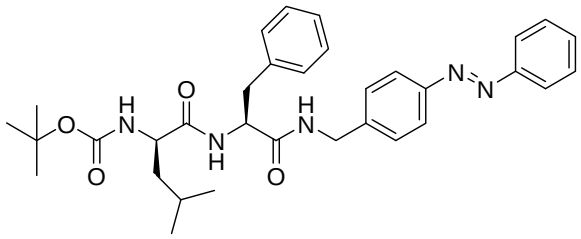

A solution of **3.14** (150 mg, 0.37 mmol) in THF (4.0 mL) was cooled to 0ºC and LiOH (0.25 M in 2:1 THF/H_2O, 2.2 mL) was added. The resulting mixture was stirred for 2 h, then diluted with DCM (50 mL) and H_2O (50 mL) and the layers were separated. The aqueous layer was acidified to pH 4 with HCl (1.0 M) and extracted with DCM (50 mL). The final organic extract was washed with brine (50 mL), dried over $MgSO_4$ and concentrated to give **3.15**[16] (60 mg, 43%) as a white solid. To a solution of **3.15** (60 mg, 0.16 mmol), **3.12** (34 mg, 1 eq) and HATU (67 mg, 1.1 eq) in DMF (3.0 mL) was added DIEA (61 μL, 45 mg, 2.2 eq) and the resulting mixture was stirred for 16 h then diluted with EtOAc (50 mL), washed with H_2O (50 mL × 2), sat $NaHCO_3$ (50 mL), brine (50 mL), dried over MgSO4 and concentrated. The crude material was purified by flash chromatography, eluting with 1:4 EtOAc/DCM to give **3.16** (65 mg, 72%) as an orange solid:

mp: 124-127 ºC

$[\alpha]_D^{20}$: -42.1º (c = 1.4, DCM)

^{1}H NMR (500 MHz, $CDCl_3$) δ 0.82-0.87 (6H, m, CH*Me*$_2$), 1.29-1.34 (11H, m), 1.56 (1H, m), 3.14-3.27 (2H, m), 3.78 (1H, m), 4.35 (1H, dd, J = 15.3, 5.2 Hz), 4.61 (1H, dd, J = 15.3, 6.3 Hz), 4.82 (2H, m), 6.14 (1H, d, J = 8.8 Hz), 7.12-7.36 (8H, m), 7.45-7.54 (3H, m), 7.84 (2H, d, J = 8.3 Hz), 7.91 (2H, d, J = 7.1 Hz).

^{13}C NMR (75 MHz, $CDCl_3$) δ 22.4, 22.7, 24.6, 28.3, 37.7, 40.9, 43.1, 54.0, 54.3, 80.4, 122.9, 123.1, 127.1, 128.1, 128.8, 129.1, 129.4, 131.0, 136.6, 141.4, 151.8, 152.7, 156.1, 170.9, 173.0.

HRMS (ES): Calcd. for $C_{33}H_{42}N_5O_4$ (MH^+) 572.3237, found 572.3265.

(*R*)-2-amino-4-methyl-*N*-((*S*)-1-oxo-3-phenyl-1-((*E*)-4-(phenylazo)benzylamino) propan-2-yl)pentanamide trifluoroacetate 3.5:

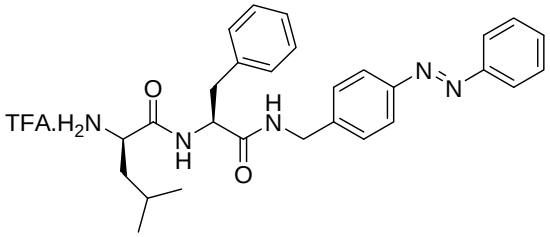

To a solution of **3.16** (65 mg, 0.11 mmol) in DCM (0.8 mL) was added TFA (0.2 mL) and the resulting mixture was stirred for 1 h, then diluted with DCM (50 mL), washed with HCl (1.0 M, 50 mL), sat $NaHCO_3$ (50 mL), brine (50 mL), dried over $MgSO_4$ and concentrated. The crude product was purified by recrystallisation from EtOAc/pet ether to give **3.5** (48 mg, 89%) as an orange solid:

mp: 161-164 ºC

$[\alpha]_D^{20}$: -8.3º (c = 0.29, MeOH)

^{1}H NMR (500 MHz, $CDCl_3$) δ 0.82-0.90 (6H, m, CH*Me*$_2$), 1.17-1.42 (3H, m), 1.49-1.67 (2H, m), 3.09 (1H, dd, J = 13.7, 7.5 Hz, CHC*H*HPh), 3.18 (1H, dd, J = 13.7, 7.5 Hz, CHCH*H*Ph), 3.28 (1H, dd, J = 9.2, 4.0 Hz), 4.42 (2H, m), 4.70 (1H, q, J = 7.5 Hz, C*H*CH$_2$Ph), 6.91 (1H, t, J = 5.8 Hz), 7.20-7.29 (7H, m), 7.44-7.53 (3H, m), 7.79-7.85 (3H, m), 7.88-7.91 (2H, m).

^{13}C NMR (75 MHz, $CDCl_3$) δ 21.3, 23.5, 24.9, 37.9, 43.1, 44.0, 53.5, 54.5, 122.9, 123.2, 127.0, 128.2, 128.7, 129.2, 129.4, 131.1, 136.9, 141.1, 151.9, 152.7, 171.1, 176.4.

HRMS (ES): Calcd. for $C_{28}H_{34}N_5O_2$ (MH^+) 472.2713, found 472.2690.

9.4 Experimental for work described in chapter 4

((*S*)-1-Benzyl-2-oxo-ethyl)-carbamic acid benzyl ester 4.11:[17, 18]

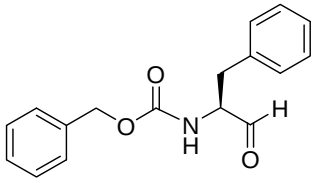

A solution of Cbz-Phe-OMe **4.10** (1.0 g, 3.2 mmol) in toluene (15 mL) was cooled to -78 ºC, then DIBAL (20% in toluene, 4.5 mL, 1.7 eq) was added, and the resulting mixture was stirred for 2.5 h at -78 ºC. Cold anhydrous MeOH (-50 ºC, 10 mL) was added and the

mixture was stirred for a further 20 min at -78 ºC then warmed to r.t. and HCl (1.0 M, 10 mL) was added. The mixture was stirred for 20 min, diluted with EtOAc (50 mL), washed with HCl (1.0 M, 50 mL × 3), sat $NaHCO_3$ (50 mL), brine (50 mL), dried over $MgSO_4$ and concentrated to give **4.11** (810 mg) which was used subsequently without further purification:

mp: 69-74 ºC (lit.[18] 78.5-80 ºC)

$[\alpha]_D^{20}$: -51.2 (c = 1.0, MeOH)

^{1}H NMR (500 MHz, $CDCl_3$) δ 3.14 (2H, d, J = 6.4 Hz, CHC*H*$_2$), 4.51 (1H, m, C*H*CH$_2$), 5.11 (2H, s, OC*H*$_2$), 5.31 (1H, d, J = 5.5 Hz, N*H*), 7.16-7.40 (10H, m), 9.63 (1H, s, C*H*O).

((*S*)-1-Benzyl-2-cyano-2-hydroxy-ethyl)-carbamic acid benzyl ester 4.12:[17, 19]

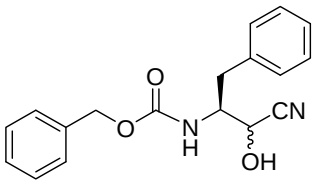

A solution of **4.11** (720 mg, 2.5 mmol) in EtOAc (4.0 mL) was cooled to 0 ºC and a solution of $NaHSO_3$ (300 mg, 1.1 eq) in H_2O (2.0 mL) was added. The resulting mixture was stirred for 30 min at 0 ºC then 20 h at 4 ºC. EtOAc (40 mL) and a solution of KCN (180 mg, 1.1 eq) in H_2O (3.0 mL) were added and the mixture was stirred vigorously at r.t. for 4.5 h then the layers were separated. The organic layer was washed with H_2O (50 mL × 2), brine (50 mL), dried over $MgSO_4$ and concentrated. The crude material was purified by flash chromatography, eluting with 1:9 EtOAc/DCM to give **4.12** (620 mg, 79 %) as a white solid:

^{1}H NMR (500 MHz, $(CD_3)_2SO$) δ 2.61 (0.4H, dd, J = 10.9, 13.0 Hz), 2.71 (0.6H, dd, J = 11.2, 13.8 Hz), 2.99 (1H, m), 3.90 (1H, m, C*H*NH), 4.41 (0.4H, m), 4.61 (0.6H, m), 4.96 (2H, s, OC*H*$_2$), 6.81 (0.6H, d, J = 5.7 Hz), 6.86 (0.4H, d, J = 7.2), 7.17-7.34 (10H, m), 7.54 (0.4H, d, J = 9.4), 7.68 (0.6H, d, J = 8.6).

(2*R*,3*S*)-3-Benzyloxycarbonylamino-2-hydroxy-4-phenyl-butyric acid methyl ester 4.13 and (2*S*,3*S*)-3-Benzyloxycarbonylamino-2-hydroxy-4-phenyl-butyric acid methyl ester 4.14:[17, 20]

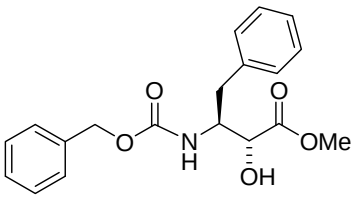

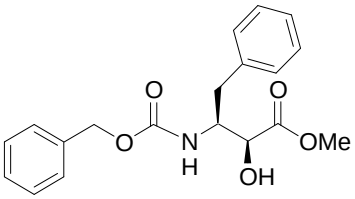

An HCl saturated mixture of ether (7.5 mL) and dry MeOH (2.5 mL) was cooled to 0 ºC and **4.12** (200 mg, 0.64 mmol) was added. The resulting mixture was stirred for 24 h at 4 ºC, then cold H_2O (0 ºC, 2.5 mL) was added slowly. The mixture was stirred at 4 ºC for 48 h, then concentrated. The crude material was purified by flash chromatography, eluting with 2:3 EtOAc/pet ether to give **4.13** (73 mg, 33%):

mp: 95-96 ºC (lit.[20] 94-95 ºC)

$[\alpha]_D^{20}$: -76.4 º (c = 1.0, MeOH)

^{1}H NMR (500 MHz, $CDCl_3$) δ 2.87-2.99 (2H, m, CHC*H*$_2$), 3.11 (1H, d, J = 3.5 Hz), 3.71 (3H, s, O*Me*), 4.08 (1H, s), 4.33 (1H, m, C*H*NH), 5.02-5.08 (3H, m), 7.19-7.38 (10H, m).

then **4.14** (42 mg, 19%):

mp: 119-120 ºC (lit.[20] 121-122 ºC)

$[\alpha]_D^{20}$: -158.0 º (c = 1.0, MeOH)

^{1}H NMR (500 MHz, $CDCl_3$) δ 2.81 (2H, m, CHC*H*$_2$), 3.19 (1H, s), 3.57 (3H, s, O*Me*), 4.32-4.43 (2H, m), 5.03-5.12 (3H, m), 7.17-7.37 (10H, m).

(2*R*,3*S*)-3-Amino-2-hydroxy-4-phenyl-butyric acid methyl ester 4.9:[21]

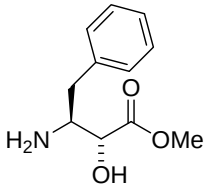

To a solution of **4.13** (40 mg, 0.064 mmol) in EtOAc (5 mL) was added Pd/C (5.0 mg). The resulting mixture was evacuated then stirred for 16 hours under a H_2 atmosphere, filtered through celite-545 filter aid and concentrated to obtain **4.9** (25 mg, qu) as a pale yellow gel which was used in subsequent reactions without further purification:

Selected peaks from ^{1}H NMR (500 MHz, $CDCl_3$) δ 2.75 (1H, dd, J = 8.3, 13.2 Hz), 2.93 (1H, dd, J = 6.5, 13.2 Hz), 3.39 (1H, s), 3.78 (3H, s, O*Me*), 4.09 (1H, s), 7.18-7.36 (5H, m). HRMS (ES): Calcd. for $C_{11}H_{16}NO_3$ (MH^+) 210.1130, found 210.1122.

(2*R*,3*S*,*E*)-methyl 3-(4-((4-((2-(tert-butoxycarbonylamino)acetamido)methyl)phenyl) diazenyl) benzamido)-2-hydroxy-4-phenylbutanoate 4.15:

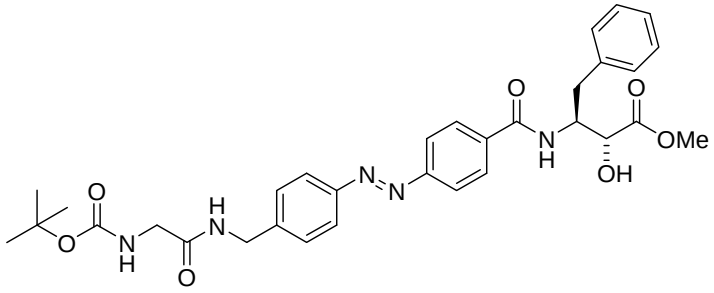

To a solution of **2.42** (20 mg, 0.048 mmol), **4.9** (10 mg, 1 eq), EDCI (10 mg, 1.1 eq) and HOBt (7.0 mg, 1.1 eq) in DMF (2.0 mL) was added DIEA (18 μL, 2.2 eq) and the resulting mixture was stirred for 16 h, diluted with EtOAc (50 mL), washed with H_2O (50 mL × 2), brine (50 mL), dried over $MgSO_4$ and concentrated. The crude product was purified by column chromatography, eluting with EtOAc to give **4.15** (20 mg, 69%) as an orange gel:

$[\alpha]_D$ = -73.9 º (c = 1.0, MeOH)

^{1}H NMR (500 MHz, $CDCl_3$) δ 1.43 (9H, s, C*Me*$_3$), 3.04-3.14 (2H, m), 3.73 (3H, s, O*Me*), 3.88 (2H, s), 4.27 (1H, d, J = 1.9 Hz), 4.45 (2H, m), 4.85 (1H, m), 5.62 (1H, s), 7.00 (1H, d, J = 9.2 Hz), 7.18-7.37 (8H, m), 7.73-7.76 (5H, m).

^{13}C NMR (126 MHz, $CDCl_3$) δ 28.3, 37.8, 42.9, 52.8, 53.7, 70.5, 80.4, 122.8, 123.3, 126.8, 127.9, 128.0, 128.6, 129.4, 135.8, 137.3, 141.5, 151.6, 154.0, 166.8, 170.1, 174.1.

HRMS (ES): Calcd. for $C_{32}H_{38}N_5O_7$ (MH^+) 604.2771, found 604.2792.

(*S*,*E*)-methyl-3-(4-((4-((2-(tert-butoxycarbonylamino)acetamido)methyl)phenyl) diazenyl)benzamido)-2-oxo-4-phenylbutanoate 4.5:

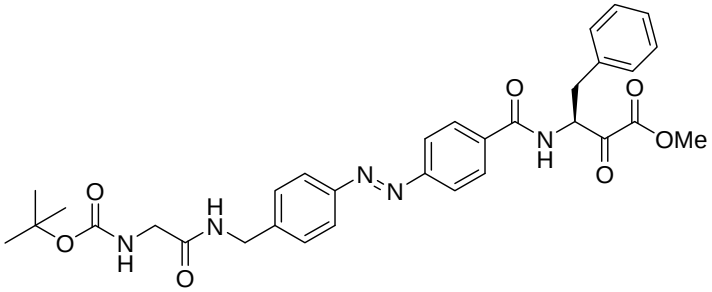

A solution of alcohol **4.15** (13 mg, 0.022 mmol) and Dess-Martin periodinane (19 mg, 2 eq) in DCM (1.0 mL) was stirred for 3 h, diluted with EtOAc (50 mL), washed with $Na_2S_2O_3$ (0.25 M in sat. $NaHCO_3$, 50 mL × 2), sat. $NaHCO_3$ (50 mL × 2), brine (50 mL), dried over $MgSO_4$ and concentrated. The crude material was purified by column chromatography, eluting with EtOAc to give **4.5** (11 mg, 83%) as an orange gel:

$[\alpha]_D$ = -85.6 º (c = 1.0, MeOH)

^{1}H NMR (300 MHz, ($CDCl_3$) δ 1.43 (9H, s, C*Me*$_3$), 3.23 (1H, dd, J = 14.1, 6.8 Hz, CHC*H*H), 3.40 (1H, dd, J = 14.3, 6.0 Hz, CHCH*H*), 3.83-3.93 (5H, m), 4.51 (2H, d, J = 5.9 Hz), 5.37 (1H, s), 5.62 (1H, q, J = 6.7 Hz, C*H*CH$_2$), 6.88-6.98 (2H, m), 7.18 (2H, d, J = 6.4 Hz), 7.25-7.39 (5H, m), 7.76-7.89 (6H, m).

^{13}C NMR (75 MHz, ($CDCl_3$) δ 28.3, 36.7, 42.9, 44.5, 53.3, 57.1, 80.4, 122.9, 123.4, 127.4, 128.1, 128.1, 128.8, 129.4, 134.7, 135.1, 141.8, 151.7, 154.4, 156.2, 160.7, 166.5, 169.8, 191.5.

HRMS (ES): Calcd. for $C_{32}H_{36}N_5O_7$ (MH^+) 602.2614, found 602.2632.

(*E*)-((4-[4-(1-Benzyl-3,3,3-trifluoro-2-hydroxy-propylcarbamoyl)-phenylazo)-benzyl carbamoyl)-methyl)-carbamic acid tert-butyl ester 4.16:

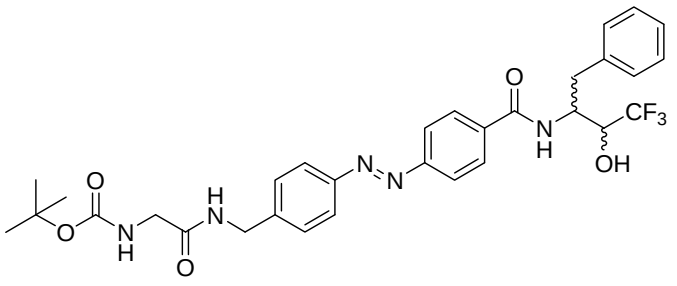

To a solution of carboxylic acid **2.42** (20 mg, 0.049 mmol), amine **4.8**[22] (supplied by Nathan Alexander[6], 11 mg, 1 eq), EDCI (10 mg, 1 eq) and HOAt (7.0 mg, 1 eq) in DMF

(3.0 mL) was added DIEA (9.0 μL, 6.7 mg, 1 eq) and the resulting mixture was stirred for 16 h, diluted with EtOAc (50 mL), washed with H_2O (50 mL × 2), brine (50 mL), dried over $MgSO_4$ and concentrated. The crude product was purified by flash chromatography, eluting with 3:2 EtOAc/DCM to give **4.16** (15 mg, 50%) as an orange solid:

^{1}H NMR (500 MHz, $(CD_3)_2CO$) δ 1.42 (9H, s, C(C*H*$_3$)$_3$), 3.17 (2H, m, CHC*H*$_2$), 3.84 (2H, d, J = 5.7 Hz), 4.23 (1H, m), 4.53 (2H, d, J = 6.0 Hz), 4.72 (1H, m), 6.35-6.40 (2H, m), 7.21 (1H, t, J = 7.4 Hz, CHCHC*H*CHCH), 7.30 (2H, t, J = 7.4 Hz, CHC*H*CHC*H*CH), 7.37 (2H, d, J = 7.4 Hz, C*H*CHCHCHC*H*), 7.50 (2H, d, J = 8.0 Hz), 7.83-7.96 (6H, m), 7.98 (2H, d, J = 8.5 Hz).

^{13}C NMR (126 MHz, $(CD_3)_2CO$) δ 28.5, 37.9, 43.0, 44.8, 52.2, 70.5 (q, J = 29.5 Hz), 79.4, 123.3, 123.8, 127.4, 128.9, 129.2, 129.3, 130.2, 137.4, 138.9, 144.5, 152.3, 154.9, 156.9, 167.3, 170.7.

^{19}F NMR (282 MHz, CD_3OD) δ -74.69 (d, J = 7.3 Hz), -75.97 (d, J = 7.4 Hz).

HRMS (ES): Calcd. for $C_{31}H_{35}F_3N_5O_5$ $(M - CF_3COO)^+$ 614.2590, found 614.2602.

(*E*)-((4-(4-(1-Benzyl-3,3,3-trifluoro-2-oxo-propylcarbamoyl)-phenylazo)-benzyl carbamoyl)-methyl)-carbamic acid tert-butyl ester 4.1:

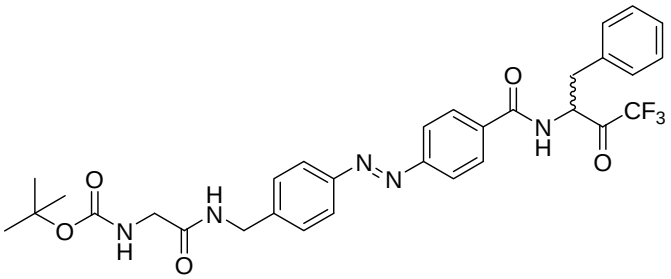

A solution of **4.16** (7.0 mg, 0.011 mmol) and Dess-Martin periodinane[23] (20 mg, 7 eq) in DCM (0.5 mL) was stirred for 3 h, diluted with EtOAc (50 mL), washed with $Na_2S_2O_3$ (0.25 M in sat. $NaHCO_3$, 50 mL), sat. $NaHCO_3$ (50 mL × 2), brine (50 mL), dried over $MgSO_4$ and concentrated. The crude material was purified by column chromatography, eluting with 4:1 EtOAc/DCM to give **4.1** (3.0 mg, 44%, predominantly hydrate isomer with traces of ketone) as an orange solid:

^{1}H NMR (500 MHz, $(CD_3)_2CO$) δ 1.42 (9H, s, C(C*H*$_3$)$_3$), 3.25 (1H, m, CHC*H*H), 3.39 (1H, m, CHCH*H*), 3.81 (2H, d, J = 5.2 Hz), 4.42 (1H, m, C*H*CH$_2$), 4.53 (2H, d, J = 5.5 Hz), 6.32 (1H, s), 6.80 (1H, s), 7.13-7.38 (6H, m), 7.51 (2H, d, J = 7.8 Hz), 7.80-7.92 (7H, m), 8.22 (1H, d, J = 8.0 Hz).

selected peaks from ^{13}C NMR (75 MHz, $(CD_3)_2CO$) δ 28.5, 33.7, 43.0, 44.8, 58.6, 79.4, 95.4 (q, J = 29.9Hz), 123.3, 123.8, 127.2, 129.0, 129.2, 129.5, 130.1, 136.7, 139.5, 144.8, 152.3, 155.1, 169.7, 170.6.

HRMS (ES): Calcd. for $C_{32}H_{37}F_3N_5O_6$ $(M + CH_3OH)^+$ 644.2696, found 644.2717.

(*E*)-Azobenzene-4,4′-dicarboxylic acid 4.20:[24]

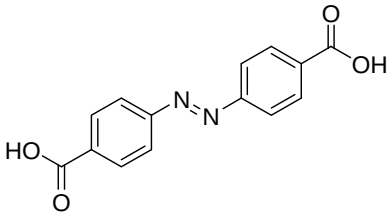

A mixture of 4-nitrobenzoic acid **4.19** (13 g, 78 mmol), NaOH (50 g) and H_2O (230 mL) was warmed to 50 ºC and a solution of glucose (100 g, 7.2 eq) in H_2O (150 mL) was added. The resulting mixture was stirred vigorously in air for 16 hours, then acidified by addition of HCl (1.0 M) and filtered to collect a brown precipitate. The crude material was recrystallised from a solution of K_2CO_3, then acidified by HCl (1.0 M) and filtered to obtain **4.20** (7.0 g, 33%) as an orange solid:

mp > 360 ºC

^{1}H NMR (300 MHz, D_2O) δ 8.01 (4H, d, J = 8.4 Hz), 7.88 (4H, d, J = 8.4 Hz).

(*E*)-Azobenzene-4,4′-diacid chloride 4.21:[24, 25]

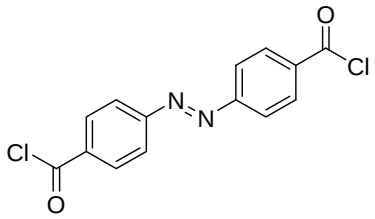

A solution of **4.20** (1.0 g, 3.7 mmol) in 1,2-dichloroethane (15 mL) was cooled to 0 ºC, and PCl_5 (2.0 g, 2.6 eq) was added. The resulting mixture was refluxed for 2 h, cooled and filtered to collect a red precipitate. The crude material was purified by flash chromatography, eluting with 1:1 DCM/pet ether to obtain **4.21** (540 mg, 47%) as a red solid:

mp: 161-163 ºC (lit.[24] 164 ºC)

^{1}H NMR (500 MHz, $CDCl_3$) δ 8.31 (4H, d, J = 8.8 Hz), 8.07 (4H, d, J = 8.8 Hz).

2-(2-(2-(2-Prop-2-ynyloxy-ethoxy)-ethoxy)-ethoxy)-ethanol 4.23:[26]

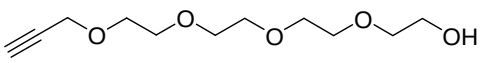

A solution of tetraethylene glycol **4.22** (8.2 g, 42 mmol) in THF (10 mL) was cooled to 0 ºC and NaH (60 % in mineral oil, 340 mg, 1 eq) was added. The resulting mixture was stirred for 20 min, then propargyl bromide (80% in toluene, 1.3 g, 8.7 mmol) was added slowly, and the mixture was stirred overnight, warming to r.t., then concentrated. The crude material was purified by flash chromatography, eluting with 1:9 MeOH/EtOAc to give **4.23** (1.1 g, 54%) as a yellow oil:

^{1}H NMR (500 MHz, $CDCl_3$) δ 2.07-2.26 (1H, br s, O*H*), 2.43 (1H, t, J = 2.4 Hz, C*H*), 3.60-3.75 (16H, m), 4.21 (2H, d, J = 2.4 Hz, CHCCH_2).

^{13}C NMR (75 MHz, $CDCl_3$) δ 58.5, 61.9, 69.2, 70.5, 70.5, 70.7, 70.7, 70.8, 73.7, 74.7, 79.7.

(*E*)-4-(4-Chlorocarbonyl-phenylazo)-benzoic acid 2-(2-(2-(2-prop-2-ynyloxy-ethoxy)-ethoxy)-ethoxy)-ethyl ester 4.24:

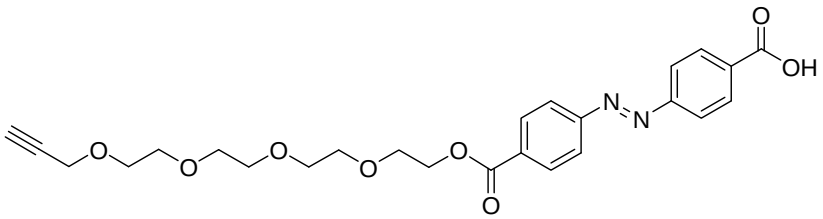

A solution of **4.23** (100 mg, 0.43 mmol) in THF (5.0 mL) was cooled to 0 ºC and TEA (1.0 mL) then a solution of **4.21** (260 mg, 2 eq) in THF (13 mL) were added. The solution was stirred for 2 h, at which point TLC showed that the acid chloride had been consumed. The mixture was diluted with EtOAc (50 mL) and filtered to obtain an orange precipitate and an orange filtrate. The ester **4.24** was not detected in either sample by ^{1}H NMR.

(*E*)-4-(4-(1-Benzyl-3,3,3-trifluoro-2-hydroxy-propylcarbamoyl)-phenylazo)-benzoyl chloride 4.25:

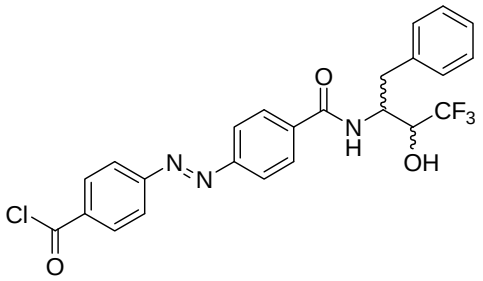

To a solution of amine **4.8**[22] (supplied by Nathan Alexander[6], 35 mg, 0.16 mmol) in DCM (5.0 mL) was added DIEA (29 μL, 22 mg, 1 eq) then a solution of **4.21** (100 mg, 2 eq) in DCM (5.0 mL) was added. The resulting mixture was stirred overnight, then washed with HCl (1.0 M, 20 mL), brine (20 mL), dried over $MgSO_4$ and concentrated. The crude product was purified by flash chromatography, eluting with 1:19 EtOAc/DCM to give **4.25** (30 mg, 38%) as a red-orange solid:

mp: 168-170 ºC

^{1}H NMR (500 MHz, $CDCl_3$) δ 3.10 (1H, dd, J = 13.8, 7.8 Hz, C*H*H), 3.33 (1H, dd, J = 13.8, 7.8 Hz, CH*H*), 4.11 (1H, m), 4.41 (1H, dq, J = 7.8, 2.2 Hz, C*H*CH_2), 4.77 (1H, d, J = 7.1 Hz), 6.62 (1H, d, J = 7.8 Hz, N*H*), 7.25-7.37 (5H, m), 7.83 (2H, d, J = 8.3 Hz), 7.98-8.04 (4H, m), 8.29 (2H, d, J = 8.4 Hz).

^{13}C NMR (75 MHz, $(CD_3)_2CO$) δ 37.9, 52.1, 70.4 (q, J = 28.5 Hz, *C*HCF_3), 123.9, 124.1, 127.4, 129.3, 129.4, 130.2, 133.5, 135.5, 138.7, 138.9, 154.7, 157.0, 167.0, 168.1.

HRMS (ES): Calcd. for $C_{25}H_{23}F_3N_3O_4$ (M – Cl + OCH_3 + H^+) 486.1641, found 486.1661.

(*E*)-4-(4-(1-Benzyl-3,3,3-trifluoro-2-hydroxy-propylcarbamoyl)-phenylazo)-benzoic acid 2-(2-(2-(2-prop-2-ynyloxy-ethoxy)-ethoxy)-ethoxy)-ethyl ester 4.26:

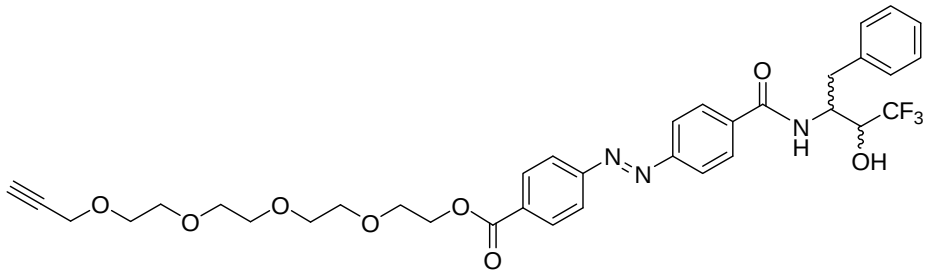

To a solution of **4.25** (20 mg, 0.042 mmol) and **4.23** (10 mg, 1 eq) in DCM (3.0 mL) was added DIEA (8.0 μL, 1 eq) and the resultant mixture was stirred for 16 h. TLC showed only returned starting materials.

(*R*)-2-*tert*-Butoxycarbonylamino-propionic acid 2-(2-(2-(2-prop-2-ynyloxy-ethoxy)-ethoxy)-ethoxy)-ethyl ester 4.27:

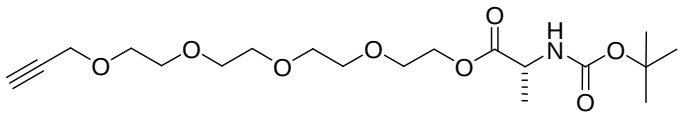

A solution of **4.23** (100 mg, 0.43 mmol), Boc-Ala-OH (82 mg, 1 eq), EDCI (83 mg, 1 eq) and DMAP (7.0 mg, 1 eq) in DCM (3.0 mL) was stirred for 16 h, diluted with EtOAc (50 mL), washed with H_2O (50 mL × 2), brine (50 mL), dried over $MgSO_4$ and concentrated. The crude product was purified by flash chromatography, eluting with 1:1 EtOAc/DCM to give **4.27** (160 mg, 94%) as a colourless oil:

$[\alpha]_D^{20}$: -127.0 º (c = 0.63, MeOH)

^{1}H NMR (500 MHz, $CDCl_3$) δ 1.39 (3H, d, J = 7.2 Hz, CH*Me*), 1.45 (9H, s, C(C*H*$_3$)$_3$), 2.43 (1H, t, J = 2.4 Hz, C*H*CCH$_2$), 3.64-3.72 (14H, m), 4.21 (2H, d, J = 2.4 Hz, CHCC*H*$_2$), 4.25-4.37 (3H, m), 5.05-5.12 (1H, br s, N*H*).

^{13}C NMR (75 MHz, $CDCl_3$) δ 18.1, 28.0, 48.9, 58.0, 64.0, 68.6, 68.7, 70.0, 70.2, 74.6, 79.3, 154.9, 173.0.

HRMS (ES): Calcd. for $C_{19}H_{33}NNaO_8$ (MNa^+) 426.2104, found 426.2090.

(*R*)-2-Amino-propionic acid 2-(2-(2-(2-prop-2-ynyloxy-ethoxy)-ethoxy)-ethoxy)-ethyl ester trifluoroacetate 4.28:

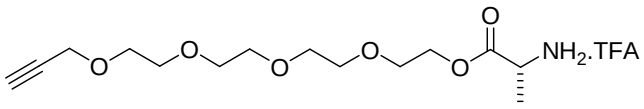

To a solution of **4.27** (150 mg, 0.37 mmol) in DCM (0.8 mL) was added TFA (0.2 mL) and the resulting mixture was stirred for 30 min then concentrated to give **4.28** (210 mg) as a pale yellow oil which was used subsequently without further purification:

Selected peaks from ^{1}H NMR (500 MHz, $CDCl_3$) δ 1.61 (3H, d, J = 7.1 Hz, *Me*), 2.51 (1H, t, J = 2.0 Hz, C*H*CCH_2), 3.63-3.77 (14H, m), 4.15-4.28 (3H, m), 4.34 (1H, m), 4.51 (1H, m).

Selected peaks from ^{13}C NMR (75 MHz, $CDCl_3$) δ 15.9, 49.4, 58.4, 65.0, 68.6, 68.8, 69.9, 70.0, 70.1, 70.1, 70.2, 75.4, 79.0, 169.8.

HRMS (ES): Calcd. for $C_{14}H_{26}NO_6$ (MH^+) 304.1760, found 304.1745.

(*R*,*E*)-2-(4-(4-Chlorocarbonyl-phenylazo)-benzoylamino)-propionic acid 2-(2-(2-(2-prop-2-ynyloxy-ethoxy)-ethoxy)-ethoxy)-ethyl ester 4.29:

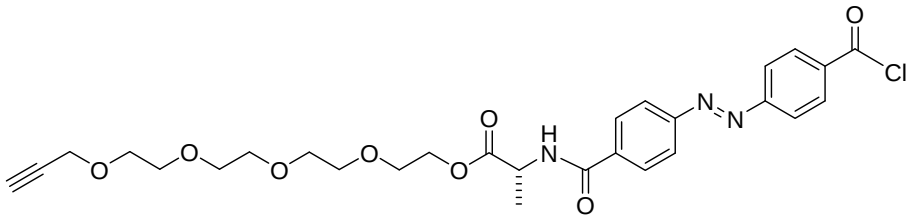

To a solution of **4.28** (68 mg, 0.16 mmol) in DCM (5.0 mL) was added DIEA (120 μL, 4 eq) then a solution of **4.21** (100 mg, 2 eq) in DCM (5.0 mL). The resultant mixture was stirred for 16 h then filtered to obtain an orange precipitate and an orange filtrate. MS showed the presence of **4.29** in the filtrate, but only traces of azobenzene products could be identified in this sample by TLC and NMR.

(*R*,*E*)-2-(4-(4-(1-Benzyl-3,3,3-trifluoro-2-hydroxy-propylcarbamoyl)-phenylazo)-benzoylamino)-propionic acid 2-(2-(2-(2-prop-2-ynyloxy-ethoxy)-ethoxy)-ethoxy)-ethyl ester 4.30:

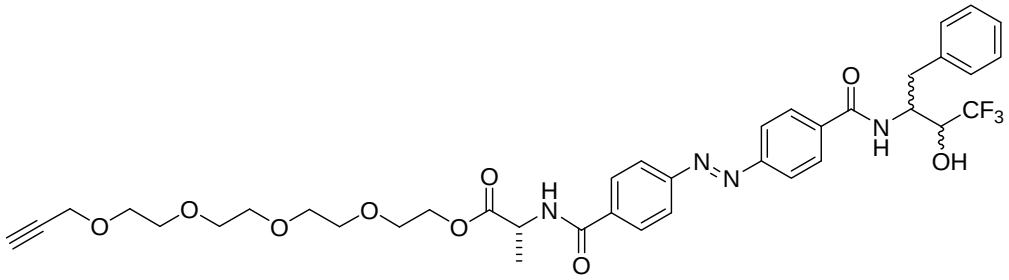

To a solution of acid chloride **4.25** (14 mg, 0.030 mmol) and alcohol **4.28** (16 mg, 1.3 eq) in DCM (2.0 mL) was added DIEA (21 μL, 16 mg, 4 eq) and the resulting mixture was stirred for 16 h, diluted with EtOAc (50 mL), washed with HCl (1.0 M, 50 mL), sat. $NaHCO_3$ (50 mL), brine (50 mL), dried over $MgSO_4$ and concentrated. The crude product was purified by flash chromatography, eluting with EtOAc to give **4.30** (16 mg, 70% over two steps) as a colourless oil:

^{1}H NMR (500 MHz, $CDCl_3$) δ 1.62 (3H, d, J = 7.2 Hz, *Me*), 2.43 (1H, t, J = 2.4 Hz, C*H*CCH$_2$O), 3.12 (1H, m, CHC*H*H), 3.23 (1H, dd, J = 13.3, 7.0 Hz, CHCH*H*), 3.62-3.70 (12H, m), 3.76 (2H, t, J = 4.7 Hz), 4.08 (1H, s), 4.17 (2H, d, J = 2.1 Hz, CHCC*H*$_2$O), 4.38 (2H, dd, J = 8.1, 3.9 Hz), 4.65 (1H, m), 4.82 (1H, p, J = 7.1 Hz, C*H*CH$_3$), 5.71 (1H, s), 7.26 (1H, t, J = 7.2 Hz), 7.30-7.37 (4H, m), 7.48-7.70 (10H, m).

^{13}C NMR (75 MHz, $CDCl_3$) δ 17.7, 37.6, 49.0, 51.1, 58.3, 64.5, 68.8, 69.0, 70.2, 70.4, 70.5, 70.5, 74.8, 79.5, 122.6, 126.9, 127.8, 128.0, 128.7, 129.4, 135.8, 136.4, 137.0, 153.2, 153.3, 167.7, 168.0, 172.7.

HRMS (ES): Calcd. for $C_{38}H_{44}F_3N_4O_9$ (MH^+) 757.3060, found 757.3094.

(*R*,*E*)-2-(4-(4-(1-Benzyl-3,3,3-trifluoro-2-oxo-propylcarbamoyl)-phenylazo)-benzoylamino)-propionic acid 2-(2-(2-(2-prop-2-ynyloxy-ethoxy)-ethoxy)-ethoxy)-ethyl ester 4.2:

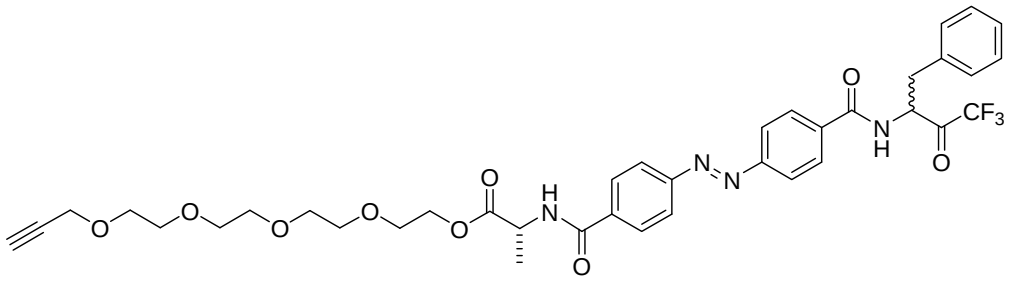

A solution of alcohol **4.30** (31 mg, 0.041 mmol) and Dess-Martin periodinane (38 mg, 3.7 eq) in DCM (3.0 mL) was stirred for 3 h, diluted with EtOAc (50 mL), washed with $Na_2S_2O_3$ (0.25 M in sat. $NaHCO_3$, 50 mL × 2), sat. $NaHCO_3$ (50 mL × 2), brine (50 mL), dried over $MgSO_4$ and concentrated. The crude material was purified by flash chromatography, eluting with EtOAc to give **4.2** (32 mg, qu, a 2:3 mixture of ketone/hydrate), as an orange gel:

$[\alpha]_D^{20}$: +21.1º (c = 0.29, MeOH)

^{1}H NMR (500 MHz, $(CD_3)_2CO$) δ 1.54 (3H, d, J = 7.3 Hz, *Me*), 2.92 (1H, t, J = 2.4 Hz, C*H*CCH$_2$O), 3.27 (1H, m, CHC*H*H), 3.40 (1H, m, CHCH*H*), 3.53-3.64 (12H, m), 3.68-3.72 (2H, m, C*H*$_2$CH$_2$OCO), 4.17 (2H, d, J = 2.4 Hz, CHCC*H*$_2$O) 4.24 (1H, m, CH$_2$C*H*HOCO), 4.31 (1H, m, CH$_2$CH*H*OCO), 4.47 (0.6H, t, J = 8.8 Hz, C*H*CH$_2$ (hydrate isomer)), 4.71 (1H, p, J = 7.3 Hz, C*H*Me), 5.26 (0.4H, dt, J = 9.3, 6.0 Hz), 6.79 (0.4H, s), 7.12 (0.4H, s), 7.19 (1H, t, J = 7.4 Hz), 7.23-7.39 (4H, m), 7.89 (2H, m), 7.94-8.01 (4H, m), 8.10 (2H, m), 8.18-8.25 (1.6H, m, N*H*CHCH$_2$(hydrate isomer) and N*H*CHMe), 8.69 (0.4H, d, J = 6.7 Hz).

HRMS (ES): Calcd. for $C_{38}H_{44}F_3N_4O_{10}$ (MH_3O^+) 773.3010, found 773.3019.

4-Nitroso-benzoic acid methyl ester 4.35:[27]

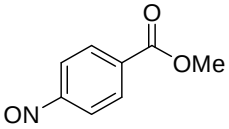

To a solution of 4-methyl aminobenzoate **4.34** (1.0 g, 6.6 mmol) in DCM (20 mL) was added Oxone (8.2 g, 2 eq) in H_2O (80 mL) and the resulting mixture was stirred vigorously for 30 min, then the layers were separated. The organic layer was washed with H_2O (50

mL), brine (50 mL), dried over $MgSO_4$ and concentrated. The crude product was purified by flash chromatography, eluting with DCM to give **4.35** (680 mg, 62%) as an green solid:
mp 123-124 ºC
^{1}H NMR (300 MHz, $CDCl_3$) δ 3.99 (3H, s, *Me*), 7.94 (2H, d, J = 8.7 Hz), 8.31 (2H, d, J = 8.7 Hz).

(*E*)-4-(4-Bromo-phenylazo)-benzoic acid methyl ester 4.37:[27]

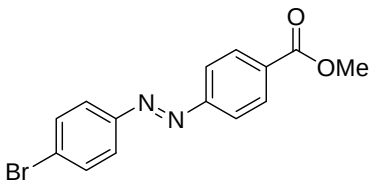

Method A:
A mixture of bromoaniline **4.36** (170 mg, 1.0 mmol), nitrosobenzene **4.35** (200 mg, 1.2 eq) and AcOH (7.0 mL) stirred for 16 h at 40 ºC, then further bromoaniline **4.36** (90 mg, 0.5 eq) was added. The mixture was stirred for a further 4 h at 40 ºC then cooled and concentrated. The crude material was purified by flash chromatography, eluting with 4:1 DCM/pet. ether to give **4.37** (99 mg, 30%) as an orange solid:
mp 136 ºC (decomp)
^{1}H NMR (300 MHz, $CDCl_3$) δ 3.96 (3H, s, *Me*), 7.67 (2H, d, J = 8.8 Hz), 7.83 (2H, d, J = 8.8 Hz), 7.95 (2H, d, J = 8.8 Hz), 8.19 (2H, d, J = 8.8 Hz).

Method B:
A mixture of nitrosobenzene **4.38** (200 mg, 1.1 mmol), 4-methyl aminobenzoate **4.34** (180 mg, 1.1 eq) and AcOH (5.0 mL) was stirred for 16 h then filtered to collect an orange precipitate. The precipitate was purified by flash chromatography, eluting with 4:1 DCM/pet ether to obtain **4.37** (180 mg, 52%) as an orange solid.

1-Bromo-4-nitroso-benzene 4.38:[27]

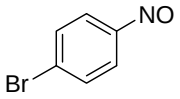

To a solution of bromoaniline **4.36** (5.0 g, 29 mmol) in DCM (90 mL) was added Oxone (36 g, 2 eq) in H_2O (360 mL) and the resulting mixture was stirred vigorously for 3 h 10 min, then the layers were separated. The organic layer was washed with HCl (1.0 M, 50 mL), sat. $NaHCO_3$ (50 mL), brine (50 mL), dried over $MgSO_4$ and concentrated. The crude product was purified by flash chromatography, eluting with 1:9 EtOAc/pet ether to give **4.38** (5.3 g, 98%) as an green solid:

^{1}H NMR (500 MHz, $CDCl_3$) δ 7.76-7.81 (4H, m).

(*E*)-4-(4-(3-Hydroxy-3-methyl-but-1-ynyl)-phenylazo)-benzoic acid methyl ester 4.39:

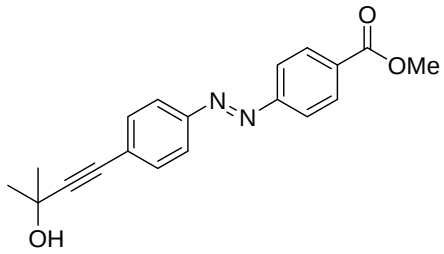

To a solution of **4.37** (3.0 g, 9.4 mmol), 2-methyl-3-butyn-2-ol (930 mg, 1.2 eq), PPh_3 (28 mg, 0.12 eq) and CuI (7.0 mg, 0.0039 eq) in TEA (50 mL) was added $PdCl_2(PPh_3)_2$ (8.0 mg, 0.012 eq). The resulting mixture was refluxed for 1 h, then cooled and concentrated. The crude product was purified by flash chromatography, eluting with 1:9 EtOAc/DCM to give **4.39** (2.8 g, 93%) as an orange solid:

mp 198-201 ºC

^{1}H NMR (500 MHz, $CDCl_3$) δ 1.65 (6H, s), 3.96 (3H, s), 7.57 (2H, d, J = 8.4 Hz), 7.90 (2H, d, J = 8.4 Hz), 7.95 (2H, d, J = 8.5 Hz), 8.19 (2H, d, J = 8.5 Hz).

^{13}C NMR (75 MHz, $CDCl_3$) δ 31.6, 52.5, 65.8, 81.9, 96.8, 122.9, 123.2, 126.3, 130.8, 132.1, 132.7, 151.8, 155.2, 166.6.

HRMS (ES): Calcd. for $C_{19}H_{19}N_2O_3$ (MH^+) 323.1396, found 323.1396.

(*E*)-4-(4-Ethynyl-phenylazo)-benzoic acid 4.40:

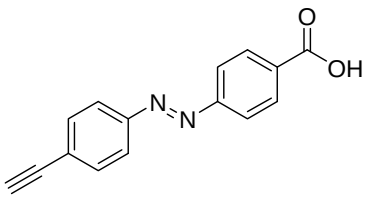

A solution of NaOH (150 mg) in butanol (8.0 mL) was heated to reflux and ester **4.39** (20 mg, 0.062 mmol) was added. The resulting mixture was refluxed for 15 min, then cooled and filtered to collect an orange precipitate which was washed with DCM (50 mL) then dissolved in MeOH (20 mL), acidified with HCl (1.0 M) and filtered to collect **4.40** (11 mg, 71%) as a pale orange solid:

mp 210 ºC (decomp)

^{1}H NMR (500 MHz, $(CD_3)_2SO$) δ 4.50 (1H, s, C*H*CC_6H_4), 7.72 (2H, d, J = 8.6 Hz), 7.94 (2H, d, J = 8.6 Hz), 7.99 (2H, d, J = 8.6 Hz), 8.15 (1H, d, J = 8.6 Hz).

^{13}C NMR (75 MHz, $(CD_3)_2SO$) δ 83.0, 83.9, 122.7, 123.1, 125.3, 130.7, 133.0, 133.1, 151.4, 154.2, 166.7.

HRMS (ES): Calcd. for $C_{15}H_{11}N_2O_2$ (MH^+) 251.0821, found 251.0819.

(*E*)-*N*-(1-Benzyl-3,3,3-trifluoro-2-hydroxy-propyl)-4-(4-ethynyl-phenylazo)-benzamide 4.41:

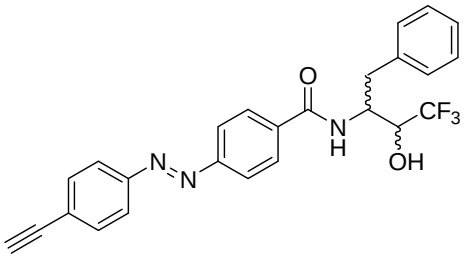

To a solution of carboxylic acid **4.40** (150 mg, 0.60 mmol), amine **4.8**[22] (supplied by Nathan Alexander[6], 130 mg, 1 eq), EDCI (120 mg, 1 eq) and HOAt (81 mg, 1 eq) in DMF (8.0 mL) was added DIEA (210 µL, 160 mg, 2 eq) and the resulting mixture was stirred for 16 h, diluted with DCM (50 mL), washed with H_2O (50 mL), brine (50 mL), dried over $MgSO_4$ and concentrated. The crude product was purified by column chromatography, eluting with a gradient from DCM to 1:19 EtOAc/DCM to give **4.41** (150 mg, 56%) as an orange solid:

mp: 173-174 ºC

^{1}H NMR (500 MHz, $CDCl_3$) δ 3.10 (1H, dd, J = 13.8, 7.7 Hz, C*H*H), 3.26 (1H, s, C*H*CC_6H_4), 3.33 (1H, dd, J = 13.8, 8.0 Hz, CH*H*), 4.10 (1H, m), 4.36 (1H, dq, J = 7.9, 2.6 Hz), 4.91 (1H, d, J = 7.3 Hz), 6.59 (1H, d, J = 7.6 Hz), 7.25-7.36 (5H, m, *Ph*), 7.65 (2H, d, J = 8.4 Hz), 7.79 (2H, d, J = 8.4 Hz), 7.94 (2H, d, J = 8.4 Hz), 7.90 (2H, d, J = 8.4 Hz).
^{13}C NMR (75 MHz, $(CD_3)_2CO$) δ 37.9, 52.2, 70.4 (q, J = 29.6 Hz, *C*HCF_3), 82.1, 83.6, 123.5, 123.9, 126.4, 127.4, 129.3, 129.3, 130.2, 133.8, 137.9, 138.9, 152.8, 154.8, 167.2.
HRMS (ES): Calcd. for $C_{25}H_{21}F_3N_3O_2$ (MH^+) 452.1586, found 452.1571.

(*E*)-*N*-(1-Benzyl-3,3,3-trifluoro-2-oxo-propyl)-4-(4-ethynyl-phenylazo)-benzamide 4.3:

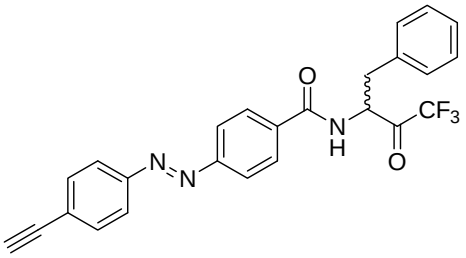

A solution of alcohol **4.41** (54 mg, 0.12 mmol) and Dess-Martin periodinane (110 mg, 3.7 eq) in DCM (5.0 mL) was stirred for 3 h, diluted with EtOAc (50 mL), washed with $Na_2S_2O_3$ (0.25 M in sat. $NaHCO_3$, 50 mL × 2), sat. $NaHCO_3$ (50 mL × 2), brine (50 mL), dried over $MgSO_4$ and concentrated. The crude material was purified by flash chromatography, eluting with 1:19 EtOAc/DCM to give **4.3** (49 mg, 91%, a 1:3 mixture of ketone/hydrate) as an orange solid:
mp: 187-189 ºC
^{1}H NMR (500 MHz, $(CD_3)_2CO$) δ 3.25 (1H, m, C*H*H), 3.38 (1H, m, CH*H*), 3.92 (1H, s, C*H*CC_6H_4), 4.40 (0.75H, m, C*H*CH_2 (hydrate isomer)), 5.24 (0.25H, m, C*H*CH_2 (ketone isomer)), 6.77 (0.75H, s, O*H*), 7.12 (0.75H, s, O*H*), 7.19 (1H, t, J = 7.3 Hz), 7.24-7.38 (4H, m), 7.72 (2H, d, J = 8.6 Hz), 7.89-8.04 (6H, m), 8.20 (0.75H, d, J = 8.4 Hz, N*H* (hydrate isomer)), 8.62 (0.25H, d, J = 7.0 Hz, N*H* (ketone isomer)).
selected peaks from ^{13}C NMR (75 MHz, $(CD_3)_2CO$) δ 33.7, 58.5, 82.1, 83.6, 95.3 (q, J = 30.1 Hz, *C*HCF_3), 123.5, 123.9, 126.5, 127.2, 129.2, 129.5, 130.1, 133.8, 137.1, 139.5, 152.8, 154.9, 169.6.
HRMS (ES): Calcd. for $C_{25}H_{19}F_3N_3O_2$ (MH^+) 450.1429, found 450.1408.

(2*R*,3*S*,*E*)-methyl 3-(4-((4-ethynylphenyl)diazenyl)benzamido)-2-hydroxy-4-phenyl butanoate 4.42:

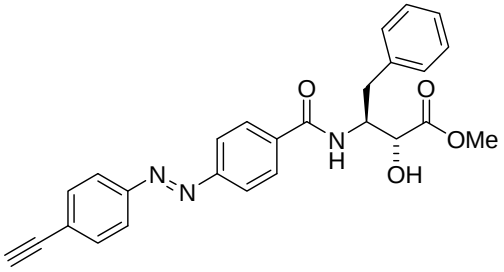

To a solution of carboxylic acid **4.39** (12 mg, 0.048 mmol), amine **4.9** (10 mg, 1 eq), EDCI (10 mg, 1.1 eq) and HOBt (7.0 mg, 1.1 eq) in DMF (2.0 mL) was added DIEA (18 μL, 2.2 eq) and the resulting mixture was stirred for 16 h, diluted with EtOAc (50 mL), washed with H_2O (50 mL × 2), brine (50 mL), dried over $MgSO_4$ and concentrated. The crude product was purified by column chromatography, eluting with 1:9 EtOAc/DCM to give **4.42** (13 mg, 61%) as an orange solid:

mp: 187-191 ºC

$[\alpha]_D$ = -130.3 º (c = 0.65, MeOH)

^{1}H NMR (500 MHz, $CDCl_3$) δ 3.02-3.14 (2H, m, CHC*H*$_2$), 3.26 (1H, s), 3.75 (3H, s, O*Me*), 4.24 (1H, d, J = 1.6 Hz), 4.84 (1H, m, C*H*NH), 6.65 (1H, d, J = 9.2 Hz, N*H*), 7.24 (1H, m), 7.30-7.37 (5H, m), 7.62 (2H, d, J = 8.5 Hz), 7.80 (2H, d, J = 8.5 Hz), 7.85-7.90 (4H, m).

^{13}C NMR (126 MHz, $CDCl_3$) δ37.9, 53.0, 53.4, 70.1, 79.9, 83.1, 123.0, 123.0, 125.3, 126.8, 128.0, 128.7, 129.4, 133.0, 136.2, 137.1, 151.9, 154.1, 166.5, 174.2.

HRMS (ES): Calcd. for $C_{26}H_{24}N_3O_4$ (MH^+) 442.1767, found 442.1769.

(*S*,*E*)-methyl 3-(4-((4-ethynylphenyl)diazenyl)benzamido)-2-oxo-4-phenylbutanoate 4.6:

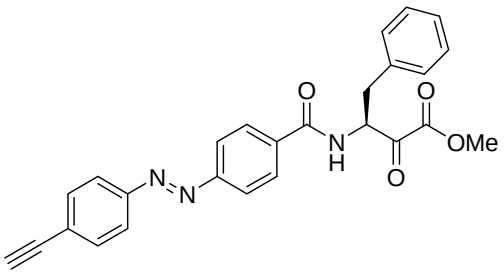

A solution of alcohol **4.42** (11 mg, 0.025 mmol) and Dess-Martin periodinane (21 mg, 2 eq) in DCM (1.0 mL) was stirred for 3 h, diluted with EtOAc (50 mL), washed with $Na_2S_2O_3$ (0.25 M in sat. $NaHCO_3$, 50 mL × 2), sat. $NaHCO_3$ (50 mL × 2), brine (50 mL),

dried over $MgSO_4$ and concentrated. The crude material was purified by column chromatography, eluting with 1:1 EtOAc/pet ether to give **4.6** (10 mg, 91%) as an orange solid:

mp: 156-161 ºC

$[\alpha]_D$ = -166.4 º (c = 1.0, MeOH)

^{1}H NMR (300 MHz, $(CD_3)_2CO$) δ 3.13 (1H, dd, J = 14.0, 9.3 Hz, CHC*H*H), 3.40 (1H, dd, J = 14.0, 5.2 Hz, CHCH*H*), 3.83 (3H, s, O*Me*), 3.92 (1H, s, C*H*CC_6H_4), 5.40 (1H, m, C*H*CH_2), 7.19-7.41 (5H, m), 7.71 (2H, d, J = 8.5 Hz), 7.89-8.06 (6H, m), 8.39 (1H, d, J = 6.6 Hz).

^{13}C NMR (75 MHz, $(CD_3)_2CO$) δ 36.1, 53.1, 58.7, 82.1, 83.6, 123.6, 123.9, 126.5, 127.6, 129.3, 129.5, 130.2, 133.9, 136.9, 138.0, 152.8, 155.0, 162.2, 167.0, 192.5.

HRMS (ES): Calcd. for $C_{26}H_{22}N_3O_4$ (MH^+) 440.1610, found 440.1628.

(*E*)-*N*-(1-Benzyl-3,3,3-trifluoro-2-hydroxy-propyl)-4-(4-(3-(2-(2-(2-(2-prop-2-ynyloxy-ethoxy)-ethoxy)-ethoxy)-ethoxy)-prop-1-ynyl)-phenylazo)-benzamide 4.48:

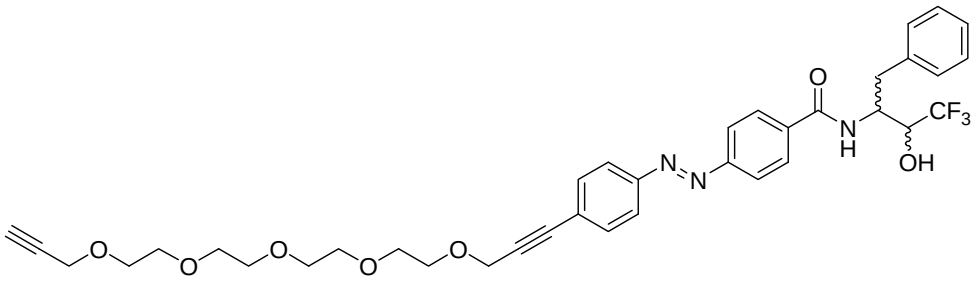

To a solution of carboxylic acid **4.47** (100 mg, 0.20 mmol), amine **4.8**[22] (supplied by Nathan Alexander[6], 44 mg, 1 eq), EDCI (43 mg, 1.1 eq) and HOBt (30 mg, 1.1 eq) in DMF (5.0 mL) was added DIEA (77 mL, 57 mg, 2.2 eq) and the resulting mixture was stirred for 19 h, diluted with EtOAc (50 mL), washed with H_2O (50 mL × 4), brine (50 mL), dried over $MgSO_4$ and concentrated. The crude product was purified by column chromatography, eluting with 2:3 EtOAc/DCM to give **4.48** (110 mg, 80%) as an orange gel:

^{1}H NMR (500 MHz, $CDCl_3$) δ 2.54 (1H, s, OCH_2CCH), 3.00-3.20 (2H, m, $CHCH_2$), 3.55-3.80 (16H, m), 4.18 (1H, t, J = 6.1 Hz), 4.24 (2H, d, J = 2.2 Hz, $CHCCH_2$), 4.52 (2H, s), 4.75 (1H, m, NHC*H*), 6.18 (1H, d, J = 7.0 Hz), 7.24-7.43 (5H, m), 7.50 (1H, d, J = 8.3 Hz), 7.61 (2H, d, J = 8.4 Hz), 7.85-7.95 (6H, m).

^{13}C NMR (126MHz, $CDCl_3$) δ 37.6 (CH*C*H_2), 51.0 (NH*C*H), 58.2, 59.0, 68.9, 69.2, 70.2, 70.3, 70.4, 70.4, 70.4, 74.7, 79.5, 85.8, 87.9, 122.9, 123.0, 125.7, 126.9, 128.0, 128.6, 129.2, 132.4, 135.8, 136.8, 151.5, 154.0, 167.6.

HRMS (ES) Calcd. for $C_{37}H_{40}F_3N_3NaO_7$ (MNa^+) 718.2716, found 718.2735.

(*E*)-*N*-(1-Benzyl-3,3,3-trifluoro-2-oxo-propyl)-4-(4-(3-(2-(2-(2-(2-prop-2-ynyloxy-ethoxy)-ethoxy)-ethoxy)-ethoxy)-prop-1-ynyl)-phenylazo)-benzamide 4.4:

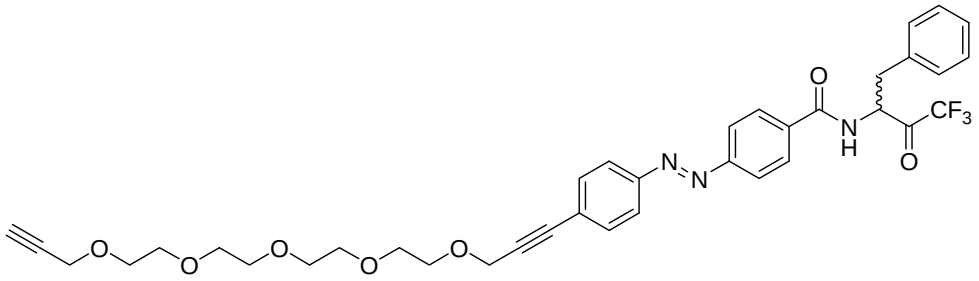

A solution of **4.48** (31 mg, 0.045 mmol) and Dess-Martin periodinane (42 mg, 3.7 eq) in DCM (2.0 mL) was stirred for 3 h, diluted with EtOAc (50 mL), washed with $Na_2S_2O_3$ (0.25 M in sat. $NaHCO_3$, 50 mL × 2), sat. $NaHCO_3$ (50 mL × 2), brine (50 mL), dried over $MgSO_4$ and concentrated. The crude material was purified by column chromatography, eluting with 1:1 EtOAc/DCM to give **4.4** (28 mg, 90%) as an orange gel:

^{1}H NMR (500 MHz, $(CD_3)_2CO$) δ 2.92 (1H, t, J = 2.4 Hz, OCH_2CCH), 3.25 (1H, dd, J = 12.1, 14.0 Hz, CH*C*H_2), 3.40 (1H, dd, J = 3.1, 14.0 Hz, CH*C*H_2), 3.55-3.65 (12, m), 3.67 (2H, m), 3.74 (2H, m), 4.17 (2H, d, J = 2.4 Hz, $CHCCH_2O$), 4.40-4.48 (3H, m), 6.80 (1H, s), 7.14 (1H, s), 7.19 (1H, t, J = 7.4 Hz), 7.27 (2H, t, J = 7.4 Hz), 7.34 (2H, d, J = 7.4 Hz), 7.67 (2H, d, J = 8.6), 7.88-7.94 (6H, m), 8.20 (1H, d, J = 8.1 Hz).

^{13}C NMR (126MHz, $(CD_3)_2CO$) δ 33.7 (CH*C*H_2), 58.5, 58.5, 59.3, 69.7, 70.0, 70.9, 71.1, 71.2, 71.2, 75.7, 80.9, 85.8, 89.8, 95.3 (q, J = 29.8, *C*CF_3), 123.4, 123.9, 127.0, 127.2, 129.2, 129.5, 130.1, 133.5, 137.0, 139.5, 152.6, 155.0, 169.6.

HMRS (ES) Calcd. for $C_{37}H_{40}F_3N_3NaO_8$ ($M + H_2O + Na^+$) 734.2665, found 734.2652.

(2R,3*S*,*E*)-methyl 3-(4-((4-(4,7,10,13,16-pentaoxanonadeca-1,18-diynyl)phenyl) diazenyl)benzamido)-2-hydroxy-4-phenylbutanoate 4.49:

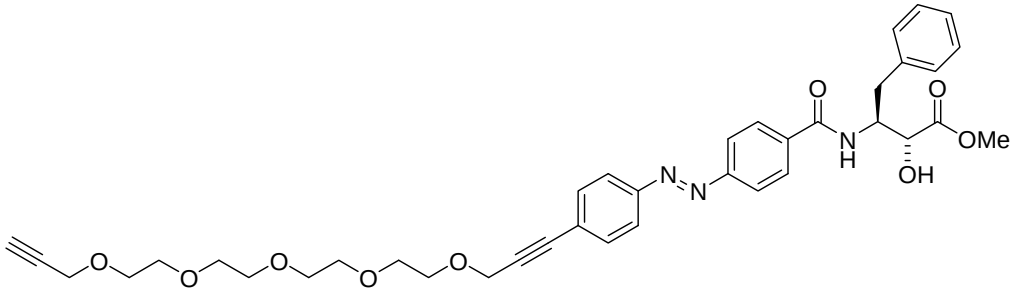

To a solution of **4.47** (24 mg, 0.048 mmol), **4.9** (10 mg, 1 eq), EDCI (10 mg, 1.1 eq) and HOBt (7.0 mg, 1.1 eq) in DMF (2.0 mL) was added DIEA (18 μL, 2.2 eq) and the resulting mixture was stirred for 16 h, diluted with EtOAc (50 mL), washed with H_2O (50 mL × 2), brine (50 mL), dried over $MgSO_4$ and concentrated. The crude product was purified by column chromatography, eluting with 1:1 EtOAc/DCM to give **4.49** (19 mg, 58%) as an orange gel:

$[\alpha]_D$ = -58.2 º (c = 0.5, MeOH)

^{1}H NMR (500 MHz, $CDCl_3$) δ 2.43 (1H, t, J = 2.4 Hz, $CHCCH_2O$), 3.01-3.14 (m, 2H, $CHCH_2$), 3.63-3.81 (19H, m), 4.20 (2H, d, J = 2.4 Hz, $CHCCH_2O$), 4.23 (1H, d, J = 1.2 Hz, CHOH), 4.47 (2H, s), 4.83 (1H, m, $CHCH_2$), 6.64 (1H, m, NH), 7.25 (1H, m), 7.30-7.37 (4H, m), 7.58 (2H, d, J = 8.3 Hz), 7.82 (2H, d, J = 8.5 Hz), 7.86-7.92 (4H, m).

^{13}C NMR (126 MHz, $CDCl_3$) δ 37.9, 53.0, 53.4, 58.3, 59.1, 69.0, 69.3, 70.1, 70.3, 70.4, 70.5, 70.5, 70.5, 70.6, 74.5, 79.6, 85.8, 88.0, 122.9, 123.0, 125.8, 126.8, 128.0, 128.6, 129.4, 132.5, 136.1, 137.1, 151.7, 154.1, 166.4, 174.1.

HRMS (ES): Calcd. for $C_{38}H_{43}N_3NaO_9$ (MNa^+) 708.2897, found 708.2913.

(*S*,*E*)-methyl 3-(4-((4-(4,7,10,13,16-pentaoxanonadeca-1,18-diynyl)phenyl)diazenyl) benzamido)-2-oxo-4-phenylbutanoate 4.7:

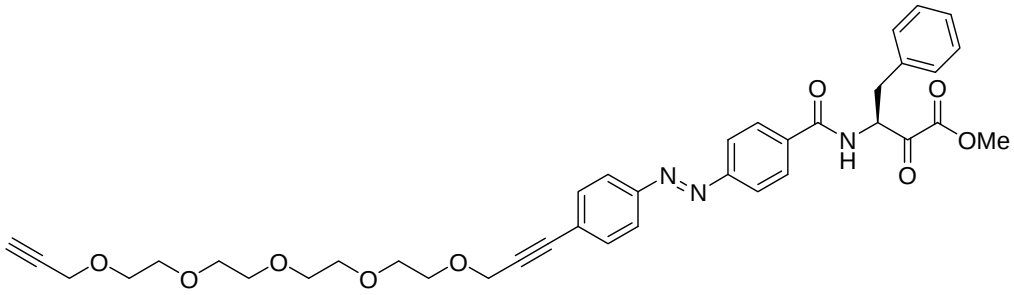

A solution of **4.49** (21 mg, 0.031 mmol) and Dess-Martin periodinane (26 mg, 2 eq) in DCM (1.0 mL) was stirred for 3 h, diluted with EtOAc (50 mL), washed with $Na_2S_2O_3$ (0.25 M in sat. $NaHCO_3$, 50 mL × 2), sat. $NaHCO_3$ (50 mL × 2), brine (50 mL), dried over $MgSO_4$ and concentrated. The crude material was purified by column chromatography, eluting with 1:1 EtOAc/DCM to give **4.7** (11 mg, 51%) as an orange gel:

$[\alpha]_D$ = -2.2 º (c = 1.0, MeOH)

^{1}H NMR (300 MHz, $CDCl_3$) δ 2.43 (1H, t, J = 2.4 Hz, C*H*CCH$_2$O), 3.24 (1H, dd, J = 14.1, 6.6 Hz, CHC*H*H), 3.40 (1H, dd, J = 14.1, 6.1 Hz, CHCH*H*), 3.64-3.82 (16H, m), 3.90 (3H, s, O*Me*), 4.20 (2H, d, J = 2.4 Hz, CHCCH$_2$O), 4.47 (2H, s), 5.64 (1H, q, J = 6.5 Hz, C*H*CH$_2$), 6.73 (1H, d, J = 6.9 Hz, N*H*), 7.17 (2H, m), 7.24-7.36 (3H, m), 7.59 (2H, d, J = 8.5 Hz), 7.81-8.00 (6H, m).

^{13}C NMR (75 MHz, $CDCl_3$) δ 36.8, 53.3, 57.0, 58.4, 59.2, 69.1, 69.3, 70.3, 70.4, 70.5, 70.5, 70.6, 70.6, 74.5, 79.6, 85.8, 88.0, 123.1, 123.1, 126.0, 127.5, 128.1, 128.8, 129.4, 132.6, 134.9, 135.0, 151.7, 154.4, 160.6, 166.3, 191.4.

HRMS (ES): Calcd. for $C_{38}H_{43}N_3NaO_{10}$ (M + H_2O + Na^+) 738.3003, found 738.3010.

9.5 Experimental for work described in chapter 5

Methanesulfonic acid 2-(2-(2-hydroxy-ethoxy)-ethoxy)-ethyl ester 5.20:[28, 29]

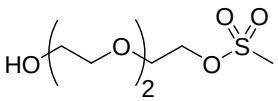

A solution of MsCl (650 mg, 6.0 mmol) in DCM (2.0 mL) was added dropwise to a solution of triethylene glycol **5.19** (750 mg, 5.0 mmol) and Ag_2O (1.3 g, 5.5 mmol) in DCM (10 mL). The resultant mixture was stirred for 68 h, filtered through Celite-545 and

concentrated. The crude material was purified by flash chromatography, eluting with 1:9 MeOH/EtOAc to give **5.20** (740 mg, 65%) as a pale yellow oil:

^{1}H NMR (500 MHz, $CDCl_3$) δ 3.07 (3H, s, *Me*), 3.60 (2H, m), 3.68 (4H, s), 3.73 (2H, m), 3.78 (2H, m), 4.38 (2H, m).

HRMS (ES): Calcd. for $C_7H_{17}O_6S$ (MH^+) 229.0746, found 229.0744.

2-(2-(2-Azido-ethoxy)-ethoxy)-ethanol 5.21:[28, 30]

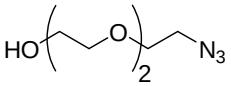

A mixture of **5.20** (400 mg, 1.8 mmol), NaN_3 (170 mg, 1.5 eq) and DMF (2.0 mL) was stirred for 2.5 h at 110 ºC, then cooled and concentrated. The crude material was purified by flash chromatography to give **5.21** (310 mg, qu) as a colourless oil:

^{1}H NMR (500 MHz, $CDCl_3$) δ 3.40 (2H, t, J = 4.9 Hz), 3.61 (2H, m), 3.65-3.70 (6H, m), 3.73 (2H, m).

5-(1,2)Dithiolan-3-yl-pentanoic acid 2-(2-(2-azido-ethoxy)-ethoxy)-ethyl ester 5.4:

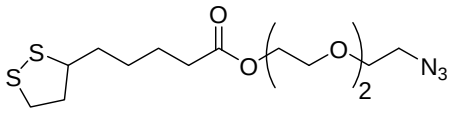

To a solution of **5.21** (100 mg, 0.57 mmol), lipoic acid **5.1** (120 mg, 1 eq) and HATU (220 mg, 1 eq) in DMF (5.0 mL) was added DIEA (200 μL, 2 eq). The resultant solution was stirred for 16 h then diluted with EtOAc (50 mL), washed with brine (50 mL × 2), dried over $MgSO_4$ and concentrated. The crude material was purified by flash chromatography, eluting with 1:19 EtOAc/DCM to give **5.4** (79 mg, 38%) as a yellow oil:

^{1}H NMR (500 MHz, $CDCl_3$) δ 1.47 (2H, m), 1.68 (4H, m), 1.91 (1H, m), 2.35 (2H, t, J = 7.4 Hz), 2.46 (1H, m), 3.14 (2H, m), 3.39 (2H, t, J = 4.8 Hz), 3.57 (1H, m), 3.65-3.73 (8H, m), 4.23 (2H, m).

^{13}C NMR (75 MHz, $CDCl_3$) δ 24.3, 28.4, 33.6, 34.3, 38.2, 39.9, 50.4, 56.0, 63.1, 68.9, 69.8, 70.3, 70.4, 173.0 (*C*OO).

HRMS (ES): Calcd. for $C_{14}H_{25}N_3NaO_4S_2$ (MNa^+) 386.1184, found 386.1166.

Methanesulfonic acid 2-(2-(2-(2-(2-(2-hydroxy-ethoxy)-ethoxy)-ethoxy)-ethoxy)-ethoxy)-ethyl ester 5.23:[29]

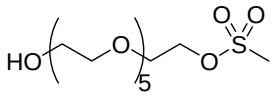

A solution of hexaethylene glycol **5.22** (11 g, 39 mmol) in THF was cooled to 0 ºC then NaH (60% in mineral oil, 520 mg, 13 mmol) was added. The mixture was stirred for 30 min, then MsCl (1.0 mL, 1.5 g, 13 mmol) was added dropwise. The resulting mixture was stirred for 16 h, warming to r.t., then concentrated. The crude material was purified by flash chromatography, eluting with 1:9 MeOH/EtOAc to give **5.23** (2.1 g, 45%) as a colourless oil:

^{1}H NMR (300 MHz, ($CDCl_3$) δ 2.84 (1H, t, J = 6.1 Hz, O*H*), 3.10 (3H, s), 3.58-3.80 (22H, m), 4.39 (2H, m).

2-(2-(2-(2-(2-(2-Azido-ethoxy)-ethoxy)-ethoxy)-ethoxy)-ethoxy)-ethanol 5.24:[31]

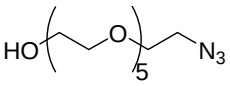

A mixture of **5.23** (1.0 g, 2.8 mmol), NaN_3 (270 mg, 1.5 eq) and DMF (3.0 mL) was stirred for 2 h 30 min at 110 ºC, cooled then concentrated. The crude product was purified by flash chromatography, eluting with 1:9 MeOH/EtOAc to give **5.24** (690 mg, 81%) as a yellow oil:

^{1}H NMR (500 MHz, ($CDCl_3$) δ 2.87 (1 H, t, J = 6.2 Hz, O*H*), 3.39 (2H, t, J = 5.1 Hz), 3.61 (2H, m), 3.64-3.69 (18H, m), 3.73 (2H, m).

5-(1,2)Dithiolan-3-yl-pentanoic acid 2-(2-(2-(2-(2-(2-azido-ethoxy)-ethoxy)-ethoxy)-ethoxy)-ethoxy)-ethyl ester 5.5:

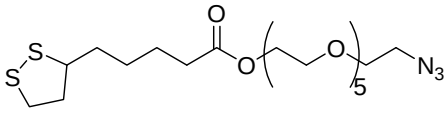

A solution of alcohol **5.24** (150 mg, 0.48 mmol), lipoic acid **5.1** (100 mg, 1 eq), EDCI (100 mg, 1.1 eq) and DMAP (20 mg, 0.34 eq) in DCM (5.0 mL) was stirred for 16 h, diluted with DCM (50 mL), washed with H_2O (50 mL), brine (50 mL), dried over $MgSO_4$ and

concentrated. The crude product was purified by flash chromatography, eluting with EtOAc to give **5.5** (180 mg, 77%) as a yellow oil:

^{1}H NMR (500 MHz, ($CDCl_3$) δ 1.47 (2H, m), 1.68 (4H, m), 1.91 (1H, m), 2.35 (2H, t, J = 7.4 Hz), 2.46 (1H, m), 3.12 (1H, m), 3.19 (1H, m), 3.39 (2H, t, J = 5.0 Hz), 3.57 (1H, m), 3.64-3.72 (20H, m), 4.23 (2H, m).

^{13}C NMR (75 MHz, $CDCl_3$) δ 24.2, 28.3, 33.5, 34.2, 38.1, 39.8, 50.2, 55.9, 63.0, 68.7, 69.6, 70.1, 70.1, 70.2, 70.2, 70.2, 70.2, 172.9.

HRMS (ES): Calcd. for $C_{20}H_{37}N_3NaO_7S_2$ (MNa^+) 518.1971, found 518.1983.

FTIR: 1734 (C=O), 2105 (N_3) cm^{-1}

5-(1,2)Dithiolan-3-yl-pentanoic acid 2-(2-hydroxy-ethoxy)-ethyl ester 5.6:

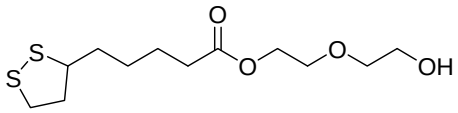

To a solution of EDCI (92 mg, 0.48 mmol), diethylene glycol (510 mg, 10 eq) and DMAP (20 mg, 0.34 eq) in DCM (5.0 mL) was added a solution of lipoic acid **5.1** (100 mg, 1 eq) in DCM (1.0 mL). The resulting mixture was stirred for 16 h then concentrated. The crude product was purified by flash chromatography, eluting with 1:19 MeOH/DCM to give **5.6** (110 mg, 78%) as a yellow oil:

^{1}H NMR (500 MHz, $CDCl_3$) δ 1.48 (2H, m), 1.60-1.76 (4H, m), 1.91 (1H, m), 2.05 (1H, s, O*H*), 2.36 (2H, t, J = 7.5 Hz), 2.46 (1H, m), 3.12 (1H, m), 3.18 (1H, m), 3.53-3.65 (3H, m), 3.68-3.77 (4H, m), 4.25 (2H, t, J = 4.8 Hz).

^{13}C NMR (75 MHz, $(CD_3)_2CO$) δ 24.6, 28.7, 34.0, 34.6, 38.5, 40.3, 56.4, 61.7, 63.4, 69.2, 72.4, 173.6.

HRMS (ES): Calcd. for $C_{12}H_{23}O_4S_2$ (MH^+) 295.1038, found 295.1043.

11-Acetylsulfanyl-undecanoic acid 5.25:[29, 32]

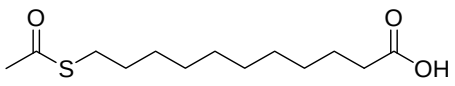

A solution of 11-mercaptoundecanoic acid **5.2** (1.0 g, 4.6 mmol) in DCM (12 mL) and AcOH (12 mL) was cooled to 0 ºC, AcCl (7.0 mL) was added and the resulting solution was stirred for 5 min, warmed to r.t. and stirred for 2 h, then washed with cold HCl (0 ºC,

0.1 M, 50 mL × 2), brine (50 mL) and concentrated. The crude product was purified by flash chromatography, eluting with 1:4 EtOAc/pet ether to give **5.25** (760 mg, 63%) as a white solid:

mp: 47-52 ºC (lit.[32] 49-50 ºC)

^{1}H NMR (500 MHz, $CDCl_3$) δ 1.24-1.39 (12H, m), 1.52-1.67 (4H, m), 2.31-2.37 (5H, m), 2.86 (2H, t, J = 7.4 Hz).

HRMS (ES): Calcd. for $C_{13}H_{25}O_3S$ (MH^+) 261.1524, found 261.1519.

(2-(2-(2-Hydroxy-ethoxy)-ethoxy)-ethoxy)-acetic acid tert-butyl ester 5.27:[33]

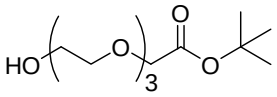

A solution of triethylene glycol **5.19** (10 g, 68 mmol) in THF (20 mL) was cooled to 0 ºC, NaH (60% in mineral oil, 540 mg, 14 mmol) was added and the resulting mixture was stirred for 30 min. *tert*-Butyl bromoacetate **5.26** (2.7 g, 14 mmol) was added dropwise over 10 min, the mixture was stirred for 16 h, warming to r.t., then concentrated. The crude product was purified by flash chromatography, eluting with EtOAc to give **5.27** (1.4 g, 38%) as a colourless oil:

^{1}H NMR (500 MHz, $CDCl_3$) δ 1.48 (9H, s, C(*Me*)$_3$), 3.62 (2H, m), 3.66-3.77 (10H, m), 4.03 (2H, s, COC*H*$_2$).

HRMS (ES): Calcd. for $C_{12}H_{24}NaO_6$ (MNa^+) 287.1471, found 287.1463.

11-Acetylsulfanyl-undecanoic acid 2-(2-(2-tert-butoxycarbonylmethoxy-ethoxy)-ethoxy)-ethyl ester 5.28:

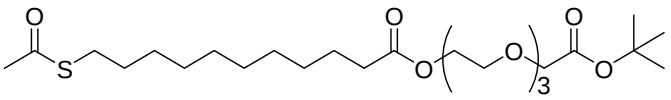

A solution of alcohol **5.27** (150 mg, 0.58 mmol), carboxylic acid **5.25** (150 mg, 1 eq), EDCI (110 mg, 1 eq) and DMAP (14 mg, 0.2 eq) in DCM (5.0 mL) was stirred for 16 h, diluted with EtOAc (50 mL), washed with brine (50 mL × 2), dried over $MgSO_4$ and concentrated. The crude material was purified by flash chromatography, eluting with a gradient of 1:19 to 1:9 EtOAc/DCM to give **5.28** (180 mg, 63%) as a colourless oil:

^{1}H NMR (500 MHz, $CDCl_3$) δ 1.23-1.38 (12H, m), 1.48 (9H, s), 1.52-1.65 (4H, m), 2.30-2.35 (5H, m), 2.86 (2H, t, J = 7.3 Hz), 3.66-3.73 (10H, m), 4.02 (2H, s), 4.22 (2H, t, J = 4.9 Hz).

^{13}C NMR (75 MHz, $CDCl_3$) δ 25.0, 28.2, 28.9, 29.2, 29.2, 29.2, 29.3, 29.4, 29.5, 29.6, 30.7, 34.3, 63.5, 69.1, 69.3, 70.6, 70.7, 70.7, 70.8, 81.6, 169.7, 173.9, 196.1.

HRMS (ES): Calcd. for $C_{25}H_{46}NaO_8S$ (MH^+) 529.2811, found 529.2835.

11-Acetylsulfanyl-undecanoic acid 2-(2-(2-carboxymethoxy-ethoxy)-ethoxy)-ethyl ester 5.7:

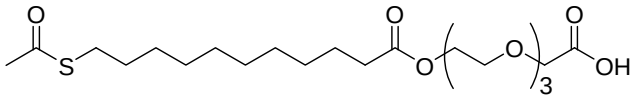

To a solution of **5.28** (50 mg, 0.099 mmol) in DCM (4.0 mL) was added TFA (1.0 mL). The reaction mixture was stirred for 1 h then concentrated. The crude material was purified by flash chromatography, eluting with 30:70:1 EtOAc/DCM/AcOH to give **5.7** (33 mg, 74%) as a colourless oil:

^{1}H NMR (500 MHz, $CDCl_3$) δ 1.24-1.38 (12H, m), 1.52-1.65 (4H, m), 2.31-2.35 (5H, m), 2.86 (2H, t, J = 7.4 Hz), 3.65-3.73 (8H, m), 3.74-3.78 (2H, m), 4.18 (2H, s), 4.24 (2H, t, J = 4.8 Hz).

^{13}C NMR (75 MHz, $CDCl_3$) δ 25.0, 28.9, 29.2, 29.2, 29.3, 29.3, 29.5, 29.5, 29.6, 30.8, 34.3, 63.4, 68.9, 69.4, 70.4, 70.5, 70.8, 71.5, 172.6, 174.0, 196.3.

HRMS (ES): Calcd. for $C_{21}H_{39}O_8S$ (MH^+) 451.2365, found 451.2383.

11-Acetylsulfanyl-undecanoic acid 2-(2-(2-(2-(2-azido-ethoxy)-ethoxy)-ethoxy)-ethoxy)-ethyl ester 5.8:

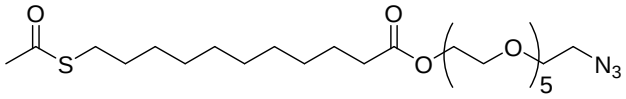

A solution of alcohol **5.24** (200 mg, 0.65 mmol), carboxylic acid **5.25** (170 mg, 1 eq), EDCI (130 mg, 1 eq) and DMAP (27 mg, 0.34 eq) in DCM (5.0 mL) was stirred for 16 h, diluted with DCM (50 mL), washed with H_2O (50 mL), brine (50 mL), dried over $MgSO_4$ and concentrated. The crude product was purified by flash chromatography, eluting with 1:9 EtOAc/pet ether to give **5.8** (100 mg, 29%) as a yellow oil:

^{1}H NMR (500 MHz, ($CDCl_3$) δ 1.24-1.38 (12H, m), 1.52-1.65 (4H, m), 2.30-2.34 (5H, m), 2.86 (2H, t, J = 7.3 Hz), 3.39 (2H, t, J = 5.0 Hz), 3.63-3.71 (20H, m), 4.22 (2H, t, J = 4.9 Hz).

^{13}C NMR (75 MHz, ($CDCl_3$) δ 25.0, 28.9, 29.2, 29.2, 29.2, 29.3, 29.4, 29.5, 29.6, 30.7, 34.3, 50.8, 63.4, 69.3, 70.1, 70.6, 70.7, 70.7, 70.8, 70.8, 173.9, 196.1.

HRMS (ES): Calcd. for $C_{25}H_{48}N_3O_8S$ (MH^+) 550.3162, found 550.3175.

FTIR: 1689 (C=O), 1734 (C=O), 2106 (N_3) cm^{-1}

11-(10-(2-(2-(2-(2-(2-(2-Azido-ethoxy)-ethoxy)-ethoxy)-ethoxy)-ethoxy)-ethoxycarbonyl)-decyldisulfanyl)-undecanoic acid 2-(2-(2-(2-2-(2-azido-ethoxy)-ethoxy)-ethoxy)-ethoxy)-ethyl ester 5.9:

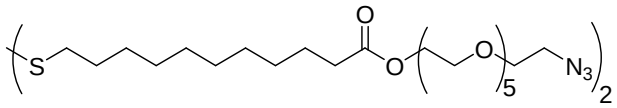

A solution of **5.8** (25 mg, 0.045 mmol) and hydrazine acetate (8.0 mg, 2 eq) in DMF (1.0 mL) was stirred for 2 d, diluted with DCM (50 mL), washed with H_2O (50 mL × 2) and concentrated. The crude material was purified by flash chromatography, eluting with 1:9 MeOH/EtOAc to give **5.9** (23 mg, qu) as a colourless oil:

^{1}H NMR (500 MHz, ($CDCl_3$) δ 1.24-1.41 (12H, m), 1.58-1.70 (4H, m), 2.32 (2H, t, J = 7.6 Hz), 2.68 (2H, t, J = 7.3 Hz), 3.39 (2H, t, J = 5.0 Hz), 3.63-3.72 (20H, m), 4.22 (2H, t, J = 4.9 Hz).

^{13}C NMR (75 MHz, ($CDCl_3$) δ 24.8, 28.4, 29.1, 29.1, 29.2, 29.3, 29.4, 34.1, 39.1, 50.6, 63.3, 69.1, 70.0, 70.5, 70.5, 70.6, 70.6, 70.6, 173.7.

HRMS (ES): Calcd. for $C_{46}H_{88}N_6NaO_{14}S_2$ (MNa^+) 1035.5698, found 1035.5697.

FTIR: 1734 (C=O), 2106 (N_3) cm^{-1}

11-Acetylsulfanyl-undecanoic acid 2-(2-hydroxy-ethoxy)-ethyl ester 5.10:

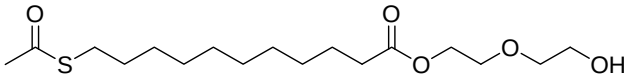

To a solution of diethylene glycol (410 mg, 10 eq), EDCI (74 mg, 1 eq) and DMAP (10 mg, 0.2 eq) in DCM (4.0 mL) was added a solution of **5.25** (100 mg, 0.38 mmol) in DCM (1.0 mL) and the resulting solution was stirred for 16 h, diluted with EtOAc (50 mL)

washed with brine (50 mL × 2), dried over $MgSO_4$ and concentrated. The crude product was purified by flash chromatography, eluting with 1:4 EtOAc/DCM to give **5.10** (100 mg, 76%) as a white solid:

mp: 24-26 ºC

^{1}H NMR (500 MHz, ($CDCl_3$) δ 1.23-1.38 (12H, m), 1.52-1.66 (4H, m), 2.31-2.36 (5H, m), 2.86 (2H, t, J = 7.4 Hz), 3.61 (2H, t, J = 4.5 Hz), 3.71 (2H, t, J = 4.8 Hz), 3.74 (2H, t, J = 4.5 Hz), 4.25 (2H, t, J = 4.8 Hz).

^{13}C NMR (75 MHz, $CDCl_3$) δ 25.0, 28.8, 29.1, 29.1, 29.2, 29.3, 29.4, 29.4, 29.5, 30.7, 34.3, 61.8, 63.3, 69.2, 72.4, 173.9, 196.1.

HRMS (ES): Calcd. for $C_{17}H_{33}O_5S$ (MH^+) 349.2048, found 349.2048.

11-(10-(2-(2-Hydroxy-ethoxy)-ethoxycarbonyl)-decyldisulfanyl)-undecanoic acid 2-(2-hydroxy-ethoxy)-ethyl ester 5.11:

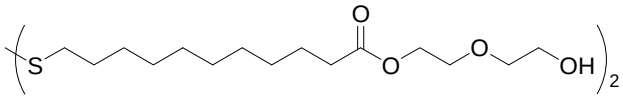

A solution of **5.10** (15 mg, 0.043 mmol) and hydrazine acetate (5.0 mg, 1 eq) in DMF (1.0 mL) was stirred for 2 d, diluted with DCM (50 mL), washed with H_2O (50 mL × 2) and concentrated. The crude material was purified by flash chromatography, eluting with EtOAc to give **5.11** (7.0 mg, 53%) as a white solid:

mp: 54-56 ºC

^{1}H NMR (500 MHz, ($CDCl_3$) δ 1.23-1.42 (12H, m), 1.64 (4H, m), 2.23-2.40 (3H, m), 2.68 (2H, t, J = 7.4 Hz), 3.61 (2H, t, J = 4.6 Hz), 3.71 (2H, t, J = 4.7 Hz), 3.74 (2H, t, J = 4.6 Hz), 4.25 (2H, t, J = 4.7 Hz).

^{13}C NMR (75 MHz, $CDCl_3$) δ 25.0, 28.6, 29.2, 29.3, 29.3, 29.5, 29.5, 34.3, 39.2, 61.8, 63.3, 69.3, 72.4, 173.9.

HRMS (ES): Calcd. for $C_{30}H_{59}O_8S_2$ (MH^+) 611.3651, found 611.3645.

(*E*)-4-(4-((2,2,2-Trifluoro-acetylamino)-methyl)-phenylazo)-benzoic acid ethyl ester 5.29:

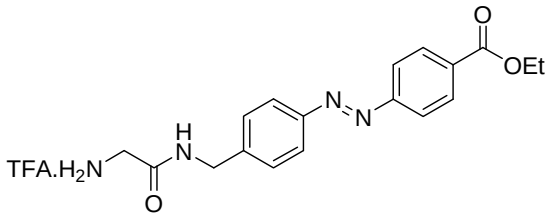

To a solution of **2.41** (12 mg, 0.027 mmol) in DCM (4.0 mL) was added TFA (1.0 mL). The reaction mixture was stirred for 1 h then concentrated to give **5.29** (12 mg, 98%) as an orange solid:

mp: 206-210 ºC

^{1}H NMR (500 MHz, (CD_3OD)) δ 1.41 (3H, t, J = 7.2 Hz, CH_2*Me*), 3.77 (2H, s), 4.40 (2H, q, J = 7.2 Hz, C*H*$_2$Me), 4.54 (2H, s), 7.52 (2H, d, J = 8.3Hz), 7.3 (2H, d, J = 8.3Hz), 7.96 (2H, d, J = 8.3Hz), 8.18 (2H, d, J = 8.3Hz).

^{13}C NMR (75 MHz, (CD_3OD)) δ 14.6 (CH_2*Me*), 41.5, 43.8, 62.5 (C*H*$_2$Me), 123.7, 124.4, 129.5, 131.6, 133.5, 143.7, 153.2, 167.3.

HRMS (ES): Calcd. for $C_{18}H_{21}N_4O_3$ (MH^+) 341.1614, found 341.1609.

4-(4-((5-(1,2)Dithiolan-3-yl-pentanoylamino)-methyl)-phenylazo)-benzoic acid ethyl ester 5.12:

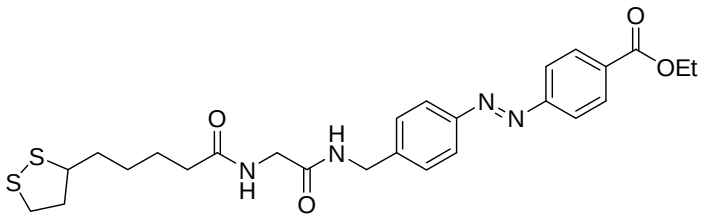

To a solution of **5.29** (12 mg, 0.026 mmol), lipoic acid **5.1** (6.0 mg, 1 eq), EDCI (6.0 mg, 1 eq) and HOBt (4.0 mg, 1 eq) in DMF (2.0 mL) was added DIEA (10 μL, 7.4 mg, 2 eq) and the resulting mixture was stirred for 16 h, diluted with EtOAc (50 mL), washed with H_2O (50 mL), brine (50 mL), dried over $MgSO_4$ and concentrated. The crude material was purified by column chromatography, eluting with 1:19 MeOH/DCM to give **5.12** (5.0 mg, 36%) as an orange solid:

mp: 163-167 ºC

^{1}H NMR (500 MHz, $CDCl_3$) δ 1.36-1.52 (5H, m), 1.57-1.73 (4H, m), 1.87 (1H, m), 2.26 (2H, t), 2.42 (1H, m), 3.05-3.19 (2H, m), 3.53 (1H, m), 4.00 (2H, d, J = 5.2 Hz), 4.42 (2H,

q, J = 7.1 Hz, CH_2Me), 4.53 (2H, d, J = 5.9 Hz), 6.40 (1H, s), 6.81 (1H, s), 7.42 (2H, d, J = 8.3 Hz), 7.88-7.97 (4H, m), 8.19 (2H, d, J = 7.9 Hz).

^{13}C NMR (75 MHz, $CDCl_3$) δ 14.5, 25.4, 29.0, 34.7, 36.1, 38.6, 40.4, 43.3, 43.6, 56.5, 61.4, 122.8, 123.6, 128.5, 130.7, 132.4, 141.7, 152.0, 155.1, 166.2, 169.2, 173.7.

HRMS (ES): Calcd. for $C_{26}H_{33}N_4O_4S_2$ (MH^+) 529.1943, found 529.1924.

(*E*)-4-(4-((2-(2-(2-(2-(2-(11-Acetylsulfanyl-undecanoyloxy)-ethoxy)-ethoxy)-ethoxy)-acetylamino)-acetylamino)-methyl)-phenylazo)-benzoic acid ethyl ester 5.13:

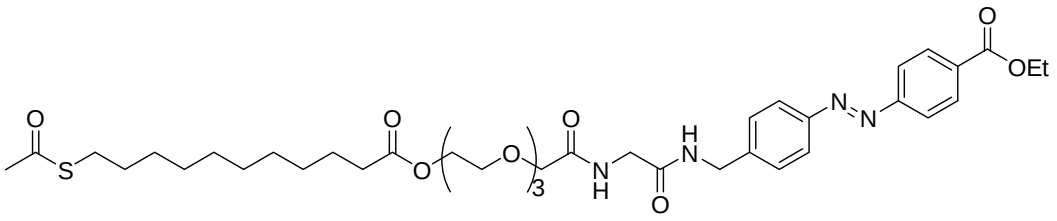

To a solution of amine **5.29** (10 mg, 0.022 mmol), carboxylic acid **5.7** (10 mg, 1 eq), EDCI (5.0 mg, 1 eq) and HOBt (3.0 mg, 1 eq) in DCM (2.0 mL) was added DIEA (12 μL, 8.9 mg, 3 eq) and the resulting mixture was stirred for 16 h, diluted with EtOAc (50 mL), washed with brine (50 mL × 2) and concentrated. The crude material was purified by column chromatography, eluting with 1:19 MeOH/DCM to give **5.13** (9.0 mg, 53%) as an orange gel:

^{1}H NMR (500 MHz, $CDCl_3$) δ 1.21-1.37 (12H, m), 1.43 (3H, t, J = 7.0 Hz), 1.50-1.63 (4H, m), 2.27-2.33 (5H, m), 2.85 (2H, t, J = 7.3 Hz), 3.61-3.71 (10H, m), 4.02-4.07 (4H, m), 4.21 (2H, t, J = 4.8 Hz), 4.42 (2H, q, J = 7.1 Hz), 4.53 (2H, d, J = 5.9 Hz), 6.99 (1H, t, J = 5.7 Hz), 7.43 (2H, d, J = 8.2 Hz), 7.80 (1H, t, J = 5.8 Hz), 7.88-7.95 (4H, m), 8.19 (2H, d, J = 8.3 Hz).

^{13}C NMR (75 MHz, $CDCl_3$) δ 14.4, 25.0, 28.9, 29.2, 29.2, 29.2, 29.3, 29.5, 29.5, 29.6, 30.8, 34.3, 43.2, 61.4, 63.3, 69.3, 70.2, 70.4, 70.4, 70.6, 71.2, 122.7, 123.5, 128.5, 130.7, 132.3, 142.0, 151.9, 155.1, 166.1, 169.2, 171.3, 173.9, 196.2.

HRMS (ES): Calcd. for $C_{39}H_{57}N_4O_{10}S$ (MH^+) 773.3795, found 773.3820.

(*E*)-4-(4-((2-Amino-acetylamino)-methyl)-phenylazo)-*N*-(1-benzyl-3,3,3-trifluoro-2-hydroxy-propyl)-benzamide trifluoroacetate 5.30:

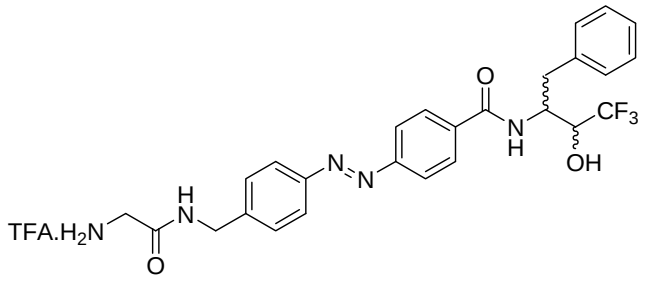

To a solution of **4.16** (10 mg, 0.016 mmol) in DCM (4.0 mL) was added TFA (1.0 mL). The reaction mixture was stirred for 80 min then concentrated. The crude material was purified by column chromatography, eluting with 1:3 EtOH–DCM to give **5.30** (6.0 mg, 60%), as an orange solid:

mp: 109–112 ºC

^{1}H NMR (500 MHz, CD_3OD) δ 3.06 (2H, d, J = 7.8 Hz), 3.76 (2H, s), 4.05 (1H, m, C*H*CH_2), 4.54 (2H, s), 4.73 (1H, t, J = 7.8 Hz, C*H*CF_3), 7.19-7.36 (5H, m), 7.51 (2H, d, J = 7.3 Hz), 7.83-7.98 (6H, m).

^{13}C NMR (75 MHz, CD_3OD) δ 37.6, 40.4, 42.7, 50.7, 69.0 (q, J = 30.9 Hz), 122.6, 123.1, 126.7, 128.3, 128.4, 128.5, 129.3, 136.7, 137.9, 142.4, 152.0, 154.4, 166.2, 168.0.

^{19}F NMR (282 MHz, (CD_3OD)) δ -75.98 (d, J = 7.2 Hz, CHC*F*$_3$), -74.68 (s, COC*F*$_3$).

HRMS (ES): Calcd. for $C_{26}H_{27}F_3N_5O_3$ ($M - CF_3COOH + H^+$) 514.2066, found 514.2058.

(*E*)-11-Acetylsulfanyl-undecanoic acid 2-(2-(2-((((4-[4-(1-benzyl-3,3,3-trifluoro-2-hydroxy-propylcarbamoyl)-phenylazo)-benzylcarbamoyl)-methyl)-carbamoyl)-methoxy)-ethoxy)-ethoxy)-ethyl ester 5.31:

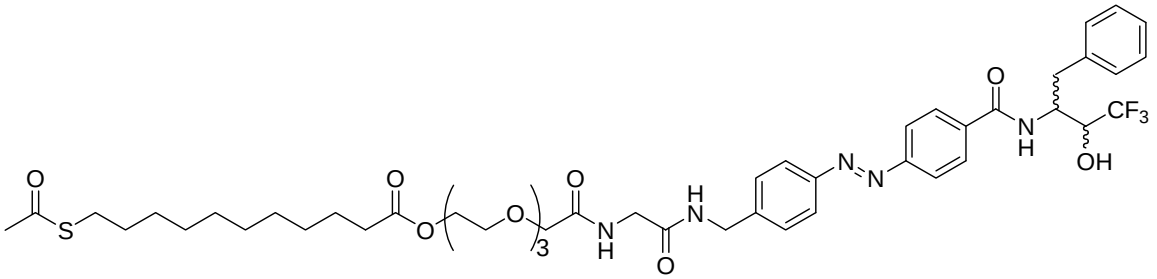

To a solution of amine **5.30** (10 mg, 0.016 mmol), carboxylic acid **5.7** (7.0 mg, 1 eq), EDCI (4.0 mg, 1 eq) and HOAt (3.0 mg, 1 eq) in DMF (2.0 mL) was added DIEA (6.0 μL, 4.5 mg, 2 eq) and the resulting mixture was stirred for 16 h, diluted with EtOAc (50 mL),

washed with H_2O (50 mL × 2), brine (50 mL), dried over $MgSO_4$ and concentrated. The crude product was purified by column chromatography, eluting with 1:19 MeOH/EtOAc to give **5.31** (15 mg, 99%) as an orange gel:

^{1}H NMR (500 MHz, $CDCl_3$) δ 1.19-1.34 (12H, m), 1.48-1.60 (4H, m), 2.25-2.31 (5H, m), 2.82 (2H, t, J = 7.3 Hz), 3.06 (1H, dd, J = 13.6, 8.5 Hz), 3.18 (1H, dd, J = 13.5, 7.1 Hz), 3.58-3.69 (10H, m), 4.00-4.09 (5H, m), 4.16-4.20 (2H, t, J = 4.9 Hz), 4.43 (2H, d, J = 5.5 Hz), 4.59 (1H, m), 7.18-7.39 (8H, m), 7.69-7.75 (5H, m), 7.84 (1H, m).

^{13}C NMR (75 MHz, $CDCl_3$) δ 124.9, 28.8, 29.1, 29.2, 29.2, 29.3, 29.4, 29.4, 29.5, 30.7, 34.2, 37.5, 42.9, 43.1, 51.6, 63.2, 69.2, 70.2, 70.4, 70.5, 71.1, 122.9, 123.4, 127.0, 128.1, 128.2, 128.8, 129.4, 135.8, 137.2, 141.6, 151.7, 154.1, 167.7, 169.5, 171.5, 174.0, 196.4.

HRMS (ES): Calcd. for $C_{47}H_{63}F_3N_5O_{10}S$ (MH^+) 946.4248, found 946.4231.

(*E*)-11-Acetylsulfanyl-undecanoic acid 2-(2-(2-((((4-(4-(1-benzyl-3,3,3-trifluoro-2-oxo-propylcarbamoyl)-phenylazo)-benzylcarbamoyl)-methyl)-carbamoyl)-methoxy)-ethoxy)-ethoxy)-ethyl ester 5.14:

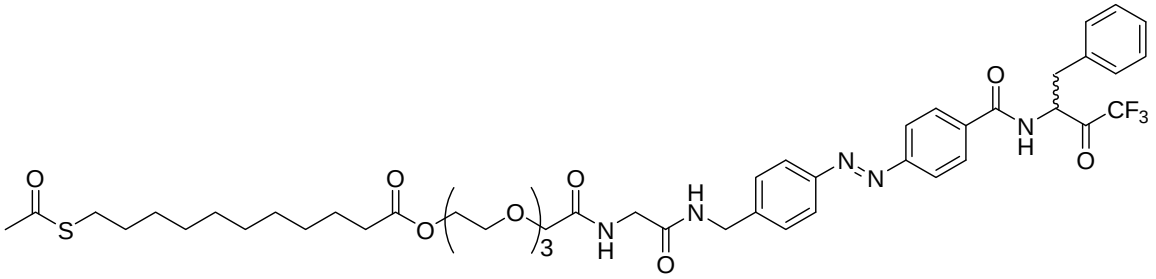

A solution of **5.31** (13 mg, 0.014 mmol) and Dess-Martin periodinane (22 mg, 3.7 eq) in DCM (1.0 mL) was stirred for 3 h, diluted with EtOAc (50 mL), washed with $Na_2S_2O_3$ (0.25 M in sat. $NaHCO_3$, 50 mL), sat. $NaHCO_3$ (50 mL × 2), brine (50 mL), dried over $MgSO_4$ and concentrated. The crude material was purified by column chromatography, eluting with 1:19 acetone/EtOAc to give **5.14** (5.0 mg, 38%) as an orange gel:

^{1}H NMR (500 MHz, $((CD_3)_2CO)$ δ 1.25-1.38 (12H, m), 1.50-1.61 (4H, m), 2.27-2.31 (5H, m), 3.26 (1H, dd, J = 13.9, 12.1 Hz), 3.38 (1H, dd, J = 14.2, 3.1 Hz), 3.58-3.72 (10H, m), 3.97-4.01 (4H, m), 4.17 (2H, t, J = 4.8 Hz), 4.40 (1H, m), 4.53 (2H, d, J = 6.0 Hz), 6.79 (1H, s), 7.14-7.21 (2H, m), 7.27 (2H, t, J = 7.6 Hz), 7.34 (2H, d, J = 7.1 Hz), 7.53 (2H, d, J = 8.5 Hz), 7.78-7.85 (2H, m), 7.88-7.92 (6H, m), 8.22 (1H, d, J = 8.2 Hz).

HRMS (ES): Calcd. for $C_{47}H_{63}F_3N_5O_{11}S$ (MH_3O^+) 962.4197, found 962.4221.

(*E*)-11-Acetylsulfanyl-undecanoic acid 2-(2-(2-(2-(2-(4-(4-(4-(1-benzyl-3,3,3-trifluoro-2-oxo-propylcarbamoyl)-phenylazo)-phenyl)-(1,2,3)triazol-1-yl)-ethoxy)-ethoxy)-ethoxy)-ethoxy)-ethyl ester 5.15:

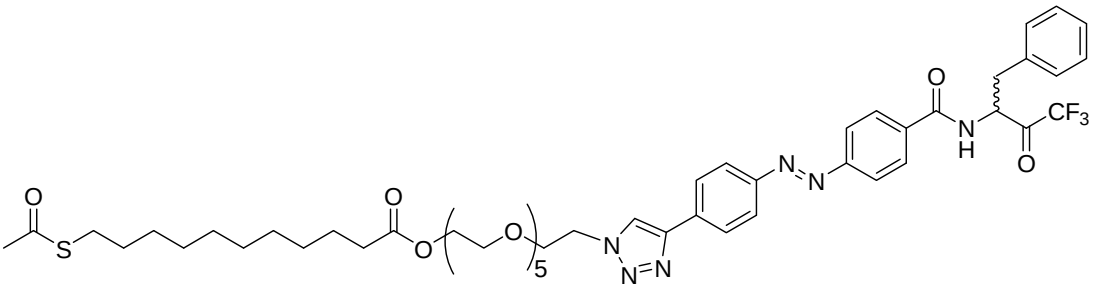

To a solution of alkyne **4.3** (17 mg, 0.038 mmol) and azide **5.8** (21 mg, 1 eq) in EtOH (9.0 mL) and H_2O (8.0 mL) was added sodium ascorbate (0.45 mg, 0.060 eq) then $CuSO_4$ (0.070 mg, 0.012 eq) and the resulting mixture was stirred for 16 h, diluted with EtOAc (50 mL), washed with H_2O (50 mL × 2), brine (50 mL), dried over $MgSO_4$ and concentrated. The crude material was purified by column chromatography, eluting with EtOAc to give **5.15** (10 mg, 26%) as an orange gel:

^{1}H NMR (500 MHz, ($(CD_3)_2CO$) δ 1.24-1.38 (12H, m), 1.50-1.62 (4H, m), 2.26-2.31 (5H, m), 2.85 (2H, t, J = 7.5 Hz), 3.27 (1H, dd, J = 14.1, 12.1 Hz), 3.40 (1H, dd, J = 14.2, 2.9 Hz), 3.51-3.68 (18H, m), 3.99 (2H, t, J = 5.1 Hz), 4.15 (2H, t, J = 4.9 Hz), 4.40 (1H, m), 4.68 (2H, t, J = 5.1 Hz), 7.16 (1H, s), 7.20 (1 H, t, J = 7.3 Hz), 7.29 (2H, t, J = 7.6 Hz), 7.35 (2H, d, J = 7.3 Hz), 7.92 (2H, d, J = 8.7 Hz), 7.96 (2H, d, J = 8.7 Hz), 8.05 (2H, d, J = 8.6 Hz), 8.16 (2H, d, J = 8.6 Hz), 8.21 (1H, d, J = 8.1 Hz), 8.57 (1H, s).

^{13}C NMR (75 MHz, $(CD_3)_2CO$) δ 25.6, 29.4, 29.4, 29.7, 29.8, 30.0, 30.1, 30.1, 30.3, 30.4, 30.6, 33.7, 33.7, 34.5, 51.0, 58.6, 63.9, 69.7, 70.0, 71.0, 71.1, 71.2, 71.2, 71.2, 71.2, 71.2, 123.3, 124.5, 127.0, 127.2, 129.2, 129.5, 130.1, 135.9, 136.7, 139.5, 146.7, 152.6, 155.2, 169.7, 173.7, 195.5.

HRMS (ES): Calcd. for $C_{50}H_{68}F_3N_6O_{11}S$ (MNa^+) 1017.4619, found 1017.4643.

1-Nitro-4-prop-2-ynyloxy-benzene 5.34:[34, 35]

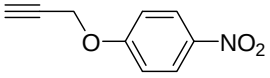

A solution of 4-nitrophenol **5.33** (5.0 g, 0.036 mol), propargyl bromide (5.2 g, 1.2 eq) and K_2CO_3 (6.0 g, 1.2 eq) in DMF (7.0 mL) was stirred for 16 h, diluted with EtOAc (50 mL),

washed with H_2O (50 mL), brine (50 mL), dried over $MgSO_4$ and concentrated. The crude material was purified by recrystallisation twice from 1:4 EtOAc/pet ether to give **5.34** (800 mg, 13%) as white crystals:

mp: 108-110 ºC

^{1}H NMR (500 MHz, $CDCl_3$) δ 2.59 (1H, t, J = 2.5 Hz, CH_2CCH), 4.80 (2H, d, J = 2.5 Hz, CH_2), 7.06 (2H, d, J = 9.3 Hz), 8.23 (2H, d, J = 9.3 Hz).

^{13}C NMR (75 MHz, $CDCl_3$) δ 56.4, 76.9, 77.2, 115.1, 125.9, 142.2, 162.4.

HRMS (ES): Calcd. for $C_9H_8NO_3$ (MH^+) 178.0504, found 178.0506.

1-Benzyl-4-(4-nitro-phenoxymethyl)-1H-(1,2,3)triazole 5.35:

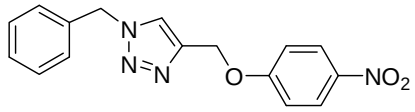

Method A:

To a solution of **5.32** (130 mg, 1.0 mmol) and **5.34** (180 mg, 1 eq) in ^{t}BuOH (1.0 mL) and H_2O (1.0 mL) was added sodium ascorbate (20 mg, 0.1 eq) then $CuSO_4$ (1.0 M in H_2O, 50 µL, 0.05 eq) and the resulting mixture was stirred for 75 min at 60 ºC, then H_2O (10 mL) and NH_3 (10% in H_2O, 1.0 mL) were added. The mixture was stirred for 5 min at 60 ºC, cooled and filtered to obtain a yellow precipitate. The precipitate was dissolved in DCM (20 mL), filtered and concentrated. The crude material was purified by flash chromatography, eluting with a gradient of DCM to 1:9 EtOAc/DCM to give **5.35** (210 mg, 69%) as a white solid:

mp: 100-103 ºC

^{1}H NMR (500 MHz, $CDCl_3$) δ 5.27 (2H, s), 5.55 (2H, s), 7.05 (2H, d, J = 9.2 Hz), 7.28 (2H, m), 7.36-7.41 (3H, m), 7.59 (1H, s, NC*H*), 8.17 (2H, d, J = 9.2 Hz).

^{13}C NMR (75 MHz, $CDCl_3$) δ 54.2, 62.3, 114.8, 123.2, 125.8, 128.0, 128.8, 129.1, 134.3, 141.6, 142.9, 163.1.

HRMS (ES): Calcd. for $C_{16}H_{15}N_4O_3$ (MH^+) 311.1144, found 311.1144.

Method B:

To a solution of **5.32** (7.0 mg, 0.05 mmol) and **5.34** (9 mg, 1 eq) in ^{t}BuOH (0.5 mL) and H_2O (0.5 mL) was added sodium ascorbate (1 mg, 0.1 eq) then $CuSO_4$ (0.25 M in H_2O, 10 µL, 0.05 eq) and the resulting mixture was stirred for 16 then diluted with DCM (10 mL),

washed with H_2O (10 mL), filtered and concentrated. ^1H NMR of the crude material revealed 11% yield of **5.35**.

Method C:

To a solution of **5.32** (7.0 mg, 0.05 mmol) and **5.34** (9 mg, 1 eq) in ^tBuOH (0.5 mL) and H_2O (0.5 mL) was added sodium ascorbate (10 mg, 1 eq) then $CuSO_4$ (1.0 M in H_2O, 50 μL, 1 eq) and the resulting mixture was stirred for 16 then diluted with DCM (10 mL), washed with H_2O (10 mL), filtered and concentrated. ^1H NMR of the crude material revealed 80% yield of **5.35**.

(*E*)-11-(10-(2-(2-(2-(2-(2-(2-(4-(4-(4-(1-benzyl-3,3,3-trifluoro-2-oxo-propylcarbamoyl)-phenylazo)-phenyl)-(1,2,3)triazol-1-yl)-ethoxy)-ethoxy)-ethoxy)-ethoxy)-ethoxycarbonyl)-decyldisulfanyl)undecanoic acid 2-(2-(2-(2-(2-(2-(4-(4-(4-(1-benzyl-3,3,3-trifluoro-2-oxo-propylcarbamoyl)-phenylazo)-phenyl)-(1,2,3)triazol-1-yl)-ethoxy)-ethoxy)-ethoxy)-ethoxy)-ethoxy)-ethyl ester 5.16:

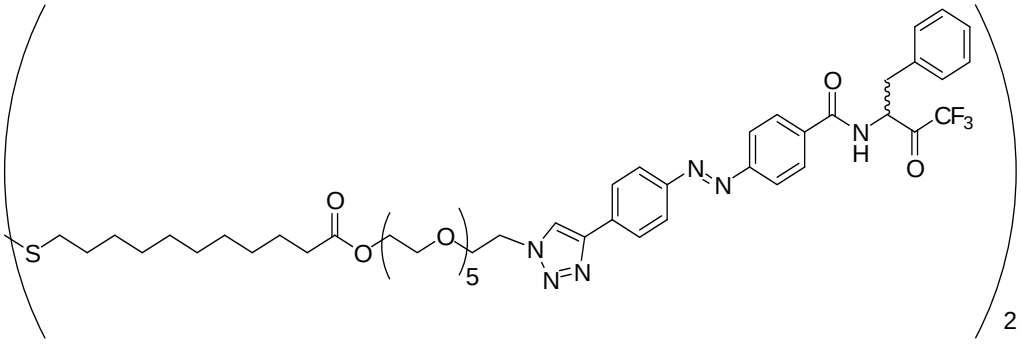

To a solution of azide **5.9** (9.0 mg, 0.0089 mmol) and alkyne **4.3** (8.0 mg, 2 eq) in ^tBuOH (0.5 mL) and H_2O (0.5 mL) was added sodium ascorbate (4.0 mg, 2.2 eq) then $CuSO_4$ (1.0 M in H_2O, 20 μL, 2.2 eq) and the resulting mixture was stirred for 16 h, diluted with EtOAc (50 mL), washed with H_2O (50 mL × 2), brine (50 mL), dried over $MgSO_4$ and concentrated. The crude material was purified by flash chromatography, eluting with 1:9 MeOH/EtOAc to give **5.16** (14 mg, 82%) as an orange gel:

^1H NMR (500 MHz, $(CD_3)_2CO$) δ 1.23-1.41 (12H, m), 1.56 (2H, m), 1.65 (2H, p, J = 7.3), 2.27 (2H, t, J = 7.4 Hz), 2.69 (2H, t, J = 7.3 Hz), 3.27 (1H, m, CHC*H*H), 3.40 (1H, m, CHCH*H*), 3.51-3.67 (18H, m), 3.98 (2H, t, J = 5.0 Hz), 4.14 (2H, t, J = 4.9 Hz), 4.41 (0.8H, m, C*H*CH_2 (hydrate isomer)), 4.67 (2H, t, J = 5.0 Hz), 5.25 (0.2H, m, C*H*CH_2 (ketone isomer)), 6.80 (1H, s), 7.15-7.21 (2H, m), 7.25-7.38 (4H, m), 7.93 (4H, m), 8.03 (2H, m),

8.14 (2H, m), 8.22 (0.8H, d, J = 8.3 Hz, N*H* (hydrate isomer)), 8.55 (1H, s, NC*H*), 8.63 (0.2H, d, J = 6.6 Hz, N*H* (ketone isomer).

^{13}C NMR (75 MHz, $(CD_3)_2CO$) δ 25.6, 29.1, 29.7, 29.9, 30.1, 30.2, 34.5, 39.3, 51.0, 64.0, 69.7, 70.0, 71.1, 71.2, 71.2, 71.2, 71.2, 71.2, 71.2, 123.3, 124.5, 127.0, 127.2, 129.2, 129.5, 130.2, 135.8, 136.7, 139.5, 146.7, 152.6, 155.2, 169.6, 173.7.

(*E*)-*N*-(1-Benzyl-3,3,3-trifluoro-2-oxo-propyl)-4-(4-(1-(2-(2-(2-(2-(2-(2-hydroxy-ethoxy)-ethoxy)-ethoxy)-ethoxy)-ethoxy)-ethyl)-1H-(1,2,3)triazol-4-yl)-phenylazo)-benzamide 5.17:

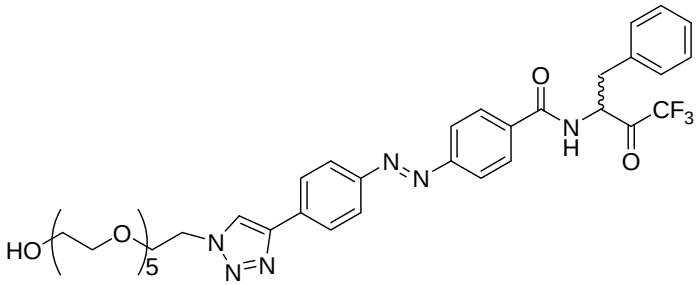

To a solution of alkyne **4.3** (13 mg, 0.029 mmol) and azide **5.24** (10 mg, 1.1 eq) in ^{t}BuOH (0.5 mL) and H_2O (0.5 mL) was added sodium ascorbate (7.0 mg, 1.1 eq) then $CuSO_4$ (1.0 M in H_2O, 32 μL, 1.1 eq) and the resulting mixture was stirred for 16 h, diluted with EtOAc (50 mL), washed with H_2O (50 mL), brine (50 mL), dried over $MgSO_4$ and concentrated. The crude material was purified by flash chromatography, eluting with 15:85 MeOH/EtOAc to give **5.17** (15 mg, 68%) as an orange gel:

^{1}H NMR (500 MHz, $(CD_3)_2CO$) δ 3.25 (1H, m, CHC*H*H), 3.39 (1H, m, CHCH*H*), 3.47-3.66 (20H, m), 3.98 (2H, t, J = 5.0 Hz), 4.41 (1H, m, C*H*CH_2), 4.67 (2H, t, J = 5.1 Hz), 6.80 (1H, s), 7.15-7.21 (2H, m), 7.25-7.41 (4H, m), 7.88-7.96 (4H, m), 8.03 (2H, d, J = 8.6 Hz), 8.14 (2H, d, J = 8.8 Hz), 8.21 (1H, d, J = 8.3 Hz), 8.56 (1H, s, NNC*H*).

^{13}C NMR (75 MHz, $CDCl_3$) δ 33.8, 51.0, 58.5, 61.9, 70.0, 71.0, 71.1, 71.2, 73.5, 123.3, 124.5, 127.0, 127.2, 129.2, 129.5, 130.1, 135.8, 136.7, 139.5, 146.7, 152.6, 155.2, 169.6.

HRMS (ES): Calcd. for $C_{37}H_{45}F_3N_6NaO_9$ (MH_3O^+) 797.3098, found 797.3126.

(*S*,*E*)-methyl 3-(4-((4-(1-(17-hydroxy-3,6,9,12,15-pentaoxaheptadecyl)-1H-1,2,3-triazol-4-yl) phenyl)diazenyl)benzamido)-2-oxo-4-phenylbutanoate 5.18:

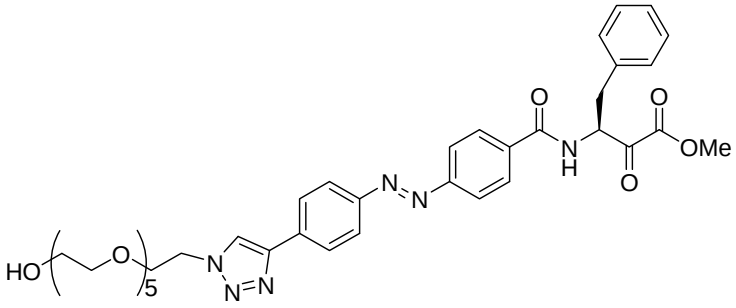

To a solution of **4.6** (5.0 mg, 0.011 mmol) and **5.24** (4.0 mg, 1.2 eq) in ^{t}BuOH (0.5 mL) and H_2O (0.5 mL) was added sodium ascorbate (2.0 mg, 1 eq) then $CuSO_4$ (1.0 M in H_2O, 11 μL, 1 eq) and the resulting mixture was stirred for 16 h, diluted with EtOAc (50 mL), washed with H_2O (50 mL), brine (50 mL), dried over $MgSO_4$ and concentrated. The crude material was purified by flash chromatography, eluting with 15:85 MeOH/EtOAc to give **5.18** (3.0 mg, 37%) as an orange gel:

$[\alpha]_D$ = -70.9 º (c = 0.19, acetone)

^{1}H NMR (500 MHz, $(CD_3)_2CO$) δ 2.91 (0.6H, m, hydrate/hemiacetal CHC*H*H), 3.09-3.26 (1H, m, hydrate/hemiacetal CHCH*H* and ketone CHC*H*H), 3.36 (0.4H, dd, J = 14.0, 5.3 Hz, ketone CHCH*H*), 3.46-3.73 (28H, m), 3.81 (1H, s, hemiacetal C(OH)O*Me*), 3.96 (2H, t, J = 5.0 Hz), 4.67 (2H, t, J = 5.0 Hz), 4.79 (0.6H, m, hydrate/hemiacetal C*H*CH_2), 5.37 (0.4H, dd, J = 9.2, 5.5 Hz, ketone C*H*CH_2), 7.07-7.16 (0.6H, m), 7.17-7.23 (2H, m), 7.27-7.36 (3H, m), 7.87-7.99 (3H, m), 7.99-8.04 (3H, m), 8.09-8.15 (2H, m), 8.60 (1H, d, J = 2.5 Hz, NNC*H*).

HRMS (ES): Calcd. for $C_{38}H_{49}N_6O_{11}$ (MH^+) 765.3459, found 765.3441.

9.6 Experimental for work described in chapter 6

Photoisomerisations

Solutions of azobenzenes (~10 mM in d_3-acetonitrile or d_6-DMSO) were photoisomerised by irradiation with UV or visible light from a 500 W Hg arc lamp. The light beam was filtered through water to reduce heat, and through a Schott UG11 filter, Corning 7-37 filter or Edmund optics 340 nm interference filter for UV, and a Corning 0–51 visible filter for

visible light. Samples were irradiated in a darkened fumehood, then encased with foil to protect from ambient light and analysed by ^{1}H NMR immediately after irradiation. NMR spectra were run with a delay time, d1, of 1 s. The use of longer delay times (e.g. 10 s) did not significantly affect integrals, except in the case of terminal alkyne protons RCC*H*, which required d1 = 10 s to obtain a meaningful integral. *E*/*Z* ratios were determined by measurement of the average *E*/*Z* integrals of appropriate non-overlapping proton resonances. Typically, α-H, NH and azobenzene signals were used depending on the degree of overlap. The major isomer was assigned the thermodynamically more stable *E* configuration based on literature precedence.[36, 37] The minor *Z* isomer characteristically gave rise to upfield signals for the aryl protons which were enhanced on irradiation.

^{1}H NMR data for azobenzene E/Z isomers obtained by photoisomerisation

E-**2.26**:

^{1}H NMR (500 MHz, CD_3CN) δ 0.81 (3H, d, J = 6.6 Hz, CH*Me*Me), 0.88 (3H, d, J = 6.6 Hz, CHMe*Me*), 1.42-1.54 (2H, m), 1.66 (1H, m), 3.40 (3H, s, O*Me*), 3.93 (1H, m, C*H*CH_2), 6.21 (1H, d, J = 8.6 Hz, N*H*), 7.58-7.63 (3H, m), 7.94-8.03 (6H, m).

Z-**2.26**:

^{1}H NMR (500 MHz, CD_3CN) δ 0.78 (3H, d, J = 6.6 Hz, CH*Me*Me), 0.86 (3H, d, J = 6.6 Hz, CHMe*Me*), 1.41-1.45 (2H, m), 1.59 (1H, m), 3.40 (3H, s, O*Me*), 3.83 (1H, m, C*H*CH_2), 6.07 (1H, d, J = 9.1 Hz, N*H*), 6.86 (2H, d, J = 7.96 Hz), 6.96 (2H, d, J = 8.68 Hz), 7.21 (1H, t, J = 7.45 Hz, CHCHC*H*CHCH), 7.31 (2H, t, J = 7.74 Hz, CHC*H*CHC*H*CH), 7.69 (2H, d, J = 8.61 Hz).

E-**2.41**:

^{1}H NMR (500 MHz, CD_3CN) δ 1.36-1.46 (12H, m, CMe_3 and CH_2*Me*), 3.69 (2H, d, *J* = 6.0 Hz), 4.38 (2H, q, *J* = 7.1 Hz, CH_2Me), 4.46 (2H, d, *J* = 6.2 Hz), 5.66 (1H, s), 7.18 (1H, s), 7.48 (2H, d, *J* = 8.2 Hz), 7.90 (2H, d, *J* = 8.2 Hz), 7.95 (2H, d, *J* = 8.7 Hz), 8.18 (2H, d, *J* = 8.7 Hz).

Z-**2.41**:

^{1}H NMR (500 MHz, CD_3CN) δ 1.32 (3H, t, *J* = 7.1 Hz, CH_2*Me*), 1.39 (9H, s, C*Me*$_3$), 3.62 (2H, d, *J* = 5.8 Hz), 4.26-4.33 (4H, m), 5.62 (1H, s), 6.82 (2H, d, *J* = 8.2 Hz), 6.90 (2H, d, *J* = 8.5 Hz), 7.03 (1H, s), 7.16 (2H, d, *J* = 8.2 Hz), 7.90 (2H, d, *J* = 8.5 Hz).

E-**2.7**:

^{1}H NMR (500 MHz, CD_3CN) δ 1.16-1.23 (12H, m, (C*Me*$_2$)$_2$), 2.77 (1H, m), 2.93-3.07 (2H, m), 7.17-7.36 (5H, m), 7.57-7.63 (3H, m), 7.88 (1H, s, N*H*), 7.92-8.00 (6H, m).

Z-**2.7**:

^{1}H NMR (500 MHz, CD_3CN) δ 1.12-1.17 (12H, m, (C*Me*$_2$)$_2$), 2.69 (1H, m), 2.87-2.99 (2H, m), 6.84 (2H, d, J = 7.6 Hz), 6.89 (2H, d, J = 6.9 Hz), 7.16-7.34 (7H, m), 7.67 (2H, d, J = 6.9 Hz), 7.76 (1H, s).

E-**2.10**:

^{1}H NMR (500 MHz, CD_3CN) δ 1.15-1.21 (12H, m, (C*Me*$_2$)$_2$), 1.42 (9H, s, C*Me*$_3$), 2.77 (1H, dd, J = 13.9, 9.9 Hz), 2.96 (1H, dd, J = 13.9, 5.3 Hz), 3.02 (1H, m), 3.69 (2H, d, J = 5.5 Hz), 4.46 (2H, d, J = 6.0 Hz), 5.67 (1H, s, N*H*), 7.15-7.38 (6H, m), 7.47 (2H, d, J = 8.1 Hz), 7.86-7.98 (6H, m).

Z-**2.10**:

^{1}H NMR (500 MHz, CD_3CN) δ 1.12-1.17 (12H, m (C*Me*$_2$)$_2$), 1.39 (9H, s, C*Me*$_3$), 2.8 (1H, m), 2.92 (2H, m), 3.62 (2H, m), 4.29 (2H, d, J = 5.9 Hz), 5.64 (1H, s, N*H*), 6.81 (2H, d, J = 8.2 Hz), 6.89 (2H, d, J = 7.8 Hz), 7.06 (1H, s, N*H*), 7.12-7.36 (7H, m), 7.69 (2H, d, J = 8.2 Hz), 7.86 (1H, s, N*H*).

E-**4.1**:

^{1}H NMR (500 MHz, CD_3CN) δ 1.42 (9H, s, C*Me*$_3$), 3.11 (1H, m, CHC*H*H), 3.29 (1H, dd, J = 14.1, 3.3 Hz, CHCH*H*), 3.69 (2H, d, J = 5.4 Hz), 4.34 (0.7H, m, hydrate C*H*CH_2), 4.45 (2H, d, J = 6.2 Hz), 5.13 (0.3H, m), 5.35 (0.3H, m), 5.68 (1H, s), 5.94 (1H, s), 6.37 (1H, s), 7.15-7.43 (7H, m), 7.47 (2H, d, J = 8.1 Hz), 7.74 (2H, d, J = 8.6 Hz), 7.85-7.92 (4H, m).

Z-**4.1**:

^{1}H NMR (500 MHz, CD_3CN) δ 1.40 (9H, s, C*Me*$_3$), 3.04 (1H, m, CHC*H*H), 3.25 (1H, dd, J = 13.9, 2.7 Hz, CHCH*H*), 3.63 (2H, d, J = 5.9 Hz), 4.23-4.33 (3H, m), 5.11 (0.3H, m), 5.34 (1H, m), 5.64 (1H, s), 5.91 (1H, s), 6.31 (1H, s), 6.77-6.84 (4H, m), 7.08 (1H, s), 7.15-7.30 (8H, m), 7.48 (2H, d, J = 8.4 Hz).

E-**4.2**:

^{1}H NMR (500 MHz, CD_3CN) δ 1.50 (3H, d, J = 7.3 Hz, Me), 2.69 (1H, t, J = 2.3 Hz, CH_2CCH), 3.12 (1H, m, CHC*H*H), 3.30 (1H, dd, J = 14.1, 2.9 Hz, CHCH*H*), 3.50-3.60 (12H, m), 3.66 (2H, t, J = 4.6 Hz), 4.14 (2H, m), 4.19-4.36 (3H, m), 4.61 (1H, m), 5.75 (1H, s), 6.20 (1H, s), 7.21 (1H, m), 7.25-7.31 (4H, m), 7.34 (1H, d, J = 8.2 Hz), 7.44 (1H, d, J = 7.0 Hz), 7.75 (2H, d, J = 8.3 Hz), 7.92 (2H, d, J = 8.3 Hz), 7.96-8.03 (4H, m).

Z-**4.2**:

^{1}H NMR (500 MHz, CD_3CN) δ 1.44 (3H, d, J = 7.3 Hz), 2.79 (1H, m, CH_2CCH), 3.04 (1H, m, CHC*H*H), 3.23 (1H, dd, J = 14.1, 2.7 Hz, CHCH*H*), 3.47-3.60 (12H, m), 3.63 (2H, t, J = 4.5 Hz), 4.13 (2H, m), 4.15-4.36 (3H, m), 4.53 (1H, m), 5.75 (1H, s), 6.17 (1H, s), 6.85 (2H, d, J = 8.5 Hz), 6.89 (2H, d, J = 8.4 Hz), 7.14-7.30 (7H, m), 7.46 (2H, d, J = 8.5 Hz), 7.73 (2H, d, J = 8.4 Hz).

E-**4.3**:

^{1}H NMR (500 MHz, CD_3CN) δ 3.08-3.20 (1H, m, CHC*H*H), 3.26-3.36 (1H, m, CHCH*H*), 3.61 (1H, s, CCC*H*), 4.31 (0.3H, m, hydrate C*H*CH_2), 5.09 (0.7H, m, ketone C*H*CH_2), 5.74 (0.3H, s, hydrate O*H*), 6.20 (1H, s, hydrate O*H*), 7.18-7.37 (6H, m), 7.67-7.77 (3H, m), 7.85-7.98 (5H, m).

Z-**4.3:**

The NMR spectra obtained for *Z*-**4.3** in d_3-acetonitrile contained a mixture of *E*- and *Z*-ketone and hydrate isomers, and peaks corresponding to each could not be fully determined. The NMR spectrum is shown in Fig. 9.1, and selected *Z* peaks were assigned for determination of *E*/*Z* composition:

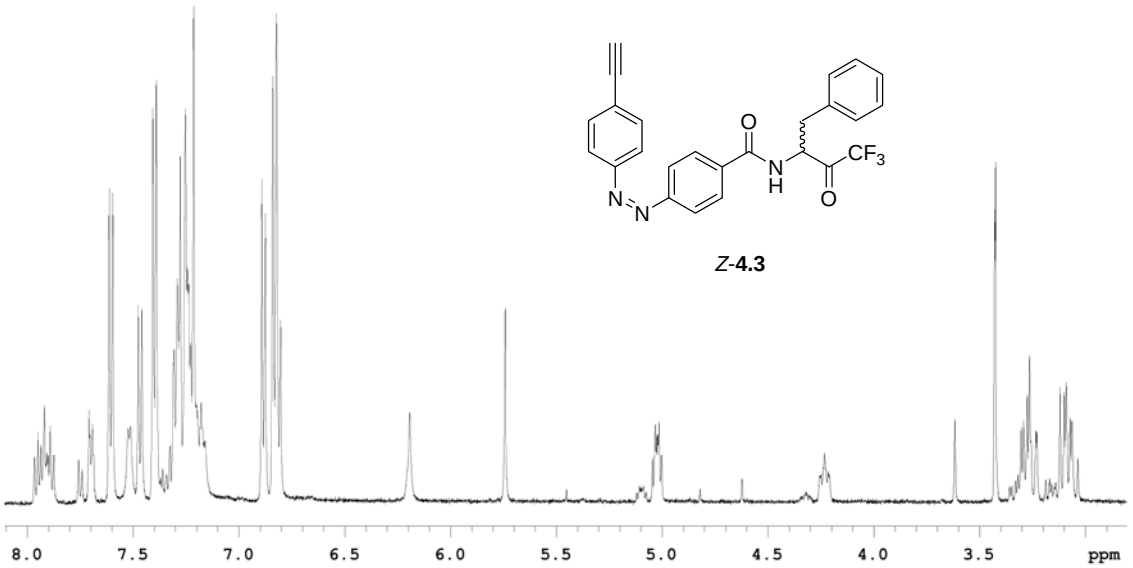

Fig. 9.1. ^{1}H NMR spectrum of a *Z*-enriched sample of **4.3**.

Selected peaks from ^{1}H NMR (500 MHz, CD_3CN) δ 3.41-3.43 (1H, m, CCC*H*), 4.23 (0.3H, m, hydrate C*H*CH_2), 5.02 (0.7H, m, ketone C*H*CH_2).

E-**4.4**:

^{1}H NMR (500 MHz, CD_3CN) δ 2.69 (1H, t, J = 2.4 Hz, CH_2CCH), 3.10 (1H, m, CHC*H*H), 3.29 (1H, dd, J = 14.3, 3.1 Hz, CHCH*H*), 3.49-3.65 (14H, m), 3.70 (2H, m), 4.14 (2H, d, J = 2.4 Hz, CH_2CCH), 4.34 (1H, m, C*H*CH_2), 4.43 (2H, s, OCH_2CC), 5.87 (1H, s), 6.27 (1H, s), 7.20 (1H, m), 7.24-7.32 (4H, m), 7.38 (1H, d, J = 8.5 Hz), 7.64 (2H, d, J = 8.3 Hz), 7.75 (2H, d, J = 8.3 Hz), 7.88-7.93 (4H, m).

Z-**4.4**:

^{1}H NMR (500 MHz, CD_3CN) δ 2.69 (1H, t, J = 2.3 Hz, CH_2CCH), 3.04 (1H, m, CHC*H*H), 3.24 (1H, dd, J = 14.0, 3.1 Hz, CHCH*H*), 3.51-3.67 (16H, m), 4.14 (2H, t, J = 2.3 Hz, CH_2CCH), 4.25 (1H, m, C*H*CH_2), 4.35 (2H, s, OCH_2CC), 5.86 (1H, s), 6.26 (1H, s), 6.78-6.85 (4H, m), 7.14-7.30 (6H, m), 7.35 (2H, d, J = 8.5 Hz), 7.47 (2H, d, J = 8.6 Hz).

E- and *Z*-**4.5**:

The NMR spectra obtained for *E*- and *Z*-**4.5** in d_3-acetonitrile contained mixtures of *E*- and *Z*- ketone and hydrate isomers, and peaks corresponding to each isomer could not be fully determined. ^{1}H NMR spectra are shown in Figs. 9.2 and 9.3, and *E* and *Z* CH_2 peaks were assigned for determination of *E*/*Z* composition:

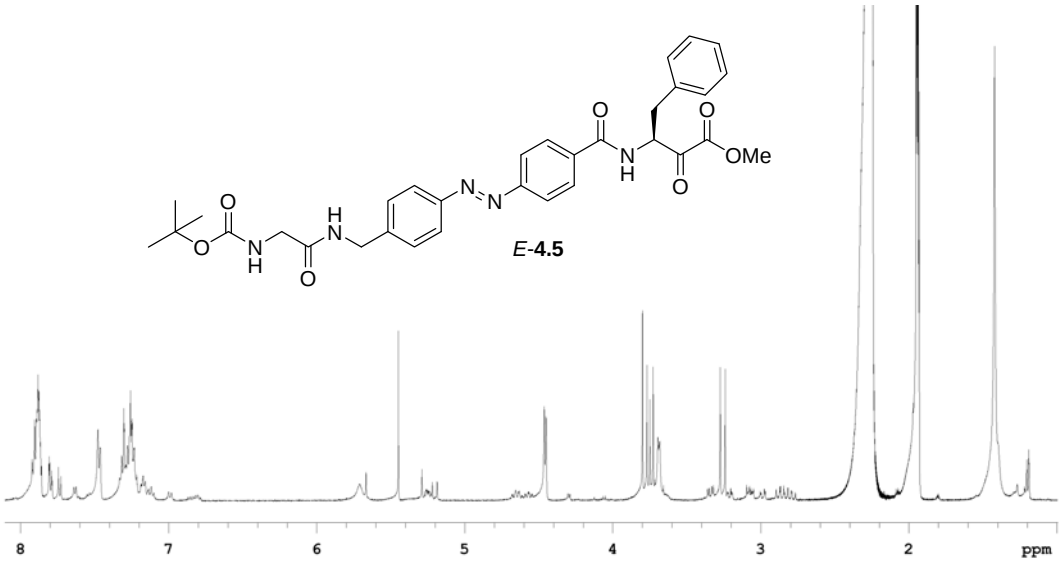

Fig. 9.2. ^{1}H NMR spectrum of *E*-**4.5**.

Selected peak from ^{1}H NMR (500 MHz, CD_3CN) δ 4.46 (2H, d, J = 6.2 Hz).

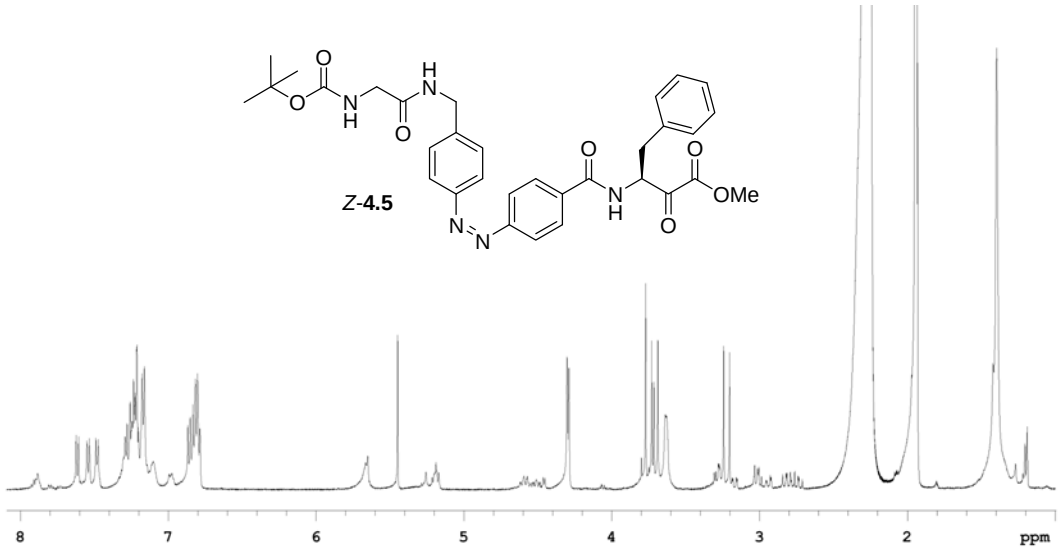

Fig. 9.3. ^{1}H NMR spectrum of a *Z*-enriched sample of **4.5**.

Selected peak from ^{1}H NMR (500 MHz, CD_3CN) δ 4.29 (2H, d, J = 6.2 Hz).

E- and *Z*-**4.6**:

The NMR spectra obtained for *E*- and *Z*-**4.6** in d_3-acetonitrile contained mixtures of *E*- and *Z*- ketone and hydrate isomers, and peaks corresponding to each isomer could not be fully determined. ^{1}H NMR spectra are shown in Figs. 9.4 and 9.5, and *E* and *Z* aryl peaks were assigned for determination of *E*/*Z* composition:

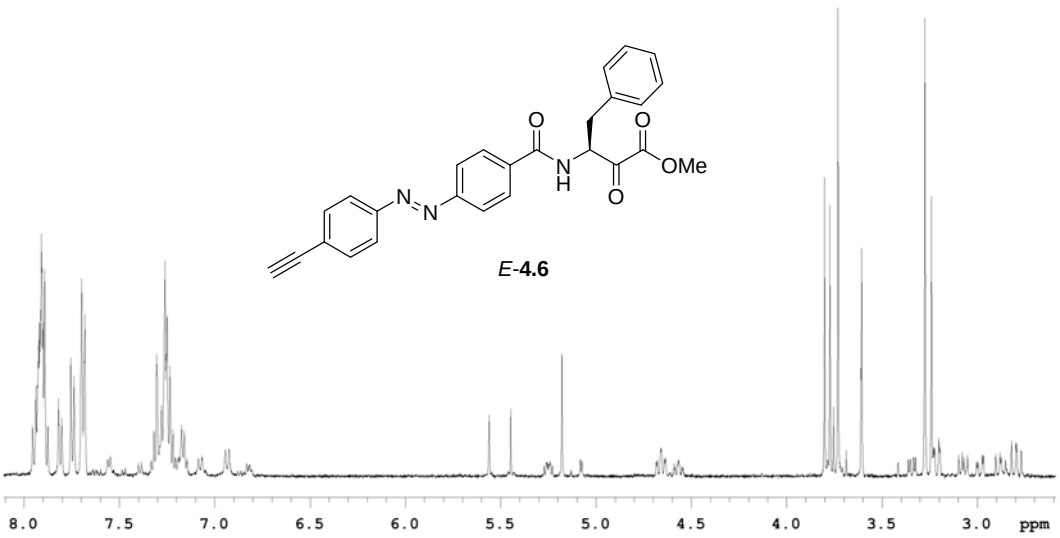

E-**4.6**

Fig. 9.4. ^{1}H NMR spectrum of *E*-**4.6**.

Selected peak from ^{1}H NMR (500 MHz, CD_3CN) δ 7.87-7.96 (6H, m).

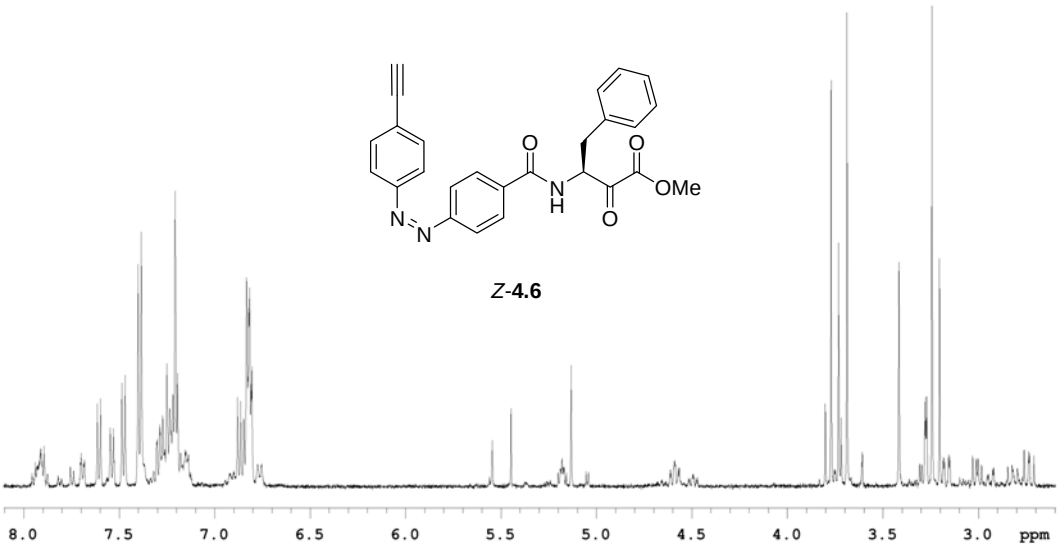

Z-**4.6**

Fig. 9.5. ^{1}H NMR spectrum of a *Z*-enriched sample of **4.6**.

Selected peak from ^{1}H NMR (500 MHz, CD_3CN) δ 6.80-6.84 (4H, m).

E- and *Z*-**4.7**:

The NMR spectra obtained for *E*- and *Z*-**4.7** in d_3-acetonitrile contained mixtures of *E*- and *Z*- ketone and hydrate isomers, and peaks corresponding to each isomer could not be fully determined. ^{1}H NMR spectra are shown in Figs. 9.6 and 9.7, and *E* and *Z* aryl peaks were assigned for determination of *E*/*Z* composition:

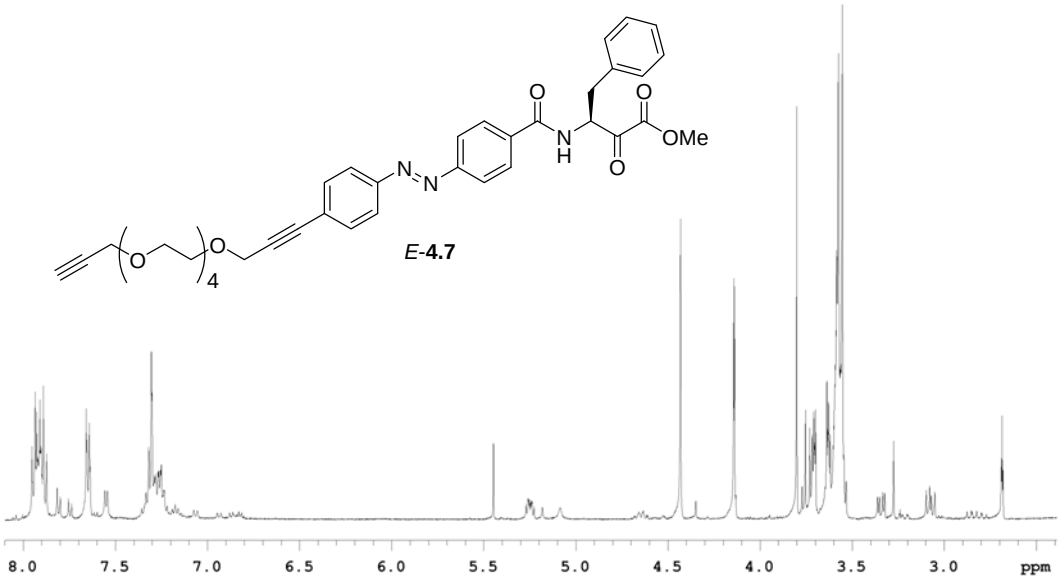

Fig. 9.6. ^{1}H NMR spectrum of *E*-**4.7**.

Selected peak from ^{1}H NMR (500 MHz, CD_3CN) δ 7.87-7.96 (6H, m).

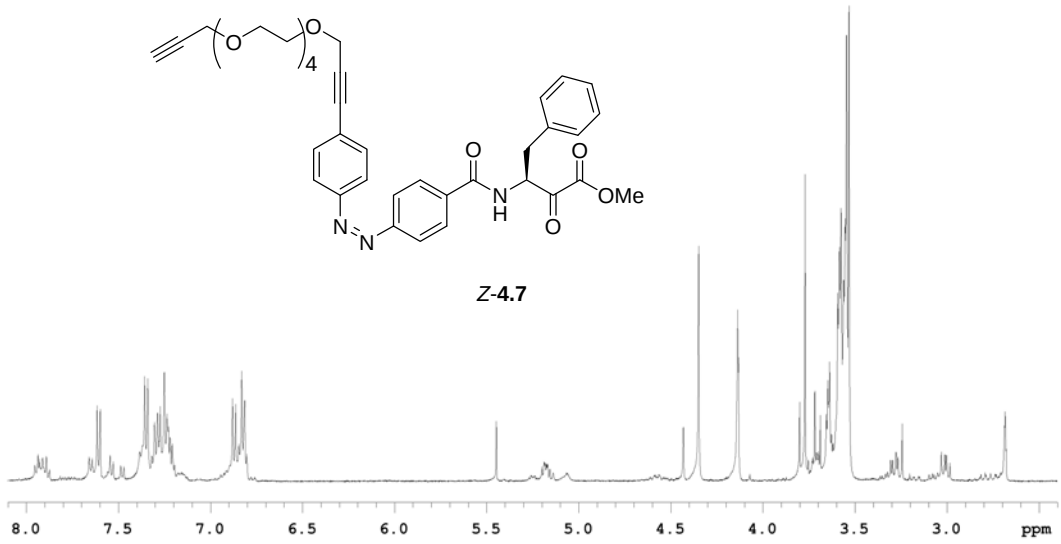

Fig. 9.7. ^{1}H NMR spectrum of a *Z*-enriched sample of **4.7**.

Selected peak from ^{1}H NMR (500 MHz, CD_3CN) δ 6.80-6.89 (4H, m).

E-**5.17**:

^{1}H NMR (500 MHz, CD_3CN) δ 2.80 (1H, m), 3.13 (1H, m), 3.29 (1H, dd, J = 14.1, 3.1 Hz), 3.40-3.64 (20H, m), 3.91 (2H, t, J = 5.0 Hz), 4.32 (1H, m), 4.59 (2H, t, J = 5.0 Hz), 5.78 (1H, s), 6.25 (1H, s), 7.21 (1H, m), 7.24-7.31 (4H, m), 7.76 (1H, d, J = 8.6 Hz), 7.91 (2H, d, J = 8.6 Hz), 8.01 (2H, d, J = 8.6 Hz), 8.08 (2H, d, J = 8.6 Hz), 8.32 (1H, s, NNNC*H*).

Z-**5.17**:

^{1}H NMR (500 MHz, CD_3CN) δ 2.88 (1H, t, J = 5.9 Hz), 3.04 (1H, m), 3.22 (1H, dd, J = 13.9, 3.2 Hz), 3.40-3.64 (20H, m), 3.86 (2H, m), 4.23 (1H, m), 4.53 (2H, m), 5.81 (1H, s), 6.22 (1H, s), 6.87 (2H, d, J = 8.6 Hz), 6.91 (2H, d, J = 8.6 Hz), 7.16-7.25 (5H, m), 7.28 (1H, m), 7.49 (2H, d, J = 8.6 Hz), 7.77 (2H, d, J = 8.6 Hz), 8.17 (1H, s, NNNC*H*).

E- and *Z*-**5.18**:

The NMR spectra obtained for *E*- and *Z*-**5.18** in d_3-acetonitrile contained mixtures of *E*- and *Z*- ketone, hydrate, and hemiacetal isomers, and peaks corresponding to each isomer could not be fully determined. ^{1}H NMR spectra are shown in Figs. 9.8 and 9.9, and *E* and *Z* triazole peaks were assigned for determination of *E*/*Z* composition:

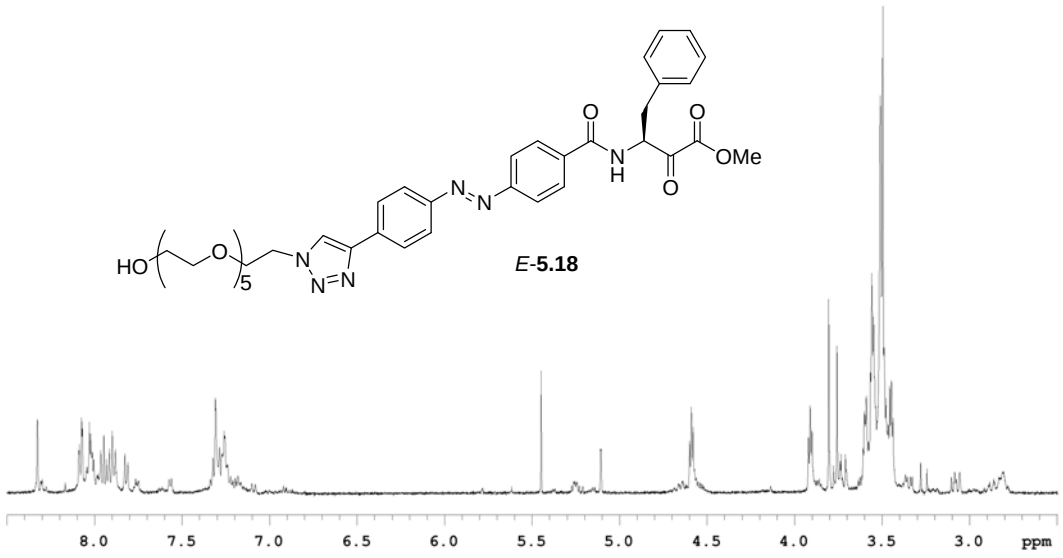

Fig. 9.8. ^{1}H NMR spectrum of *E*-**5.18**.

Selected peak from ^{1}H NMR (500 MHz, CD_3CN) δ 8.33 (1H, s, NNNC*H*).

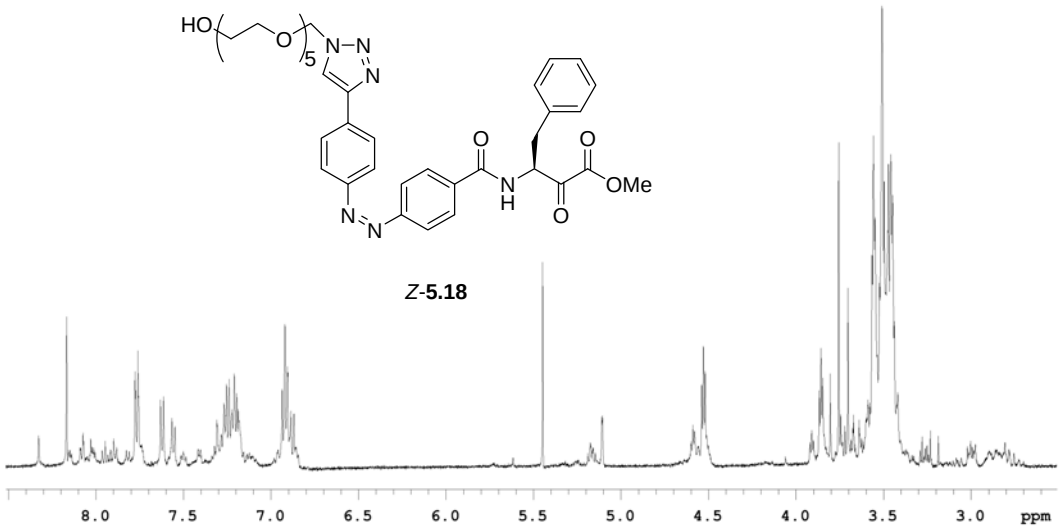

Fig. 9.9. ^{1}H NMR spectrum of a *Z*-enriched sample of **5.18**.

Selected peak from ^{1}H NMR (500 MHz, CD_3CN) δ 8.17 (1H, s, NNNC*H*).

E-**5.12**:

^{1}H NMR (500 MHz, CD_3CN) δ 1.35-1.46 (5H, m), 1.55-1.64 (4H, m), 1.69 (1H, m), 1.86 (1H, m), 2.41 (1H, m), 3.08 (1H, m), 3.16 (1H, m), 3.56 (1H, m), 3.80 (2H, d, J = 5.8 Hz), 4.38 (2H, q, J = 7.1 Hz, C*H*$_2$Me), 4.45 (2H, d, J = 6.2 Hz), 6.74 (1H, s), 7.13 (1H, t, J = 5.7 Hz), 7.47 (2H, d, J = 8.2 Hz), 7.91 (2H, d, J = 8.2 Hz), 7.95 (2H, d, J = 8.3 Hz), 8.18 (2H, d, J = 8.3 Hz).

The NMR spectrum obtained for *Z*-**5.12** contained only a small amount of *Z*-**5.12**, and few peaks corresponding to this isomer could be identified, as given below.

Z-**5.12**:

Selected peaks from ^{1}H NMR (500 MHz, CD_3CN) δ 3.73 (2H, d, J = 6.2 Hz), 4.25-4.32 (4H, m), 6.82 (2H, d, J = 7.9 Hz), 6.90 (2H, d, J = 8.1 Hz).

E-**5.13**:

^{1}H NMR (500 MHz, CD_3CN) δ 1.18-1.35 (12H, m), 1.38 (3H, t, J = 7.1 Hz, CH_2*Me*), 1.47-1.56 (4H, m), 2.23-2.29 (5H, m), 2.81 (2H, m), 3.52-3.68 (10H, m), 3.89 (2H, d, J = 6.0 Hz), 3.98 (2H, s, COC*H*$_2$O), 4.12 (2H, m), 4.38 (2H, q, J = 7.1 Hz, C*H*$_2$Me), 4.46 (2H,

d, J = 6.1 Hz), 7.18 (1H, m), 7.48 (2H, d, J = 8.4 Hz), 7.58 (1H, m), 7.91 (2H, d, J = 8.4 Hz), 7.95 (2H, d, J = 8.6 Hz), 8.18 (2H, d, J = 8.6 Hz).

Z-**5.13**:

^{1}H NMR (500 MHz, CD_3CN) δ 1.23-1.35 (15H, m), 1.49-1.56 (4H, m), 2.24-2.29 (5H, m), 2.83 (2H, m), 3.51-3.65 (10H, m), 3.83 (2H, d, J = 6.1 Hz), 3.95 (1H, s, COCH_2O), 4.11 (2H, m), 4.27-4.33 (4H, m), 6.82 (2H, d, J = 8.3 Hz), 6.90 (2H, d, J = 8.5 Hz), 7.04 (1H, m), 7.17 (2H, d, J = 8.3 Hz), 7.54 (1H, m), 7.91 (2H, d, J = 8.5 Hz).

*Isolation of Z-**2.7***

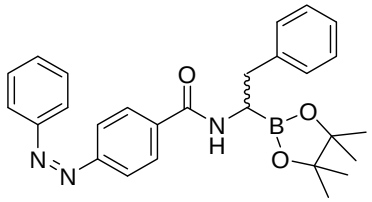

A solution of *E*-**2.7** (10 mg, 0.02 mmol) in 3:7 EtOAc–DCM (2.0 mL) was exposed to ambient indoor lighting and daylight for 2 d, giving a mixture of *E*- and *Z*-**2.7** (by TLC). The isomers were separated by flash chromatography, eluting with 3:7 EtOAc–DCM to give *Z*-**2.7** (1.0 mg, 7%, >95% *Z* isomer by ^{1}H NMR):

^{1}H NMR (500 MHz, $CDCl_3$) δ 1.27 (6H, s, (CMe_2)$_2$), 1.28 (6H, s, (CMe_2)$_2$), 2.76 (1H, dd, *J* = 12,14), 3.03 (1H, dd, *J* = 14, 4.3), 3.09 (1H, m), 6.80 (3H, m), 6.85 (2H, d, *J* = 8.5), 7.18 (1H, t, *J* = 9.3), 7.23 (5H, m), 7.33 (2H, t, *J* = 7.5), 7.62 (2H, d, *J* = 8.5).

α-Chymotrypsin assays

Buffer solution (Tris): Tris(hydroxymethyl)aminomethane (12 g), $CaCl_2.6H_2O$ (4.4 g) and Triton X-100 (0.50 g) were dissolved in Milli-Q deionised water (750 mL), adjusted to pH 7.8 with HCl solution (1.0 M) and made up to 1.0 L with Milli-Q water.

Substrate solution: *N*-succinyl-Ala-Ala-Pro-Phe-4-nitroanilide (21 mg) was dissolved in Tris buffer solution (10 mL) by ultrasonication. The solution was stored at −18 ºC for up to two weeks. The concentration of the solution was determined at the start of each day from its UV spectrum (ε_{315} =14 000 $Lmol^{-1}cm^{-1}$).

Enzyme solution: a stock solution was prepared from α-chymotrypsin (15 mg) in HCl solution (10 mL, pH 3, made up by dilution of conc. HCl with Milli-Q water). The stock solution was stored at −18 ºC for up to 1 month. Each day an enzyme solution was prepared: stock solution (200 μL, or 100 μL for assay of trifluoromethylketones and α-ketoesters) and Triton X-100 (25 mg) were made up to 50 mL with Milli-Q water.

Inhibition of α-chymotrypsin was determined with Suc–Ala–Ala–Pro–Phe–4-nitroanilide as the substrate by an assay procedure developed from the technique described by Geiger,[38] except that the order of addition of enzyme and substrate was inverted, and in some cases only one substrate concentration was used, in order to obtain inhibition constants as IC_{50} rather than K_i. Inhibitors were dissolved in acetonitrile or DMSO at a series of dilutions ranging from 0.001 – 500 μM as appropriate for each compound (see assay data below for the concentrations used in each assay). For each rate measurement, inhibitor solution (or acetonitrile blank, 50 μL), substrate solution (30-150 μL) and buffer solution (to make up the total volume to 1020 μL) were mixed in a cuvette, and incubated for 5 min at 25 ºC. Enzyme solution (30 μL) was added, and the absorbance at 405 nm was monitored for 5 min (or 10 min for trifluoromethylketones). An absorbance *vs.* time plot was obtained, and the slope used to find the initial rate V_0 (or final rate for trifluoromethylketones) in μmol s^{-1} mg^{-1} (μmol of substrate hydrolysed per second per mg of enzyme) using the following equation:

$$V_0 = \frac{slope \cdot V \cdot 10^6}{\varepsilon_{405} \cdot l \cdot m_E} = 606 \cdot slope$$

Where V is the volume of the assay solution (0.001050 L), ε_{405} is the molar absorptivity coefficient of 4-nitroaniline (10200 L mol^{-1} cm^{-1}), l is the path length of the cell (1 cm) and m_E is the mass of enzyme used in the assay (1.7×10^{-4} mg).

For IC_{50} assays, % inhibition values were calculated from V_0 (or slopes) using the following formula:

$$\%\ \text{inhibition} = \frac{V_{0([I]=0)} - V_0}{V_{0([I]=0)}} \cdot 100$$

Where $V_{0([I]=0)}$ is the initial rate in the absence of inhibitor.

The rate data (V_0 and % inhibition) was analysed to give K_i or IC_{50} inhibition constants. Details of these analyses are given in chapter 6.

The uncertainty in affinity constants was not studied comprehensively, but is estimated at ±20%, with ±10% estimated for increases/decreases in inhibition on photoisomerisation. These estimated errors are based on measurement uncertainties and observed discrepancies between *E*:*Z* compositions and IC_{50} values in photoswitching assays, as follows:

It is apparent that the *Z* isomer of the trifluoromethylketone and α-ketoester inhibitors is the most potent (see chapter 6, Table 6.4). Therefore, the IC_{50} value obtained for each inhibitor before irradiation (5-7% Z, see chapter 6, Table 6.2) is expected to be slightly higher than, and similar to, the value obtained after visible irradiation (8-21% Z, Table 6.2). However, some inhibitors (**4.2**, **4.7** and **5.17**) exhibit up to 10% greater IC_{50} values after visible irradiation than obtained before irradiation. This discrepancy must be due to experimental error, and is used to estimate ±10% uncertainty in IC_{50} increases/decreases on photoswitching. This maximum observed error also gives an estimated ±10% error for assays, not including uncertainty in the measurement of inhibitor concentrations.

The total uncertainty in affinity constants also includes measurement errors, primarily weighing balance uncertainties and the possible presence of solvents or minor impurities in inhibitor samples. These measurement errors are estimated at ±10%, which gives a total estimated error of ±20% (including the 10% assay error described above). While it is recognised that this estimation is not a rigorous calculation of uncertainties, the limited analysis was considered sufficient for the purposes of this study.

Assay data (slopes of absorbance vs. time plots and derived initial rates, V_0)

Table 9.1. Data for assay of α-chymotrypsin.

Substrate concentration (μM)	Slope (A.U. s^{-1})	V_0 (μmol s^{-1} mg^{-1})
83	0.0014	0.85
170	0.0017	1.0
250	0.0018	1.1
330	0.0018	1.1
420	0.0019	1.1

Table 9.2. Data for assay of α-chymotrypsin in the presence of acetonitrile.

Substrate concentration (μM)	Slope (A.U. s^{-1})	V_0 (μmol s^{-1} mg^{-1})
83	0.0017	1.0
170	0.0024	1.4
250	0.0019	1.1
330	0.0019	1.2
420	0.0020	1.2

Table 9.3. Data for assay of α-chymotrypsin in the presence of DMSO.

Substrate concentration (μM)	Slope (A.U. s^{-1})	V_0 (μmol s^{-1} mg^{-1})
83	0.0014	0.84
170	0.0016	0.98
250	0.0017	1.0
330	0.0018	1.1
420	0.0018	1.1

Table 9.4. Data for assay of the inhibition of α-chymotrypsin by **2.12**.

Inhibitor and Substrate concentrations (μM)	Slope (A.U. s^{-1})	V_0 (μmol s^{-1} mg^{-1})
0, 82	0.0016	0.99
0, 170	0.0017	1.0
0, 250	0.0018	1.1
0, 330	0.0020	1.2
0, 410	0.0021	1.2
17, 82	0.00057	0.35
17, 170	0.00088	0.54
17, 250	0.0011	0.69
17, 330	0.0013	0.78
17, 410	0.0014	0.86
35, 82	0.00037	0.22
35, 170	0.00063	0.38
35, 150	0.00086	0.52
35, 330	0.00098	0.60
35, 410	0.0011	0.69
52, 82	0.00030	0.18
52, 170	0.00048	0.29
52, 250	0.00062	0.38
52, 330	0.00076	0.46
52, 410	0.00088	0.53
69, 82	0.00023	0.14
69, 170	0.00042	0.26
69, 250	0.00056	0.34
69, 330	0.00067	0.40
69, 410	0.00084	0.51

Table 9.5. Data for assay of the inhibition of α-chymotrypsin by **2.1**.

Inhibitor concentration (μM)	Slope (A.U. s^{-1})	V_0 (μmol s^{-1} mg^{-1})	% Inhibition
0	0.0019	1.1	0
15	0.0018	1.1	6.5

Table 9.6. Data for assay of the inhibition of α-chymotrypsin by **2.2**.

Inhibitor concentration (μM)	Slope (A.U. s^{-1})	V_0 (μmol s^{-1} mg^{-1})	% Inhibition
0	0.0019	1.1	0
25	0.0017	1.0	8.6

Table 9.7. Data for assay of the inhibition of α-chymotrypsin by **2.6**.

Inhibitor concentration (μM)	Slope (A.U. s^{-1})	V_0 (μmol s^{-1} mg^{-1})	% Inhibition
0	0.0019	1.1	0
200	0.0018	1.1	3.1

Table 9.8. Data for assay of the inhibition of α-chymotrypsin by **2.7**.

Inhibitor concentration (μM)	Slope (A.U. s^{-1})	V_0 (μmol s^{-1} mg^{-1})	% Inhibition
0	0.0023	1.4	0
0.41	0.0020	1.2	12
0.81	0.0019	1.2	17
1.6	0.0015	0.92	34
3.2	0.0011	0.66	52

Table 9.9. Data for assay of the inhibition of α-chymotrypsin by chromatographically isolated *Z*-**2.7**.

Inhibitor concentration (μM)	Slope (A.U. s^{-1})	V_0 (μmol s^{-1} mg^{-1})	% Inhibition
0	0.0018	1.1	0
0.81	0.0016	0.94	16
1.6	0.0014	0.83	26
3.2	0.0011	0.64	43
6.5	0.00075	0.45	60

Table 9.10. Data for assay of the inhibition of α-chymotrypsin by **2.8**.

Inhibitor concentration (μM)	Slope (A.U. s^{-1})	V_0 (μmol s^{-1} mg^{-1})	% Inhibition
0	0.0016	0.96	0
4.2	0.0014	0.86	10
8.4	0.0012	0.70	27
14	0.00079	0.48	50
21	0.00071	0.43	55
42	0.00050	0.30	69

Table 9.11. Data for assay of the inhibition of α-chymotrypsin by **2.9**.

Inhibitor concentration (μM)	Slope (A.U. s^{-1})	V_0 (μmol s^{-1} mg^{-1})	% Inhibition
0	0.0016	0.96	0
0.52	0.0011	0.67	30
1.1	0.00090	0.55	43
2.1	0.00059	0.36	63
4.2	0.00036	0.22	77
8.4	0.00022	0.14	86

Table 9.12. Data for assay of the inhibition of α-chymotrypsin by **2.10**.

Inhibitor concentration (μM)	Slope (A.U. s^{-1})	V_0 (μmol s^{-1} mg^{-1})	% Inhibition
0	0.0019	1.1	0
5.1	0.0013	0.78	30
10	0.00087	0.53	53
20	0.00060	0.36	68
41	0.00040	0.25	78

Table 9.13. Data for assay of the inhibition of α-chymotrypsin by **2.11**.

Inhibitor concentration (μM)	Slope (A.U. s^{-1})	V_0 (μmol s^{-1} mg^{-1})	% Inhibition
0	0.0018	1.1	0
5.5	0.0012	0.74	33
11	0.00088	0.53	52
22	0.00057	0.34	69
44	0.00036	0.22	80
88	0.00022	0.13	88

Table 9.14. Data for assay of the inhibition of α-chymotrypsin by **2.7** after UV irradiation.

Inhibitor concentration (μM)	Slope (A.U. s^{-1})	V_0 (μmol s^{-1} mg^{-1})	% Inhibition
0	0.0017	1.2	0
1.7	0.0014	0.84	28
3.5	0.0011	0.68	41
7.0	0.00086	0.52	55
14	0.00052	0.32	72

Table 9.15. Data for assay of the inhibition of α-chymotrypsin by **2.7** after UV, vis irradiation.

Inhibitor concentration (μM)	Slope (A.U. s^{-1})	V_0 (μmol s^{-1} mg^{-1})	% Inhibition
0	0.0019	1.2	0
0.87	0.0017	1.0	10
1.7	0.0016	0.96	17
3.5	0.0013	0.78	33
7.0	0.00089	0.54	54

Table 9.16. Data for assay of the inhibition of α-chymotrypsin by **2.7** after UV, vis, UV irradiation.

Inhibitor concentration (μM)	Slope (A.U. s^{-1})	V_0 (μmol s^{-1} mg^{-1})	% Inhibition
0	0.0019	1.2	0
2.2	0.0016	0.99	14
4.4	0.0014	0.87	25
8.7	0.0011	0.70	39
17	0.00078	0.47	59

Table 9.17. Data for assay of the inhibition of α-chymotrypsin by **2.7** after UV, vis, UV, vis irradiation.

Inhibitor concentration (μM)	Slope (A.U. s^{-1})	V_0 (μmol s^{-1} mg^{-1})	% Inhibition
0	0.0016	1.1	0
2.2	0.0015	1.0	12
4.4	0.0013	0.93	18
8.7	0.0011	0.80	30
17	0.0019	0.64	44

Table 9.18. Data for assay of the inhibition of α-chymotrypsin by **2.10** after UV irradiation.

Inhibitor concentration (μM)	Slope (A.U. s^{-1})	V_0 (μmol s^{-1} mg^{-1})	% Inhibition
0	0.0019	1.1	0
2.6	0.0014	0.82	27
5.1	0.0011	0.66	41
10	0.00072	0.44	61
20	0.00045	0.27	76
41	0.00025	0.15	86

Table 9.19. Data for assay of the inhibition of α-chymotrypsin by **2.10** after UV, vis irradiation.

Inhibitor concentration (μM)	Slope (A.U. s^{-1})	V_0 (μmol s^{-1} mg^{-1})	% Inhibition
0	0.0019	1.1	0
5.1	0.0012	0.74	35
10	0.0011	0.67	41
20	0.00072	0.43	62
41	0.00055	0.33	71

Table 9.20. Data for assay of the inhibition of α-chymotrypsin by **2.10** after UV, vis, UV irradiation.

Inhibitor concentration (μM)	Slope (A.U. s^{-1})	V_0 (μmol s^{-1} mg^{-1})	% Inhibition
0	0.0019	1.1	0
5.1	0.0012	0.75	34
10	0.00098	0.60	47
20	0.00054	0.33	71
41	0.00037	0.22	80

Table 9.21. Data for assay of the inhibition of α-chymotrypsin by **3.3**.

Inhibitor concentration (μM)	Slope (A.U. s^{-1})	V_0 (μmol s^{-1} mg^{-1})	% Inhibition
0	0.0013	0.80	0
60	0.0013	0.78	1.6

Table 9.22. Data for assay of the inhibition of α-chymotrypsin by **3.4**.

Inhibitor concentration (μM)	Slope (A.U. s^{-1})	V_0 (μmol s^{-1} mg^{-1})	% Inhibition
0	0.0012	0.75	0
91	0.0012	0.72	3.7

Table 9.23. Data for assay of the inhibition of α-chymotrypsin by **3.10**.

Inhibitor and Substrate concentrations (μM)	Slope (A.U. s^{-1})	V_0 (μmol s^{-1} mg^{-1})
0, 89	0.0011	0.65
0, 180	0.0013	0.80
0, 270	0.0015	0.88
0, 350	0.0015	0.90
0, 440	0.0015	0.93
11, 89	0.00074	0.45
11, 180	0.0012	0.73
11, 270	0.0013	0.77
11, 350	0.0014	0.85
11, 440	0.0014	0.85
21, 89	0.00061	0.37
21, 180	0.00088	0.53
21, 270	0.0011	0.65
21, 350	0.0012	0.75
21, 440	0.0013	0.78

Table 9.24. Data for assay of the inhibition of α-chymotrypsin by **4.1**.

Inhibitor concentration (μM)	Slope (A.U. s^{-1})	V_0 (μmol s^{-1} mg^{-1})	% Inhibition
0	0.00075	0.45	0
4.9	0.00066	0.40	11
9.7	0.00056	0.34	26
19	0.00047	0.28	37
39	0.00033	0.20	56

Table 9.25. Data for assay of the inhibition of α-chymotrypsin by **4.1** after UV irradiation.

Inhibitor concentration (μM)	Slope (A.U. s^{-1})	V_0 (μmol s^{-1} mg^{-1})	% Inhibition
0	0.00075	0.45	0
4.9	0.00056	0.34	25
9.7	0.00043	0.26	43
19	0.00029	0.18	61
39	0.00016	0.097	79

Table 9.26. Data for assay of the inhibition of α-chymotrypsin by **4.1** after UV, vis irradiation.

Inhibitor concentration (μM)	Slope (A.U. s^{-1})	V_0 (μmol s^{-1} mg^{-1})	% Inhibition
0	0.00075	0.45	0
4.9	0.00066	0.40	12
9.7	0.00056	0.34	24
19	0.00043	0.26	43
39	0.00075	0.19	57

Table 9.27. Data for assay of the inhibition of α-chymotrypsin by **4.2**.

Inhibitor concentration (μM)	Slope (A.U. s^{-1})	V_0 (μmol s^{-1} mg^{-1})	% Inhibition
0	0.00068	0.41	0
3.3	0.00067	0.40	1.7
6.6	0.00054	0.33	20
13	0.00041	0.25	39
26	0.00026	0.16	62
53	0.00019	0.11	73

Table 9.28. Data for assay of the inhibition of α-chymotrypsin by **4.2** after UV irradiation.

Inhibitor concentration (μM)	Slope (A.U. s^{-1})	V_0 (μmol s^{-1} mg^{-1})	% Inhibition
0	0.00068	0.41	0
3.3	0.00061	0.37	10
6.6	0.00052	0.32	23
13	0.00036	0.22	46
26	0.00024	0.14	65
53	0.00016	0.095	77

Table 9.29. Data for assay of the inhibition of α-chymotrypsin by **4.2** after UV, vis irradiation.

Inhibitor concentration (μM)	Slope (A.U. s^{-1})	V_0 (μmol s^{-1} mg^{-1})	% Inhibition
0	0.00068	0.41	0
3.3	0.00067	0.40	1.7
6.6	0.00056	0.34	17
13	0.00042	0.25	38
26	0.00027	0.16	61
53	0.00019	0.11	72

Table 9.30. Data for assay of the inhibition of α-chymotrypsin by **4.3**.

Inhibitor concentration (μM)	Slope (A.U. s^{-1})	V_0 (μmol s^{-1} mg^{-1})	% Inhibition
0	0.00072	0.44	0
11	0.00063	0.38	13
21	0.00054	0.33	25
42	0.00045	0.27	38
85	0.00039	0.24	46

Table 9.31. Data for assay of the inhibition of α-chymotrypsin by **4.3** after UV irradiation.

Inhibitor concentration (μM)	Slope (A.U. s^{-1})	V_0 (μmol s^{-1} mg^{-1})	% Inhibition
0	0.00072	0.44	0
2.7	0.00066	0.40	9
5.3	0.00056	0.34	23
11	0.00043	0.26	41
21	0.00031	0.19	57
42	0.00019	0.11	74
85	0.00012	0.073	83

Table 9.32. Data for assay of the inhibition of α-chymotrypsin by **4.3** after UV, vis irradiation.

Inhibitor concentration (μM)	Slope (A.U. s^{-1})	V_0 (μmol s^{-1} mg^{-1})	% Inhibition
0	0.00072	0.44	0
5.3	0.00070	0.42	3.8
11	0.00062	0.38	14
21	0.00054	0.33	25
42	0.00045	0.27	38
85	0.00037	0.22	49

Table 9.33. Data for assay of the inhibition of α-chymotrypsin by **4.4**.

Inhibitor concentration (μM)	Slope (A.U. s^{-1})	V_0 (μmol s^{-1} mg^{-1})	% Inhibition
0	0.00053	0.32	0
51	0.00029	0.17	46

Table 9.34. Data for assay of the inhibition of α-chymotrypsin by **4.4** after UV irradiation.

Inhibitor concentration (μM)	Slope (A.U. s^{-1})	V_0 (μmol s^{-1} mg^{-1})	% Inhibition
0	0.00053	0.32	0
3.2	0.00046	0.28	13
6.4	0.00036	0.22	31
13	0.00029	0.17	46
26	0.00017	0.10	68
51	0.000091	0.055	83

Table 9.35. Data for assay of the inhibition of α-chymotrypsin by **4.4** after UV, vis irradiation.

Inhibitor concentration (μM)	Slope (A.U. s^{-1})	V_0 (μmol s^{-1} mg^{-1})	% Inhibition
0	0.00053	0.32	0
51	0.00031	0.19	42

Table 9.36. Data for assay of the inhibition of α-chymotrypsin by **4.5**.

Inhibitor concentration (μM)	Slope (A.U. s^{-1})	V_0 (μmol s^{-1} mg^{-1})	% Inhibition
0	0.00068	0.41	0
0.18	0.00061	0.37	11
0.36	0.00051	0.31	26
0.73	0.00034	0.21	50
1.5	0.00018	0.11	74
2.9	0.000092	0.056	87
15	0.0000078	0.0047	99

Table 9.37. Data for assay of the inhibition of α-chymotrypsin by **4.5** after UV irradiation.

Inhibitor concentration (μM)	Slope (A.U. s^{-1})	V_0 (μmol s^{-1} mg^{-1})	% Inhibition
0	0.00068	0.41	0
0.090	0.00054	0.33	20
0.18	0.00039	0.24	43
0.36	0.00026	0.16	61
0.73	0.000094	0.057	86
1.5	0.000071	0.043	90

Table 9.38. Data for assay of the inhibition of α-chymotrypsin by **4.5** after UV, vis irradiation.

Inhibitor concentration (μM)	Slope (A.U. s^{-1})	V_0 (μmol s^{-1} mg^{-1})	% Inhibition
0	0.00068	0.41	0
0.18	0.00057	0.34	17
0.36	0.00044	0.27	36
0.73	0.00032	0.20	53
1.5	0.00015	0.091	78

Table 9.39. Data for assay of the inhibition of α-chymotrypsin by **4.6**.

Inhibitor concentration (μM)	Slope (A.U. s^{-1})	V_0 (μmol s^{-1} mg^{-1})	% Inhibition
0	0.00066	0.40	0
0.42	0.00050	0.30	24
0.85	0.00035	0.21	48
1.7	0.00025	0.15	63
3.4	0.000093	0.057	86
6.8	0.000052	0.032	92

Table 9.40. Data for assay of the inhibition of α-chymotrypsin by **4.6** after UV irradiation.

Inhibitor concentration (μM)	Slope (A.U. s^{-1})	V_0 (μmol s^{-1} mg^{-1})	% Inhibition
0	0.00066	0.40	0
0.17	0.00051	0.31	23
0.34	0.00044	0.27	34
0.68	0.00024	0.15	64
1.4	0.00011	0.069	83

Table 9.41. Data for assay of the inhibition of α-chymotrypsin by **4.6** after UV, vis irradiation.

Inhibitor concentration (μM)	Slope (A.U. s^{-1})	V_0 (μmol s^{-1} mg^{-1})	% Inhibition
0	0.00066	0.40	0
0.42	0.00045	0.27	32
0.85	0.00033	0.20	50
1.7	0.00020	0.12	69
3.4	0.00012	0.071	82
6.8	0.000057	0.035	91

Table 9.42. Data for assay of the inhibition of α-chymotrypsin by **4.7**.

Inhibitor concentration (μM)	Slope (A.U. s^{-1})	V_0 (μmol s^{-1} mg^{-1})	% Inhibition
0	0.00059	0.36	0
0.58	0.00048	0.29	19
1.2	0.00038	0.23	36
2.3	0.00029	0.18	51
4.6	0.00015	0.089	75
9.3	0.000062	0.038	89
23	0.000028	0.017	95

Table 9.43. Data for assay of the inhibition of α-chymotrypsin by **4.7** after UV irradiation.

Inhibitor concentration (μM)	Slope (A.U. s^{-1})	V_0 (μmol s^{-1} mg^{-1})	% Inhibition
0	0.00059	0.36	0
0.29	0.00045	0.27	25
0.58	0.00033	0.20	44
1.2	0.00022	0.13	63
2.3	0.00011	0.69	81

Table 9.44. Data for assay of the inhibition of α-chymotrypsin by **4.7** after UV, vis irradiation.

Inhibitor concentration (μM)	Slope (A.U. s^{-1})	V_0 (μmol s^{-1} mg^{-1})	% Inhibition
0	0.00059	0.36	0
0.58	0.00051	0.31	14
1.2	0.00041	0.25	31
2.3	0.00029	0.18	51
4.6	0.00014	0.082	77
9.3	0.000071	0.043	81

Table 9.45. Data for assay of the inhibition of α-chymotrypsin by **5.17**.

Inhibitor concentration (μM)	Slope (A.U. s^{-1})	V_0 (μmol s^{-1} mg^{-1})	% Inhibition
0	0.00061	0.37	0
3.0	0.00060	0.37	1.7
5.9	0.00052	0.32	15
12	0.00041	0.25	34
24	0.00025	0.15	59
47	0.00015	0.089	76
94	0.000087	0.053	86

Table 9.46. Data for assay of the inhibition of α-chymotrypsin by **5.17** after UV irradiation.

Inhibitor concentration (μM)	Slope (A.U. s^{-1})	V_0 (μmol s^{-1} mg^{-1})	% Inhibition
0	0.00061	0.37	0
3.0	0.00059	0.36	4.2
5.9	0.00043	0.26	30
12	0.00030	0.18	51
24	0.00020	0.12	68
47	0.00011	0.067	82

Table 9.47. Data for assay of the inhibition of α-chymotrypsin by **5.17** after UV, vis irradiation.

Inhibitor concentration (μM)	Slope (A.U. s^{-1})	V_0 (μmol s^{-1} mg^{-1})	% Inhibition
0	0.00061	0.37	0
5.9	0.00056	0.34	8.9
12	0.00041	0.25	34
24	0.00027	0.16	57
47	0.00016	0.098	74

Table 9.48. Data for assay of the inhibition of α-chymotrypsin by **5.18**.

Inhibitor concentration (μM)	Slope (A.U. s^{-1})	V_0 (μmol s^{-1} mg^{-1})	% Inhibition
0	0.00045	0.27	0
0.13	0.00037	0.22	19
0.27	0.00030	0.18	34
0.53	0.00019	0.12	58
1.1	0.00014	0.084	69
2.1	0.000069	0.042	85

Table 9.49. Data for assay of the inhibition of α-chymotrypsin by **5.18** after UV irradiation.

Inhibitor concentration (μM)	Slope (A.U. s^{-1})	V_0 (μmol s^{-1} mg^{-1})	% Inhibition
0	0.00045	0.27	0
0.067	0.00033	0.20	28
0.13	0.00028	0.17	38
0.27	0.00019	0.11	59
0.53	0.000097	0.059	78
1.1	0.000058	0.035	87

Table 9.50. Data for assay of the inhibition of α-chymotrypsin by **5.18** after UV, vis irradiation.

Inhibitor concentration (μM)	Slope (A.U. s^{-1})	V_0 (μmol s^{-1} mg^{-1})	% Inhibition
0	0.00045	0.27	0
0.13	0.00037	0.22	19
0.27	0.00023	0.14	48
0.53	0.00022	0.14	50
1.1	0.00014	0.085	69
2.1	0.000049	0.030	89

9.7 Experimental for work described in chapter 7

Surface preparation

Gold film substrates were prepared by evaporative deposition of gold onto pieces of silicon wafer, previously coated with titanium. Silica samples were initially prepared by spin-coating a Si(100) wafer with a protective layer of AZ1813 photoresist, cutting into 10 × 10 mm squares, removing photoresist and cleaning by ultrasonication in acetone, methanol then isopropanol (for 5 s each), and drying under N_2. Ti (40 nm) then Au (200 nm) were deposited onto the wafer pieces using a Balzer vacuum evaporator. The substrates were stored in a vacuum dessicator before use.

A polycrystalline gold plug electrode (geometric surface area 0.3 cm^2) was used in electrochemistry experiments. This electrode was cleaned before use in freshly prepared piranha solution (1:3 H_2O_2/H_2SO_4), followed by annealing in a H_2 flame then scanning between potentials of -0.2 V and 1.45 V in $HClO_4$ (0.01 M) at 20 mVs^{-1} until a stable CV was obtained (several hours).

Contact angle measurements

Contact angle measurements were made by placing several (typically 2-3) water drops (2 μL) on each substrate, then recording a photograph of each drop 30 s after placement. The drops were analysed using an axisymmetric drop shape analysis program[39] to obtain contact angle measurements. All measurements for each surface were averaged. Error is estimated to be ± 3º, since the standard deviations for measurements ranged from 0.4º to 2.2º.

Cyclic voltammetry

Cyclic voltammetry was carried out using a computer controlled EG&G PAR 273A potentiostat. Either the gold plug electrode or a gold film was used as working electrode, with a Pt or Au electrode as auxiliary, and a saturated calomel electrode (SCE) as reference. The gold plug electrode was mounted in an electrochemical cell, in contact with

the solution by a hanging meniscus that exposed only the circular bottom face of the electrode to the solution. Gold film electrodes were mounted in a cell that exposed a circular region (approximate surface area = 0.3) to the cell solution.[40] Solutions were degassed with N_2 gas for 20 min prior to any scans below -0.3 V. All CVs were recorded at room temperature using a scan rate of 300 mV s^{-1} unless otherwise stated.

Quartz crystal microbalance

QCM was carried out using a Q-sense E4 instrument linked to a peristaltic pump, using gold coated quartz crystals. Tris buffer (as described above for enzyme assays but without Triton X-100 surfactant) was used as the running buffer in all experiments, flowing at 100 μL min^{-1}. Analysis of results was carried out using the Qtools software.

Surface plasmon resonance

SPR was carried out using a Biacore 2000 instrument. All solutions were filtered through a 0.22 μM filter and centrifuged (1300 rpm, 10 sec) before use. HEPES buffer (0.01 M, pH 7.4 containing 0.15 M NaCl and 3 mM EDTA) was used as the running buffer for surface modifications, and Tris buffer (as described above for enzyme assays except containing 12.5 μL P20 surfactant instead of Triton X-100) was used in all other experiments. Analysis of results was carried out using BIAevaluation software.

Compound **4.4** was immobilised on an SPR chip as follows: A Biacore CM5 chip was docked in the SPR instrument and prepared by priming and running a sensorgram in HEPES buffer at 100 μL min^{-1} flow rate then successively injecting NaOH (50 mM, 20 μL × 2), HCl (10 mM, 20 μL × 2), and SDS (0.1%, 20 μL × 2). Surface modification was then carried out at 5 μL min^{-1} flow rate by injection of 35 μL EDCI/NHS, followed by **7.1** (11 mg/mL in HEPES buffer, 3 × 5 μL) then ethanolamine (1 M, pH 8.5, 35 μL). During attachment of **7.1**, the SPR response increased by 147 RU from the initial baseline obtained before EDCI/NHS injection. The chip was then undocked and removed from the instrument and rinsed with water. A solution of **4.4** (0.30 mg, 0.44 μmol), CuBr (0.063 mg, 0.44 μmol), 2,6-lutidine (0.094 mg, 0.88 μmol), 2,2'-bipyridine (0.14 mg, 0.88 μmol), sodium ascorbate (0.17 mg, 0.88 μmol) in 1:1 DMF/H_2O (150 μL) was pipetted onto the

surface and left for 1 h at room temperature. The surface was then rinsed successively with 1:1 DMF/H_2O, H_2O, 0.1 M EDTA, 1:1 DMF/H_2O, and H_2O then redocked in the SPR instrument. A sensorgram was run in Tris buffer for several hours in order to obtain a stable baseline. A reference cell was prepared using the same method except omitting the injection of **7.1**.

Enzyme binding to this modified surface was monitored by running sensorgrams in Tris buffer at 30 μL min^{-1}. For photoswitching experiments, the chip was removed from the instrument after regeneration, rinsed with water and irradiated with UV or visible light (as detailed above for solution-phase photoisomerisation) for 10 min, then replaced in the SPR instrument.

9.8 References

1. Armarego, W. L. F.; Chai, C. L. L., *Purification of laboratory chemicals*. 5 ed.; Butterworth-Heinemann: **2003**.
2. *Organic Syntheses*. Vol. 25, p 86.
3. Harvey, A. J. PhD thesis. University of Canterbury, **2000**.
4. Harvey, A. J.; Abell, A. D., *Bioorg. Med. Chem. Lett.* **2001**, 11, 2441.
5. Desai, R. D.; Mehta, C. V., *Indian J. Pharm.* **1951**, 13, 211.
6. Alexander, N. A. PhD thesis. University of Canterbury, **2006**.
7. Kettner, C. A.; Shenvi, A. B., *Biol. Chem.* **1984**, 259, 15106.
8. Ulysse, L.; Chmielewski, J., *Bioorg. Med. Chem. Lett.* **1994**, 4, 2145.
9. Martichonok, V.; Jones, J. B., *J. Am. Chem. Soc.* **1996**, 118, 950.
10. Matteson, D. S.; Sadhu, K. M.; Lienhard, G. E., *J. Am. Chem. Soc.* **1981**, 103, 5241.
11. Hagiwara, D.; Miyake, H.; Morimoto, H.; Murai, M.; Fujii, T.; Matsuo, M., *J. Med. Chem.* **1992**, 35, 3184.
12. Ramalingam, B.; Neuburger, M.; Pfaltz, A., *Synthesis* **2007**, 4, 572.
13. Zhang, D.; Xing, X.; Cuny, G. D., *J. Org. Chem.* **2006**, 71, 1750.
14. Shimohigashi, Y.; Maeda, I.; Nose, T.; Ikesue, K.; Sakamoto, H.; Ogawa, T.; Ide, Y.; Kawahara, M.; Nezu, T.; Terada, Y.; Kawano, K.; Ohno, M., *J. Chem. Soc. Perkin Trans. 1* **1996**, 2479.
15. Oshita, S.; Matsumoto, A., *Chemistry Letters* **2003**, 32, (8), 712.

16. Sakamoto, H.; Shimohigashi, Y.; Maeda, I.; Nose, T.; Nakashima, K.; Nakamura, I.; Ogawa, T.; Ohno, M.; Kawano, K., *Journal of Molecular Recognition* **1993**, 6, (2), 95.

17. Foulds, G. PhD thesis. University of Canterbury, **1996**.

18. Kashima, C.; Harada, K.; Fujioka, Y.; Maruyama, T.; Omote, Y., *J. Chem. Soc. Perkin Trans. 1* **1988**, 3, 535.

19. Akahoshi, F.; Ashimori, A.; Sakashita, H.; Yoshimura, T.; Imada, T.; Nakajima, M.; Mitsutomi, N.; Kuwahara, S.; Ohtsuka, T.; Fukaya, C.; Miyazaki, M.; Nakamura, N., *J. Med. Chem.* **2001**, 44, 1286.

20. Herranz, R.; Castro-Pichel, J.; Vinuesa, S.; Garcia-Lopez, M. T., *J. Org. Chem.* **1990**, 55, 2232.

21. Yuan, W.; Munoz, B.; Wong, C.-H.; Haeggstriim, J. Z.; Wetterholm, A.; Samuelsson, B., *J. Med. Chem.* **1993**, 36, 211.

22. Peet, N. P.; Burkhart, J. P.; Angelastro, M. R.; Giroux, E. L.; Mehdi, S.; Bey, P.; Kolb, M.; Neises, B.; Schirlin, D., *J. Med. Chem.* **1990**, 33, (1), 394.

23. Dess, D. B.; Martin, J. C., *J. Org. Chem.* **1983**, 48, 4155.

24. Tomlinson, M. L., *J. Chem. Soc.* **1946**, 756.

25. Ameerunisha, S.; Zacharias, P. S., *J. Chem. Soc. Perkin Trans. 2* **1995**, 1679.

26. Fujiwara, K.; Murata, Y.; Wan, T. S. M.; Komatsu, K., *Tetrahedron* **1998**, 54, 2049.

27. Priewisch, B.; Rueck-Braun, K., *J. Org. Chem.* **2005**, 70, 2350-2352.

28. Lebeau, L.; Oudet, P.; Mioskowski, C., *Helv. Chim. Acta.* **1991**, 74, (8), 1697.

29. Svedhem, S.; Hollander, C.-A.; Shi, J.; Konradsson, P.; Liedberg, B.; Svensson, S. C. T., *J. Org. Chem.* **2001**, 66, 4494.

30. Rensen, P. C. N.; Leeuwen, S. H. v.; Sliedregt, L. A. J. M.; Berkel, T. J. C. v.; Biessen, E. A. L., *J. Med. Chem.* **2004**, 47, 5798.

31. Zych, A. J.; Iverson, B. L., *J. Am. Chem. Soc.* **2000**, 122, 8898.

32. Blackman, L. C. F.; Dewar, M. J. S., *J. Chem. Soc.* **1957**, 171.

33. Warnecke, A.; Kratz, F., *Bioconjugate Chem.* **2003**, 14, (2), 377.

34. Li, H.; Cheng, F.; Duft, A. M.; Adronov, A., *J. Am. Chem. Soc.* **2005**, 127, (41), 14518.

35. Sharpless, W. D.; Wu, P.; Hansen, T. V.; Lindberg, J. G., *J. Chem. Ed.* **2005**, 82, (12), 1833.

36. Harvey, A. J.; Abell, A. D., *Tetrahedron* **2000**, 56, (50), 9763.

37. Westmark, P. R.; Kelly, J. P.; Smith, B. D., *J. Am. Chem. Soc.* **1993**, 115, 3416.

38. Geiger, R., *Methods of Enzymatic Analysis*. 3 ed.; Verlag Chemie: Weinheim, **1984**; Vol. 5, p 99-129.

39. Stalder, A. F.; Kulik, G.; Sage, D.; Barbieri, L.; Hoffmann, P., *Colloid. Surface. A* **2006**, 286, (1-3), 92.

40. Brooksby, P. A.; Downard, A. J., *Langmuir* **2004**, 20, 5038.